BEAM TO COLUMN BOLTED CONNECTIONS

JOHN GRAHAM

A THESIS SUBMITTED FOR THE DEGREE

OF

DOCTOR OF PHILOSOPHY

DEPARTMENT OF CIVIL ENGINEERING

THE UNIVERSITY OF ASTON IN BIRMINGHAM

OCTOBER 1981

TO MY

MOTHER AND FATHER

THE UNIVERSITY OF ASTON IN BIRMINGHAM

BEAM TO COLUMN BOLTED CONNECTIONS

by

JOHN GRAHAM

THESIS SUBMITTED FOR THE DEGREE OF DOCTOR OF PHILOSOPHY 1981

SUMMARY

This thesis examines the behaviour of extended end plate, beam to column connections, subject to shear and bending forces. The effect of varying the bending moment/shear ratio and the thickness of the end plate and column flange for an unstiffened column section is shown. Particular attention is given to rotation, slip, local deformation and prying forces in the bolts. A total of twenty one tests using HSFG bolts are reported. Five associated tee stub tests with varying plate thickness and bolt preload are also reported and show that at failure prying forces in the tee stub bolts were approximately twice the corresponding value obtained in the beam to column tests.

Work hardening of the end plate and column flange was found to be important in fixing limits to deformations in the tee stubs and rotations in the beam to column connections.

Theoretical methods are developed for the determination of slip, stiffness, elastic load and ultimate load for beam to column connections and are compared with the experimental results reported and those from other investigations (6, 19, 22, 30, 31, 33). Design methods by other authors (20, 31, 35, 46) are also compared with the experimental results and conclusions made as to their suitability.

The behaviour of individual HSFG bolts in direct and torque tension is also examined. Twenty five torque tension tests are reported where torque wrench, 'Coronet' load indicating washer and bolt extension tightening control methods are compared with shank tensions obtained from strain gauge readings. These results are then compared with eleven similar direct tension tests. A method to determine bolt force from its extension, induced by either tightening or applying direct tension, is developed and compared with experimental results by other authors (59, 61).

BOLTS CONNECTIONS JOINTS MOMENT SHEAR

ACKNOWLEDGEMENTS

The author would like to thank his supervisor Dr. C.S. Bahia and advisor Dr. L.H. Martin for their encouragement and advice throughout the period of this research.

The author is deeply indebted to Mr. M. Turan, a postgraduate research student within the Civil Engineering Department, for his assistance in preparing and testing several of the specimens. Thanks are also due to Mr. S.M. Wagstaff, a technician within the department, for his help with the preparation of some specimens, Miss S.P. Warburton for her comments on the script and Miss P.L. Howson for typing the thesis neatly and efficiently.

Finally, the author would like to thank the Department of Education for Northern Ireland for providing the studentship.

NOTATION

a_c	column flange edge distance
a_p	tee stub or end plate edge distance
A	constant of integration
A_b	net area of a bolt
A_s	gross area of a bolt
b_c	distance from centre of bolt hole to the web of a column flange
b_p	distance from centre of bolt hole to the web of a tee stub or end plate
b_1	distance from centre of bolt hole to the strain gauge adjacent to the weld of a tee stub, end plate or column flange
B	constant of integration
c	compressive force between plates
C	vertical bolt pitch
d	bolt diameter
d_1	effective bolt diameter
d_b	distance from centre of rotation to the extreme edge of an end plate
d_f	distance from centre of rotation to the centroid of the tensile bolts
d_t	distance from centre of rotation to the centre of the compression zone bolts
e	bolt extension
e_{be}	linear elastic bolt extension due to applied load

e_{bp}	linear elastic bolt extension due to prestress
E	Young's modulus of elasticity
E_b	Young's modulus of elasticity for a bolt
E_c	Young's modulus of elasticity for a column flange
E_p	Young's modulus of elasticity for a tee stub or end plate
F	applied load per bolt to a tee stub or end plate
F_e	applied load per bolt to a tee stub or end plate in the linear elastic range
F_u	applied load per bolt to a tee stub or end plate at failure
F_s	bolt preload
F_b	bolt force
F_{be}	bolt force in the linear elastic range
F_{bu}	ultimate tensile strength of a bolt
g	gauge length of a bolt
g_c, g_p	proportion of the grip length of a bolt related to one plate, generally the plate thickness plus one washer
I_c	second moment of area per bolt for a column flange
I_p	second moment of area per bolt for a tee stub or end plate
k	elastic stiffness of a joint
K	torque coefficient

l	half span in a strip beam test
l_n	nut thickness
L	span in beam to column tests
L_1	unthreaded length of a bolt
L_2	$(g - L_1)$
m	elastic moment of resistance per bolt
m_h	work hardened moment of resistance per unit length
m_p	theoretical plastic moment of resistance per strip beam or per bolt for a tee stub or beam to column connection
m_p'	theoretical plastic moment of resistance per bolt at the bolt line of a tee stub
m_{ch}	work hardened moment of resistance per bolt for a column flange at the first discontinuity
m_{ph}	work hardened moment of resistance per strip beam or per bolt for a tee stub or end plate at the first discontinuity
M	applied bending moment at a beam to column connection
M_p	theoretical plastic moment of resistance
M_p'	plastic moment of resistance for the beam section
M_s	applied bending moment at a beam to column connection at final slip
M_u	applied bending moment at a beam to column connection at failure

M_{bh} moment applied to a beam to column connection at the discontinuity limit for the tensile bolts

M_{ch} moment applied to a beam to column connection at the lower bound discontinuity limit for the column flange

M_{cy} moment applied to a beam to column connection at the upper bound discontinuity limit for the column flange

M_{ph} moment applied to a beam to column connection at the discontinuity limit for the end plate

n_c number of bolts positioned near the compression flange

n_t number of bolts around the tension flange

Q_b prying force per bolt

Q_{be} prying force per bolt in the linear elastic range

Q_{bs} prying force per bolt at final slip

Q_{bu} prying force per bolt at failure

Q_u total prying force at the extremity of the end plate in the beam to column connections

r absolute value of the correlation coefficient for a linear regression analysis

S_{be} linear elastic strain in a bolt due to the external load

S_{bs} strain in a bolt due to the prestress force = F_s/A_bE_b

S_{bu}	strain in a bolt from the external load at failure
t	strip beam thickness
t_c	column flange thickness
t_p	tee stub or end plate thickness
t_w	total washer thickness
T	total ply thickness
T_s	torque applied to a bolt shank
V	applied shear force at a beam to column connection
V_s	applied shear force at a beam to column connection at final slip
V_u	applied shear force at a beam to column connection at failure
w	strip beam width
w_c	effective width of column flange per bolt in the linear elastic range
w_{ce}	effective width of column flange in the linear elastic range
w_{cy}	equivalent width of column flange per bolt at work hardened yield
w_p	width of tee stub or end plate per bolt
W	applied load to a strip beam
α	empirical constant
δ	$(e_{be} - e_{bp})$
δ_f	deflection at the toe of a column flange
ε	strain in a bolt
μ	coefficient of slip
μ_t	coefficient of thread friction

σ	elastic stress value obtained from strain gauge reading
σ_b	tensile stress applied to the net area of a bolt
σ_s	tensile stress applied to the gross area of a bolt
σ_y	yield stress
$\sigma_{y0.2}$	0.2% yield stress of a bolt in direct tension
$\sigma_{yt0.2}$	0.2% yield stress of a bolt in torque tension
σ_{cy}	yield stress of a column flange
σ_{py}	yield stress of a tee stub or end plate
τ	uniform shear stress across the threaded area of a bolt
ϕ	rotation
ϕ_j	elastic rotation of a connection
Δ	central deflection of a strip beam
Δ_c	deflection at the toe of a column flange in the linear elastic range
Δ_p	deflection of the extended portion of the end plate in the linear elastic range

NOTE: Some notations not included in the above list, will be specifically defined when they are first introduced.

CONTENTS

LIST OF TABLES

CHAPTER SIX

APPENDIX A-2 TO CHAPTER TWO

LIST OF FIGURES

LIST OF PLATES

CHAPTER ONE

INTRODUCTION AND REVIEW OF PREVIOUS RESEARCH

1.1 Introduction

Structural steel frames are formed by the assembly of individual members, by means of connections.

Structural connections should reflect the assumptions made in the design of the adjacent members of a framework. The principal requirements being sufficient strength and stiffness combined with adequate rotation capacity.

Beam to column connections may be divided into three main groups:

a) flexible or pinned

b) semi-rigid

c) rigid

and the type is determined by the amount of restraint offered by the joint against end rotation of the beam.

Structural steel work is normally fabricated some distance from the site and delivered in lengths suitable for transportation. The members are then connected on site, but due to carriage limitations some connections or splices may be unavoidable. The economics of steel structures are largely governed by fabrication and erection costs. Both

of these processes are dependent on the type and extent of the connections throughout a structure.

Although joints are important in the overall cost of some frameworks they are usually given little attention by designers and lack of knowledge of how particular connections behave is certainly one reason for this. To reduce costs, one solution would be to produce simple and efficient joint designs and is the main theme of this research project.

1.1.1. Beam to Column Connections

Modern practice is moving towards welded shop joints with bolted site joints, thus producing a more efficient and cheaper fabrication technique, and eliminating unnecessary material and labour costs. This can be observed in some typical beam to column connections shown in Figure 1.1. Pinned or simply supported joints may be represented by Figures 1.1 (a) and 1.1 (b). Figure 1.1 (a) shows a pre-drilled end plate, fillet welded to the beam and site connected with either grade 4.6 bolts or grade 8.8 precision bolts. Clearance holes are provided in both the end plate and column. The connection is kept within the depth of the beam. A seating cleat, which facilitates erection may be used as illustrated in Figure 1.1 (b). This method allows more end rotation than the previous arrangement, with a top cleat ensuring lateral restraint. The connection

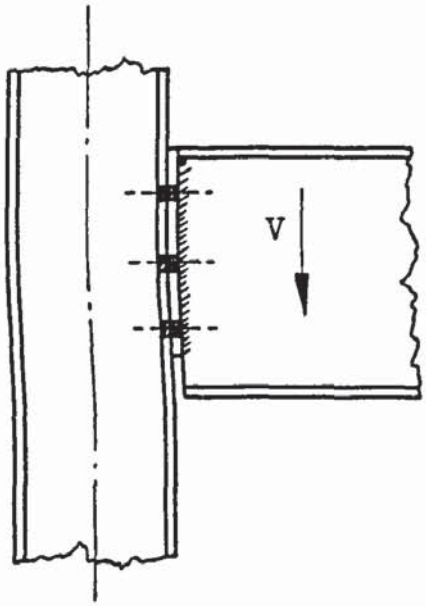

(a) Short end plate

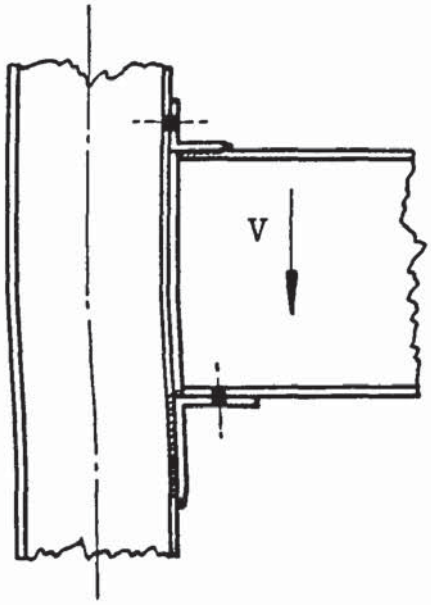

(b) Seating cleat

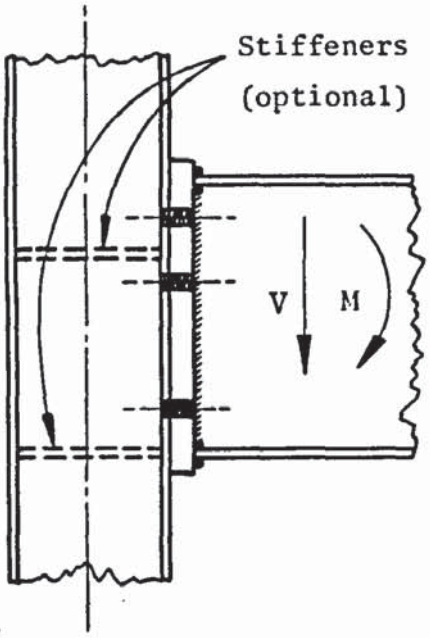

(c) Flush end plate

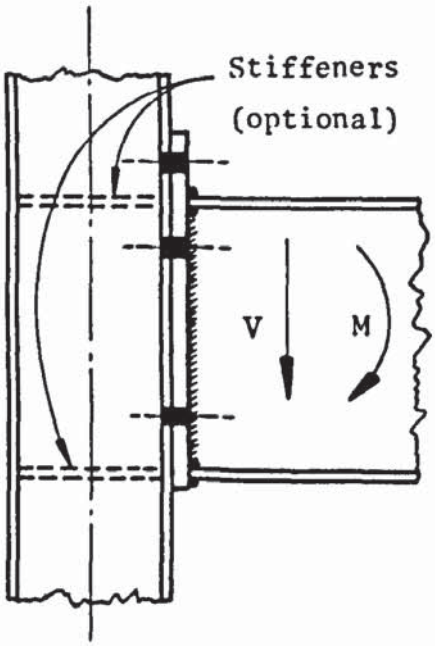

(d) Extended end plate

FIGURE 1.1 TYPICAL BEAM TO COLUMN CONNECTIONS

is made outside the depth of the beam, normally with grade 4.6 bolts. The end plate method is usually preferred by the industry.

Typical semi-rigid or rigid moment connections are represented by Figures 1.1 (c) and 1.1 (d). These are similar to the connection shown in Figure 1.1 (a), with the end plate either flush (Figure 1.1 (c)) or extended (Figure 1.1 (d)). Fillet welds or full penetration butt welds, or a combination of the two may be used. Site assembly is normally with high strength friction grip bolts (HSFG). As rotation normally occurs about the beam compression flange, the effective arm to the bolts increases as the end plate extends, as shown in Figure 1.1 (d). This results in smaller bolt sizes, with a decrease in the corresponding tensile and compressive forces being applied to the column. Thinner end plates are normally associated with this arrangement, resulting in the extended end plate system being usually preferred in practice.

If the connection is subjected to wind reversal, it may become necessary to have similar details around both flanges.

1.1.2. High Strength Friction Grip Bolts

With the introduction of HSFG bolts in the early fifties in the USA, extensive research has been carried out in America

and Europe. These bolts soon replaced rivets and black bolts as the main structural fastener and are still very popular today. Various types of friction grip bolts are now available and sophisticated methods of tightening have been introduced.

HSFG fasteners consist of high tensile bolts and nuts with hardened steel washers. The bolts are tightened to a pre-determined shank tension and in shear connections the load is transferred between the plies by friction. The bolts do not act in shear or bearing as in ordinary bolted joints. When placed in a tension joint, the connected parts can not separate until the torqued shank tension is exceeded by the applied tension. When joints similar to those shown in Figures 1.1 (c) and 1.1 (d) are subjected to flexural and shear loading, the advantages of using HSFG bolts can readily be seen. Fewer bolts are required due to the increase in force that can be transmitted in both shear and in tension, also greater fixity can be obtained, due to the absence of slip between the column flange and end plate. Although high strength bolts are individually more expensive than ordinary bolts, the decrease in number results in less fabrication time producing a more economic and efficient solution.

1.1.3. Extended End Plate Connections

The behaviour of beam to column connections have been

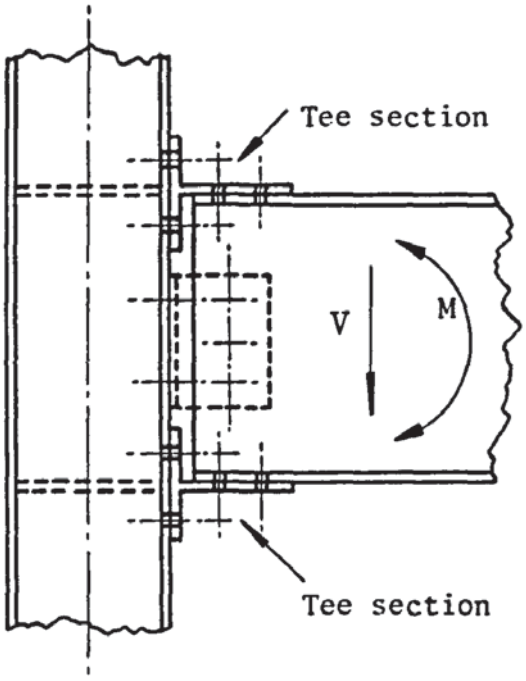

FIGURE 1.2 TYPICAL BEAM TO COLUMN TEE SECTION CONNECTION

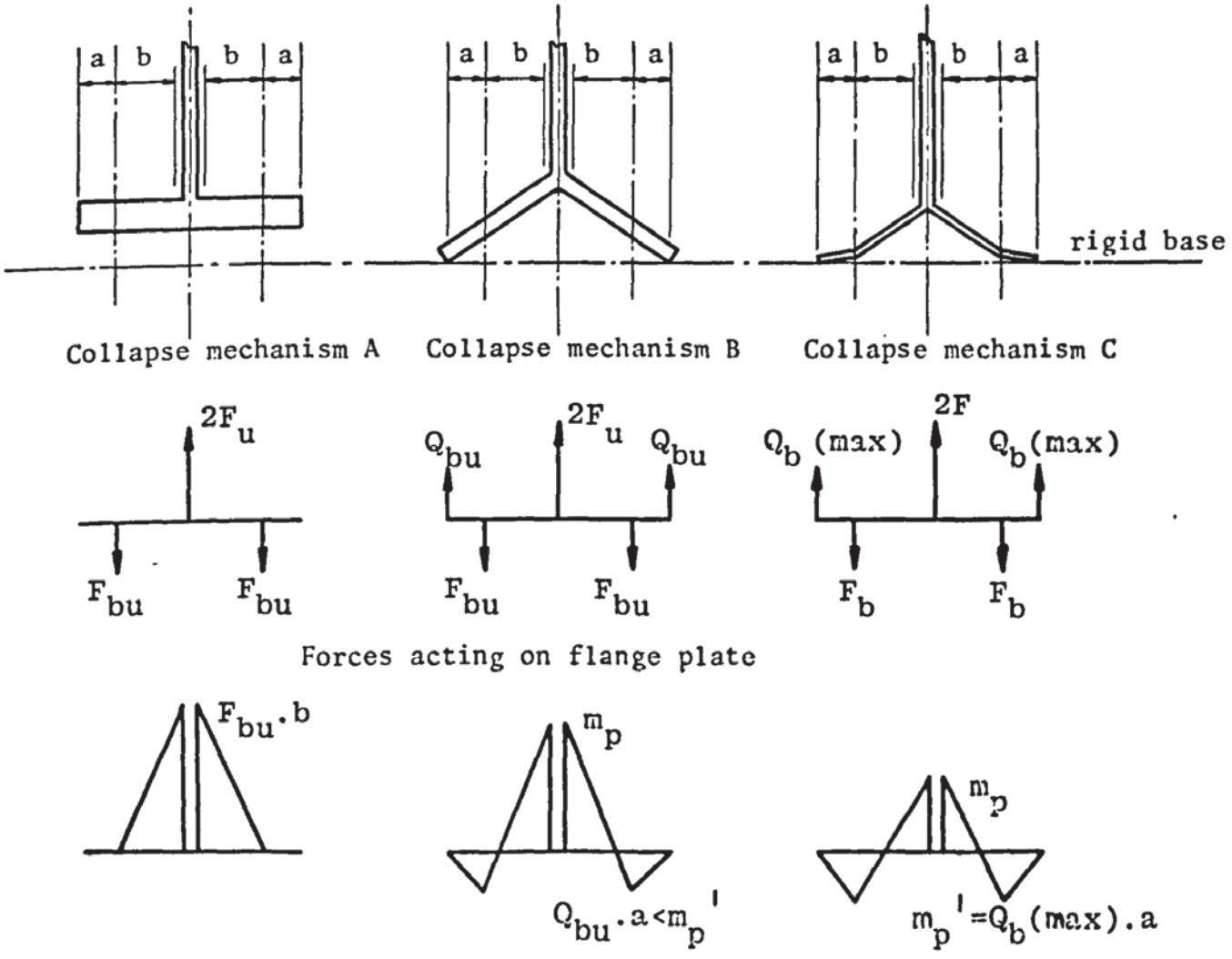

FIGURE 1.3 COLLAPSE MECHANISMS OF TEE SECTION FLANGE

investigated by several researchers and the extended end plate joint has been given much attention in recent years. This type of rigid connection became more favourable than joints formed with tee stubs, as shown in Figure 1.2, because of the reduced amount of material and labour time involved.

This research programme is limited to the performance of extended end plate, beam to unstiffened column connections, using HSFG bolts under static loading conditions.

1.2 Review of Previous Research

Between 1929 and 1936, the Steel Structures Research Committee investigated several aspects of riveted and bolted connections, to establish a basis for analysis of steel framed buildings.

In 1934, Batho and Bateman[1] in a second report for the Committee suggested the use of high tensile bolts in structural frames to prevent slipping. Batho and Rowan[2] in the same report, studied the effects of moment and shear applied to several types of beam to stanchion joints. Tee sections, web cleat and flange cleat riveted connections, together with flange cleat connections using high tensile bolts were examined. The tee or split I section detail, similar to that shown in Figure 1.2, proved to be the most

rigid of those tested. In the final report[3], a semi-graphical solution was given for determining the end moments in a beam, based on the experimental curves of the connections. BS449[4] and B/20[5] recommended this approach for semi-continuous steel frames.

In the mid-fifties Munse[6] studied the effect of initial bolt pretension in both shear and tension joints subjected to static and fatigue loading. He concluded that reduced preload in high strength bolts, induced slip at lower shear loads. He also concluded that joints with reduced preload in bolts subjected to tensile forces provided lower resistance in fatigue type loading conditions. The importance of preload and its control was evident from this investigation.

In 1959, Munse et al[7] investigated the efficiency of tee stub joints connected by either high strength bolts or rivets, using either two lines or four lines of fasteners. The latter type carried a large portion of the applied load in the inner fasteners while the remaining fasteners were relatively ineffective. This type of connection was therefore uneconomical and indicates why in later years, research and practice concentrated on tee stubs with two lines of fasteners. From the twenty eight tests reported Munse et al[7] observed the ultimate load of the bolted joints to be approximately 14% greater than the corresponding riveted joints. This result, plus the

observations made by Munse[6] gives some indication why rivets have been superseded by high strength bolts, as the main structural fasteners.

To establish methods of analysis and design of high strength bolted connections, Schutz[8] reported the results of several tests on tension and moment joints. The tension series consisted of six tee stub connections. The formation of plastic hinges along both the bolt and web line of the flange, as indicated by Mechanism C in Figure 1.3, was taken as the ultimate limit state for design purposes. Two beam to column tee section joints with stiffened flanges, similar to Figure 1.2, were also tested. From the results Schutz[8] also recommended Mechanism C in Figure 1.3, as the governing failure mode for design of tee section and extended end plate joints. The region around the tension flange of an extended end plate connection was considered to behave as a tee section.

The two tests on connections reported by Ranger[9] were designed to provide a fixed end connection for the main beams of a multi-storey building. A haunch was provided at the beam end with an end plate welded to both the beam and haunch. The beam was then connected to the column flange with high strength bolts. Full depth stiffeners were used within the column opposite both the tension and compression flanges. The results of the tests were considered sufficient to corroborate the design basis.

Similar connections may be found in many industrial buildings today, e.g. eaves and valley details of portal frames.

During the fifties considerable interest was expressed concerning the plastic behaviour and analysis of steel structures, due to the resulting lightweight frames that could be obtained. The natural progression of this work, led Johnson et al[10] to turn their attention towards the behaviour of the connections in such structures. The object of the series of experiments reported, was to determine whether the full plastic moment of the connected members could be developed in certain types of rigid joints employing high strength bolts. In addition to studying two beam splice connections, four beam to column joints were investigated. A haunch detail similar to that used by Ranger[9] and an extended end plate joint were discussed and compared with two flange or wing plate types. The joints behaved in a rigid manner at the early stages of loading and developed the full plastic moment of the connected member producing a plastic hinge with adequate rotation capacity within the member.

Although some steel structures in the late fifties, normally portal frames, were being designed plastically, their connections were still analysed by elastic principles. In an attempt to provide continuity between the two Sherbourne[11] proposed that joint failure should coincide with that of the connected beam, resulting in more efficient

and less expensive connections. Sherbourne's[11] experimental programme was limited to an extended end plate connection, similar to a joint type investigated by Johnson et al[10]. The moment to shear ratio was kept constant throughout the five tests, in which the bolts, end plate and compression flange stiffeners were studied. The experimental results showed that little variation in the rigidity of the connections occurred, when various compression flange stiffener sizes were used. Sherbourne[11] therefore suggested the use of thin stiffeners, whenever possible, as a more economical solution to column web stiffening. He also suggested that sufficient rotation capacity could be achieved if plastic deformation of the end plate occurred, thus equalizing the forces on the bolts and increasing the strength of the assembly.

Plastic design equations were developed for the compression flange stiffener size and the end plate thickness. The end plate was assumed to act as a fixed end beam spanning between the bolts which were positioned either side of the beam tension flange. Prying action was neglected.

Douty and McGuire[12] provided more information on the elastic and plastic performance of high strength bolted connections in 1965, by examining tee stub connections and joints similar to those shown in Figures 1.1 (c), 1.1 (d) and 1.2. The behaviour of tee stub joints attracted special

interest due to their associated behaviour with tee section and extended end plate joints which was suggested earlier by Schutz[8]. Twenty seven tee stub tests with rigid and flexible bases were investigated, considering parameters such as flange thickness, bolt diameter and edge distance. One extended end plate and three tee section beam to column connections were tested, together with one extended butt plate and five flush plate beam to beam joints. They suggested from the experimental evidence that the behaviour of the tee section joints, were compatible with that of the tee stub connections. Also the extended end plate joints were stiffened slightly from the presence of the beam web and end plate. One important observation made was that prying force was reduced as flange plate thickness increased. This meant that prying action could be controlled to some degree with a subsequent reduction in tensile bolt force.

Semi-empirical equations were developed for the computation of the prying force ratio, at working and ultimate loads for tee stub connections. These equations also applied to tee section and extended end plate moment joints considering the end plate around the tension flange as an equivalent tee stub.

In 1965, Bannister[13] published the results of six tee section and one angle section moment connection tests using HSFG bolts and subjected to pure moment. The test specimens

were similar to those reported by Batho and Rowan[2] and the results were similar.

In 1966, Bannister[14] discussed the moment angle change relationships for the connections reported in his earlier paper[13]. He also reported on further tests undertaken on three symmetrical frames with tee section joints. It was suggested that these frames could be considered rigidly jointed when the stress in the connected beam was kept below 5 tons/sq. in. (77N/mm^2) approximately.

In Japan, beam to column connections were usually designed as rigid moment resisting components, due to the large lateral forces that could be applied to a structure during an earth tremor. Tee section connections, similar to Figure 1.2, were not very common in Japan therefore Naka et al[15] investigated the stiffness and strength characteristics of this type of joint when subjected to cyclic loading. Fourteen tests were reported consisting of tee stubs in tension and tee section moment connections with rivets, welds and high strength bolts used as the fastener types. Rib plates to strengthen the tee section flange were used in some cases, although they did not improve the joint stiffness significantly. In general the high strength bolted tee section arrangement gave the required strength stiffness and ductility for it to be considered as a rigid connection in practical use.

Also in Japan Konishi and Yamakawa[16] investigated the behaviour of beam splice butt plate joints subjected to pure moment. The test specimens consisted of two beams connected together with either an extended or flush end plate. The plate thicknesses and high strength bolt diameter were constant for both tests. The extended end plate arrangement had four bolts symmetrically positioned around the tension flange and two bolts placed near to the compression flange. The flush end plate system however had four bolts positioned near each beam flange. The experimental results showed that the extended end plate joint was the stiffer of the two and although the maximum joint deformation occurred opposite the tension flange in both tests it was not as great in the extended end plate joint. Equations were developed, based on elastic principles from the theory postulated by Douty and McGuire[12] to determine the tensile bolt force and moment at which plate separation occurred.

In 1968 for his PhD thesis, Mann[17] attempted to determine the influence of beam to column connections on the strength and stiffness of plastically designed rigid steel frames. He showed that for braced multi-storey frameworks, the increase in flexibility compared to welded joints was beneficial in levelling end and centre moments in the beams.

Six tests were performed on a one sided beam to column connection, in preference to a cruciform arrangement

previously used by other authors. The extended end plate method was used exclusively, with four HSFG bolts symmetrically placed around the tension flange. Shear plates, rarely used in practice, were positioned below the end plate to prevent slip taking place. Mild and high yield steel sections were used. Mann[17] showed that high yield steel plates provided stiffer connections, while plate thickness had a significant effect on the mode of failure and magnitude of the failure moment. Failure of the end plate as the design criteria for a connection would only be valid if the column flange was relatively thick and this was the case throughout Mann's[17] test programme. An equation for the end plate thickness was developed, based on what he considered to be the collapse mechanism of the end plate. The tee stub analogy was not considered. The equation $P_u = M/3.6\ d_f$ was suggested for the ultimate tensile strength of the bolts (P_u) based on the bolts utilizing 20% of their ultimate strength in resisting prying forces. Several of the six tests were loaded up to 0.6 M_p on a few successive cycles. The initial tension in the bolts varied from hand tight to full preload. The results of these tests provided proof of increased stiffness with increased preload, thereby decreasing deflections at working load level.

Mann[17] also performed twenty two tests on beams with stiffened webs, to simulate conditions around the compression

flange of a beam to column connection. The stiffening plates did not extend the full depth of the web. He developed an equation for the resistance of such a stiffened section, which was similar to an equation developed by Sherbourne[11].

In 1970, the equation for end plate thickness suggested by Mann[17] was slightly refined by Surtees and Mann[18] so that it could be used for design purposes. They also suggested that the force in the bolts (P) be determined from $P = M_p/3\ d_f$.

In 1969, Struik[19] performed twenty one tee stub tests, to enable him to develop a procedure to determine the influence of prying forces on extended end plate beam to column moment connections. Parameters such as flange thickness, edge distance, bolt type (either black or HSFG) and preload, were considered. The bolt diameter was kept constant throughout the test series. His experimental results showed that the magnitude of the prying forces were dependent on the thickness of the flange plate and initial bolt tension. Prying forces reduced as the flange plate thickness increased and were smaller in comparison, to a similar specimen with less initial bolt tension, at the same applied load. The failure load however, was the same for each test with the same thickness regardless of the initial bolt tension. There was not enough information available, concerning the influence of edge distances on prying action, for any firm conclusions to be made.

Struik[19] developed equations for the elastic and plastic design of the flange plate, which included a curvature factor for the flexural behaviour of the plate. Fisher and Struik[20] recommended a similar design procedure which involved the three mechanisms shown in Figure 1.3.

Plastic analysis of steel structures at the beginning of the seventies was generally accepted in practice, although connections were designed to elastic principles, as before. This may have been considered safe practice but was certainly uneconomical and tended to produce plastic hinges in the connected members at points remote from the connections, due to the unnecessarily stiff joints.

In an attempt to rectify this situation Bailey[21] designed thirteen extended end plate beam to column connections in accordance with the equations developed by Sherbourne[11]. He subsequently tested them to study their behaviour under maximum moment or maximum shear conditions. The column section was kept constant while different beam sections, end plate dimensions, friction grip bolt size and number varied. Five mild steel assemblies with four friction grip nominally tightened bolts, symmetrically placed around the tension flange with the compression bolts omitted, were subjected to maximum moment conditions. This resulted in no slip taking place. Similar results were obtained from three similar high yield steel connec-

tions. The interfacial pressure between the end plate and column flange within the compression zone was therefore adequate to resist the vertical shear force. This led Bailey[21] to suggest that HSFG bolts were not beneficial in these cases and that high tensile bolts were just as satisfactory. From his test results however, it would appear that reducing the bolt preload reduced the joint rigidity, therefore high tensile bolts would not be advantageous in these cases as they are not normally pre-loaded. Five other mild steel connections with the number of friction bolts and their preload varied, were subjected to maximum shear conditions. Slip occurred in only three specimens but not enough to induce bearing on the bolts. From these results he suggested a reduction of 50% in the minimum preload of the compression zone bolts and developed equations to determine the slip resistance force.

In several of the connections tested the end plate remained elastic throughout the loading range while plasticity occurred in the column flanges and connecting beams. In these cases thicker end plates were used than those calculated from Sherbourne's[11] equation. In one case a much thinner end plate was used than was calculated resulting in the end plate deforming plastically while only elastic deformation occurred in the beam. Slightly lesser thicknesses than those calculated resulted in all the components other than the bolts, reaching their plastic stress simultaneously.

In 1972, de Back and Zoetemeijer[22] adopted an analytical approach towards the design of tee stub connections and proposed failure to be one of three collapse mechanisms shown in Figure 1.3. Mechanism A had no prying force constituent and bolt failure was the governing criteria. The formation of a plastic hinge along the web line which coincided with bolt failure gave Mechanism B. Bolt failure would not be considered in Mechanism C as plastic hinges formed at both web and bolt lines. From these three mechanisms, equations representing the limiting conditions were developed. The results from these equations appeared to be acceptable with the experimental results from Struik[19] and four similar tests performed by de Back and Zoetemeijer[22], in which Mechanism A and B failures occurred.

De Back and Zoetemeijer[22] also suggested that the tension zone of an extended end plate, beam to column connection could be represented by a tee stub model. These were similar to the tee stub tests reported by other authors except a dummy column section was provided between the tee stubs. Seven of these models were examined with varying tee stub flange thickness and column section size. Although the tension strips were not in alignment the results from the tee stub flange equations compared favourably with experimental values. The flanges of the artificial column were not stiffened and deformed extensively. De Back and Zoetemeijer[22] suggested that the strength of the column flange could be

computed similar to that of a tee stub, on the understanding that an imaginary effective yielded length of column flange was taken. An empirical equation for the yielded length was given and when substituted into the derived equations gave results compatible with those obtained experimentally.

In 1972, Agerskov and Thomsen[23] published the results of an experimental investigation of fifteen prestressed butt plate joints in rolled beams. For each beam section used three or four tests were carried out with uniform bolt groups and constant bolt diameter but with the plate thickness varied in order to evaluate its effect on the strength and stiffness of each connection. The butt plate extended below the tension flange with a row of high strength bolts placed either side. Each joint was subjected to pure moment and they concluded that prying action must be taken into account in the design of the bolts and that the rotation capacity of such a connection was suitable for practical use in plastically designed structures. The investigation also revealed that the bolt prestress had a significant effect on the stiffness of the joint. A similar observation was made by Mann[17].

In 1974, in a second report supplementing his earlier work, Agerskov[24], examined the behaviour of four tee stub connections. The dimensions of the tee stubs were similar, while the number, diameter, and pretension of the bolts

varied. The main concern of this report was the relationship of prying force within the connections and the development of a method to determine its magnitude. From his own test observations Agerskov[24] rejected the assumption of the formation of a mechanism with plastic hinges at the bolt and web lines, as depicted by Mechanism C in Figure 1.3. In his theoretical approach towards determining prying forces he considered three possible ways failure could take place. Firstly, ultimate load was defined as the load when bolt separation occurred before the reduced yield moment of the end plate took place adjacent to the tension flange. Secondly, the ultimate load was reached when the reduced yield moment of the end plate occurred adjacent to the tension flange before bolt separation took place. Finally, no prying force existed when the reduced yield moment of the end plate was reached. He argued that these definitions of ultimate load would result in some strength reserve due to strain hardening, while heavy plastic deformations of the end plate would be avoided. He also suggested that when the load was increased past the ultimate, the moments at the bolt lines were almost unchanged while plastication took place in the region of the beam tension flange, with the additional load carried through strain hardening. The test and theoretical results proved to be quite compatible for his interpretation of ultimate load. The developed equations were somewhat lengthy for practical design purposes and a digital computer programme was given as an aid to shorten design time.

In 1975, Agerskov[25] investigated different variables in a computer analysis of 2750 beam to column connections using some German standard end plate details. From the results obtained, combinations of various parameters were studied in order to establish diagrams for the purpose of yielding prying force ratios, as a direct function of certain combinations of the independent variables. These diagrams were condensed into one design chart enabling less design time than the original equations required. On comparison with a similar graph given in the AISC Manual[26] there was considerable deviation between the two curves, probably due to the different interpretations of ultimate load. Agerskov[25] suggested that his method could be employed in designing beam to stiffened column moment connections using cantilevering end plates, although the majority of his experimental results were obtained from beam butt plate joints. Agerskov's three reports[23, 24, 25] were summarized in two papers published in America[27, 28].

From existing tee stub test data, Kato and McGuire[29] attempted to present a better understanding of the behaviour of tee stub flange to column connections. They considered four possible modes of failure, based on high strength bolts being used and tightened to their yield loads. Each case is now summarized.

a) Separation did not occur before the ultimate strength of the tee flange was reached.

This referred to very flexible flanges with respect to the bolts. The yield strength of the tee flange was defined as the load that would cause a collapse mechanism to form, similar to Mechanism C in Figure 1.3. Ultimate load was taken as the product of the yield load and the ultimate to yield flange plate stress ratio.

b) Separation occurred in the range from yield strength to ultimate strength state of the tee flange.

The yield load was identical to case (a), while ultimate strength of the system was the load at which the bolts reached their ultimate stress.

c) Separation occurred in the range from elastic limit to yield strength of the tee flange.

Moments at the web and bolt lines were considered equal at the elastic limit state. Yield strength and ultimate strength of the connection were stated to be governed by the yield load and ultimate load of the bolts respectively.

d) Separation occurred before the tee flange reached its elastic limit.

This referred to a rigid flange plate with respect to the bolts, similar to Mechanism A in Figure 1.3. Yield load occurred when separation took place, while the summation

of the ultimate bolt forces governed ultimate load.

Equations were developed for each case and from these a plastic design method was suggested for tee stub flange to column connections which made the joints 30% stronger than the connecting members.

The test programme carried out by Nair et al[30] was initiated by the test results obtained by Munse et al[7]. The experimental work of Nair et al[30] included static and fatigue tests on tee stubs with a row of high strength bolts placed either side of the tensile strip. The tee stubs had constant flange thickness, length and bolt diameter while the remaining geometric parameters varied. Prying force was measured from the comparison of results from sixteen tee connections and four similar dimensioned single bolt tests. Test results revealed the ultimate prying ratio to vary between 2% and 50%, and was highest when large bolt spacings were used. A finite element method was adopted to analyse the tee stub and an analytical model was defined. The yield strength of the steel was assigned a value of 38 ksi (260 N/mm^2), while the minimum permissible bolt pretension was considered to be initially present. Connection failure was taken as bolt failure, or when plastic hinges formed at both web and bolt lines, similar to Mechanism C in Figure 1.3. For simplicity, semi-empirical equations were suggested for the determination of prying force at ultimate load, for A325 and A490

high tensile strength bolts. These equations were only applicable to the specific combination of bolt and plate material for which they were developed.

Before 1974, several investigators concentrated mainly on the behaviour of tee stubs in tee section moment connections, or its equivalent in an extended end plate, beam to column moment connection. The column flange was considered strong and stiff enough to be of secondary importance, which was usually ensured by placing stiffeners within the column, opposite the beam tension flange. De Back and Zoetemeijer[22] suggested that the column flange could be designed in the same way as a tee stub, using an effective length of flange that they defined empirically. In 1974, Zoetemeijer[31] analysed this concept further by performing several more tests and examining previous test results[22].

He reported the results of four tee stubs and twenty four tee stub models, five of which had stiffening plates parallel to the column flanges. From the flange deformation patterns, Zoetemeijer[31] suggested two flange collapse mechanisms. He termed these Mechanism I, in which bolt fracture was the determining factor and Mechanism II, in which collapse of the column flange was the determining factor. Design equations were established for each mechanism from yield line theory and optimisation of the straight yield line patterns. The solution was applicable to both unstiffened and parallel stiffened column flanges

and was similar to the equations developed by de Back and Zoetemeijer[22], but with an analytically derived effective length. The results from the equations were quite favourable with the corresponding test observations, but were based on the limitations imposed by the strength of the materials of the connections. In order to establish if adequate rotation capacity occurred in a connection designed by the derived equations, twenty three bolted beam to column connections were tested. The connections were designed to fail by Mechanism II, failure by Mechanism I was not considered. Different types of moment joints were examined among them tee sections (with and without web cleats), together with extended and flush end plates. Preload was a varying factor, along with parallel stiffening plates, column section type and bolt diameter. From the experimental observations the flange collapse mechanism was acceptable up to a beam span of thirty times the beam depth.

As the previous beam to column tests consisted of oversize tee stubs and end plates, four additional tests were performed in an effort to provide realistic impressions of the rotations that would occur. The tests consisted of full scale frameworks incorporating four joints designed in accordance with the proposed equations, although the governing mechanisms were not stated. Each frame had a different connection system for each test, i.e. extended end plate, flush end plate tee section and flange plus web cleat joints. The results revealed that the joints

had sufficient strength, stiffness and rotation capacity. The proposed equations were developed from tee stub model tests and were applicable to extended end plate joints, but Zoetemeijer[31] applied them to other joint arrangements with apparently successful results.

Packer[32] also simulated conditions around the tension flange of a beam to column connection with tee stub model tests which included transverse stiffeners in a few specimens. A series of eight models were tested varying column flange thickness, bolt preload, bolt spacing and type of stiffener. Full depth stiffeners were used in two tests, one fully welded around the flange and web, while the web weld was neglected in the other. It was reported that the omission of the web weld did not alter the yield load of these two models, which were more efficient than the single test incorporating triangular stiffeners. From the results of the unstiffened tests, Packer[32] produced seven yield line flange collapse patterns consisting of straight and curved boundaries. An equation was developed for each pattern which predicted the collapse yield load of the unstiffened column flange. An equation, hence pattern was then selected that best represented the results of the models tested. The procedure was repeated for the tests that included stiffeners. Two flange collapse patterns were considered. He also suggested a second collapse mechanism for unstiffened column flanges, in which the bolts were the determining factor, similar to Zoetemeijer[31],

but no test results were available to confirm the results from the corresponding equation. He suggested that the design of tee stubs be governed by the equations established by Zoetemeijer[31], which were formed from the three collapse Mechanisms A, B and C shown in Figure 1.3.

Packer[32] also tested five beam to column joints, to determine if the developed equations from the tee stub models were applicable to extended end plate connections. Three specimens were unstiffened around the tension zone while the column flange thickness varied. The column flanges of one connection were transversely stiffened with full depth stiffeners in the tension zone while the remaining test represented a balanced beam to column joint in a multi-storey building. A constant vertical load of 150 kN (50 N/mm^2) was applied to the column to study its effect on the yield load of the column flange within the connection. The yield load was in fact smaller than that of a similar test specimen whose column was unloaded. End plate thickness and bolt size were constant throughout the test programme.

From these results Packer and Morris[33] gave design recommendations for stiffened and unstiffened column flanges. They also recommended that the bolt design be governed by the equation given by Surtees and Mann[18] who assumed a prying force ratio of 33%. Extended end plate design equations were also given considering the end plate as a tee stub flange and failure mode as Mechanims C, as shown

in Figure 1.3. This equation was the same as that suggested by Schutz[8]. A Mechanism C failure did occur in two of the beam to column test specimens although one experimental result was slightly incompatible with that predicted and was on the non-conservative side. They concluded that a joint designed by their recommended procedure would have yielded when the moment capacity of the connection reached the required M_p' value, but would have only limited distortions which would not inhibit joint strength or rotation capacity. This method was intended to produce a plastic hinge within the parent beam. The test results reflected the design method in so far as the yield moment was obtained by the commencement of non linear behaviour in the moment rotation curves.

Packer and Morris[34] considered their design method as a lower bound solution, limiting end plate and column flange deformation and minimizing the detrimental effect that column flange distortions might have on the structural performance of the column member as a strut. The method suggested by Surtees and Mann[18] for end plate design was considered by Packer and Morris[34] to be an upper bound solution for limiting the strength of a joint. This method produced what Packer and Morris[34] termed quasi-hinge formation, which was the occurrence of plastic deformation within a connection capable of producing sufficient rotation capacity. This in simple terms was the

formation of a plastic hinge within the connection, with the deformation of the column flange and end plate not having the limiting influence on the design of a balanced moment joint.

In 1979, Mann and Morris[35] recommended a design procedure for extended end plate, beam to column connections. The design guide was mainly a combination of the equations suggested by Surtees and Mann[18] and Packer and Morris[33]. The equation given for the design of the end plate was similar to that suggested by Packer and Morris[33] except the bolt holes were ignored. Little attention was given to shearing forces and the possibility of slip occurring.

Krishnamurthy[36] was more realistic in this analytical approach towards extended end plate moment connections, by including empirical moment and material coefficients. These were for the stiffening effect of the beam web on the end plate and the various common combination of materials and bolts that could be obtained. These coefficients were applicable to the now traditional method of considering the portion of end plate symmetrical around the tension flange as an equivalent tee section. His research apparently covered thirty eight end plate and hanger connections although very little information was given about them. He did however state that six end plate specimens designed in accordance with his proposed elastic theory showed no signs of distress when the ultimate capacities

of the connected beams were reached. Emphasis was on the explanation of his theoretical investigation which included two and three dimensional finite element analysis. An elastic design procedure for the end plate was the final outcome. Krishnamurthy[37] compared his design procedure to both the allowable stress method given in the AISC Manual[26] and proposed method by Agerskov[28]. Krishnamurthy[37] agreed with Agerskov[28] that the AISC Manual[26] method, based on the work by Nair et al[30] was very conservative. He also showed that the method recommended by Agerskov[28] was also on the safe side.

In 1979, Krishnamurthy et al[38] attempted to determine the rotation of an end plate moment connection, from a computer analysis and resulting empirical equations. Fifteen beam butt plate splice tests were performed to check the validity of the analysis, but no details of the test specimens or results were given. They emphasized that the analysis applied only to symmetrical end plate connections or to beam to column end plate connections with very thick or stiffened flanges.

In 1980, Grundy et al[39] reported the results of two cruciform extended end plate, beam to column connections. Each specimen had eight high strength bolts symmetrically placed around the tension flange, with two high strength bolts placed close to the compression flange. A working stress design guide was given which included a constant prying force of

20% applied tension for the design of the bolts.

In 1981, an International Conference on Joints in Structural Steelwork was held at Teeside Polytechnic, Middlesbrough. Some of the papers presented at this Conference are now reviewed.

Morris and Newsome[40] investigated the effects of the out of balance moment on the column web panel of portal frame eaves connections. Four tests were carried out with different stiffening arrangements. The results of these tests indicated that a new form of stiffening termed the Morris stiffener was the most effective and economic stiffening arrangement for this type of joint.

Mann and Morris[41] reported the results of six flush end plate, beam to column connections which were tested to study the effect of lack of fit on the overall behaviour of these joints. These tests were divided into two groups, one set with 12 mm thick end plates and the other with 20 mm thick end plates. Within each group there was three different specimens, one with perfect fit, one with imperfect fit while the third was fitted with shims between the end plate and column flange faces. The concluded that small lacks of fit, approximately 1 mm, had no effect on the ultimate strength or stiffness of flush end plate connections. However, initial lack of fit was found to have an effect on the preload achieved in HSFG bolts produced by recognised tightening methods.

Bouwman[42] examined the behaviour of bolted tee stub joints subjected to dynamic tensile load. The location of the contact forces were established by placing loose shims between the faces of the flange plates. The position of the shims had a significant effect on the load resisted by the bolts. Therefore in connections subjected to fatigue loading the preload of the bolts are not only important but also the position of the contact forces.

Tarpy and Cardinal[43] presented an analytical study of extended end plate, beam to column connections. The finite element method was used based on a linear elastic model and equations predicting the behaviour of these joints were developed. The results from these equations appeared favourable when compared with a few experimental results.

1.3 British, American and European Design Practice

In the UK steel buildings were usually designed to elastic principles to BS449[4] supplemented by the Steel Designers Manual[44] in which there was a chapter devoted to plastic theory and design. Practical plastic design was covered more comprehensively by Morris and Randall[45] for Constrado who gave design examples of typical frameworks. Connection design was not included. The DOE in their CHRAC Report[46] gave a guide for the plastic design of extended end plate, beam to column connections, based on the work by Surtees

and Mann[18]. The guide ensured that plastic zones within the column flanges did not exist, by providing empirical equations for the limiting stiffened and unstiffened flange thickness. Plastic hinge formation, either within the connection or parent beam was acceptable. The introduction of limit state design to structural steelwork was implemented in draft form[5] in 1977 and like BS449[4] was intended purely as a specification for structural steelwork and not as a design guide. The draft form[5] is at present under review towards a final version, which should be published in 1981. In 1980, CIRIA[47] produced a working stress design guide for friction grip bolted connections, which gave amongst other proposals, recommendations towards the design of tee section hanger connections, flush and extended end plate moment connections. Although prying action has been known to exist for a number of years it has never been incorporated in British design practice to BS449[4] or included in the Steel Designers Manual[44]. The CIRIA Report[47] remedied this by giving an empirical equation to determine prying force in tee section connections and extended end plate joints. The region around the tension flange of the extended end plate connection was considered as an equivalent tee stub.

In American, steel buildings have been designed in accordance with the AISC Manual[26] since 1970, either to allowable stress or plastic design specifications. Since 1971, the ASCE Manual No. 41[48] has been used in conjunction

with the AISC Manual[26] for the plastic analysis and design of steel structures. Each manual recommended a different approach to the design of extended end plate bolted connections. In the AISC Manual[26], prying force was determined from the equations developed by Nair et al[30], while in the ASCE Manual[48] prying force was established by a simplified version of an equation developed by Douty and McGuire[12]. The ASCE Manual[48] also suggested a minimum tee stub flange thickness and extended end plate thickness, determined from an equation similar to that given by Schutz[8]. Both manuals recommended the equations developed by Graham et al[49] for the design of the column web, column flange and stiffeners of a beam to column connection.

In 1978, the European Convention for Constructional Steelwork[50] published its recommendations for the design of steel structures to limit state philosophy. A method similar to that suggested by Zoetemeijer[31] was given for the extended end plate thickness of a beam to column connection. The column flange suitability within the tension zone of this type of connection was checked by a method similar to that suggested by Fisher and Struik[30]. A method to determine the slip resistance force of extended end plate connections was also suggested. Little guidance was given concerning the strength of the column web panel.

1.4 Conclusions

From the survey it was concluded that further work was required to determine the magnitude of prying forces at bolt failure for tee stubs and beam to column connections. Further work was also required to limit rotation in beam to column connections. There was some work on tee stubs but there was a shortage of experimental results on beam to column connections where slip into bearing took place and also where bolt failure occurred. In many cases there was insufficient data on yield strengths. The experimental work in this research project therefore reports beam to column tests and associated tee stub tests together with material properties.

CHAPTER TWO

BOLT CALIBRATION AND TIGHTENING CONTROL

2.1 Introduction

The main experimental programme of joints, reported in Chapter Four, required the accurate measurement of axial force in the bolts during tightening and testing. One method of measurement is the use of electrical resistance strain gauges attached to the bolts, this is not only expensive but also time consuming. In order to economize tensile forces in the bolts were determined from their extension, by means of a calibration curve. Individual fasteners were tested in direct and torque tension. The effects of torque control and load indicating tightening methods on the axial forces in the bolts were also studied.

In practice HSFG bolts are tightened to a specified minimum shank tension[26, 51, 52, 53], to enable shear load to be transmitted by means of friction between the clamped surfaces. Greater shearing forces can therefore be allowed with larger bolt preloads, while the stiffness of a moment connection is also increased[17, 23]. The need for suitable and simple tightening control methods can readily be appreciated, especially after the recent incident in America where a sports stadium collapsed due to insufficient tightening of some high strength bolts. This resulted in fatigue failure of the bolts due to the dynamic wind

loading conditions[54]. Research in the fifties and sixties produced torque control and turn of nut tightening methods, or a combination of the two[55, 56, 57, 58, 59, 60, 61]. In the sixties, load indicating washers and load indicating bolts were introduced into structural practice, with apparently better control over bolt preload than previous methods[58, 60, 62]. In recent years torque control and part turn methods have given way to direct tension indication by load indicating washers, which have proved more popular than load indicating bolts due to their versatility[63,64]

2.2 Experimental Work

Several M16 and M20 general grade HSFG bolts to BS4395 Part I[52] were tested in direct and torque tension with mild steel connecting plates. M16 bolts were selected at random from a batch of 500 bolts supplied for the beam to column connection tests. All bolts were 70 mm long.

2.2.1 Direct Tension Tests

Six M16 and five M20 bolts had FLA-3-11 3mm strain gauges attached equidistant around the unthreaded portion of each bolt. Initially three strain gauges were used on the M16 bolts. When two strain gauges were attached to a few M16 bolts there appeared to be no difference between the behaviour of these bolts and bolts with three strain gauges

attached. Therefore two strain gauges were used on the remaining bolt shanks throughout the test series. The connecting wires were taken through 3mm diameter holes drilled in the bolt head and connected to the extension box of a Peekel. Each bolt was placed in the testing rig shown in Plate 2.1. Details of the test rig are shown in Figures 2.1 and 2.2 for M16 and M20 bolts respectively. Dimensions of test specimens are given in Tables A2.1 and A2.2. The base plate of each rig half was 20mm thick and had a 24mm diameter hole, through which the bolts were centrally placed. The hole diameter was larger than that recommended by BS449[4] for a 20mm diameter bolt, so that strain gauges attached to the bolt were not damaged during testing. A 24mm diameter hardened steel washer was placed under the head of an M20 bolt to enable free passage of the strain gauge wires. A 20mm diameter hardened steel washer was placed beneath the nut. Hardened steel sleeves were used to decrease the rig hole diameter and a 20mm diameter hardened steel washer placed under the bolt head for four M16 bolts. Some difficulty was experienced in providing enough clearance for the strain gauges when the sleeves were used. Therefore, for the final two M16 bolts 16mm and 20mm diameter hardened steel washers only were used under the bolt head and nut respectively. The extension of each bolt was taken at regular load intervals from an extensometer placed on demec spots attached to the bolt head and toe with epoxy resin. An initial torque of 14Nm

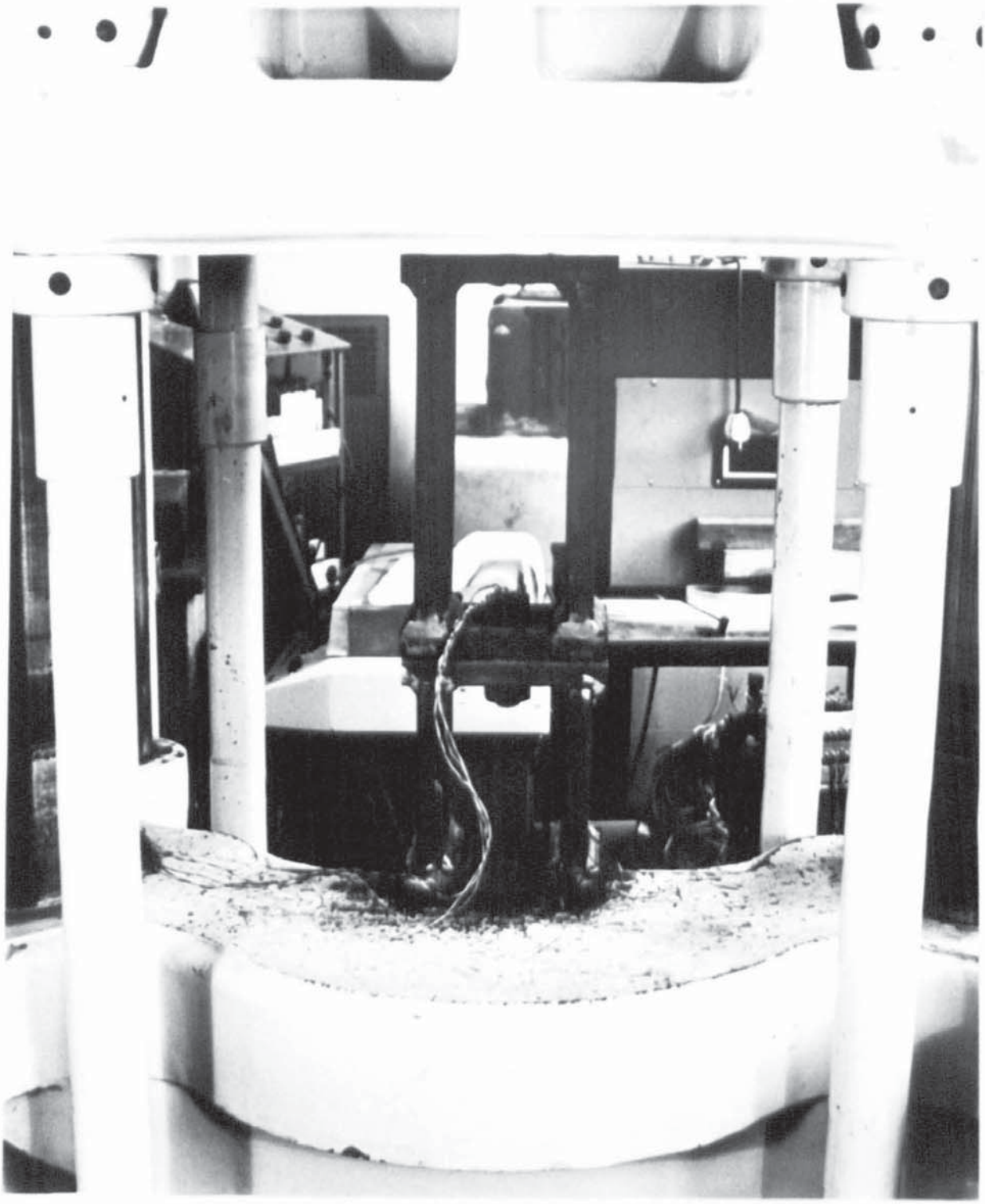

PLATE 2.1 TYPICAL DIRECT TENSION TEST

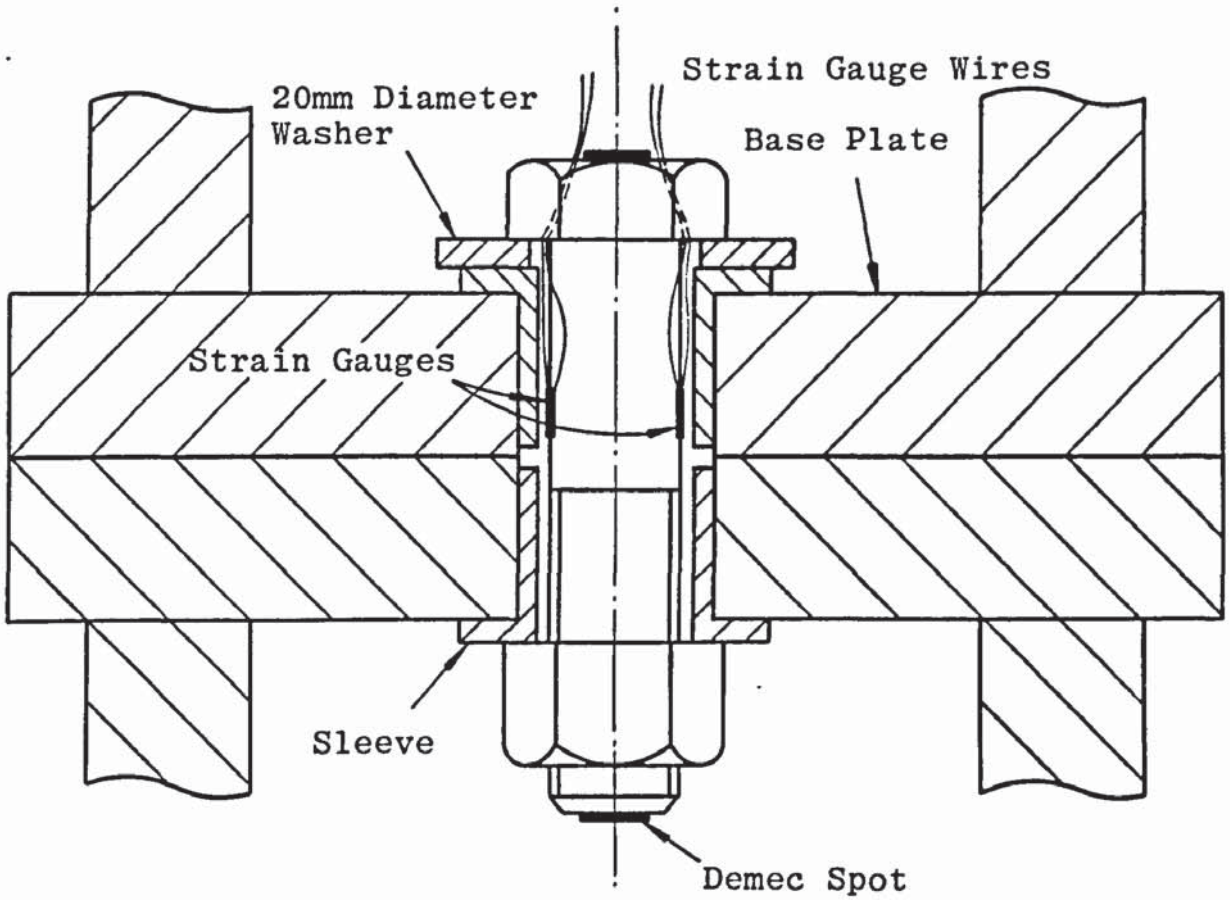

FIGURE 2.1 TYPICAL DIRECT TENSION TEST M16 BOLT

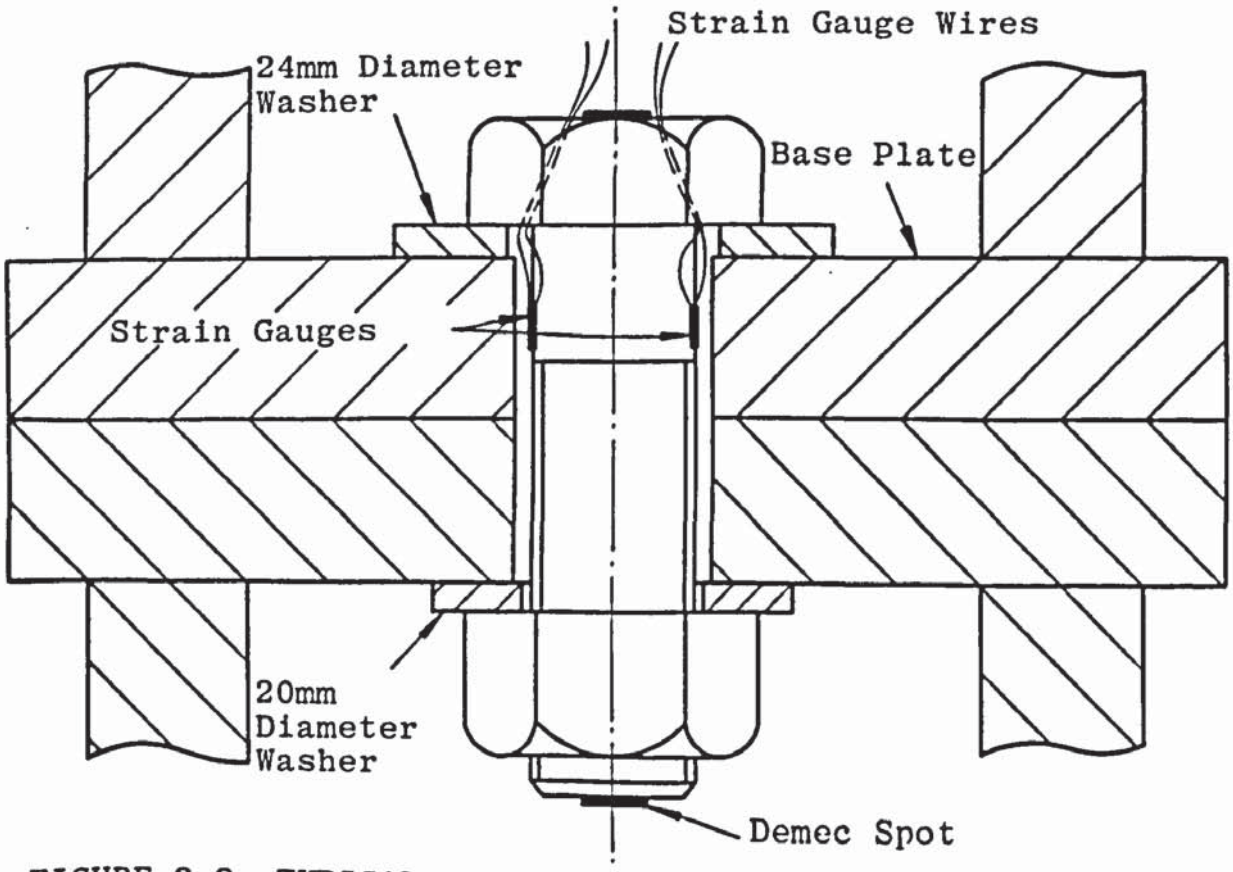

FIGURE 2.2 TYPICAL DIRECT TENSION TEST M20 BOLT

was applied to each bolt to achieve a snug fit before loading. The extensometer was graduated in increments of 0.002mm.

The relationship between applied load and extension for a typical M16 and M20 bolt is shown in Figure 2.3 and for all tests in Figure A2.1. Extension readings at 90 kN and 155 kN for M16 and M20 bolts respectively are given in Table A2.3. These shank tensions were selected as they were within the linear elastic range of each type of bolt. The maximum coefficient of variation of extension within the elastic range is approximately 5% for both M16 and M20 bolts. Experimental data for typical direct tension bolt tests 16.DT.2 and 20.DT.2 are given in Appendix A-2. A typical stress strain relationship for each type of bolt based on the full area of the bolt, A_s, and the mean strain gauge readings are shown in Figure A2.2. The E_b values obtained from these stress strain relationships are given in Table A2.3. The presence of the bolt head was considered to have an influence on the shank strain near to the bolt head when a tensile force was applied to the bolt. Due to the small unthreaded length of the M20 bolts strain gauges were positioned near to the head of the bolt which would account for the comparatively high E_b values obtained. To obtain a more realistic E_b value, bolts from each batch were machined to a reduced diameter and with two 3mm strain gauges placed diametrically opposite tested in direct tension. A typical detail is given in Figure 2.4. E_b values

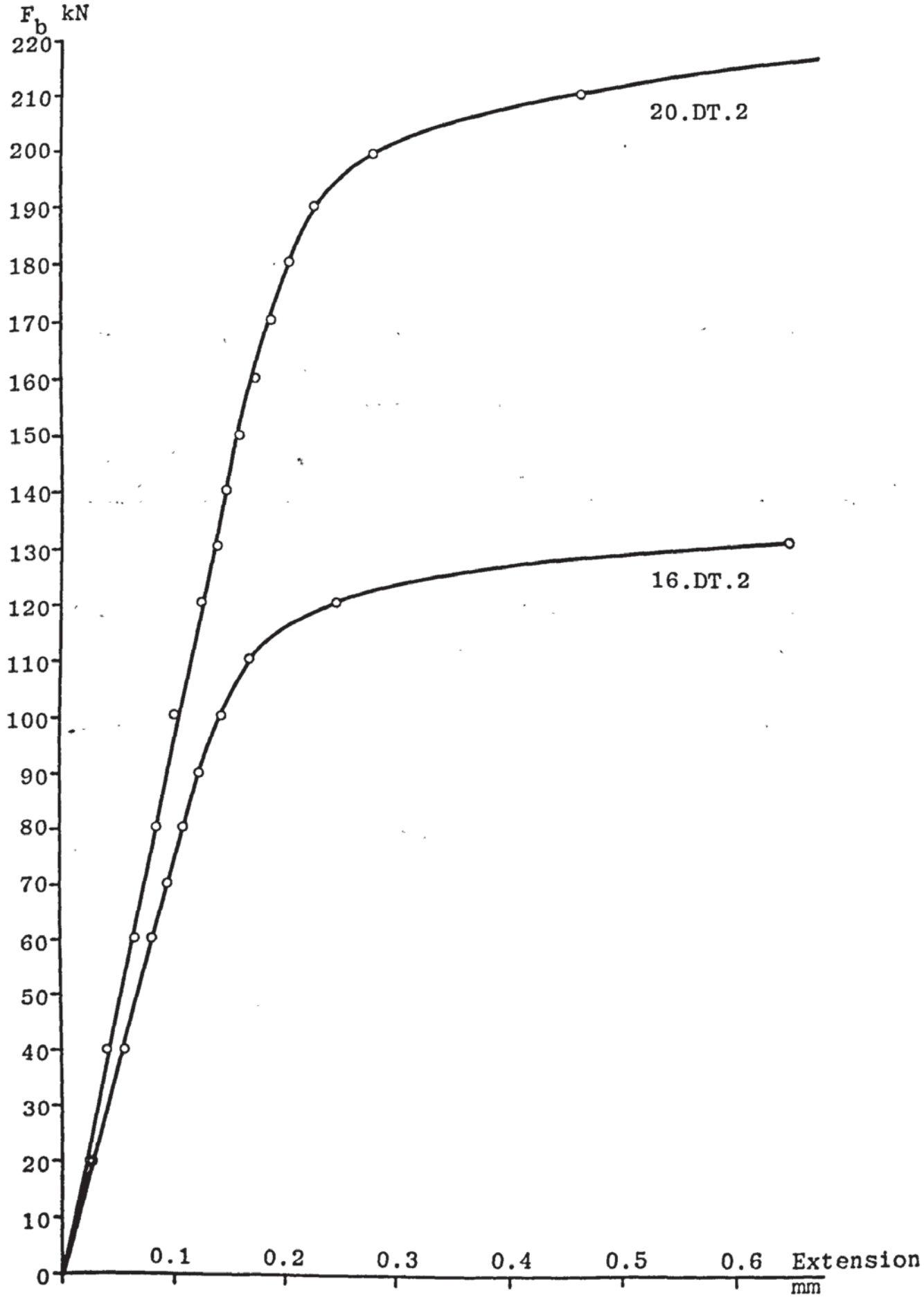

FIGURE 2.3 RELATIONSHIP BETWEEN TENSILE BOLT FORCE AND EXTENSION FOR A TYPICAL DIRECT TENSION M16 AND M20 BOLT

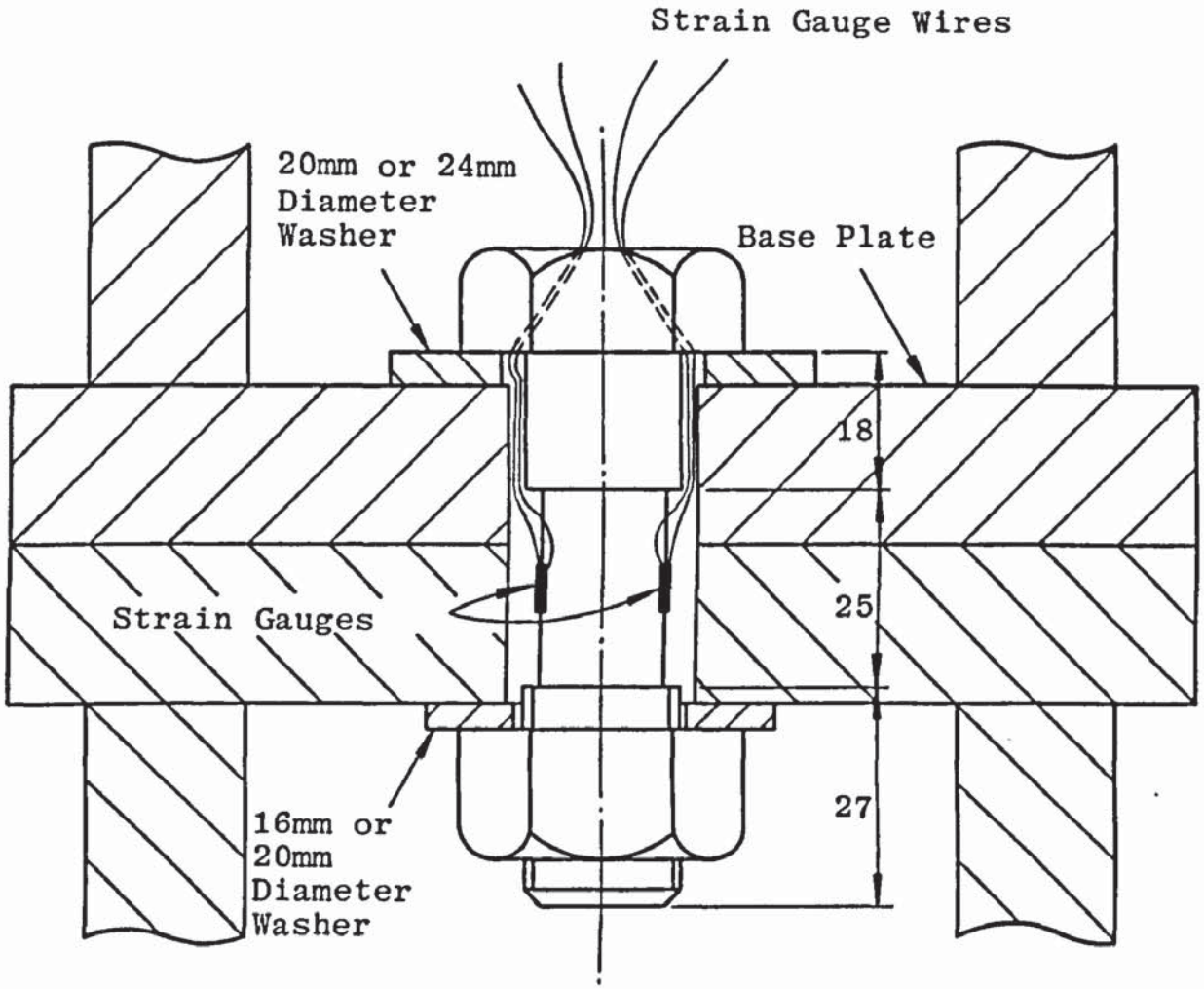

FIGURE 2.4 TYPICAL REDUCED DIAMETER DIRECT TENSION TEST

for the reduced M16 and M20 bolts are given in Table A2.4. Stress strain relationships for R16.DT.1 and R20.DT.3 are shown in Figure 2.5. The experimental data obtained from these two tests are given in Appendix A-2. The ultimate strength from direct tension tests of several M16 and M20 bolts selected at random from each batch are given in Table A2.5.

2.2.2 Torque Tension Tests

Six M16 and nineteen M20 bolts from the same batch as the direct tension tests and prepared similarly, were tested in torque tension, see Plate 2.2 and Figure 2.6. Varying thicknesses of connecting plates were used and in all but two M20 bolts, 'coronet' load indicating washers (LIW) were placed under the nut in conjunction with hardened nut face washers. In tests 20.TT.12 and 20.TT.13 LIW's were placed under a 24mm diameter washer, which in each case was situated below the bolt head. This washer was used in these tests so that enough clearance was provided for the strain gauge wires at the bolt head. The washers did not bear fully on the protrusions of the LIW's, therefore the gap and load relationship for these tests are not shown. The LIW's were used in these tests to compare the effects of bolt head and nut seating arrangements on the behaviour of the bolts. The flange of a 356 x 171 x 67UB had 24mm diameter holes drilled at 100mm centres along its

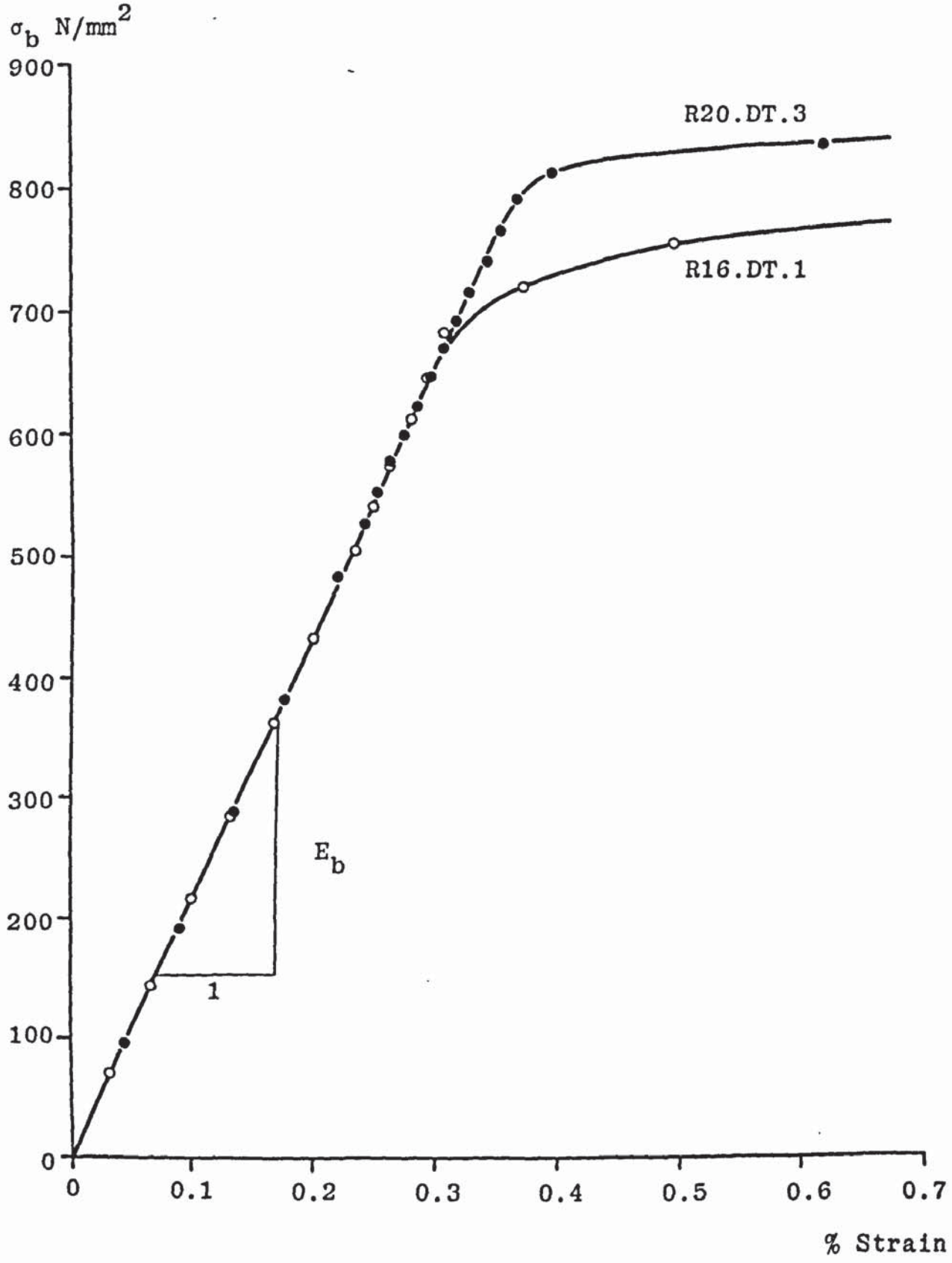

FIGURE 2.5 RELATIONSHIP BETWEEN STRESS AND STRAIN FOR A TYPICAL REDUCED M16 AND M20 BOLT

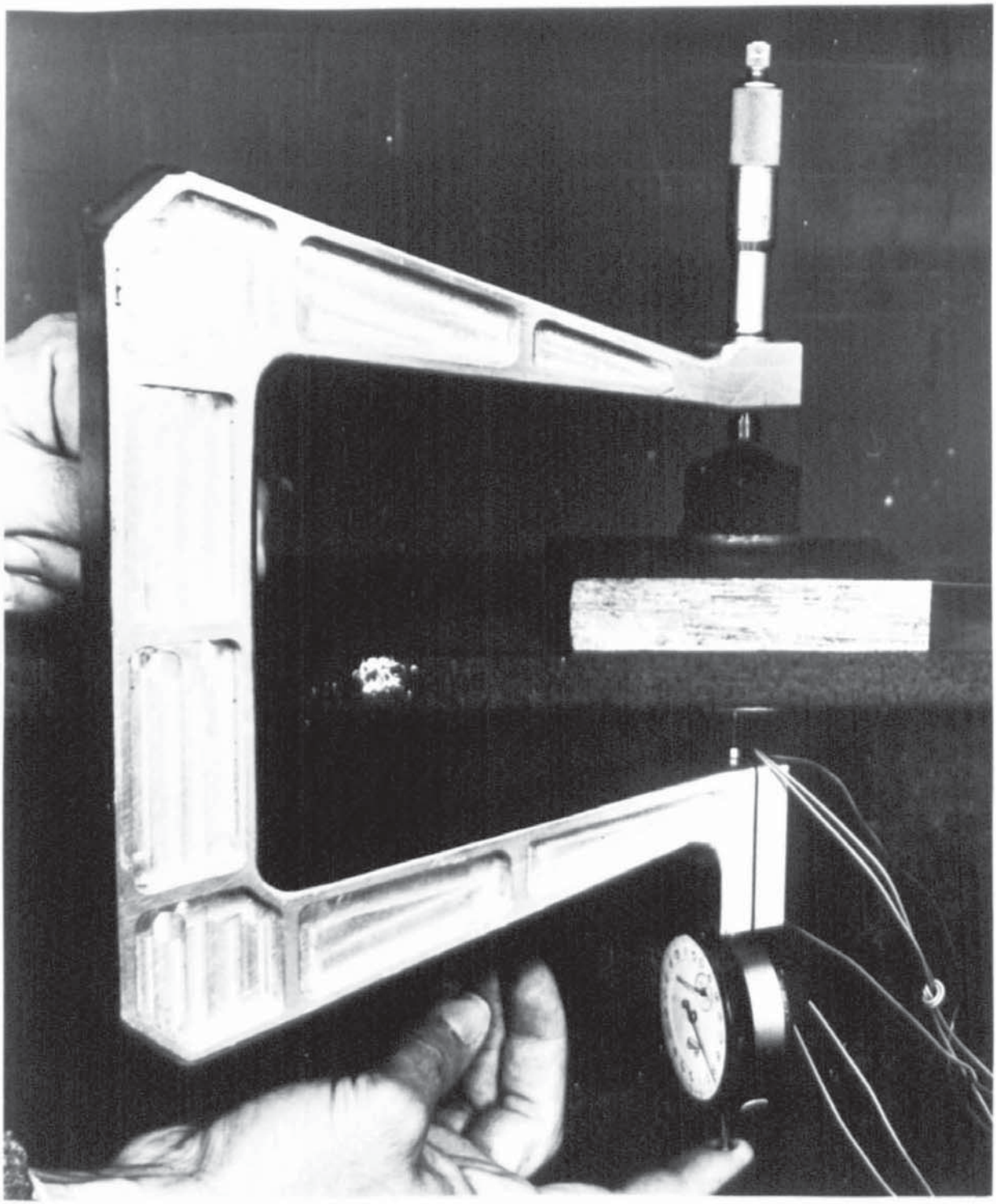

PLATE 2.2 TYPICAL TORQUE TENSION TEST

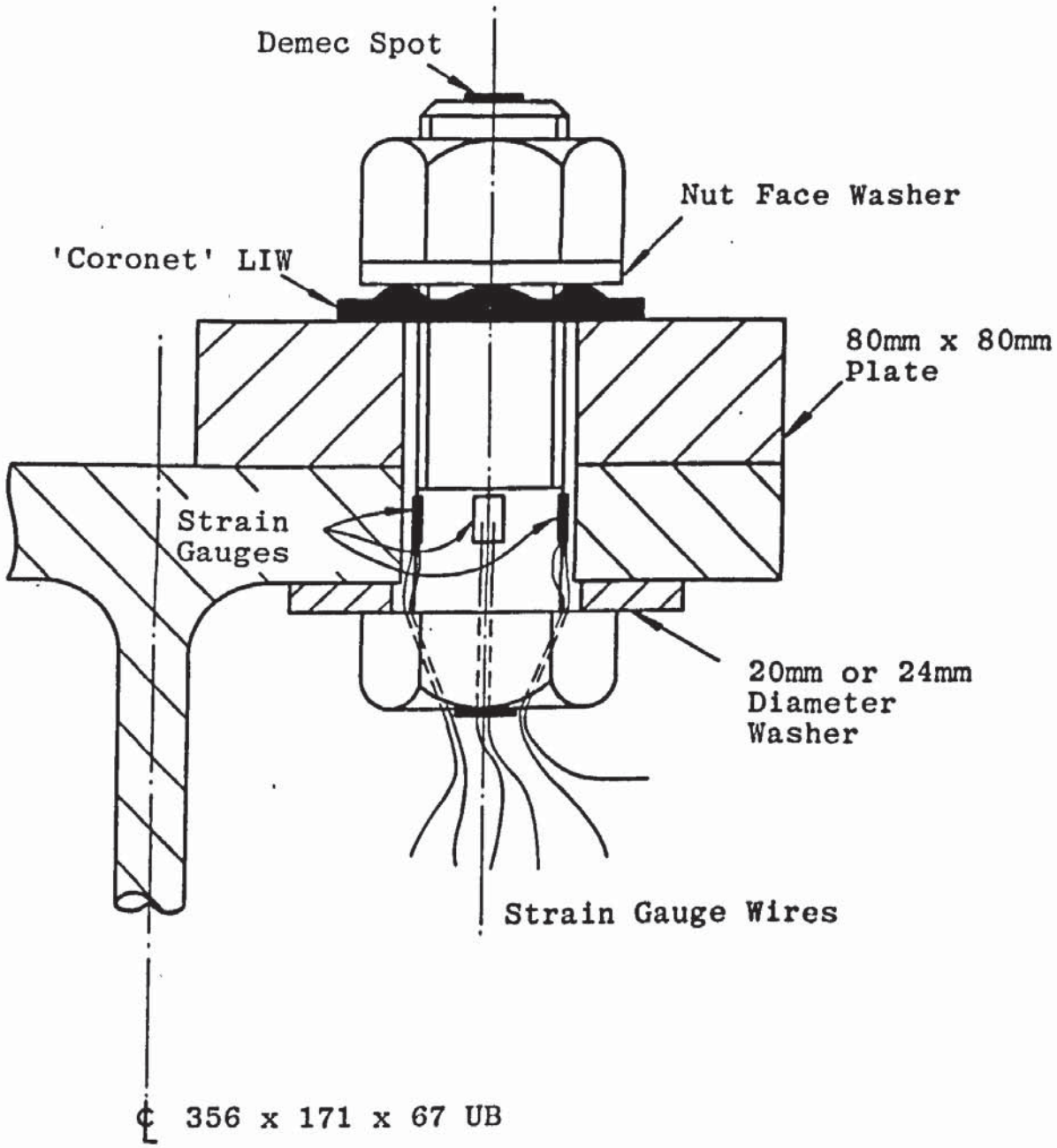

FIGURE 2.6 TYPICAL TORQUE TENSION TEST

length and 90mm centres across its width. Each torque tension test was performed at a different position and 80mm x 80mm mild steel plates were used to vary the grip length. 20mm and 24mm diameter holes were drilled in these plates for M16 and M20 bolts respectively. Mean dimensions and details of each test are given in Tables A2.6 and A2.7 for M16 and M20 bolts respectively. Test series 1 and 2 refer to different grip lengths. At regular increments of applied torque, bolt extension, strain gauge reading and LIW gap were measured using extensometer, Peekel and feeler gauges respectively. The relationship between axial bolt force from mean strain gauge readings and extension, torque and mean LIW gap, for a typical M16 bolt is shown in Figure 2.7 and for six tests in Figure A2.3. A similar relationship for a typical M20 bolt from series 1 and 2, is shown in Figures 2.8 and 2.9 respectively. The relationship between bolt force and extension, torque and LIW gap for the M20 bolt series 1 is shown in Figures A2.4, A2.5 and A2.6. There is little difference between the behaviour of bolts subject to different seating arrangements. A similar relationship for the M20 bolts series 2 is shown in Figure A2.7. The experimental data obtained from typical torque tension tests 16.TT.1, 20.TT.10 and 20.TT.16 is given in Appendix A-2.

BS4604 Part 1[53] recommends that general grade HSFG bolts in structural steelwork be tightened to a minimum shank

FIGURE 2.7 RELATIONSHIP BETWEEN TENSILE BOLT FORCE AND EXTENSION, TORQUE AND AVERAGE LIW GAP FOR A TYPICAL TORQUE TENSION M16 BOLT

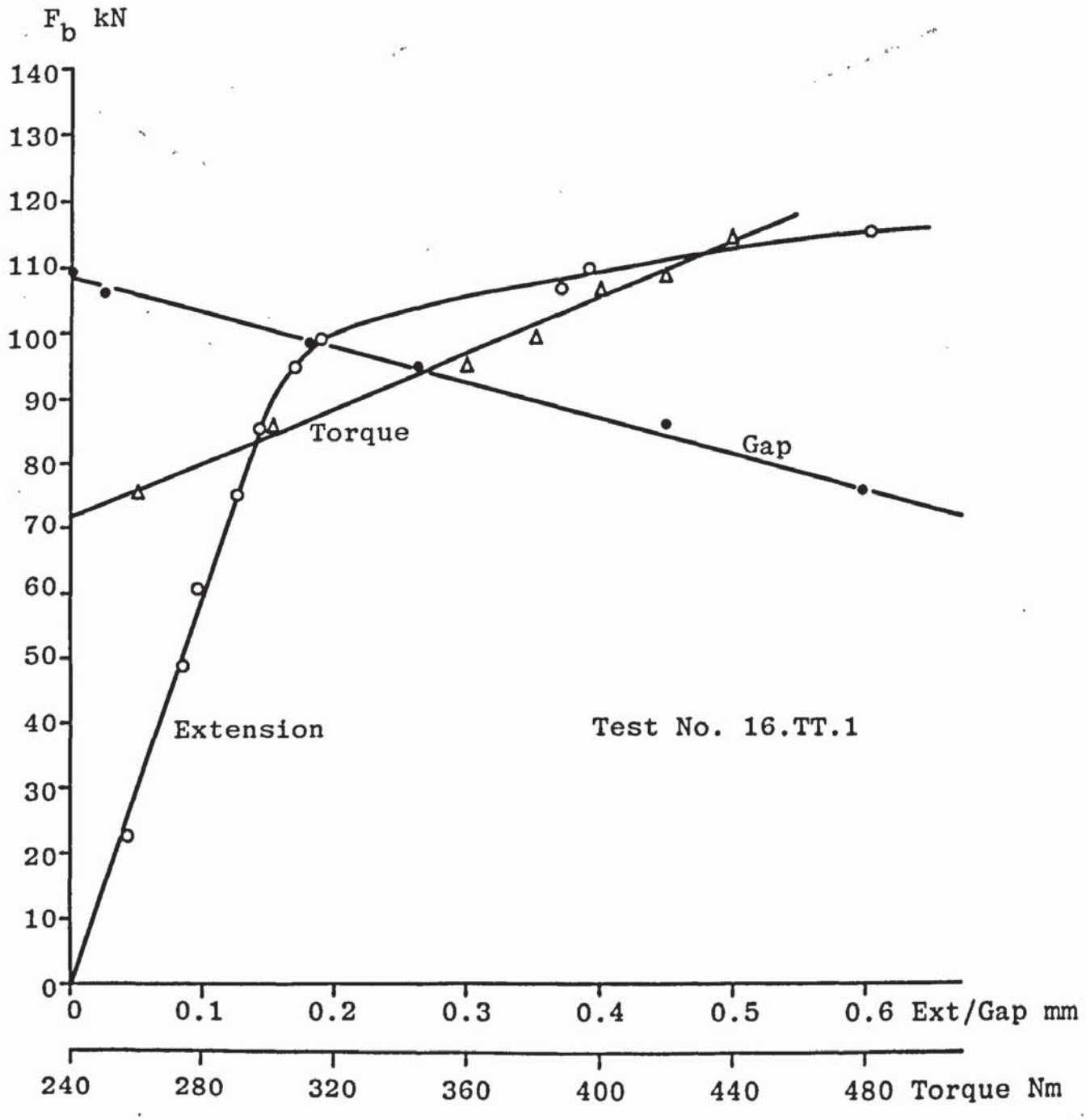

FIGURE 2.8 RELATIONSHIP BETWEEN TENSILE BOLT FORCE AND EXTENSION, TORQUE AND AVERAGE LIW GAP FOR A TYPICAL TORQUE TENSION M20 BOLT SERIES 1

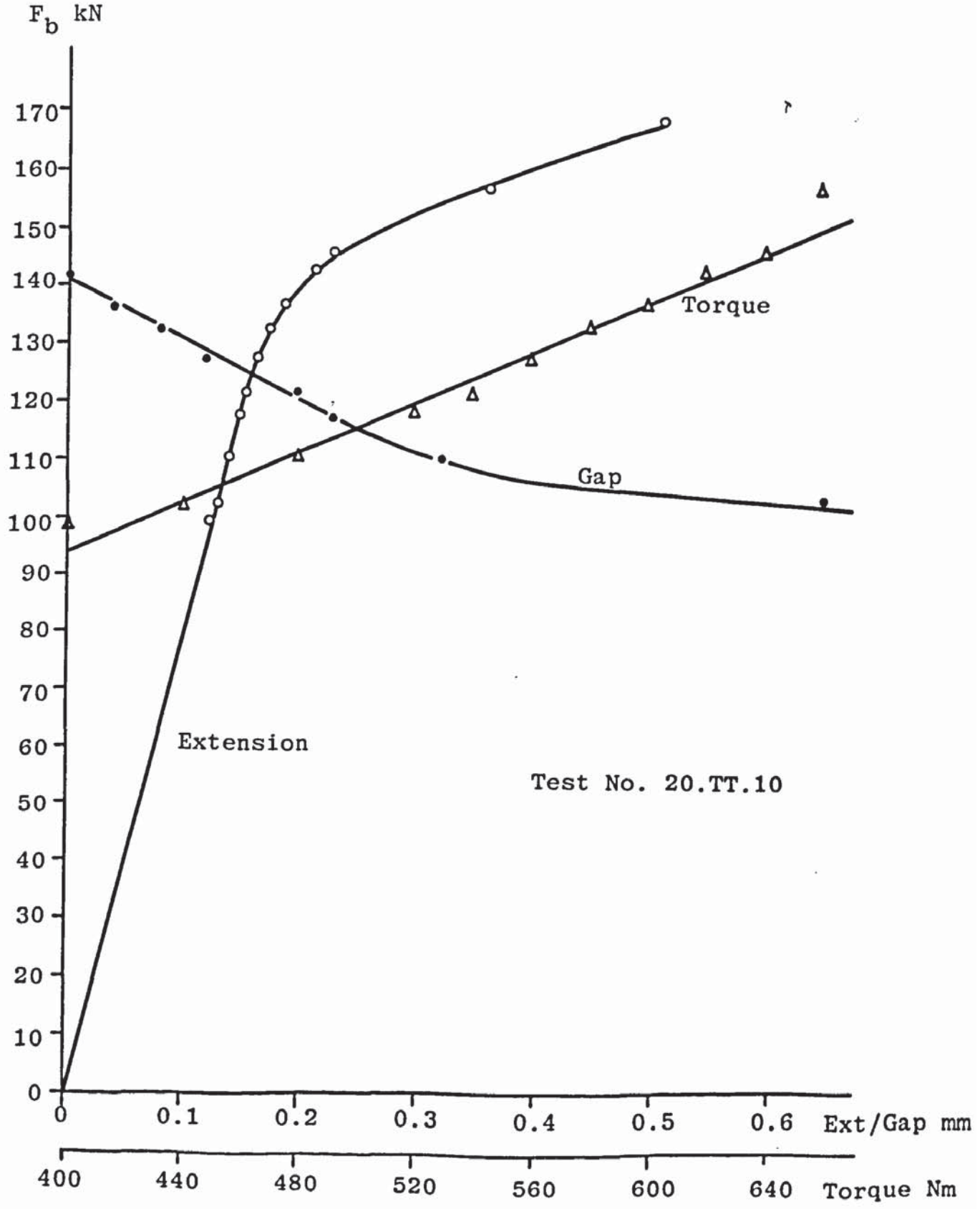

FIGURE 2.9 RELATIONSHIP BETWEEN TENSILE BOLT FORCE AND EXTENSION, TORQUE AND AVERAGE LIW GAP FOR A TYPICAL TORQUE TENSION M20 BOLT SERIES 2

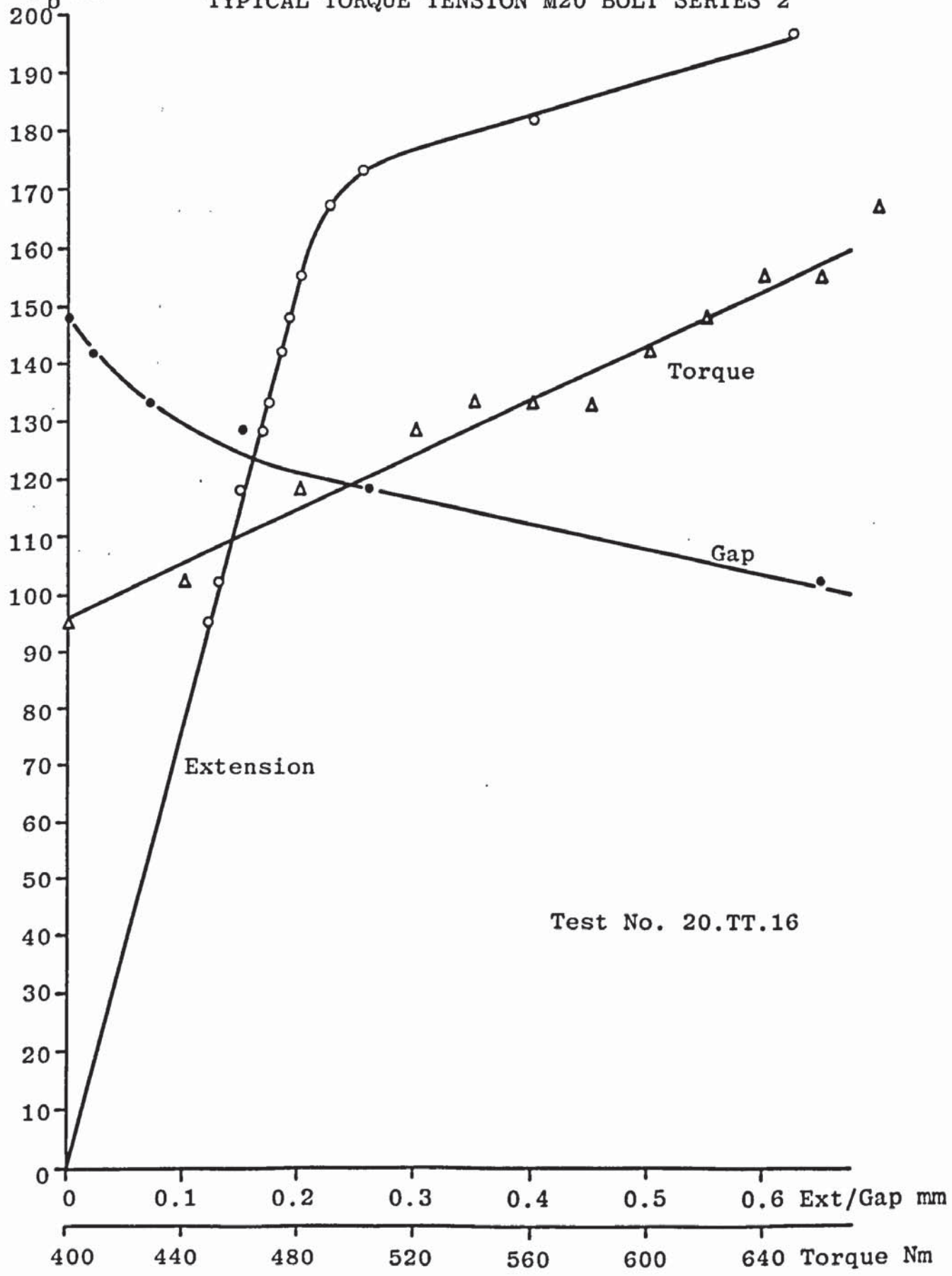

tension. For M16 and M20 bolts these preloads are 92 kN and 144 kN respectively. The appropriate values of extension, torque and average measured gap at the specified tension for each torque tension test are given in Tables 2.1, 2.2 and 2.3 for M16, M20 series 1 and M20 series 2 respectively. Cooper and Turner, the manufacturer of 'coronet' load indicating washers, specify average measured gaps at which the induced shank tension will not be less than that given in BS4604[53]. The recommended average measured gap, for LIW's with nut face washers fitted under the nut of general grade M16 and M20 bolts, is 0.25mm. The corresponding bolt tensions at this gap, recorded during the torque tension tests, are also given in Tables 2.1, 2.2 and 2.3. M16 bolts with LIW's flattened to an average measured gap of 0.25mm have a mean shank tension of 90 kN, with a coefficient of variation of 3.5%. The measured shank tension is slightly smaller than that given by the manufacturer and may be considered acceptable. However, at the recommended shank tension of 92 kN a mean average measured gap of 0.215mm with a coefficient of variation of 26.8% was recorded. It therefore appears from these tests that the average measured gap of M16 LIW's, placed under the nut, at the recommended shank tension from BS4604[53], has a considerable amount of scatter.

The amount of torque required to induce shank tension in a bolt depends upon the friction between the threads of the nut and bolt, together with the friction between the

Shank Tension	92 kN			
Test No.	Extension mm	Torque Nm	Average Measured LIW Gap mm	Shank Tension at 0.25mm LIW Gap kN
16.TT.1	0.156	338	0.30	95.0
16.TT.2	0.140	370	0.24	91.5
16.TT.3	0.142	310	0.20	89.0
16.TT.4	0.140	300	0.11	84.5
16.TT.5	0.190	325	0.24	91.0
16.TT.6	0.215	370	0.20	89.0
Mean	0.164 ±0.029	335.5 ±27.1	0.215 ±0.058	90.0 ±3.2
Coefficient of Variation	17.6%	8.1%	26.8%	3.5%

TABLE 2.1 SHANK TENSION, EXTENSION, TORQUE AND LIW GAP RELATIONSHIP FOR M16 BOLTS

Shank Tension	144 kN			
Test No.	Extension mm	Torque Nm	Average Measured LIW Gap mm	Shank Tension at 0.25mm LIW Gap kN
20.TT.1	0.380	657	0	108.0
20.TT.2	0.260	652	0.10	131.0
20.TT.3	0.335	658	0.05	123.5
20.TT.4	0.230	622	0.01	108.0
20.TT.5	0.345	705	0.01	119.5
20.TT.6	0.235	669	0.08	126.0
20.TT.7	0.400	599	0.06	123.0
20.TT.8	0.300	561	0	111.5
20.TT.9	0.185	586	0.11	134.5
20.TT.10	0.230	638	0	115.0
20.TT.11	0.170	598	0.06	126.5
20.TT.12	0.207	631	-	-
20.TT.13	0.165	608	-	-
Mean	0.265 ±0.077	629.5 ±37.7	0.044 ±0.040	120.6 ±8.6
Coefficient of Variation	28.9%	6.0%	91.3%	7.1%

TABLE 2.2 SHANK TENSION, EXTENSION, TORQUE AND LIW GAP RELATIONSHIP FOR M20 BOLTS SERIES 1

Shank Tension	144 kN			
Test No.	Extension mm	Torque Nm	Average Measured LIW Gap mm	Shank Tension at 0.25mm LIW GAP kN
20.TT.14	0.206	642	0.05	119.0
20.TT.15	0.195	627	0	112.5
20.TT.16	0.185	601	0.01	118.5
20.TT.17	0.180	614	0.02	113.0
20.TT.18	0.230	599	0	103.5
20.TT.19	0.275	658	0.05	110.0
Mean	0.212 ±0.033	623.5 ±21.4	0.022 ±0.021	112.8 ±5.3
Coefficient of Variation	15.4%	3.4%	97.6%	4.7%

TABLE 2.3 SHANK TENSION, EXTENSION, TORQUE AND LIW GAP RELATIONSHIP FOR M20 BOLTS SERIES 2

nutface and washer. For this reason no values of torque to achieve specified bolt preloads are given in BS4604[53]. From Table 2.1, the mean torque required to induce the minimum shank tension of 92 kN for M16 bolts was 335.5 Nm. This value was fairly consistent with each test result considering a coefficient of variation of 8.1%. The coefficient of variation for the extension of these bolts was 17.6% which may be considered quite large. This large variation was mainly due to each bolt having a different amount of linear and non-linear deformation at a load of 92 kN. From Table 2.2, the mean shank tension of the M20 series 1 bolts, at an average measured 'coronet' LIW gap of 0.25 mm was 120.6 kN. This value is approximately 16% below the required minimum of 144 kN for M20 bolts and is consistent throughout this test series, with a coefficient of variation of 7.1%. The mean average gap of the load indicators at 144 kN is a lot less than that recommended by the manufacturers, with an extremely large coefficient of variation, 91.3%, see Table 2.2. Similar results were obtained for the M20 series 2 bolts and are given in Table 2.3. The mean torques required to induce a shank tension of 144 kN in the M20 series 1 and 2 bolts are almost identical, with values of 629.5 Nm and 623.5 Nm respectively. Coefficients of variation are small and similar to that obtained for M16 bolts. Mean extensions and coefficients of variation for bolt series 1 and 2 at 144 kN shank tension are also given in Tables 2.2 and 2.3 respectively.

The majority of these extension variations at 144 kN may be accounted for by the varying amounts of linear and non-linear deformation, similar to the M16 bolts.

In general it may be stated from these tests, that at the minimum shank tension from BS4604[53] the torque control method proved to be the most consistent. The M16 and M20 bolts fitted with 'coronet' LIW's under the nut had approximately 2% and 19% less shank tension respectively, than the minimum specified at the manufacturers recommended average measured gap.

As some M16 and M20 bolts had non-linear deformation at the minimum preloads it was decided to examine the tightening control methods within the linear elastic range, especially that of extension near the elastic limit. Each method was therefore studied at shank tensions of 75 kN and 115 kN for M16 and M20 bolts respectively. The results for M16 bolts are given in Table 2.4 and indicate the compatability of the control methods. The results for M20 bolts are given in Tables 2.5 and 2.6, for series 1 and 2 respectively. The mean extensions for M20 bolt test series 1 and 2 are 0.140 mm and 0.153 mm respectively, with a common coefficient of variation of approximately 7%. This is similar to the variation obtained from the M16 bolts. Mean torque values for M20 bolt test series 1 and 2 are approximately the same, with similar small coefficients of variation. There is a considerable difference

Shank Tension	75 kN		
Test No.	Extension mm	Torque Nm	Average Measured LIW Gap mm
16.TT.1	0.125	256	0.59
16.TT.2	0.115	307	0.48
16.TT.3	0.115	240	0.44
16.TT.4	0.115	247	0.44
16.TT.5	0.137	252	0.55
16.TT.6	0.147	295	0.47
Mean	0.126 ±0.012	266.2 ±25.3	0.495 ±0.056
Coefficient of Variation	9.9%	9.5%	11.4%

TABLE 2.4 SHANK TENSION, EXTENSION, TORQUE AND LIW GAP RELATIONSHIP FOR M16 BOLTS

Shank Tension	115 kN		
Test No.	Extension mm	Torque Nm	Average Measured LIW Gap mm
20.TT.1	0.127	528	0.13
20.TT.2	0.140	532	0.55
20.TT.3	0.152	532	0.35
20.TT.4	0.148	528	0.17
20.TT.5	0.142	587	0.34
20.TT.6	0.133	564	0.45
20.TT.7	0.139	518	0.40
20.TT.8	0.156	461	0.18
20.TT.9	0.129	498	0.62
20.TT.10	0.145	500	0.25
20.TT.11	0.124	519	0.51
20.TT.12	0.158	527	-
20.TT.13	0.131	508	-
Mean	0.140 ±0.011	523.2 ±29.4	0.359 ±0.157
Coefficient of Variation	7.6%	5.6%	43.6%

TABLE 2.5 SHANK TENSION, EXTENSION, TORQUE AND LIW GAP RELATIONSHIP FOR M20 BOLTS SERIES 1

Shank Tension	115 kN		
Test No.	Extension mm	Torque Nm	Average Measured LIW Gap mm
20.TT.14	0.160	533	0.33
20.TT.15	0.144	516	0.15
20.TT.16	0.148	480	0.33
20.TT.17	0.144	506	0.22
20.TT.18	0.173	497	0.05
20.TT.19	0.146	562	0.21
Mean	0.153 ±0.011	515.7 ±26.3	0.215 ±0.098
Coefficient of Variation	7.0%	5.1%	45.7%

TABLE 2.6 SHANK TENSION, EXTENSION, TORQUE AND LIW GAP RELATIONSHIP FOR M20 BOLTS SERIES 2

however, between the mean average measured LIW gap of series 1 and 2, at 115 kN. Their coefficients of variations are similar but considerably large and unacceptable. The results from Tables 2.4, 2.5 and 2.6 indicate that at a shank tension of 75 kN and 115 kN for these M16 and M20 bolts respectively, the torque control method again proved to be the most consistent. Controlling tightening by means of extension, within the linear elastic range of these bolts also proved to be consistent and acceptable.

From these results it would seem reasonable to adopt the torque control method of tightening in the main beam to column connections. However, torque control method is dependent on the bolt thread condition which may vary throughout the batch. In the main test joints, different grip lenths than those in the single bolt tests, are used. This means that the mean torques obtained for these single bolt tests might not be acceptable. More control tests would therefore have to be performed in conjunction with the main tests, to provide enough evidence about these factors. A similar argument may be made concerning tightening control by means of bolt extension. However, if a stress strain relationship for any bolt type is determined from the load extension curves of direct and torque tension tests, then bolt force may be determined whatever the grip length.

2.3 Theoretical Work

Bending of the bolts may be noticed from the strain gauge readings of the torque tension tests in Appendix A-2. This accounts for the variation in extension when compared to similar direct tension tests. Bending of bolts during tightening was also observed by Pyrnne[60].

When determining linear elastic bolt extension it is assumed for simplicity that no bending occurs. Therefore from Figure 2.10

$$e = \frac{F_b}{E_b}\left[\frac{L_1}{A_s} + \frac{L_2}{A_b}\right] \qquad 2.1$$

The gauge length is assumed to be

$$g = T + t_w + l_n.\alpha \qquad 2.2$$

where α is an empirical constant depending on whether the bolt is subjected to direct or torque tension.

Therefore

$$e = \frac{F_b}{E_b}\left[\frac{L_1}{A_s} + \frac{(g - L_1)}{A_b}\right] \qquad 2.3$$

which is the general equation for bolt extension.

M16 Bolts

From Tables A2.1 and A2.6 L_1 = 30 mm, A_s = 208.67 mm^2

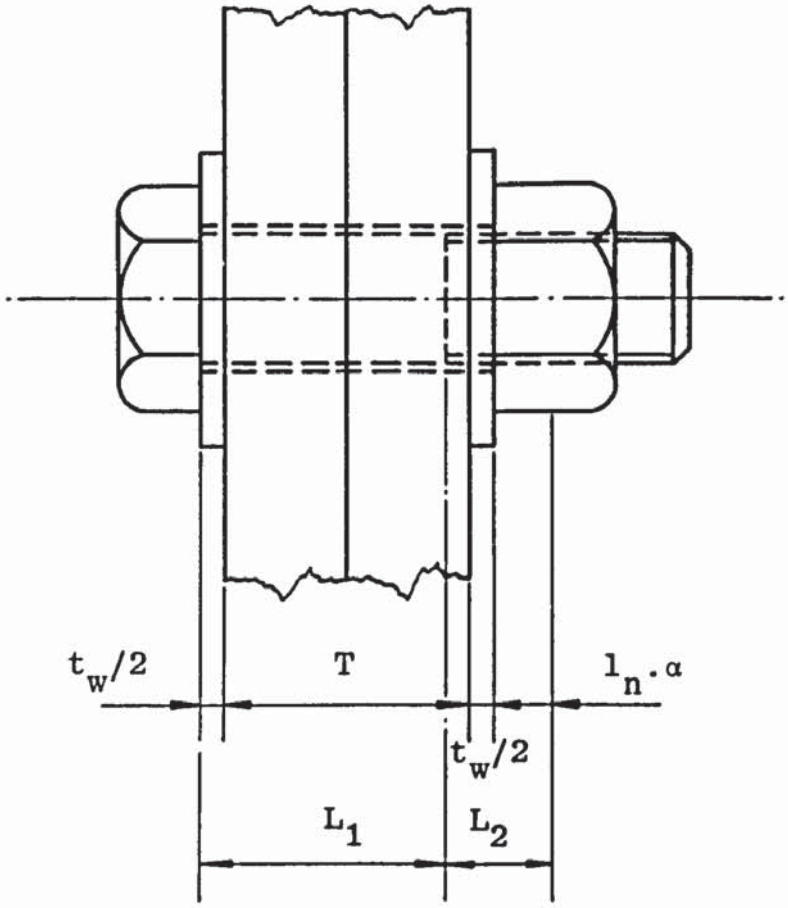

FIGURE 2.10 GENERAL BOLT DIMENSIONS

from BS4395[52] $A_b = 157\ mm^2$

therefore $A_s/A_b = 1.329$

substituting into 2.3 gives

$$e = \frac{F_b}{A_s.E_b} \left[1.329\ g - 9.87\right] \qquad 2.4$$

or

$$e = \frac{F_b}{A_b.E_b} \left[g - 7.44\right] \qquad 2.5$$

M20 Bolts

From Tables A2.2 and A2.7 $L_1 = 17$ mm, $A_b = 305.42\ mm^2$

from BS4395[52] $A_b = 245\ mm^2$

therefore $A_s/A_b = 1.247$

substituting into 2.3 gives

$$e = \frac{F_b}{A_s.E_b} \left[1.247\ g - 4.20\right] \qquad 2.6$$

or

$$e = \frac{F_b}{A_b.E_b} \left[g - 3.367\right] \qquad 2.7$$

The only unknown value in the right hand side of each equation is that of the empirical constant α. Therefore rearranging equations 2.5 and 2.7 gives

$$\alpha = \frac{1}{l_n} \left[\frac{A_b.E_b.e}{F_b} + 7.44 - (T + t_w)\right] \qquad 2.8$$

for M16 bolts and

$$\alpha = \frac{1}{l_n} \left[\frac{A_b.E_b.e}{F_b} + 3.367 - (T + t_w)\right] \qquad 2.9$$

for M20 bolts respectively.

α values, for the direct and torque tension tests of M16 bolts, obtained from equation 2.8 are given in Tables 2.7 and 2.8 respectively. α values, for the direct tension tests of M20 bolts, obtained from equation 2.9 are given in Table 2.9. Similarly α values, for the torque tension tests of M20 bolts series 1 and 2, obtained from equation 2.9 are given in Tables 2.10 and 2.11 respectively. E_b was taken as 210 kN/mm^2 for all tests. LIW thickness was taken as the mean thickness of the washer with and without protrusions. The mean value of α is approximately 0.5 for both bolt sizes in direct tension, however from Tables 2.7 and 2.9 the amount of variation is quite large. Nevertheless, taking α = 0.5 for the purposes of determining the gauge length g and hence substituting into equations 2.5 and 2.7, gives shank tension values similar to that actually observed for each M16 and M20 bolt in direct tension. In fact the mean calculated shank tensions are 89.5 kN and 154.5 kN, compared to actual values of 90 kN and 155 kN for M16 and M20 bolts respectively. From Tables 2.8, 2.10 and 2.11 the approximate mean value of α for torque tension tests is 1.0 for each bolt size. Similar to the direct tension tests the coefficients of variation of α are quite large. But taking α = 1.0, the calculated shank tensions using equations 2.5 and 2.7 are approximately equal to the actual tensions, for M16 and M20 bolts respectively in torque tension. Mean calculated shank tensions

Shank Tension		90 kN			
Test No.	Extension e mm	Gauge Length $g = T + t_w + l_n.\alpha$ mm	α Equation 2.8	F_b cal. using $\alpha = 0.5$ kN	$\frac{F_b \text{ test}}{F_b \text{ cal}}$
16.DT.1	0.143	$40.66 + 9.75 + 14.98\alpha$	0.629	93.4	0.96
16.DT.2	0.126	$40.66 + 9.81 + 15.02\alpha$	0.208	82.2	1.09
16.DT.3	0.126	$40.66 + 9.75 + 14.96\alpha$	0.213	82.3	1.09
16.DT.4	0.140	$40.66 + 9.75 + 14.88\alpha$	0.559	91.6	0.98
16.DT.5	0.135	$40.66 + 7.08 + 15.50\alpha$	0.591	92.6	0.97
16.DT.6	0.137	$40.66 + 6.85 + 15.00\alpha$	0.675	95.0	0.95
Mean	0.135 ±0.007		0.479 ±0.193	89.5 ±5.2	1.01 ±0.06
Coefficient of Variation	4.8%		40.3%	5.9%	5.9%

1) DT : Denotes Direct Tension Test

TABLE 2.7 α VALUE AND CALCULATED SHANK TENSION FOR M16 BOLTS

Shank Tension		75 kN			
Test No.	Extension e mm	Gauge Length $g = T + t_w + l_n.\alpha$ mm	α Equation 2.8	F_b cal. using $\alpha = 1.0$ kN	$\frac{F_b \text{ test}}{F_b \text{ cal}}$
16.TT.1	0.125	35.42 + 11.12 + 15.03α	1.055	76.1	0.99
16.TT.2	0.115	35.39 + 11.19 + 14.79α	0.772	70.3	1.07
16.TT.3	0.115	35.40 + 11.06 + 15.57α	0.741	69.5	1.08
16.TT.4	0.115	36.40 + 10.93 + 14.91α	0.782	70.5	1.06
16.TT.5	0.137	36.43 + 10.93 + 15.13α	1.342	82.1	0.91
16.TT.6	0.147	36.28 + 11.20 + 15.13α	1.625	87.8	0.85
Mean	0.126 ±0.012		1.053 ±0.332	76.1 ±6.8	0.99 ±0.087
Coefficient of Variation	9.9%		31.5%	9.0%	8.8%

1) TT : Denotes Torque Tension Test

TABLE 2.8 α VALUE AND CALCULATED SHANK TENSION FOR M16 BOLTS

Shank Tension		155 kN			
Test No.	Extension e mm	Gauge Length $g = T + t_w + 1_n.\alpha$ mm	α Equation 2.9	F_b cal. using $\alpha = 0.5$ kN	$\frac{F_b \text{ test}}{F_b \text{ cal.}}$
20.DT.1	0.170	40.66 + 7.57 + 17.95α	0.644	162.5	0.95
20.DT.2	0.163	40.66 + 7.48 + 18.17α	0.514	155.7	1.00
20.DT.3	0.148	40.66 + 7.55 + 18.02α	0.238	141.4	1.10
20.DT.4	0.170	40.66 + 7.64 + 18.05α	0.637	162.1	0.96
20.DT.5	0.158	40.66 + 7.63 + 18.08α	0.416	150.6	1.03
Mean	0.162 ±0.008		0.490 ±0.152	154.5 ±7.9	1.01 ±0.054
Coefficient of Variation	5.1%		30.9%	5.1%	5.4%

1) DT : Denotes Direct Tension Test

TABLE 2.9 α VALUE AND CALCULATED SHANK TENSION FOR M20 BOLTS

Shank Tension		115 kN			
Test No.	Extension e mm	Gauge Length $g = T + t_w + l_n.\alpha$ mm	α Equation 2.9	F_b cal. using $\alpha = 1.0$ kN	$\frac{F_b \text{ test}}{F_b \text{ cal.}}$
20.TT.1	0.127	36.19 + 12.27 + 17.18α	0.658	103.9	1.11
20.TT.2	0.140	36.38 + 12.26 + 18.10α	0.964	113.8	1.01
20.TT.3	0.152	36.43 + 12.26 + 18.09α	1.254	123.3	0.93
20.TT.4	0.148	35.35 + 12.28 + 17.85α	1.230	122.6	0.94
20.TT.5	0.142	35.46 + 12.16 + 18.28α	1.055	116.8	0.98
20.TT.6	0.133	35.48 + 12.26 + 18.08α	0.837	109.6	1.05
20.TT.7	0.139	36.41 + 12.22 + 17.92α	0.944	113.2	1.02
20.TT.8	0.156	36.61 + 12.18 + 18.24α	1.336	126.1	0.91
20.TT.9	0.129	36.55 + 12.23 + 18.03α	0.682	104.6	1.10
20.TT.10	0.145	35.41 + 12.28 + 17.64α	1.165	120.4	0.96
20.TT.11	0.124	35.59 + 12.05 + 17.79α	0.630	102.8	1.12
20.TT.12	0.158	35.38 + 12.19 + 18.04α	1.468	130.6	0.88
20.TT.13	0.131	36.26 + 12.24 + 17.86α	0.754	107.0	1.07
Mean	0.140 ±0.011		0.998 ±0.267	115.0 ±8.8	1.01 ±0.077
Coefficient of Variation	7.6%		26.7%	7.6%	7.6%

1) TT : Denotes Torque Tension Test

TABLE 2.10 α VALUE AND CALCULATED SHANK TENSION FOR M20 BOLTS SERIES 1

Shank Tension		115 kN			
Test No.	Extension e mm	Gauge Length $g = T + t_w + l_n.\alpha$ mm	α Equation 2.9	F_b cal. using $\alpha = 1.0$ kN	$\frac{F_b \text{ test}}{F_b \text{ cal.}}$
20.TT.14	0.160	$40.27 + 12.20 + 17.99\alpha$	1.250	122.7	0.94
20.TT.15	0.144	$40.37 + 12.24 + 17.84\alpha$	0.851	110.4	1.04
20.TT.16	0.148	$41.20 + 12.23 + 17.99\alpha$	0.898	111.9	1.03
20.TT.17	0.144	$40.24 + 12.22 + 18.13\alpha$	0.846	110.2	1.04
20.TT.18	0.173	$41.16 + 12.49 + 18.15\alpha$	1.494	130.1	0.88
20.TT.19	0.146	$41.22 + 12.24 + 17.98\alpha$	0.847	110.3	1.04
Mean	0.153 ± 0.011		1.031 ± 0.252	115.9 ± 7.7	1.00 ± 0.063
Coefficient of Variation	7.0%		24.4%	6.7%	6.3%

1) TT : Denotes Torque Tension Test

TABLE 2.11 α VALUE AND CALCULATED SHANK TENSION FOR M20 BOLTS SERIES 2

using α= 1.0 are 76.1 kN, 115.0 kN and 115.9 kN, compared to actual values of 75 kN, 115 kN and 115 kN for M16, M20 series 1 and 2 respectively. From test results by Rumpf and Fisher[59], Table A2.8 and Sterling et al[61], Table A2.9, the calculated shank tensions using equations 2.2 and 2.3 with α = 0.5 and 1.0 for direct and torque tension tests respectively, proved favourable with the actual values in approximately 85% of the tests. Therefore α values of 0.5 and 1.0 for direct and torque tension tests respectively appear to be suitable.

From equations 2.5 and 2.7 strain may be expressed as

$$e/(g - 7.44) \qquad 2.10$$

for M16 bolts and

$$e/(g - 3.367) \qquad 2.11$$

for M20 bolts respectively. g is found from equation 2.2 with the value of α depending on the type of tension test. The stress strain relationships for typical M16 and M20 bolts in direct and torque tension are shown in Figures 2.11 and 2.12 respectively. The value of α was taken as 0.5 in direct tension and 1.0 in torque tension. Detailed calculations for the construction of these curves may be found in Appendix A-2. The 0.2% yield stresses found from these and similar relationships are given in Table A2.10 for all bolts tested. There is approximately 12% difference between the mean 0.2% yield stresses of M16 bolts in direct and torque tension. This difference is approximately 25% and 17% for M20 series 1 and 2 bolts

FIGURE 2.11 RELATIONSHIP BETWEEN STRESS AND STRAIN FOR A TYPICAL DIRECT AND TORQUE TENSION M16 BOLT

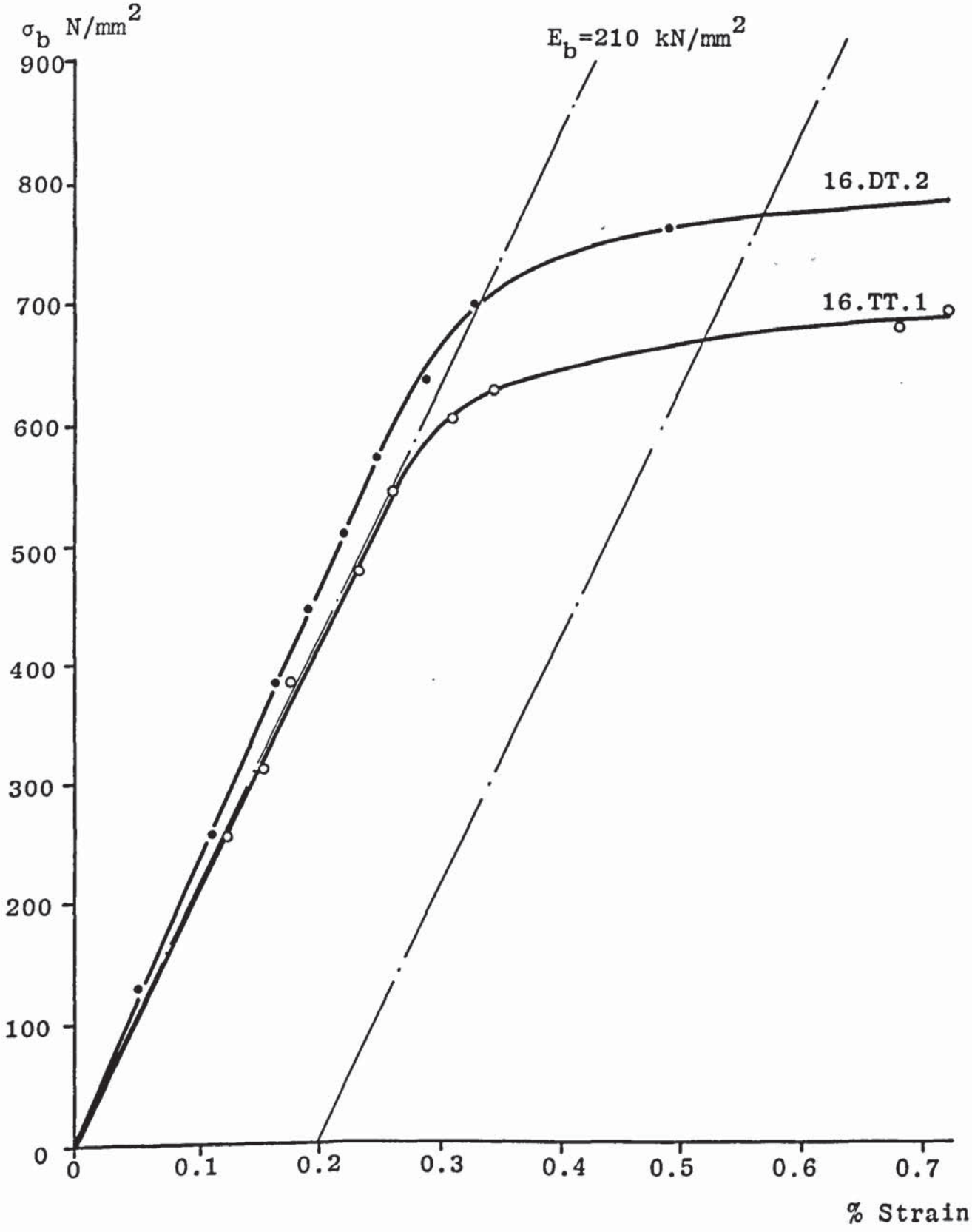

FIGURE 2.12 RELATIONSHIP BETWEEN STRESS AND STRAIN FOR A TYPICAL DIRECT AND TORQUE TENSION M20 BOLT

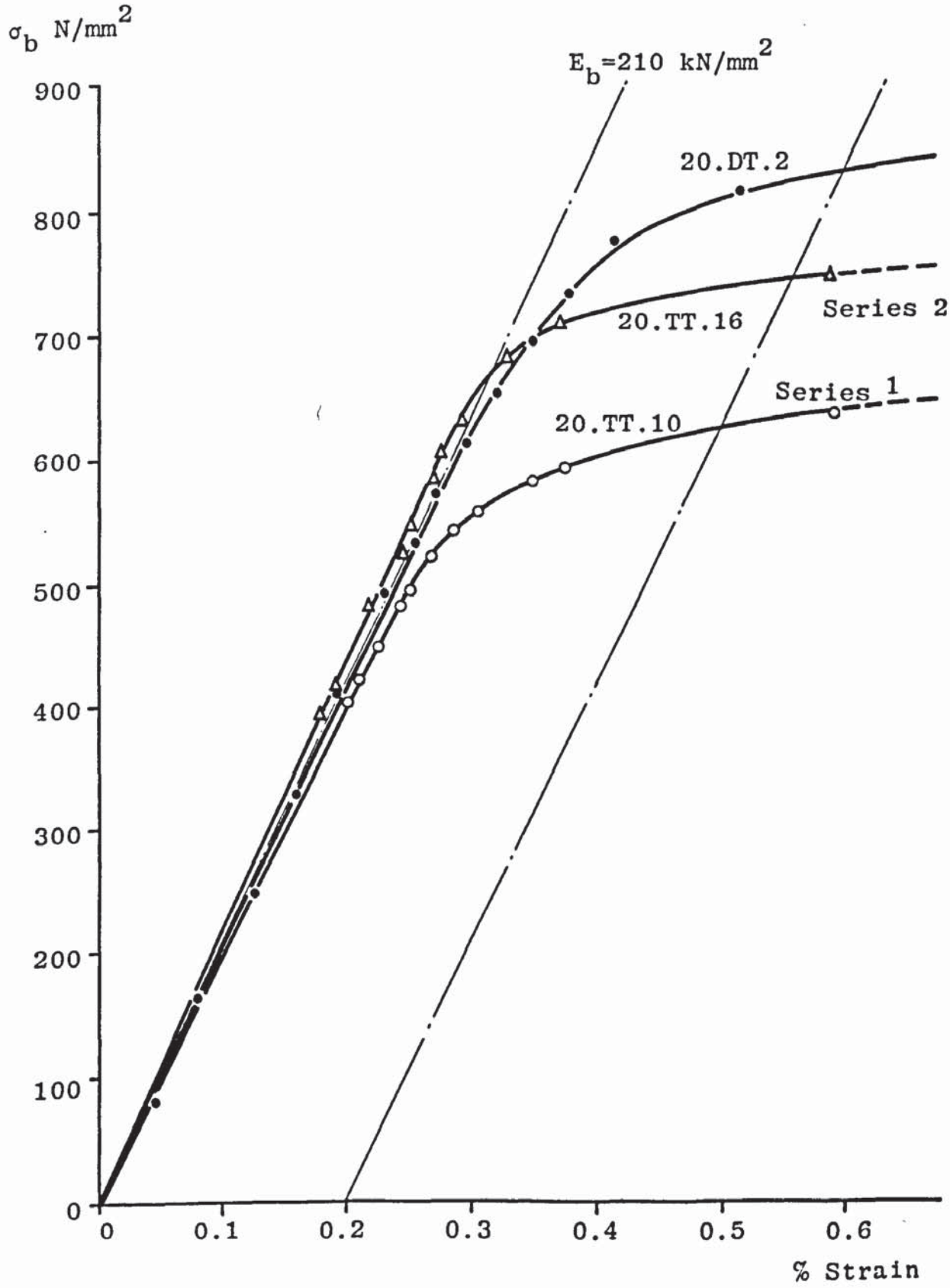

respectively. These values are similar to those quoted by Rumpf and Fisher[59] and Sterling et al[61]. The decrease in yield stress is due to torsional shear stress being induced by tightening, caused by friction between the bolt and nut threads. Assuming uniform shear stress across the threaded cross section then

$$T_s = \pi . d_1^3 . \tau/12 \qquad 2.12$$

the average coefficient of friction of the threads may be expressed as

$$\mu_t = 2 . T_s/F_b.d_1 \qquad 2.13$$

therefore using von Mises yield criterion and substituting equation 2.12 into equation 2.13 gives

$$\mu_t = \frac{2 (\sigma_{y0.2}^2 - \sigma_{yt0.2}^2)^{\frac{1}{2}}}{3.\sqrt{3}.\sigma_{yt0.2}} \qquad 2.14$$

Using the experimental 0.2% yield stresses μ_t has been found from equation 2.14 for each bolt type and the values are given in Table 2.12.

Gill[51] suggested that a mean torque coefficient K of 0.18 based on 433 torque tension tests, could be used in the equation $T = K.d.F_b$ for the applied torque. He assumed that the applied torque was absorbed in equal amounts at the thread and washer faces. Therefore torque applied to a bolt shank may be expressed as

$$T_s = K.d.F_b/2 \qquad 2.15$$

Bolt Type	μ_t Equation 2.14
M16	0.206
M20 Series 1	0.345
M20 Series 2	0.254

TABLE 2.12 COEFFICIENTS OF THREAD FRICTION

Cullimore[58] observed that approximately 60% of the applied torque was applied to the bolt shank, in several experiments with ½ inch BSF bolts. Using a K value of 0.15 he showed that

$$T_s = K.d_1.F_b/2 \qquad 2.16$$

Assuming $d \simeq d_1$ and equating 2.13, 2.15 and 2.16 gives

$$\mu_t = K = 0.18 \qquad 2.17$$

A mean coefficient of thread fiction therefore appears to be 0.18. This was confirmed by the results of Blagden[65] for ¾ inch UNC standard and 'v' quality high strength bolts, with good profile and surface finish together with good lubrication. The μ_t value obtained for the M16 bolts compares favourably with the friction value of 0.2 obtained by Blagden[65] for standard high strength bolts, with poor profile and rough surface finish together with good lubrication. Blagden[65] also obtained μ_t values of 0.36 and 0.34, for site conditioned ¾ inch standard and 'v' quality high strength bolts respectively. Site conditioning was obtained by washing the bolts in warm water and then applying mud to the threads of the standard bolts only. Both bolt types were tested dry. The threads of all the bolts tested in this investigation appeared to be in good condition. However, most, if not all of the lubricant was removed during the test preparation process. The mechanical properties of the 'v' quality bolts tested by Blagden[65] were similar to the M20 bolts reported herein, with similar values of μ_t

obtained for similar thread conditions.

2.4 Bolt Calibration Curve

The beam to column joints, reported later, were to be connected with M16 HSFG bolts from the same batch as those investigated in this chapter. The main purpose of this investigation was to provide a stress-strain curve for these bolts. From the results obtained a calibration curve has been constructed and is shown in Figure 2.13. The curve is the line of best fit through the stress strain relationships of the M16 bolts in direct tension. A similar curve may be constructed for bolts in torque tension. Both curves are similar within the linear elastic range and if bolt preload is kept within this range discontinuity is avoided. An initial preload of 75 kN is acceptable. Strain is obtained from equation 2.10 with $\alpha = 1{\cdot}0$ when bolt extensions are less than or equal to that due to the initial preload. A value of $\alpha = 0{\cdot}5$ is used when the extensions are greater than that due to the initial preload.

FIGURE 2.13 RELATIONSHIP BETWEEN STRESS AND STRAIN FOR M16 BOLTS

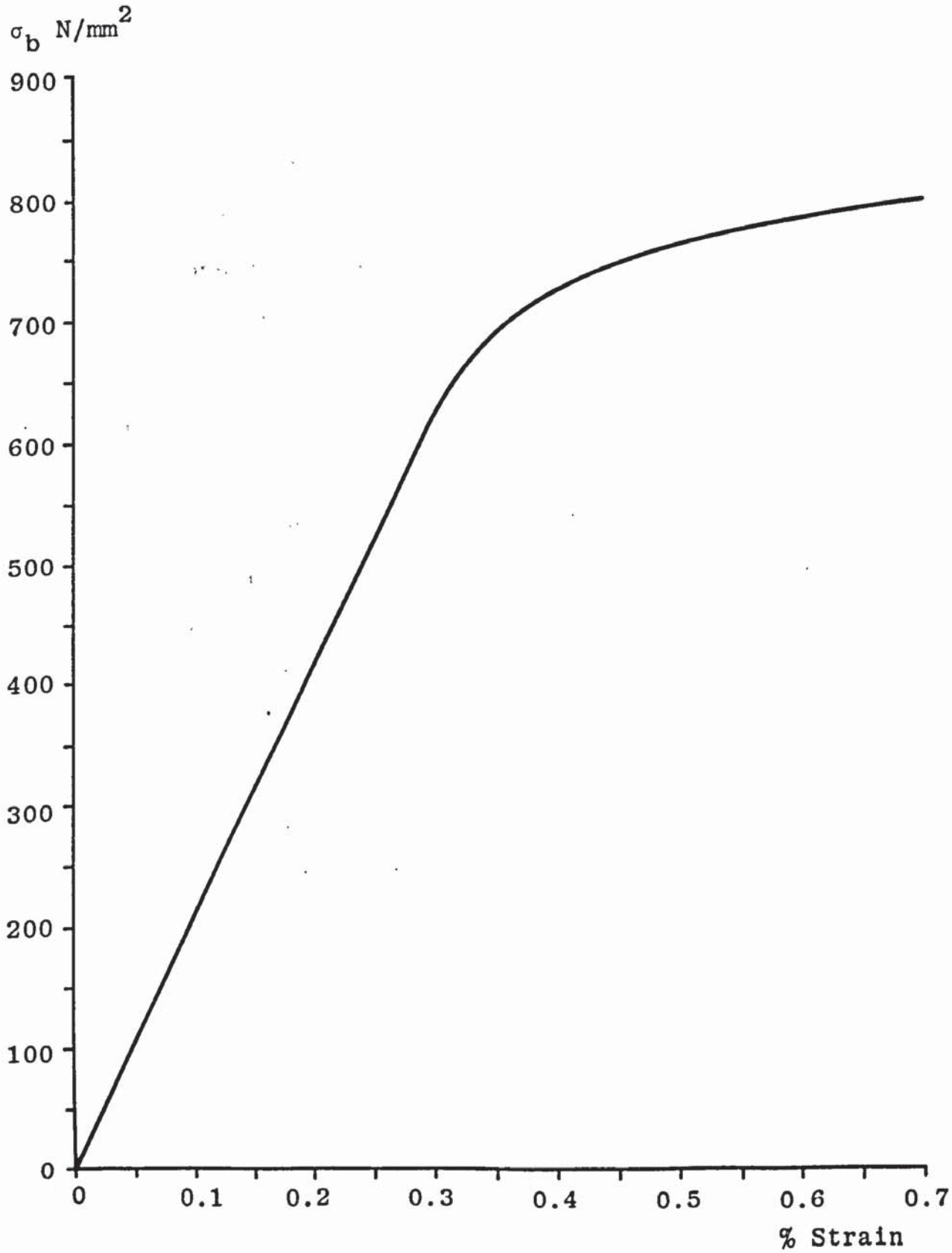

CHAPTER THREE

EXPERIMENTAL INVESTIGATION OF TEE STUB CONNECTIONS

3.1 Introduction

The tension region of an extended end plate, beam to column joint, can be represented by a tee stub connection. This chapter reports the results of tee stub tests where the dimensions and details approximate to the beam to column connections reported later.

3.2 Experimental Work

The mechanical properties of tee stub flange plates should be the same to ensure that tee stub tests are comparable. The flange plate thickness varied throughout this investigation therefore, plates from the same batch were machined to the required thickness. It was not known what effect machining had on the mechanical properties of mild steel so, several tensile tests on machined plates were carried out to examine this effect.

3.2.1 Mechanical Properties of Machined Mild Steel.

Several straight parallel tensile test specimens, approximately 250mm long were cut from a 20mm thick grade 43A mild steel plate to BS4360[66]. The specimens were

machined to the required width, which varied throughout the test series. The machining processes used in reducing the widths were shaping, dry milling and wet milling. Specimen thickness also varied and was either kept at 20mm or shaped to the required size on one surface only. A similar procedure was used on the tee stub flanges. The test pieces were tested in tension with the yield stresses and E values computed from load extension graphical outputs using a Baldwin strain plotter. The results are given in Table A3.1. From these results it is concluded that there is virtually no difference in yield stress, ultimate stress and Young's modulus for shaped, dry milled and wet milled mild steel.

3.2.2 Tee Stub Connections

A series of five tests on tee stubs simulating the tension zone of an extended end plate beam to column connection were undertaken. The dimensions of these specimens shown in Figures 3.1 and 3.2 approximate to the beam to column connections reported later. Electrical resistance strain gauges, FLA-3-11, were placed at the bolt line and adjacent to the welds to detect yielding of the plate. 16mm diameter HSFG bolts from the same batch as those used in the single bolt direct tension and torque tension tests, reported earlier, were used for the tee stubs. Axial bolt force was determined from three FLA-3-11 strain gauges attached

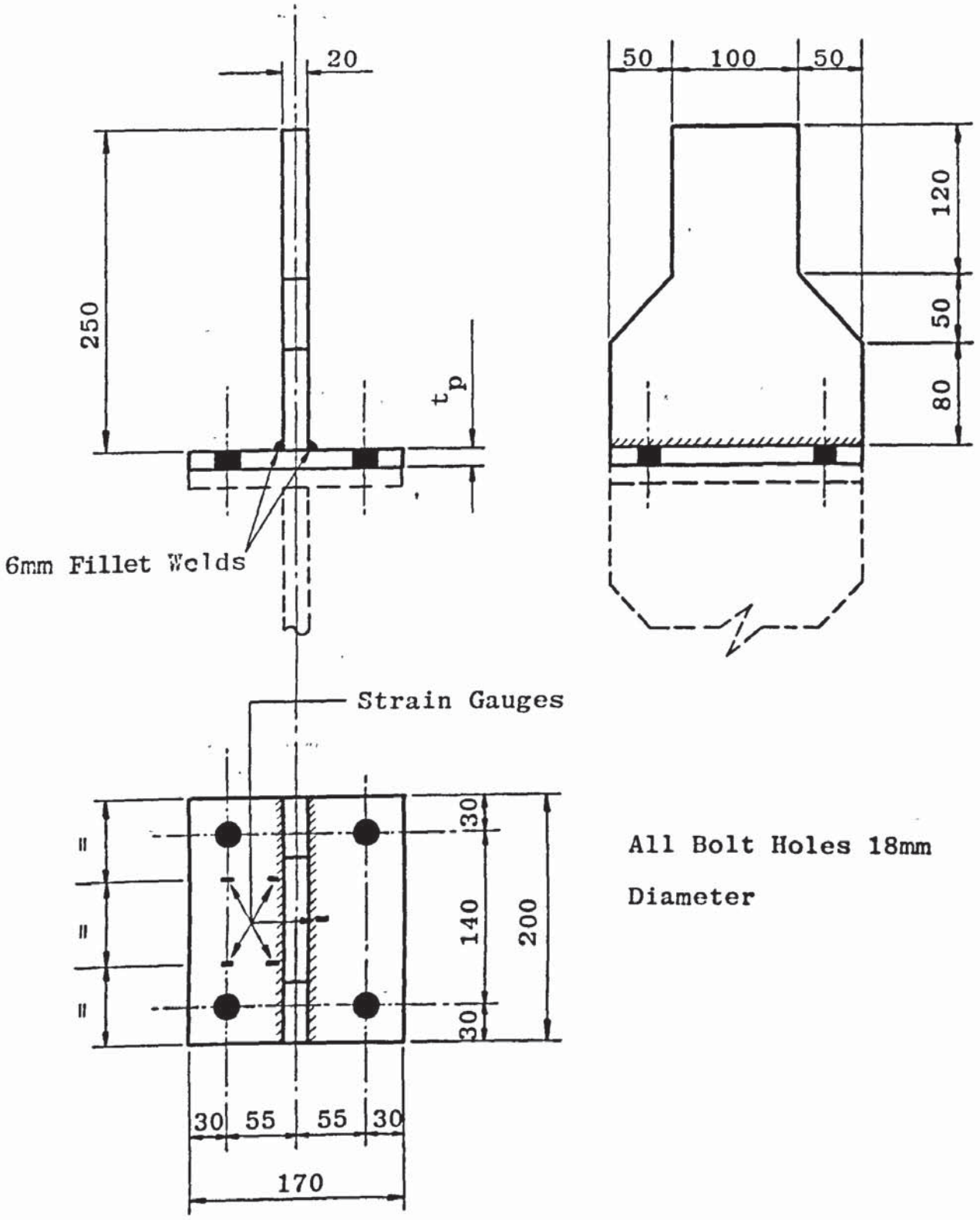

FIGURE 3.1 TEE STUB ARRANGEMENT FOR TESTS TS1, TS2, TS3 AND TS4.

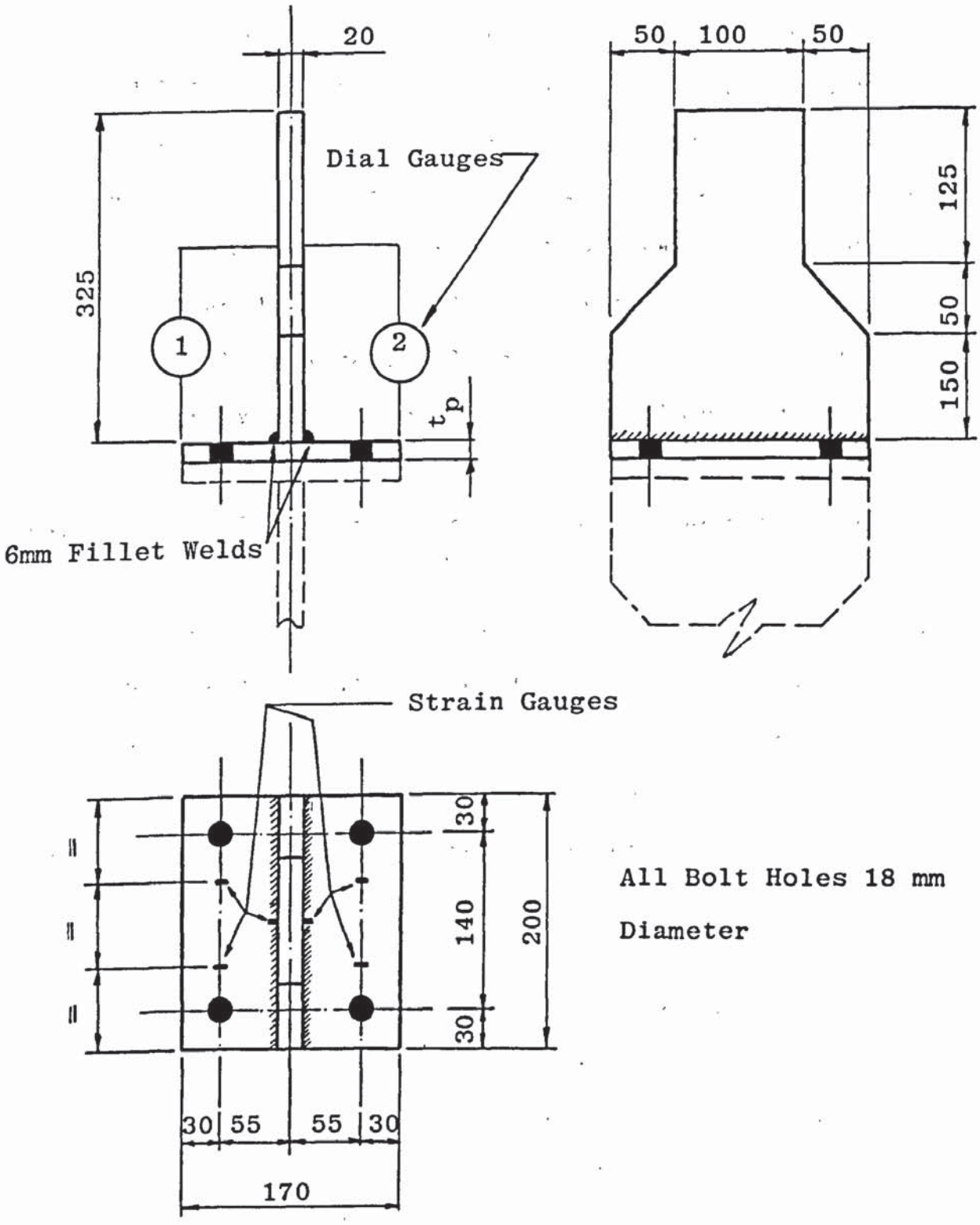

FIGURE 3.2 TEE STUB ARRANGEMENT FOR TEST TS5

to each bolt at 120° intervals in the case of Tests TS1, TS2 and TS3. The strain gauges wires passed through 3mm diameter holes drilled in the bolt head. The wires were attached to the extension box of a Peekel from which strain readings were recorded. The diameter of each bolt hole was 18mm leaving little clearance for the strain gauges and their wires. Clearance for the wires was provided by two or three 20mm diameter hardened steel washers placed beneath the bolt head. A 16mm diameter hardened steel washer was placed under the nut. A demec spot was attached to the head and toe of each bolt for all tests, except TS5, to enable bolt extension to be measured at each load interval. From these extensions, axial bolt force was determined from the calibration graph shown in Figure 2.13. Strain gauges were not attached to the bolts in Test TS4. Two 16mm diameter hardened steel washers were placed under the nut of each bolt in Test TS4. This increased the grip length as the unthreaded bolt length was greater than the plate thicknesses plus two washers in some cases. A 16mm diameter hardened steel washer was used under each bolt head. In Test TS5, axial bolt force was measured using a TML BTM-8A bolt strain gauge which was situated in a hole drilled along the vertical axis of each bolt and attached in accordance with the manufacturers instructions. Strain readings were recorded from a Peekel as before. Two 16mm diameter hardened steel washers were placed under the nut of each bolt. One 16mm diameter hardened steel washer was placed under each bolt head.

During Test TS5 flange plate deflections were recorded from magnetic dial gauges positioned as shown in Figure 3.2. Details of each tee stub test is given in Table 3.1. Variation in yield stress of the flange plate was eliminated by using plate from the same batch for all tests, except TS5, and machining down to the required thickness. The results from five straight parallel test specimens taken from the same batch as the flange plates for Tests TS1, TS2, TS3 and TS4 are given in Table A3.2. The results of two tensile specimens, taken from the same steel plate as the flange plate of Test TS5, are given in Table A3.3. Grade 43A mild steel plates to BS4360[66] were used for the tee stub flanges. During assembly each bolt was tightened in turn with increased torque until the required preload was reached. Some of the strain gauges attached to the circumference of the bolts failed to function properly during tightening. This was probably due to a break in the gauges electrical circuit caused by contact between the gauge and its surroundings. In Tests TS1, TS2 and TS3 axial bolt force from the strain gauges was therefore determined from two, three and four bolts respectively, as each of their three gauges worked normally.

The initial bolt tension and flange plate thickness were varied in order to study their influence on the behaviour of these connections. The relationships between applied load and bolt force for Tests TS1, TS2, TS3, TS4 and TS5 are shown in Figures 3.3, 3.4, 3.5, 3.6 and 3.7 respectively.

Test No.		TS1	TS2	TS3	TS4	TS5
t_p	mm	20.1	12.5	15.9	12.7	15.4
20mm Dia.,	mm	3.66	3.64	3.71	-	-
Mean Washer	mm	3.66	3.63	3.66	-	-
Thickness	mm	-	3.66	3.64	-	-
16mm Dia.,	mm	3.09	3.19	3.22	3.23	3.10
Mean Washer	mm	-	-	-	3.27	3.21
Thickness	mm	-	-	-	3.25	3.28
Mean Nut Thickness	mm	14.92	14.96	15.07	15.50	15.48
F_s	kN	80.3	93.0	76.3	40.0	45.8
F_u	kN	119.0	87.2	97.7	94.7	104.7
Q_{bu}	kN	21.0	52.8	42.3	45.3	35.3
Mode of Failure		Bolt failed in all tests				

TABLE 3.1 MEAN DIMENSIONS AND EXPERIMENTAL RESULTS FOR TEE STUB TESTS

FIGURE 3.3 RELATIONSHIP BETWEEN APPLIED LOAD AND BOLT FORCE FOR TS1

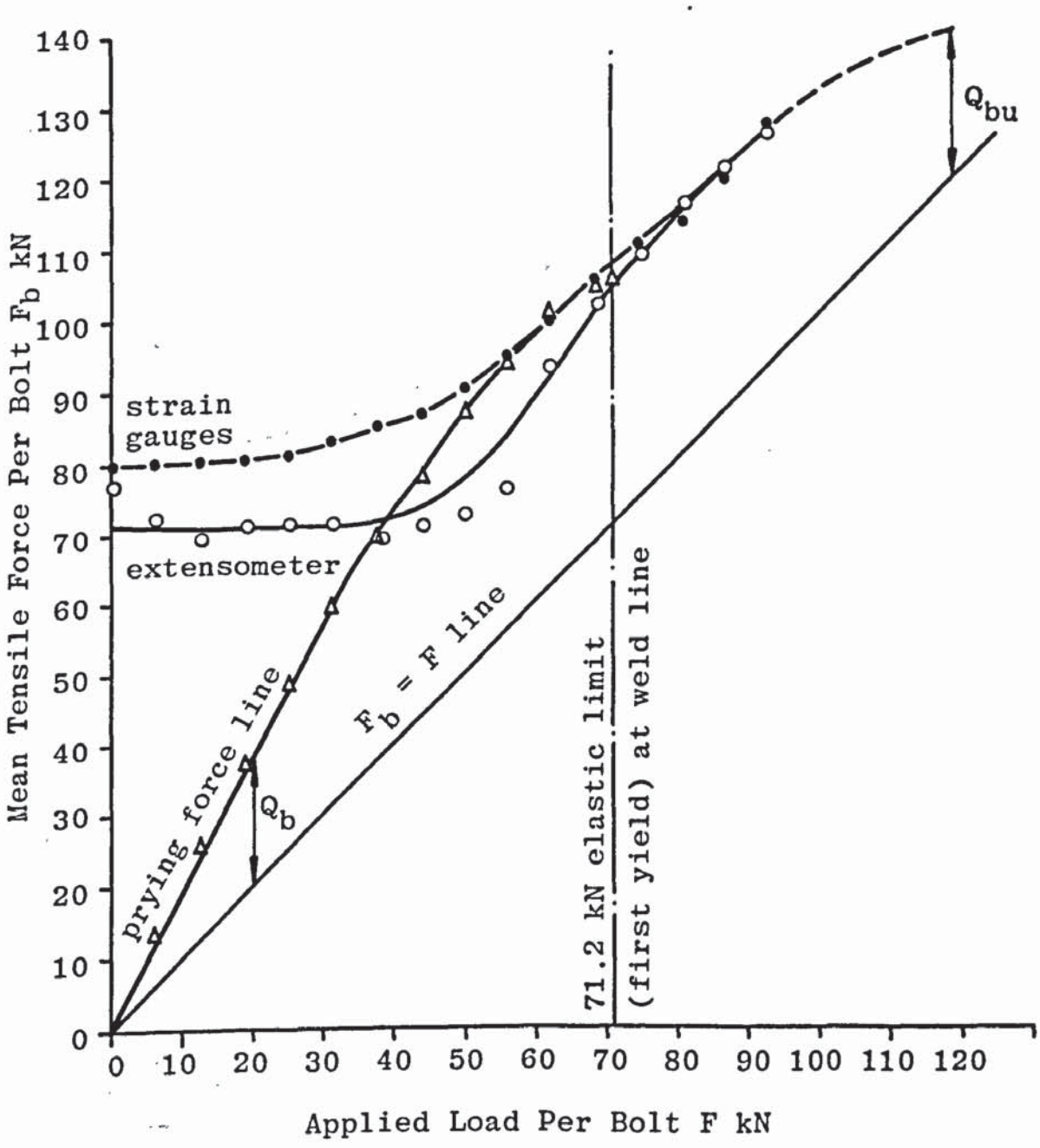

FIGURE 3.4 RELATIONSHIP BETWEEN APPLIED LOAD AND BOLT FORCE FOR TS2

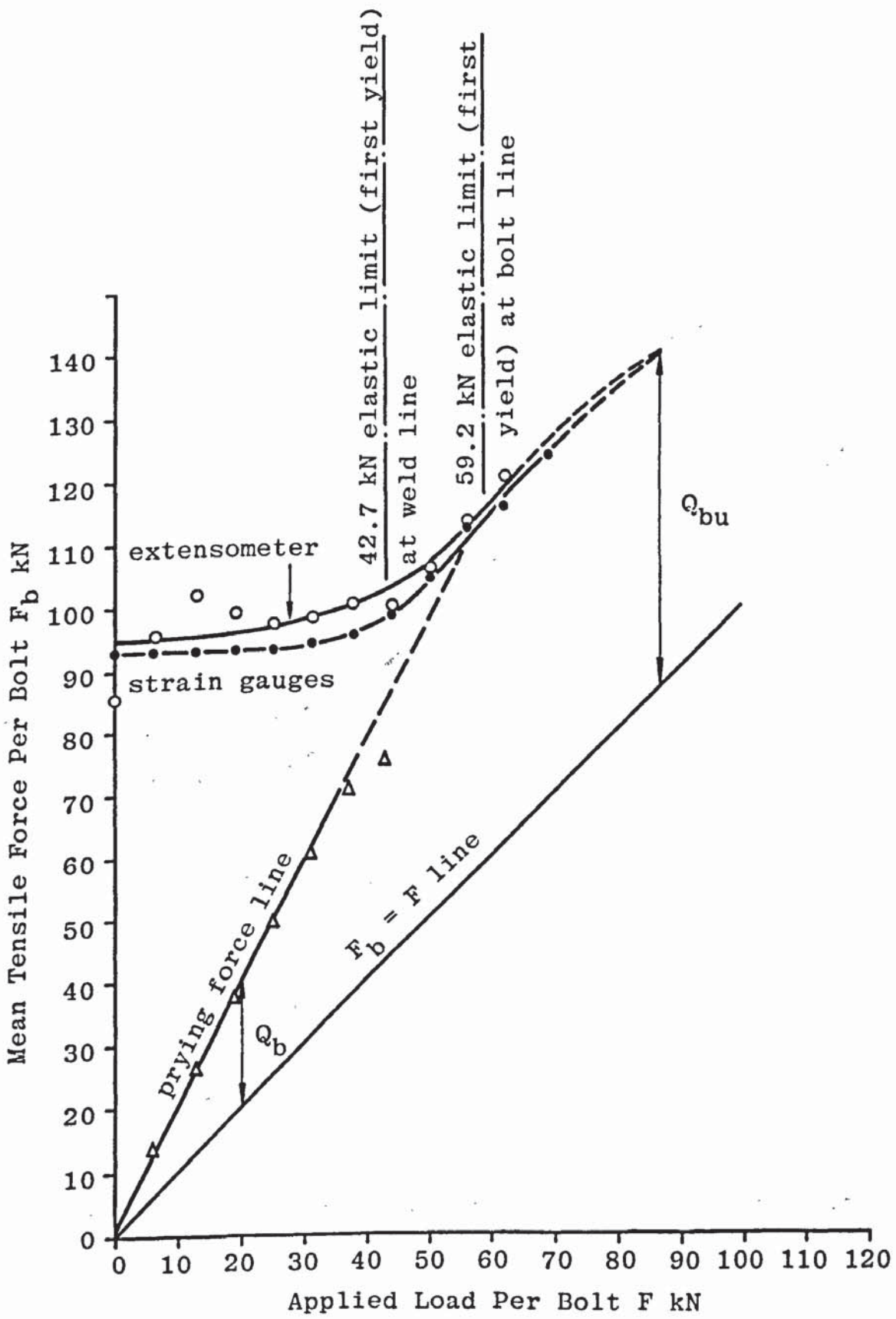

FIGURE 3.5 RELATIONSHIP BETWEEN APPLIED LOAD AND BOLT FORCE FOR TS3

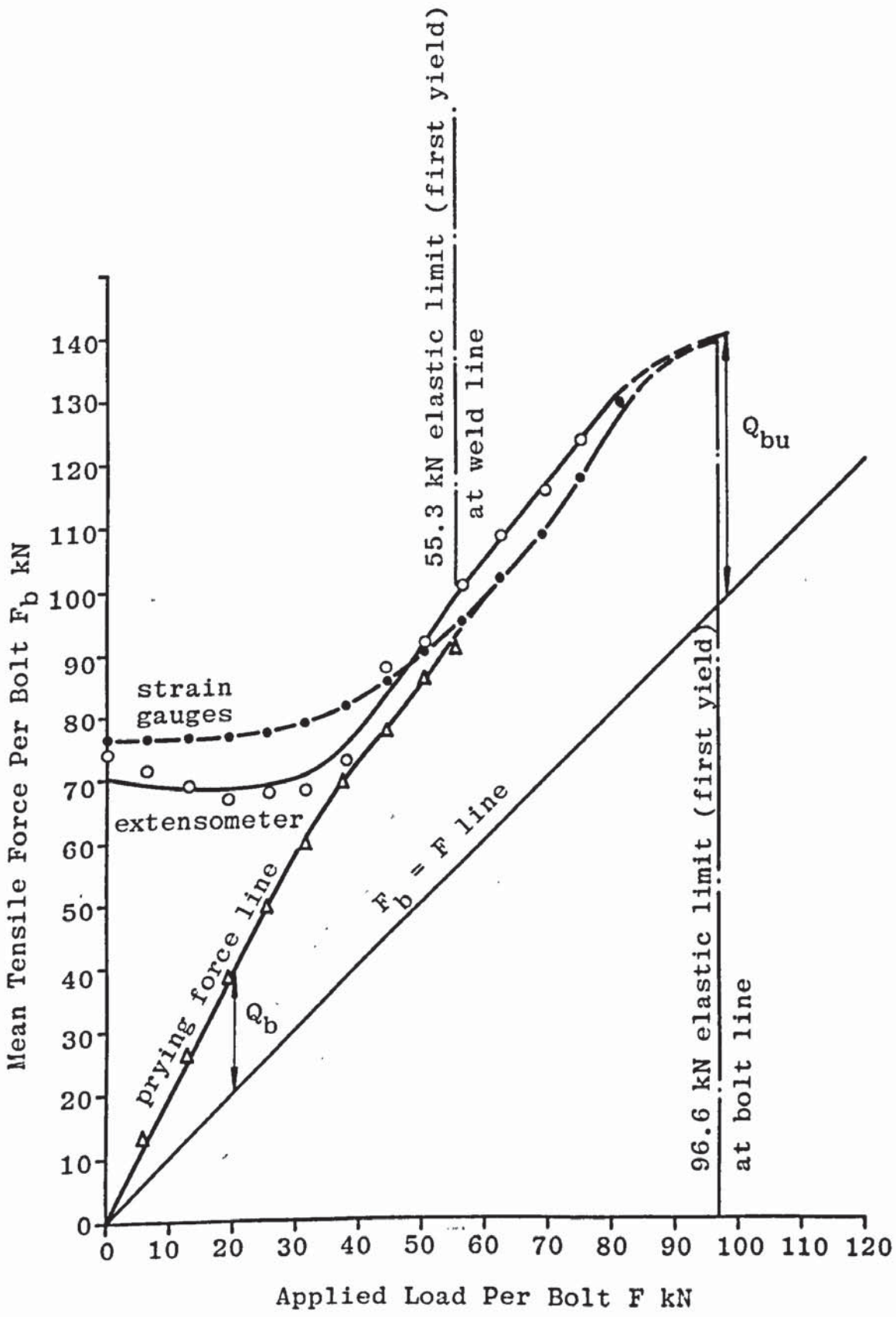

FIGURE 3.6 RELATIONSHIP BETWEEN APPLIED LOAD AND BOLT FORCE FOR TS4

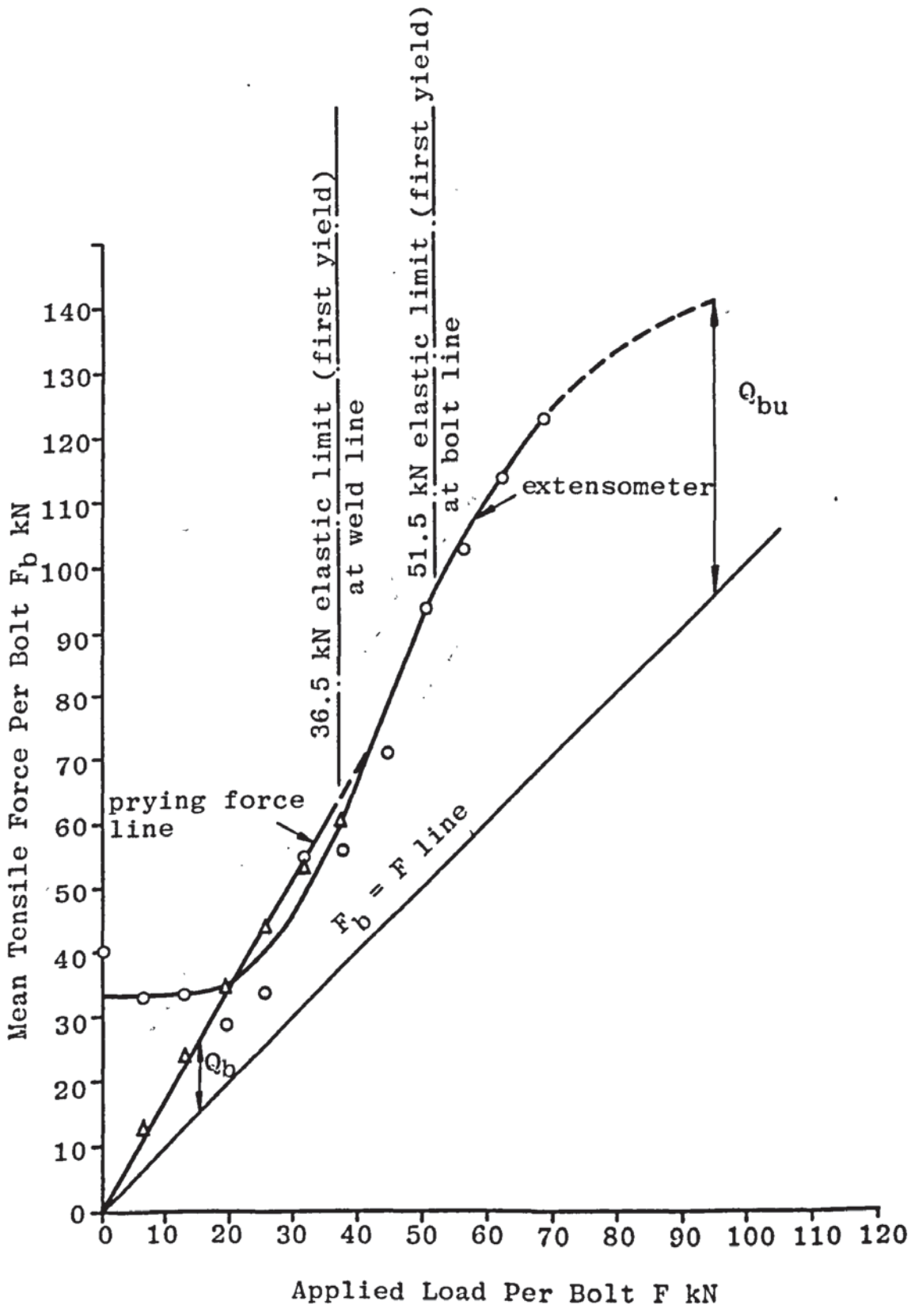

FIGURE 3.7 RELATIONSHIP BETWEEN APPLIED LOAD AND BOLT FORCE FOR TS5

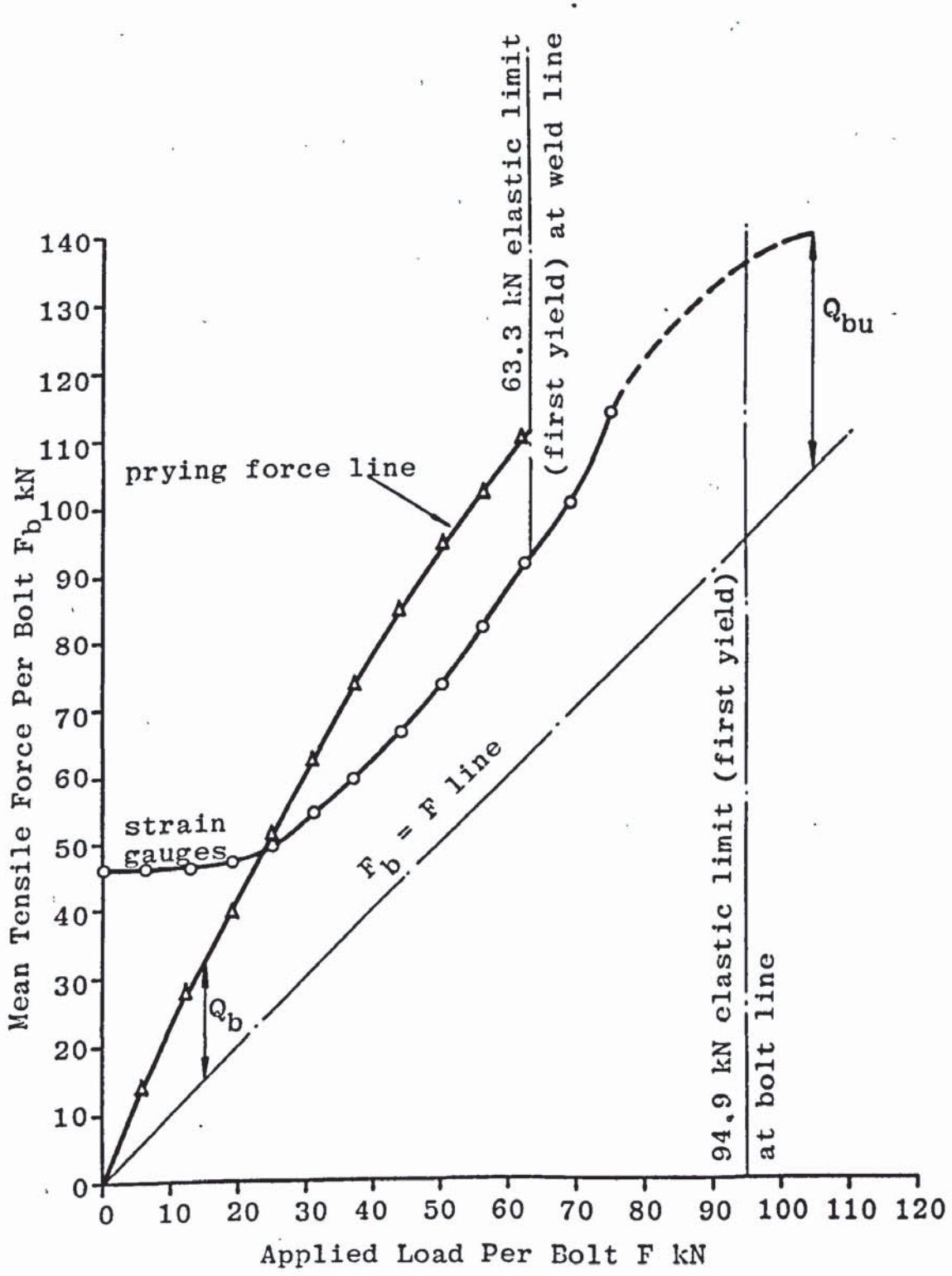

The experimental results for a typical tee stub TS5 are given in Appendix A-3. Plate flexure during each test resulted in bending of the bolts. Therefore extensions recorded during each test resulted in bending of the bolts. Therefore extensions recorded during each test were not the axial extensions but the vertical increase in length between the centre of the bolt head and toe. There is however good correlation between the axial bolt forces determined from the strain gauges and the apparent extensions. The difference between the two methods may also be considered acceptable. For these reasons bolt force in Test TS4 was determined from the extension only. The last recorded bolt force in each test was approximately 90% of the full tensile strength at approximately 80% of the maximum applied load. It therefore appears that the full tensile strength of the bolts were developed at failure despite bending distortions at earlier stages of loading.

Due to the flexure behaviour of tee stub flanges, the outer parts of the plates are forced against each other and prying forces are developed. The prying forces are shown in the applied load, bolt force relationship for each tee stub test. It should be noted that the prying force remains approximately constant once separation has occurred in Tests TS1, TS2, TS3 and TS5. In Appendix A-3 it is shown that the prying force, assumed acting at the extreme edge of the flange, can be determined using the

mean strains obtained at the weld line at any loading stage within the elastic range. A prying force line is also shown in the applied load, bolt force relationship for each test and shows that prying force increased approximately linearly until separation occurred. Prying force was not determined using the mean strains obtained at the bolt line, because it was considered that the simple bending theory was invalid at this section for relatively thick plates. For smaller plate thicknesses out of plane bending was observed along the bolt line, therefore the strains obtained did not reflect the true behaviour along the tee stub length. The first yield or elastic limit at the weld and bolt lines from the mean strains obtained are also indicated on the applied load bolt force relationship for each test specimen. A general view of the test pieces after failure is given in Plate 3.1. From the patterns in the 'snowcem' it can be seen that plastic deformation took place at and near to the web in each specimen. In the case of the relatively thin plates, Tests TS2 and TS4, plastic deformation also occurred at the bolt line together with double curvature of the flange plate.

A check on the equilibrium of moments about the web for the tee stub model shown in Figure 3.8, assuming a plastic hinge at the web and the value of the bolt and prying forces measured in each test, showed an out of balance moment. This moment may be balanced by a moment at the bolt line as assumed by Struik[19], Fisher and Struik[20]

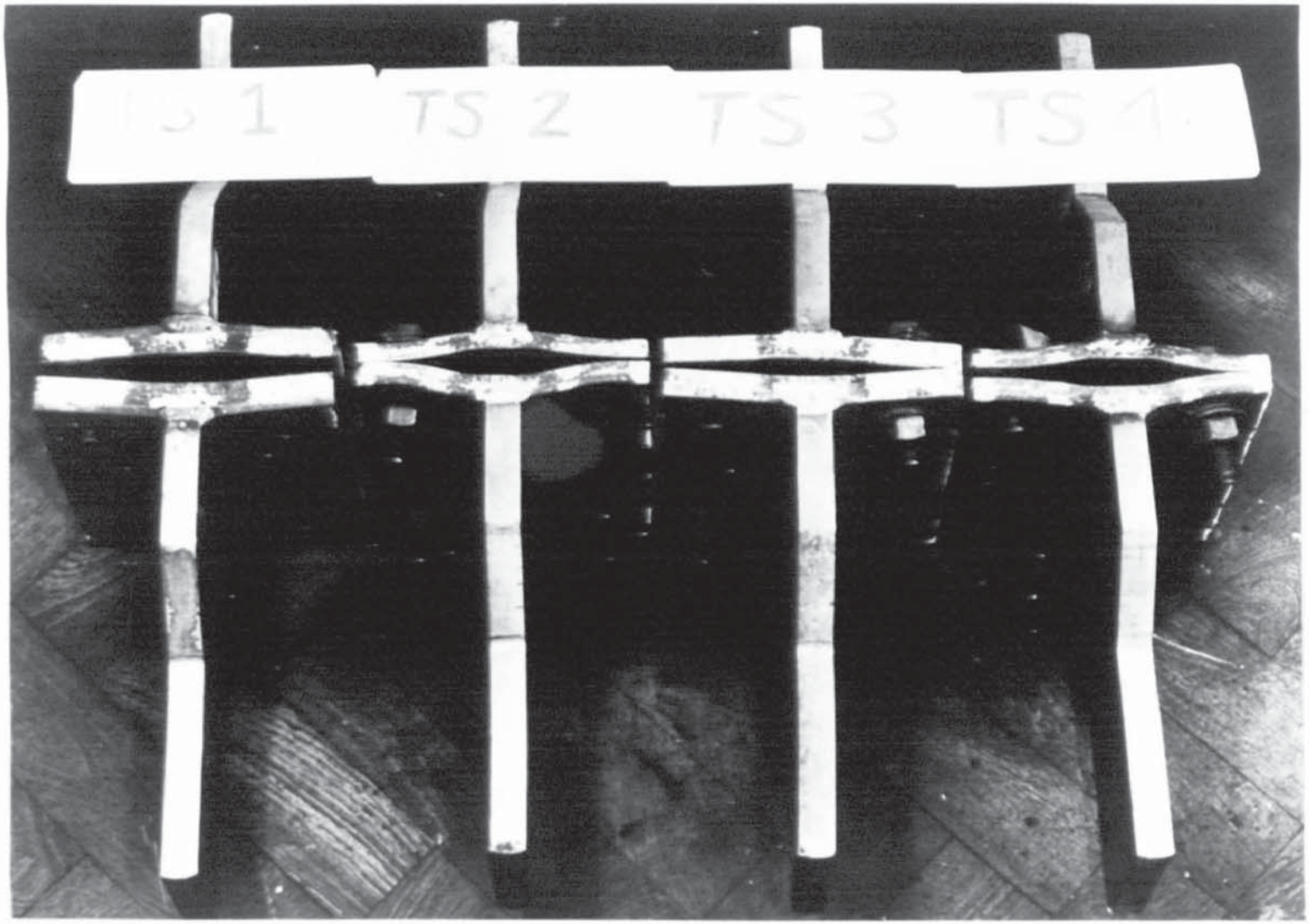

PLATE 3.1 TEE STUB SPECIMENS AFTER FAILURE

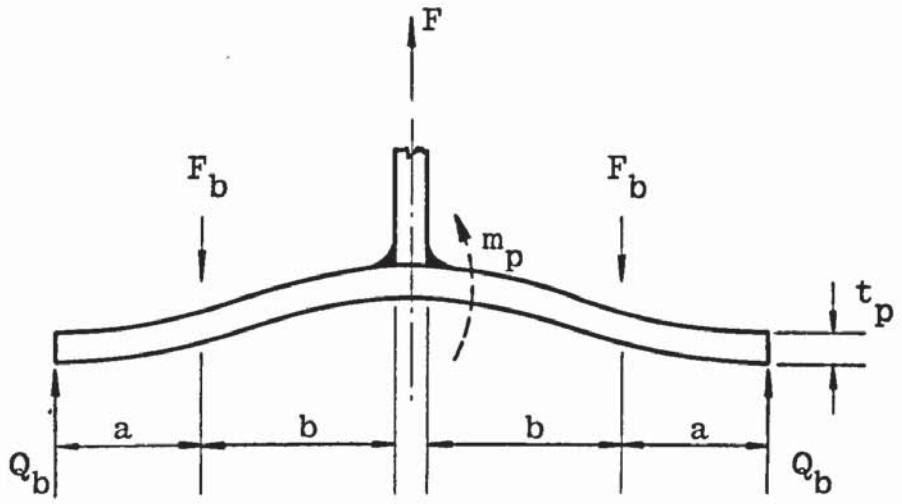

FIGURE 3.8 THEORETICAL MODEL OF A TEE STUB

and Kennedy et al[67]. Another approach would be to reduce the dimension b or increase the resistance of the plastic hinge as assumed by de Back and Zoetemeijer[22] and Douty[68]. A moment from the bolt at the bolt line was rejected because the bolt achieved the full tensile strength at failure. Also reducing the value of b did not appear to fit the deformed shape of the specimen at failure.

3.2.3 Simply Supported Rectangular Steel Strip Tests

To obtain further information on the resistance of the plastic hinge, separate experiments were conducted on simply supported rectangular steel strips with either a central point load or partial UDL. Eight steel strips were cut from the end plate of the beam to column connection CS2-5, after the test was discontinued. The strips were taken from the end plate within the beam depth, as yielding did not appear to have occurred within this zone. Six steel strips were cut from an unused end plate with a yield strength of 328.1 N/mm^2. One steel strip was cut from the same type steel as that used for Test TS5. The main variables were the span and the thickness of the strips. Details of the test specimens are given in Table 3.2. Some specimens were machined down from their original thickness on one surface only to provide consistency with the tee stub flange plates. Each specimen rested on knife edge supports. The central deflections of the strips were recorded during the tests.

Specimen	t mm	2l mm	w mm	l/t	W at m_p kN
B1	15.0	160	20.2	5.33	6.5
B2	12.3	160	19.5	6.50	4.2
B3	15.0	100	20.0	3.33	10.3
B4	12.0	100	18.7	4.17	6.2
B5	15.1	60	19.7	1.99	17.1
B6	12.2	60	20.1	2.46	11.4
B7*	15.1	100	20.0	3.31	11.3
B8*	11.9	100	19.9	4.20	7.0
B9	12.3	100	19.6	4.07	9.7
B10	15.0	100	20.0	3.34	14.7
B11	20.2	100	19.8	2.48	26.5
B12*	12.1	100	19.9	4.12	10.4
B13*	15.0	100	19.9	3.34	15.9
B14*	20.2	100	20.0	2.48	28.8
B15*	15.1	110	20.1	3.65	11.6

Note: σ_y (B1 to B8) 229 N/mm^2, σ_y(B9 to B14) 328.1 N/mm^2
σ_y (B15) 277.3 N/mm^2

Specimens marked thus * had a partial UDL.

Other specimens loaded via a knife edge.

TABLE 3.2 MEAN DIMENSIONS OF RECTANGULAR STEEL STRIP TEST SPECIMENS

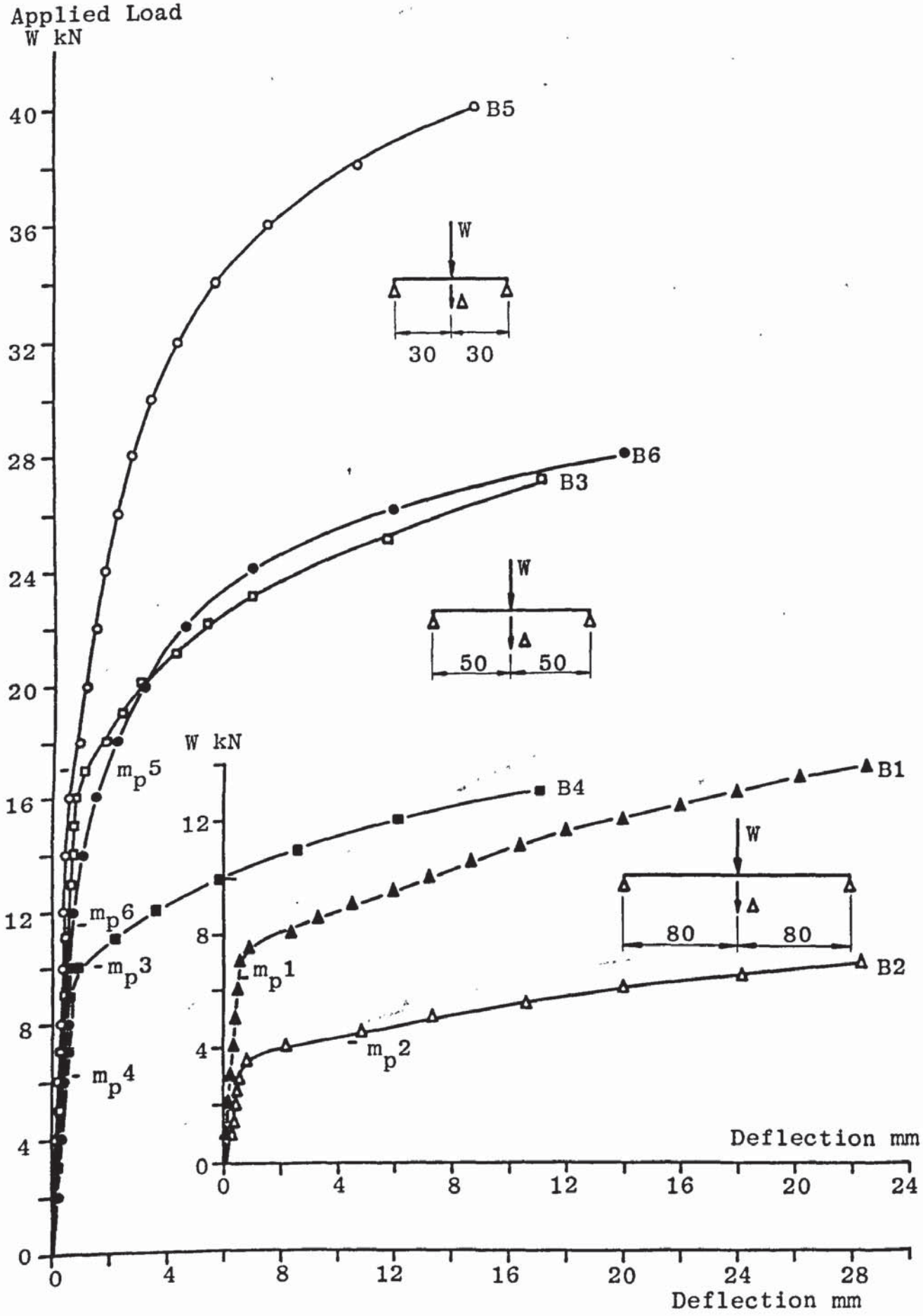

FIGURE 3.9 RELATIONSHIP BETWEEN LOAD AND DEFLECTION FOR STRIP BEAM TESTS

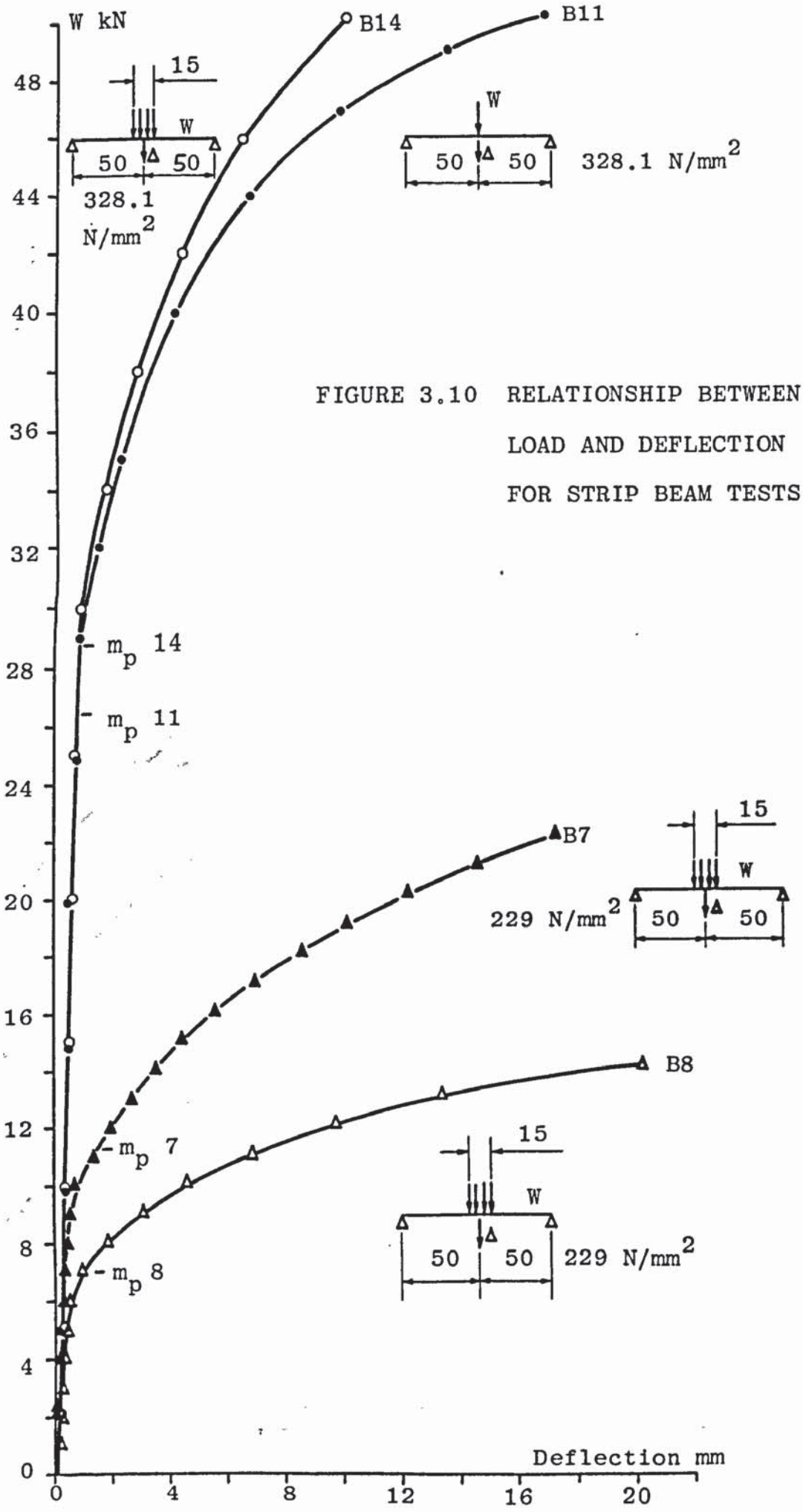

FIGURE 3.10 RELATIONSHIP BETWEEN LOAD AND DEFLECTION FOR STRIP BEAM TESTS

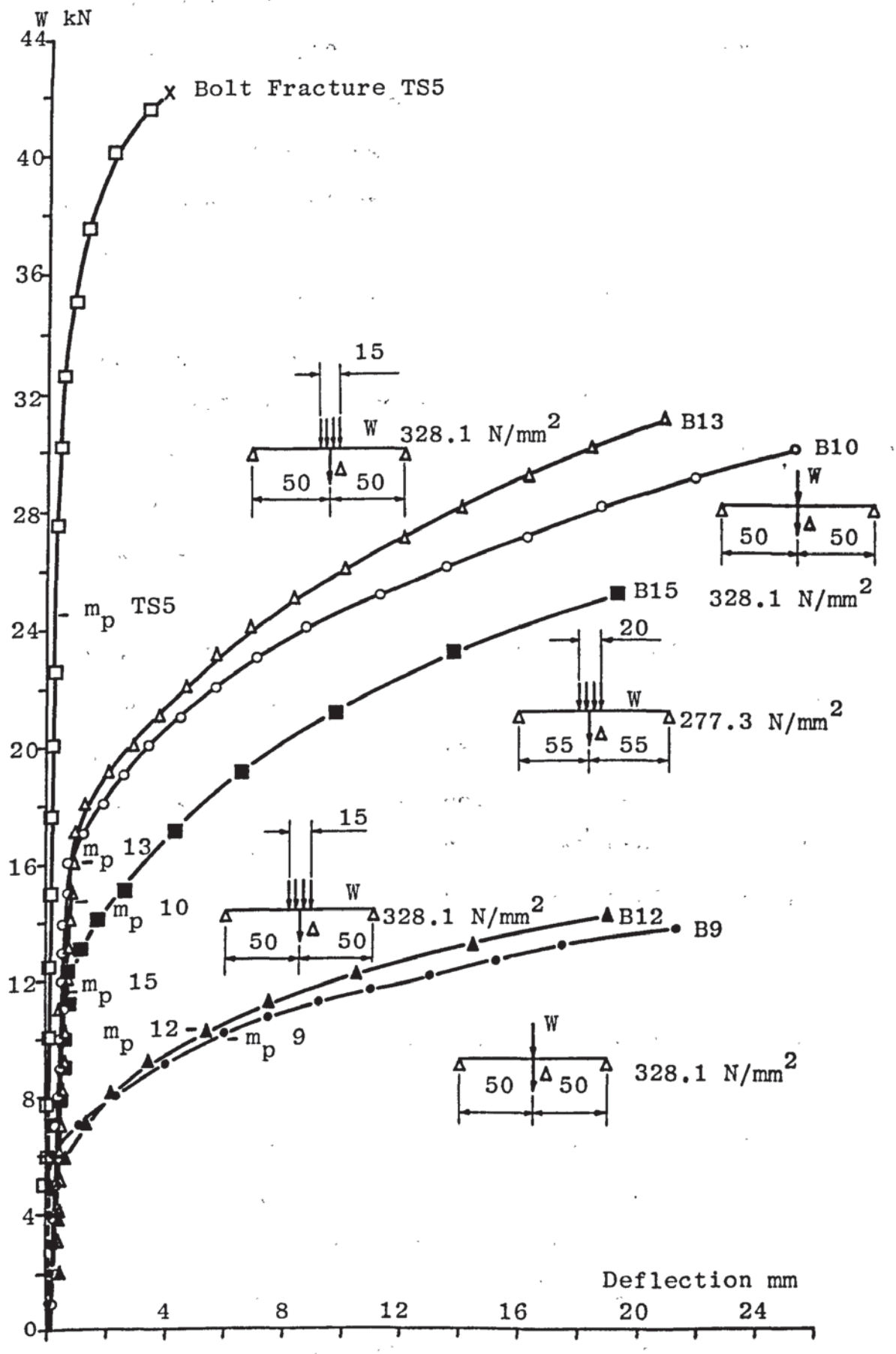

FIGURE 3.11 RELATIONSHIP BETWEEN LOAD AND DEFLECTION FOR STRIP BEAM TESTS

The load-deflection relationships of the strips are shown in Figures 3.9, 3.10 and 3.11 and the load at which the theoretical plastic hinge formed is indicated. It should be noted that for cases where l/t is small the moment of resistance of the plastic hinge is greater than m_p and is related to the deflection of the beam. It should also be noted that there is little difference between the load-deflection relationships of 328.1 N/mm^2 steel strips loaded via a central knife edge or partial UDL. In 229 N/mm^2 steel strips however there is a greater difference between the load-deflection relationships for these two types of loading arrangements.

Benham and Warnock[69] showed that the bending stresses, induced in a beam deformed by a concentrated load, were less than those associated with the simple bending theory and reduced as the span decreased. This does not confirm the results obtained from the 328.1 N/mm^2 steel strips but appears to be true for the 229 N/mm^2 steel strips although further investigation is needed.

The steel strip beams may be related to the tee stub tests if the dimension 2b in the tee stubs is assumed to approximate to the span 2l in the beam tests. The approximate deflections at the web of the tee stubs after failure are given in Table 3.3. Relating these deflections to the strip beam tests with 2b = 90mm the moments of resistance at the plastic hinges were determined from Figures 3.9,

Test No	t_p mm	b/t_p	Approximate Deflection mm	Moment of Resistance
TS1	20.1	2.24	5	1.4 m_p
TS2	12.5	3.60	9	2.6 m_p 2.0 m_p*
TS3	15.9	2.83	6	1.7 m_p
TS4	12.7	3.54	8.5	2.6 m_p 2.0 m_p*
TS5	15.4	2.93	4	1.5 m_p*

Note: * moments of resistance determined from strip tests with UDL

TABLE 3.3 DEFLECTION RECORDINGS AT FAILURE

3.10 and 3.11 considering specimens with a yield strength of 229 N/mm^2 and 277.3 N/mm^2 only. The corresponding moments of resistance are also given in Table 3.3. b/t_p values were linearly interpolated. The results from the strip tests indicate that for the tee stub tests the plastic moment of resistance at the plastic hinge adjacent to the web was not limited to m_p but increased as the value b/constant t_p decreased. The values are higher than the fixed value of 4/3 m_p given by de Back and Zoetemeijer[22].

The load deflection relationship for Test TS5 is also shown in Figure 3.11 although the applied load is related to a 20mm wide strip of flange plate i.e. actual load/10. The deflection of the tee stub is approximately linear and differs from the load-deflection relationship of the associated strip test B15. However, the moments of resistance obtained from the steel strip tests using the tee stub deflections at failure are similar to those obtained using the experimental values of F_{bu} and Q_{bu}.

CHAPTER FOUR

EXPERIMENTAL INVESTIGATION OF BEAM TO COLUMN CONNECTIONS

4.1 Introduction

The experiments dealt with in this chapter relate to a typical internal beam to column connection subject to static load. The joint consists of an extended welded end plate connected to the column flange with HSFG bolts. This type of connection has become popular in recent years and is common in many modern steel structures.

4.2 Test Specimens

The test rig shown in Figure 4.1 was used for twenty one beam to column connections subjected to varying moment to shear ratios. The maximum beam span L was approximately 1200mm to suit the laboratory facilities. The beam size selected was a 356 x 171 x 45 UB in order to avoid local flange buckling, lateral instability effects and plastic deformation. These factors have influenced the results of other investigations[11,17,21,32]. Full depth stiffeners, 12mm thick, were used at the points of support. The column section consisted of mild steel plates welded together and was preferred to a rolled 200 x 200 UC due to the variation present in column flange dimensions within that serial size. The variation in web thickness also might have caused pre-

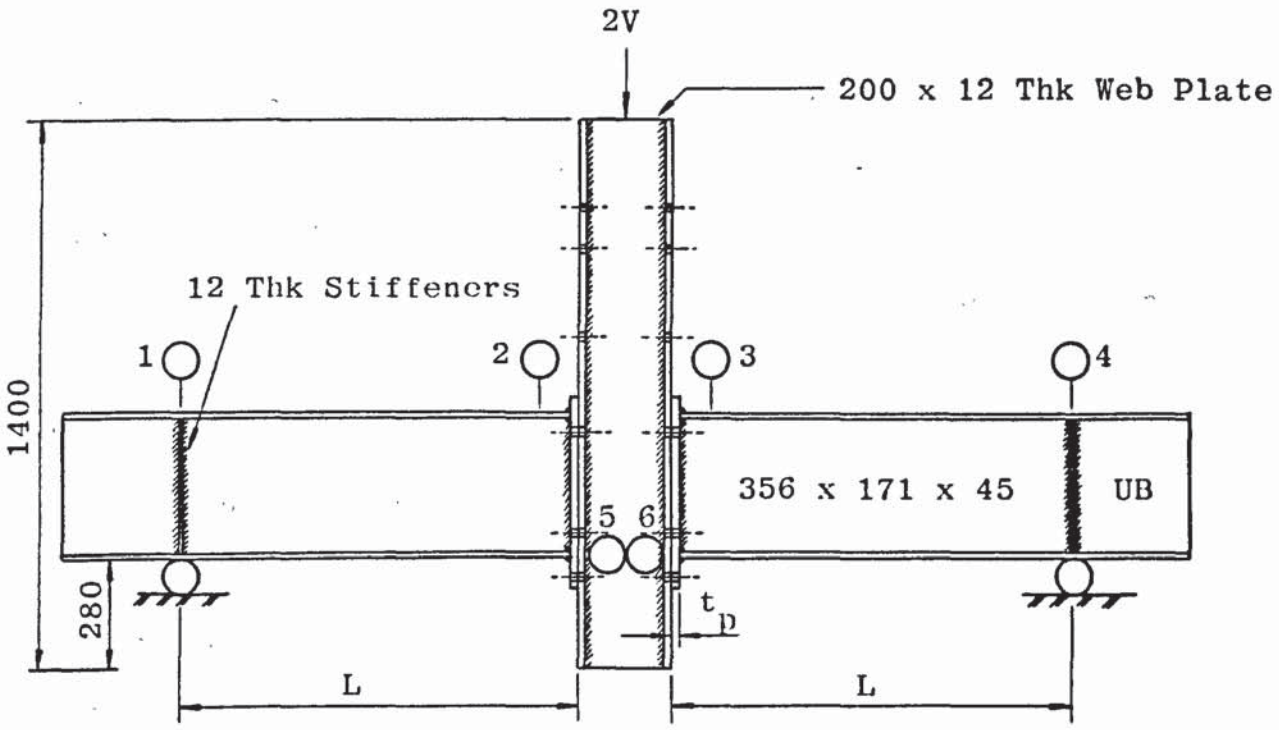

(a) Test Specimen

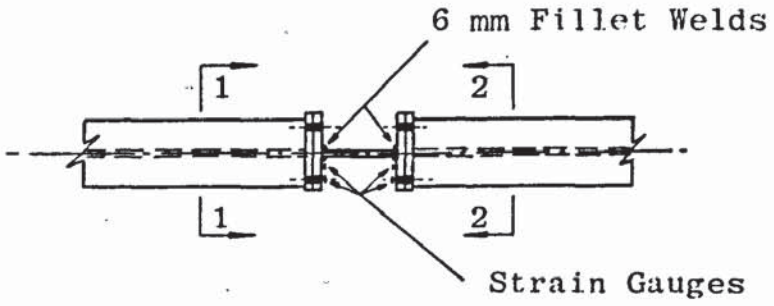

(b) Plan on Test Specimen

(c) Section 1-1

(d) Section 2-2

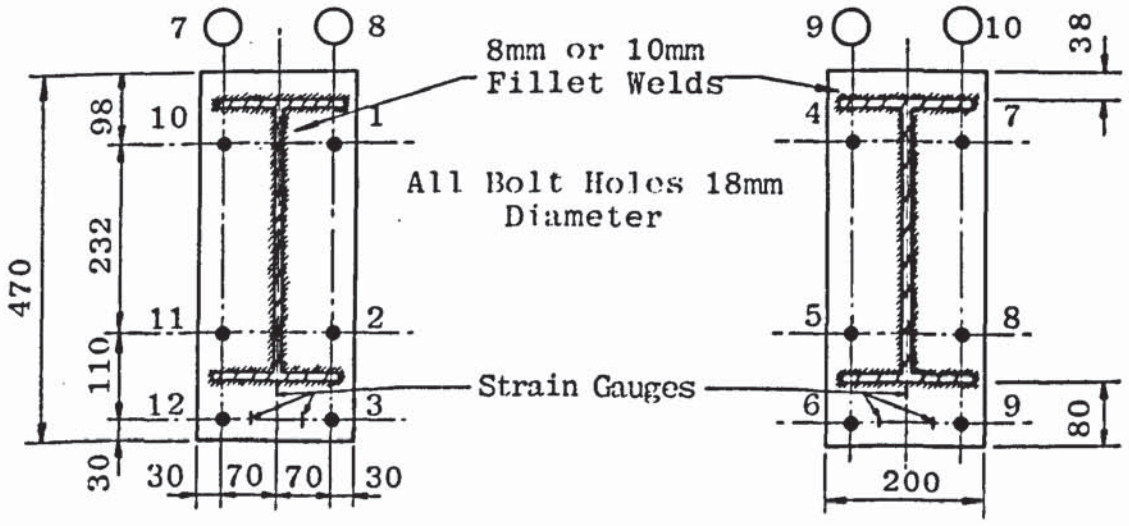

FIGURE 4.1 TEST RIG FOR BEAM TO COLUMN CONNECTIONS

mature failure due to its instability, therefore the web plate thickness was kept constant at 12mm. No stiffeners were used within the column depth. This was acceptable using the equations of Chen and Newlin[70] for column web strength and buckling. Chen and Newlin[70] showed that these equations produced conservative results. The maximum beam flange force was taken at the elastic limit of the beam. The cruciform arrangement ensured that no shear deformation occurred in the column. Each column was fabricated so that two tests could be performed with each by simply reversing the section. The edge distance to all bolt holes was 30mm in accordance with BS449[4]. The horizontal bolt pitch was 140mm as recommended in the Steel Designers Manual[44]. Each joint had six bolts, two placed close to the compression flange while the remaining four were symmetrically placed around the tension flange. The bolts within the depth of the beam were symmetrically placed around the x-x axis of the beam. M16 HSFG bolts were used from the same batch as those used for the single bolt and tee stub tests reported earlier. All bolts were tightened to an initial shank tension of 75 kN. Each bolt had a hardened steel washer placed under the bolt head and nut. 8mm or 10mm fillet welds were used for connecting the end plate to the beam section. The test specimens were of grade 43A mild steel to BS4360[66].

Four beams were initially fabricated for each test series, two at 1100mm length and two at 1500mm length. A maximum

number of three tests were obtained from the 1500mm lengths. A maximum number of two tests were obtained from the 1100mm lengths. After each test the end plate and at least 200mm of the beam length were removed by sawing. This ensured that any plastic deformation in the beam was removed. An end plate was then welded to the remaining length. This process enabled one specimen to be tested while the other was fabricated, thus optimizing the time available.

4.3 Instrumentation

The rotation of each joint was found from readings taken from dial gauges 1, 2, 3 and 4 in Figure 4.1. Each dial gauge was graduated in 0.01mm increments. Magnetic dial gauges 5 and 6 in Figure 4.1 were positioned on one side of the column web to record column flange deformations at the toe, opposite the beam tension flange. Each dial gauge was graduated in 0.01mm increments. Slip readings were recorded on magnetic dial gauges 7, 8, 9 and 10 in Figure 4.1 for each vertical row of bolts. These dial gauges were graduated in 0.002mm increments. All the bolts were installed so that slip was possible. Each bolt had a demec spot attached to the bolt head and toe with epoxy resin. These spots enabled bolt extensions to be measured during tightening and testing and the appropriate forces found from the calibration graph in Chapter Two.

On the extended portion of the end plate FLA-3-11 3mm

electrical resistance strain gauges were attached adjacent to the weld and at the bolt line, to detect yielding of the plate. Similar strain gauges were attached opposite the beam tension flange on the inside face of the column flange, adjacent to the weld and at the bolt line. The number and position of the strain gauges on the column flange varied for each test series. More information concerning this will be given later. Strain gauge wires were connected to the extension box of a Peekel from which strain readings were recorded. Each connection was given a coating of 'snowcem' so that any yield line patterns in the end plate and column flange could be observed. Each test specimen was placed on two greased roller supports. Load was applied from a 1000 kN hydraulic ram via a knife edge to the centre of a cap plate attached to the top of the column. A general view of the test rig before testing is shown in Plate 4.1.

4.4. Experimental Results

The joints tested were divided into six series of connections with varying end plate and column flange thickness. In each series there was a maximum number of five joints, each with a different beam span, i.e. moment to shear ratio. Steel was ordered in three batches. Firstly for the exploratory tests P1 and P2. Secondly for connection series CS1 and CS2 and, finally, for connection series CS3, CS4 and CS5. Straight tensile test specimens were cut from each

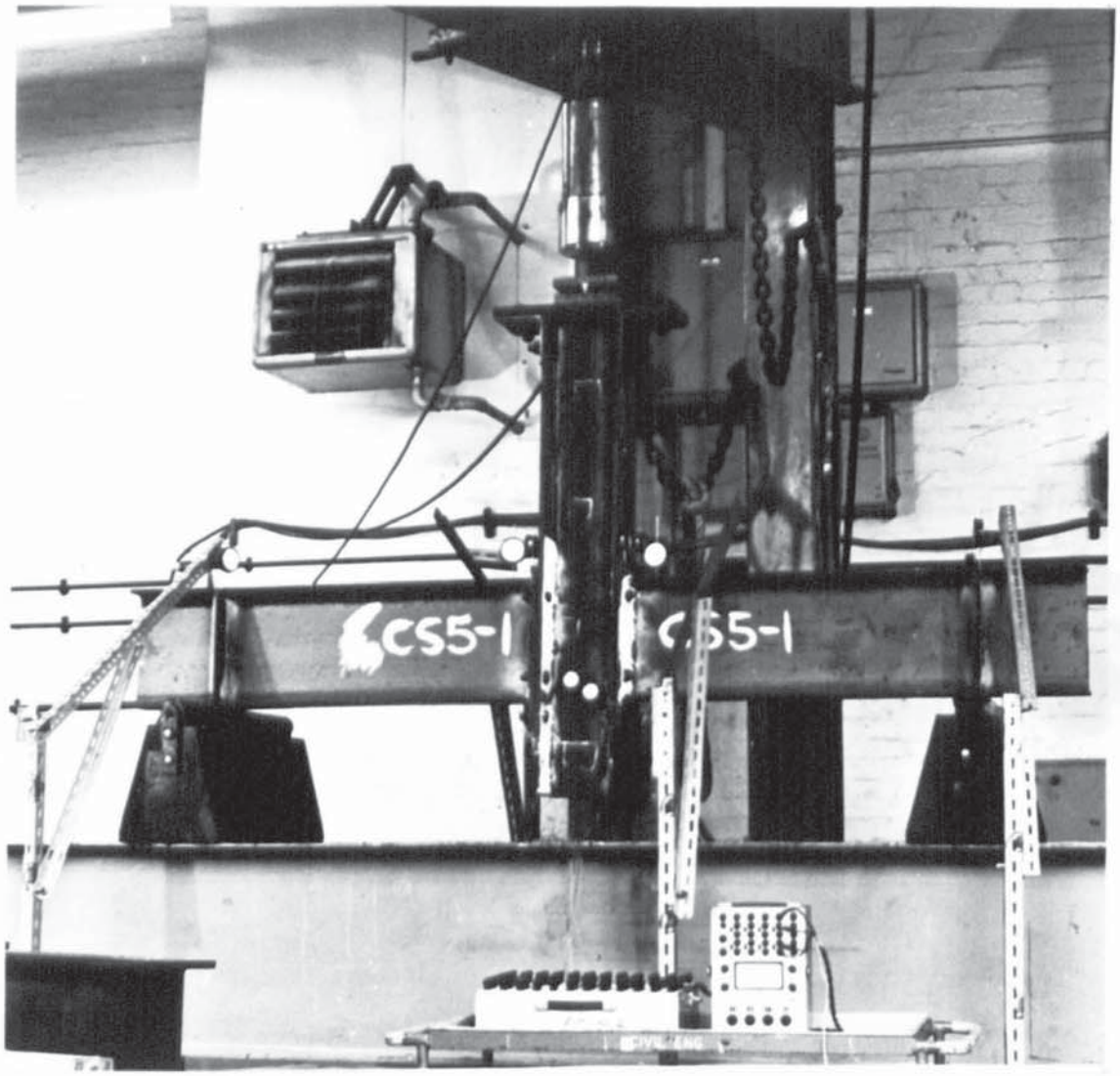

PLATE 4.1 GENERAL VIEW OF TEST RIG FOR BEAM TO COLUMN CONNECTIONS

flat strip plate and beam length delivered. The specimens were machined parallel and tested in direct tension and the yield stresses computed from load extension graphical outputs using a Baldwin strain plotter. The test results for the three steel batches are given in Tables A4.1, A4.2, A4.3 and A4.4.

4.4.1 Exploratory Tests P1 and P2

Tests P1 and P2 were considered exploratory and details of the specimens are given in Table 4.1. All welds were 10mm fillets. The object of these tests was to examine the suitability of the test rig. For this reason test P1 was not instrumented except for tightening the bolts to an initial shank tension of 75 kN. 'Snowcem' was applied to the connection in an attempt to establish the applied load at yield and yield patterns. This load was difficult to determine from the brittle coating and strain gauges were used to determine yield in subsequent tests.

Test P2 was not fully instrumented, flange deformation and slip values were not recorded. Two 3mm strain gauges were attached to each inside face of the column adjacent to the weld and at the bolt line opposite the beam tension flange. Bolt extensions and dial gauge readings were recorded at regular intervals during testing. The applied moment-rotation relationship and bolt force-applied moment relationship for joint P2 are shown in Figures 4.2 and 4.3 respectively.

Test No.	P1	P2	CS1-1	CS1-2	CS1-3	CS1-4	CS1-5
t_p mm	12	20	15	15	15	15	15
t_c mm	20	20	15	15	15	15	15
L mm	1.200	1.120	1.216	1.015	0.810	0.565	0.315
σ_{py} N/mm^2	347.6	238.4	229.0	229.0	229.0	229.0	229.0
σ_{cy} N/mm^2	238.4	238.4	229.0	229.0	229.0	229.0	229.0
LRM Rotation rads $x10^{-3}$	-	29.06	67.04	68.52	41.98	49.22	2.58
LRM Col. Flg. Deform. mm	-	-	12.02	12.95	11.38	13.47	1.31
LRM Slip - Deform. mm	-	-	0.242	0.166	0.267	0.504	1.994
M_u kNm	218.3	196.0	176.3	164.4	160.5	167.5	135.8*
V_u kN	181.9	175.0	145.0	162.0	198.1	296.5	431.1*
Q_u kN	—	58.4	72.3	99.8	108.8	92.6	*
Mode of Failure	BF	BF	BF, EPF CFF	BF	CFF	BF	*

Abbreviations used: LRM, Last Recorded Mean; BF, Bolt Fracture; EPF, End Plate Fracture; CFF, Column Flange Fracture; *, Test discontinued due to damage to hydraulic ram.

TABLE 4.1 EXPERIMENTAL RESULTS FOR BEAM TO COLUMN CONNECTIONS P1, P2 AND SERIES CS1

Abbreviations used: EP, First Yield Weld Line End Plate; CF, First Yield Weld Line Column Flange

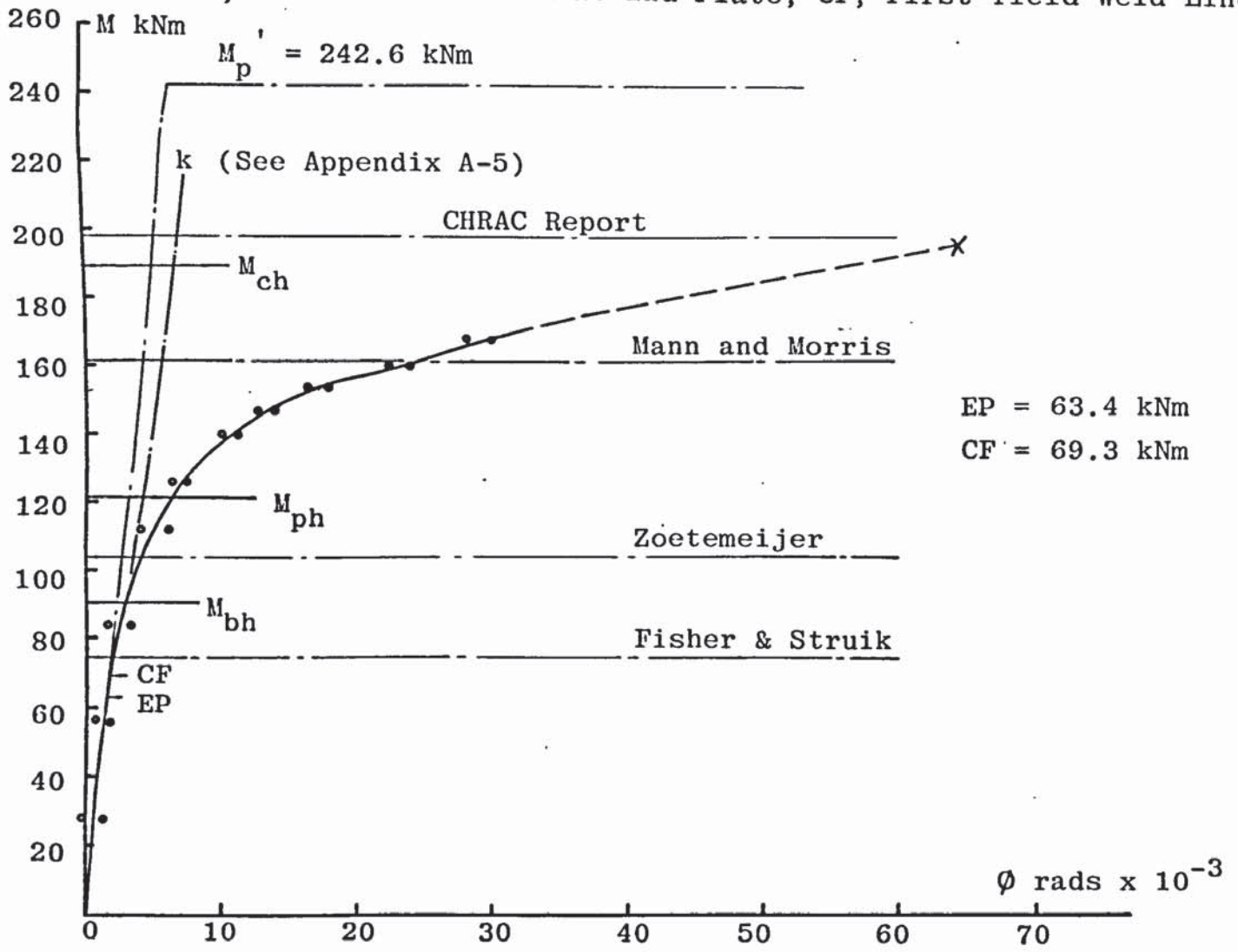

FIGURE 4.2 APPLIED MOMENT-ROTATION RELATIONSHIP FOR TEST P2

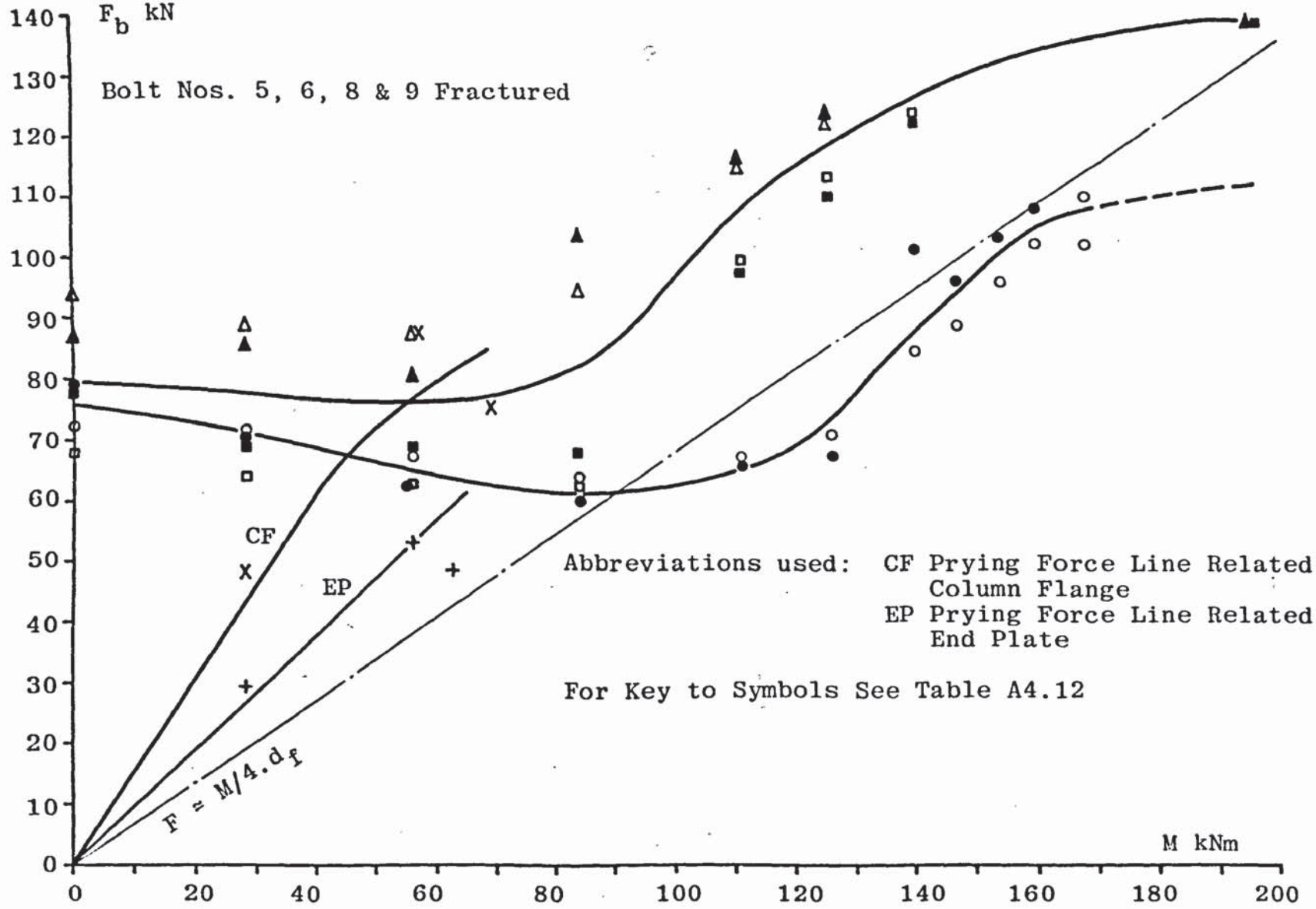

FIGURE 4.3 APPLIED MOMENT - BOLT FORCE RELATIONSHIP FOR TEST P2

The average moments at which first yield was obtained from the strain gauges adjacent to the welds of the end plate and column flange are indicated on Figure 4.2. At ultimate load tensile bolt fracture occurred.

4.4.2 Connection Series CS1

The test rig proved satisfactory therefore the member sizes were kept the same for connection series CS1. The column welds were reduced to 6mm fillets while the end plate profile fillet weld remained at 10mm. This series consisted of five tests with a 15mm thick end plate and column flange. Details of the test specimens are given in Table 4.1. Each test was fully instrumented. From the results of P2 it was considered that a strain gauge along the bolt line of the column flange was not necessary. Therefore only one strain gauge was used on each column face adjacent to the weld line opposite the beam tension flange.

The moment-rotation relationship, bolt force-applied moment relationship and moment-column flange deformation relationship for test CS1-1 are shown in Figures 4.4, 4.5 and 4.6 respectively. The shear force-slip relationship for this test is included in Figure 4.6. The experimental results for the other four tests in this series are shown in Appendix A-4. The average moments at which first yield was obtained from the strain gauges adjacent to the welds of the end plate and column flange for test CS1-1 are

Abbreviations used: EP, First Yield Weld Line End Plate; CF, First Yield Weld Line Column Flange

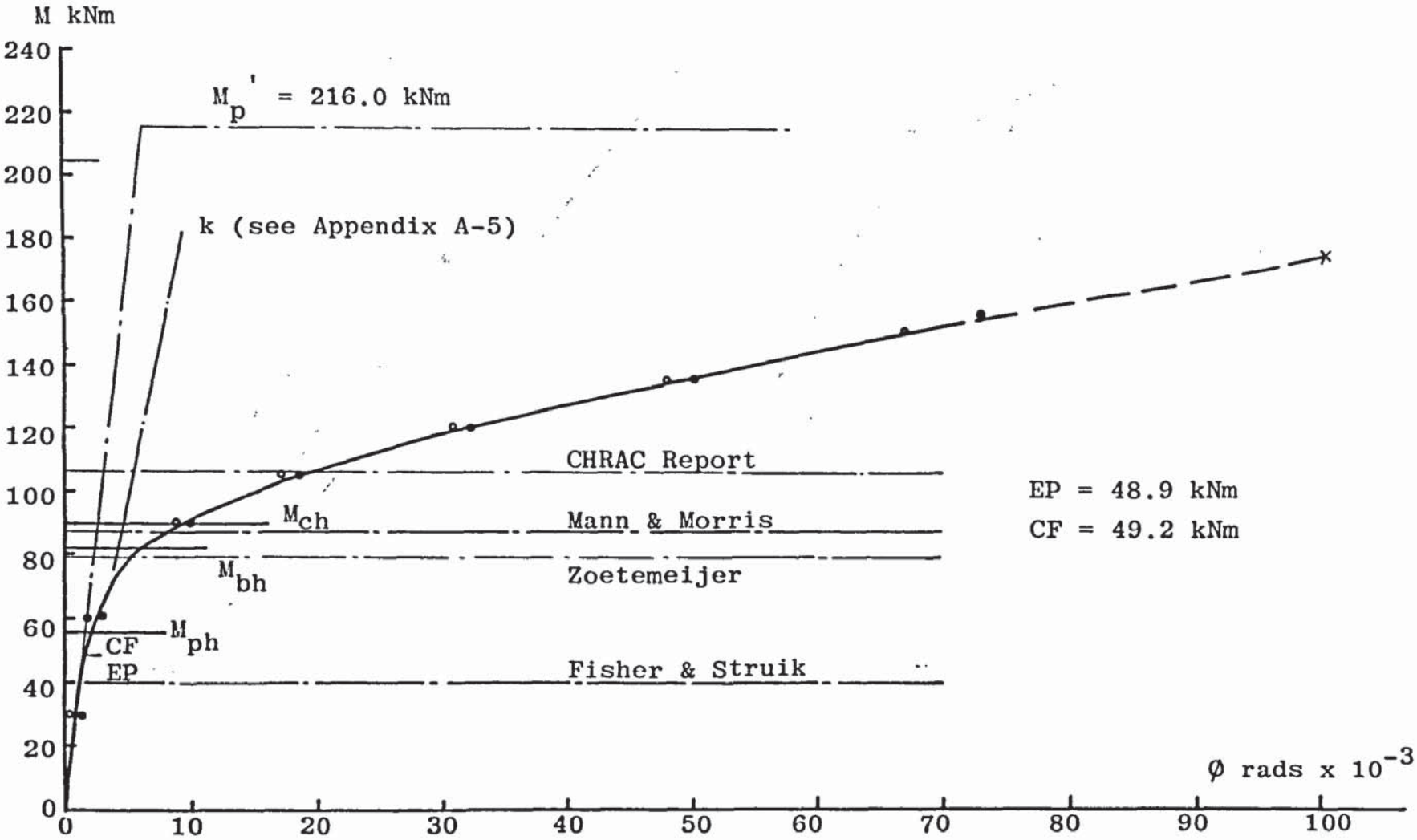

FIGURE 4.4 APPLIED MOMENT-ROTATION RELATIONSHIP FOR TEST CS1-1

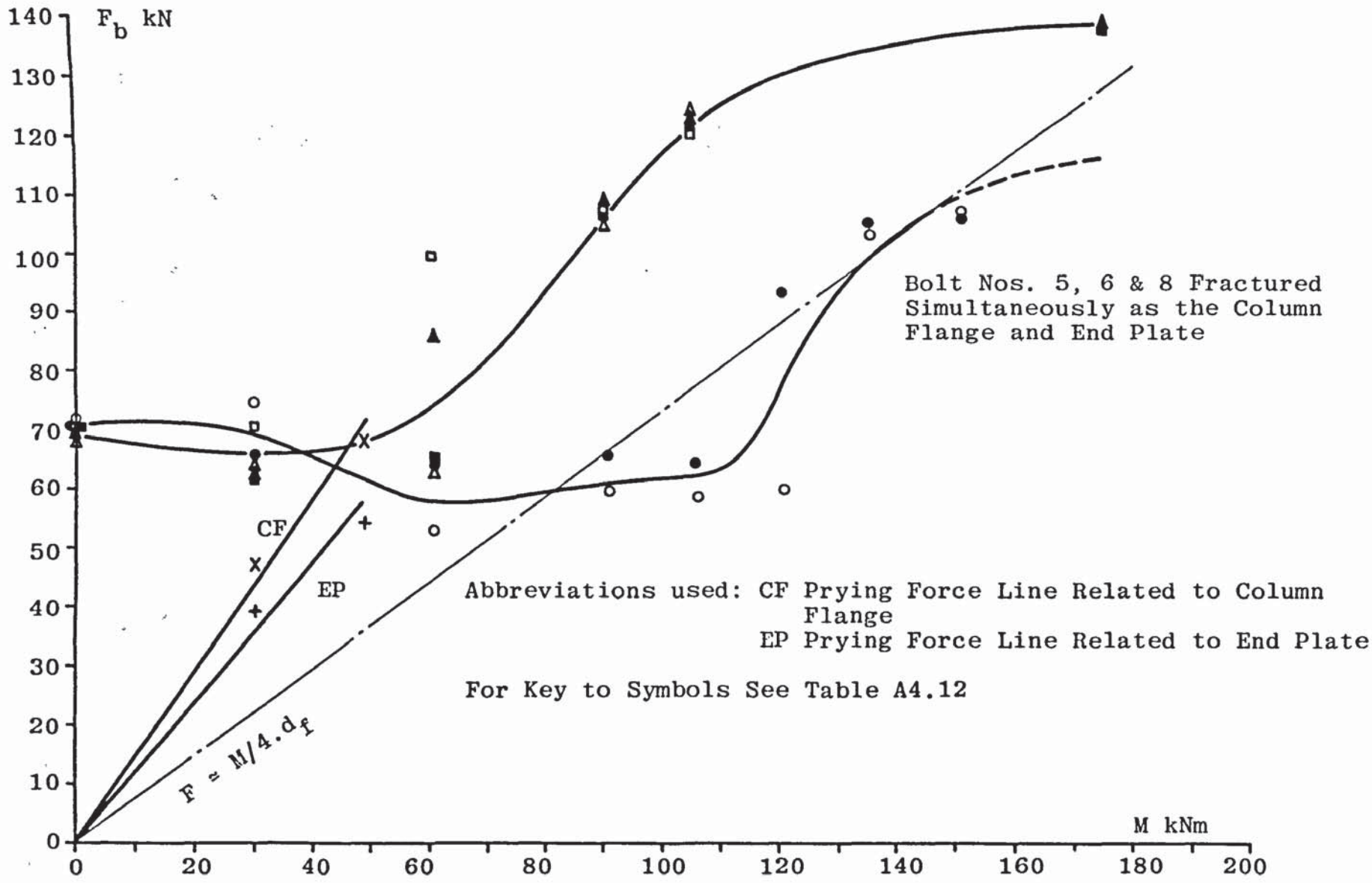

FIGURE 4.5 APPLIED MOMENT - BOLT FORCE RELATIONSHIP FOR TEST CS1-1

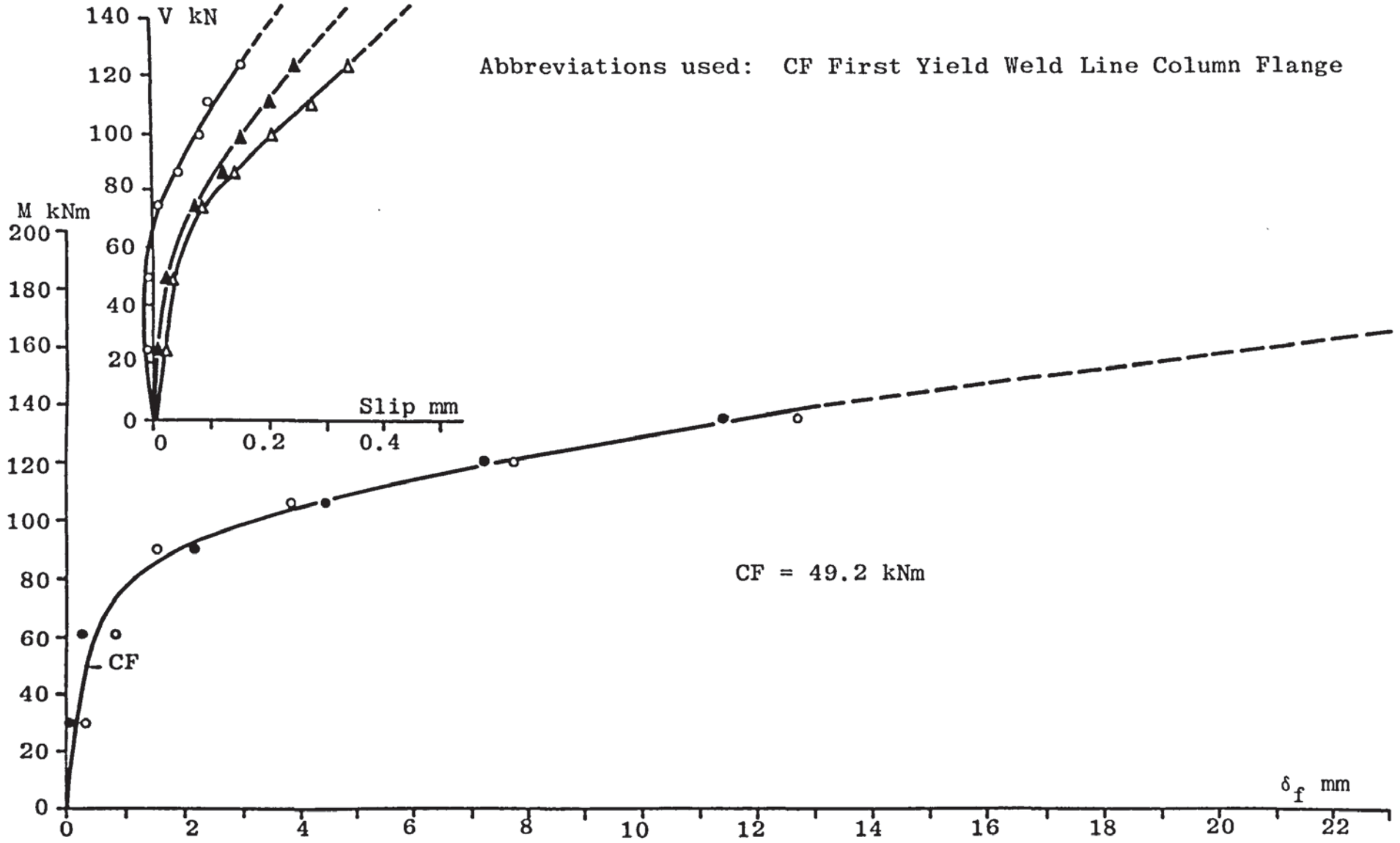

FIGURE 4.6 APPLIED MOMENT - COLUMN FLANGE DEFLECTION RELATIONSHIP AND SHEAR FORCE - SLIP RELATIONSHIP FOR TEST CS1-1

indicated on Figures 4.4 and 4.6. These moments for the other four tests are also indicated on the graphical results shown in Appendix A-4. There was a large initial increase in bolt force around the tension zone of tests CS1-3 and CS1-4 compared with the other three tests in this series. This may have been due to plate distortion caused by heat losses after welding, especially on the less stiff regions i.e. column flanges and extended portion of end plate. This would result in the end plate not being flush with the column flange, although every effort was made to minimize this effect. Therefore after tightening there may have been little or no compressive force between the end plate and column flange at the bolt positions. This could result in large bolt forces at the early stages of loading.

In tests CS1-2 and CS1-4 bolt fracture occurred. A fracture approximately 200mm long adjacent to the weld line of the column flange opposite the beam tension flange took place in test CS1-3. A similar fracture occurred in test CS1-1 together with a fracture approximately 100mm long adjacent to the weld of the extended portion of the end plate. Bolt fracture also occurred in this test. In test CS1-5 where the moment to shear ratio was small the bolts slipped into bearing during the test with a loud retort. Experimental readings were stopped shortly after slip occurred as a safety precaution and dial gauges etc. removed from the test area. Load was applied at regular intervals until the bolts securing the casing around the bottom of

CS1-1

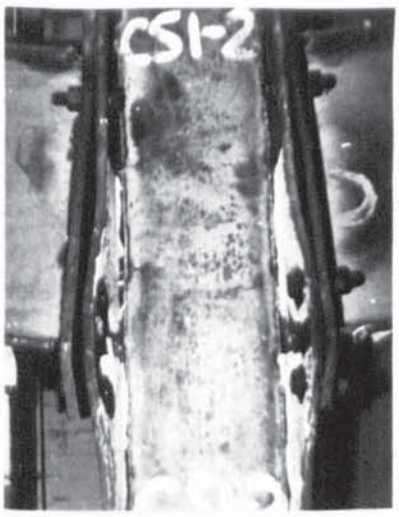

CS1-2

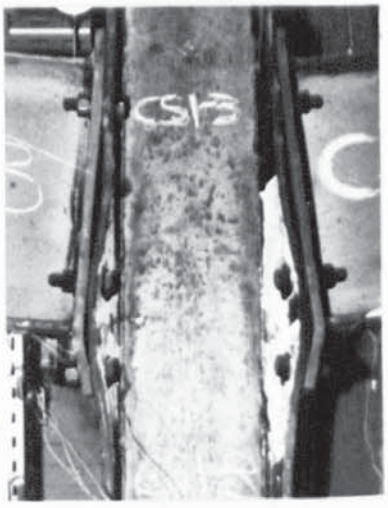

CS1-3

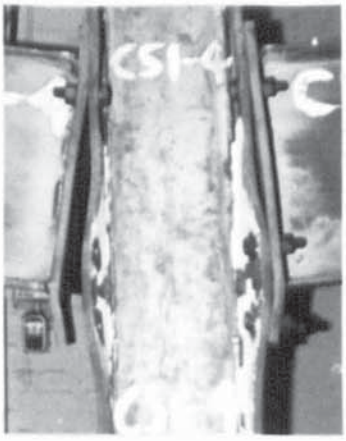

CS1-4

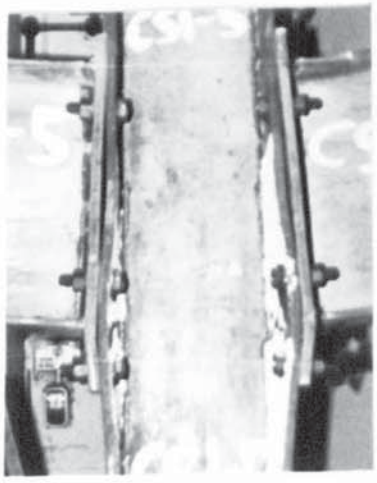

CS1-5

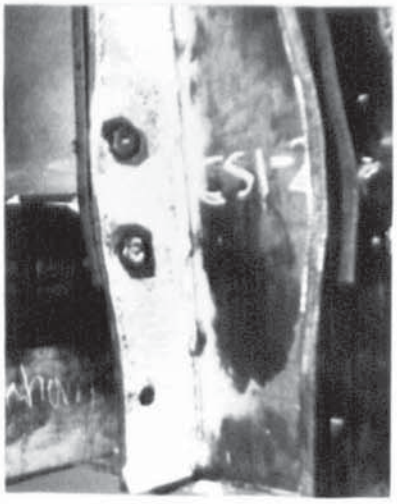

Typical Column Flange
Yield Pattern

PLATE 4.2 TEST SPECIMENS FOR SERIES CS1 AFTER FAILURE

CS1-4 TOP

CS1-5 TOP

CS1-4 MIDDLE

CS1-5 MIDDLE

CS1-4 BOTTOM

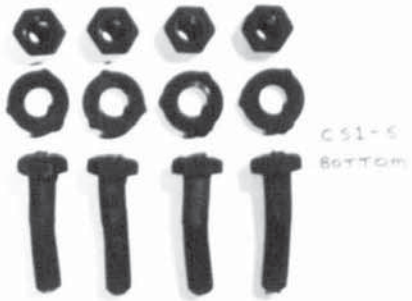

CS1-5 BOTTOM

PLATE 4.3 TYPICAL BOLT DEFORMATIONS FOR TEST SERIES CS1

the hydraulic ram sheared. At this stage the test was discontinued. The effect of slip on the moment-rotation characteristics of this joint may be seen from Figure A4-11.

The test specimens after failure are shown in Plate 4.2. A typical yield pattern in the 'snowcem' for the inside face of a column flange in this series is also shown in Plate 4.2. Bolt deformations for test CS1-4, a typical joint where slip did not occur, are shown in Plate 4.3. Bolt deformations for test CS1-5 where slip did occur are also shown in Plate 4.3. Bolts termed top, middle and bottom in Plate 4.3 refer to their location in the connection. Top, refers to the compression zone bolts. Middle, refers to the tension zone bolts within the beam depth. Bottom, refers to the tension zone bolts outside the beam depth.

4.4.3 Connection Series CS2

This series consisted of five tests with steel from the same batch as series CS1. Column flanges were machined down to approximately 12mm thick on the outside surface only. These plates were welded to the column web with 6mm fillets. The end plate remained at 15mm thick but the weld size was reduced to an 8mm fillet to reduce heat distortion. Details of the test specimens are given in Table 4.2. Strain gauges were attached to the column flanges adjacent to the weld line and at the bolt line opposite the beam tension flange.

Test No	CS2-1	CS2-2	CS2-3	CS2-4	CS2-5
t_p mm	15	15	15	15	15
t_c mm	11.8	11.95	12.0	11.74	11.6
L m	1.218	1.010	0.815	0.565	0.317
σ_{py} N/mm^2	229.0	229.0	229.0	229.0	229.0
σ_{cy} N/mm^2	229.0	229.0	229.0	229.0	229.0
LRM Rotation rads $x10^{-3}$	58.04	67.65	54.56	55.58	37.45
LRM Col. Flg. Deform. mm	16.93	24.22	16.20	18.98	16.90
LRM Slip - Deform mm	0.273	0.303	0.261	0.517	2.606
M_u kNm	163.9	163.6	164.5	159.1	106.6*
V_u kN	134.6	162.0	201.8	281.6	336.4*
Q_u kN	101.0	101.7	99.6	112.1	*
Mode of failure	BF,CFF	BF	CFF	BF,CFF	*

Abbreviations used: LRM, Last Recorded Mean; BF, Bolt Fracture; CFF, Column Flange Fracture; *, Test discontinued due to damage to hydraulic ram

TABLE 4.2 EXPERIMENTAL RESULTS FOR BEAM TO COLUMN CONNECTION SERIES CS2

The moment-rotation relationship, bolt force-applied moment relationship and moment-column flange deformation relationship for a typical test CS2-2 are shown in Figures 4.7, 4.8 and 4.9 respectively. The shear force-slip relationship for this test is included in Figure 4.9. The graphical results for the other four tests in this series are shown in Appendix A-4. The average moments at which first yield was obtained from the strain gauges are indicated on these figures. Large initial increases in bolt force around the tension zone occurred in tests CS2-1 and CS2-4. This was probably due to the loss of compression between the plates at the bolt positions due to heat distortion although the end plate weld size was reduced to minimize this effect.

A fracture approximately 200mm long adjacent to the weld line of the column flange occurred in tests CS2-1 and CS2-3 similar to two tests in series CS1. Similar fractures at ultimate load took place in both column flanges of test CS2-4. Bolt fracture also occurred in tests CS2-1, CS2-2 and CS2-4. In test CS2-5 the bolts slipped into bearing during the test. From Figure A4-27 it can be seen that the right hand side joint slipped suddenly while the left hand side joint gradually slipped into bearing. Damage to the hydraulic ram similar to test CS1-5 forced test CS2-5 to be discontinued before failure occurred.

The test specimens after failure are shown in Plates 4.4 and 4.5 A typical yield pattern in the 'snowcem' for the

Abbreviations used: EP, First Yield Weld Line End Plate; CF, First Yield Weld Line Column Flange; CFB, First Yield Bolt Line Column Flange

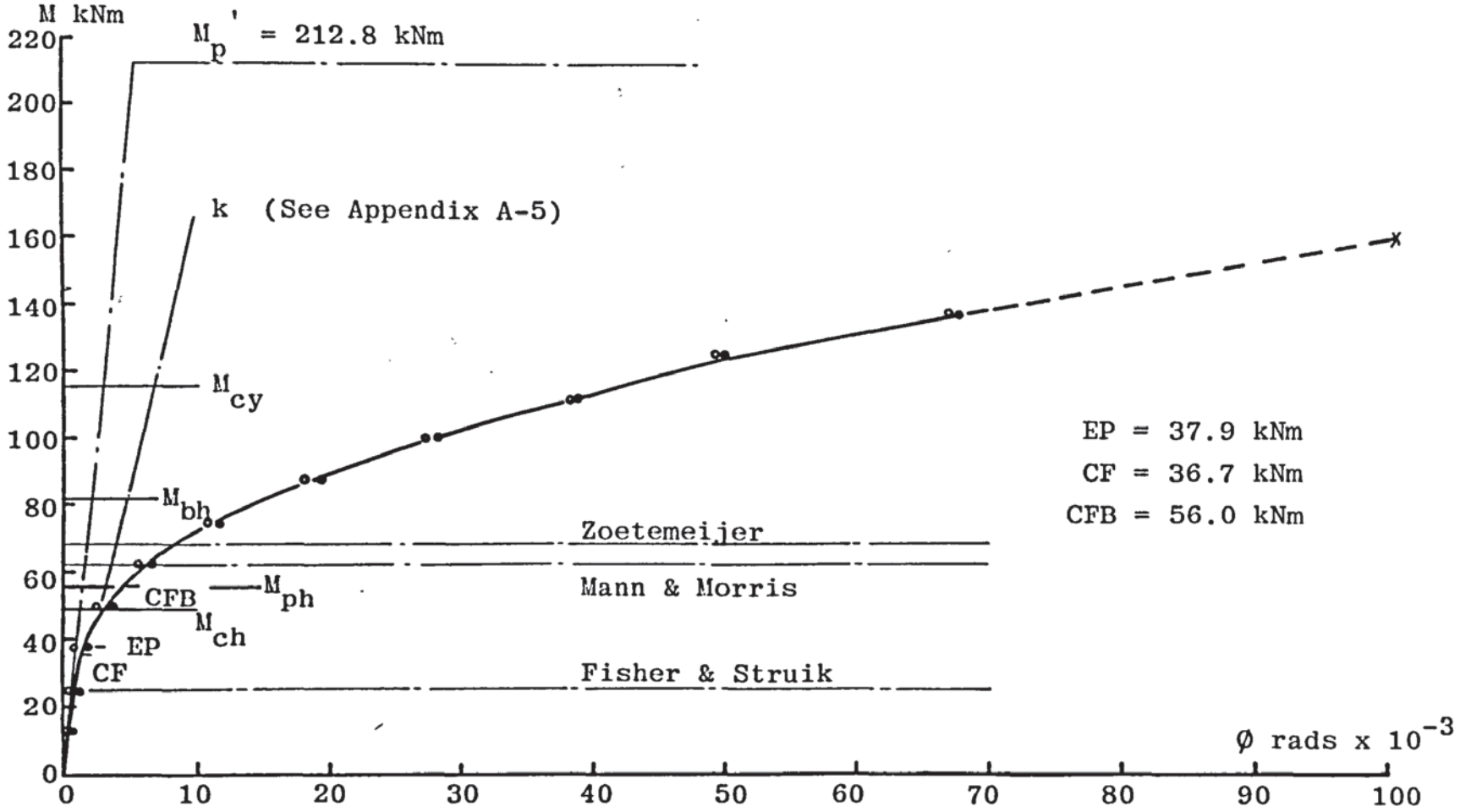

FIGURE 4.7 APPLIED MOMENT-ROTATION RELATIONSHIP FOR TEST CS2-2

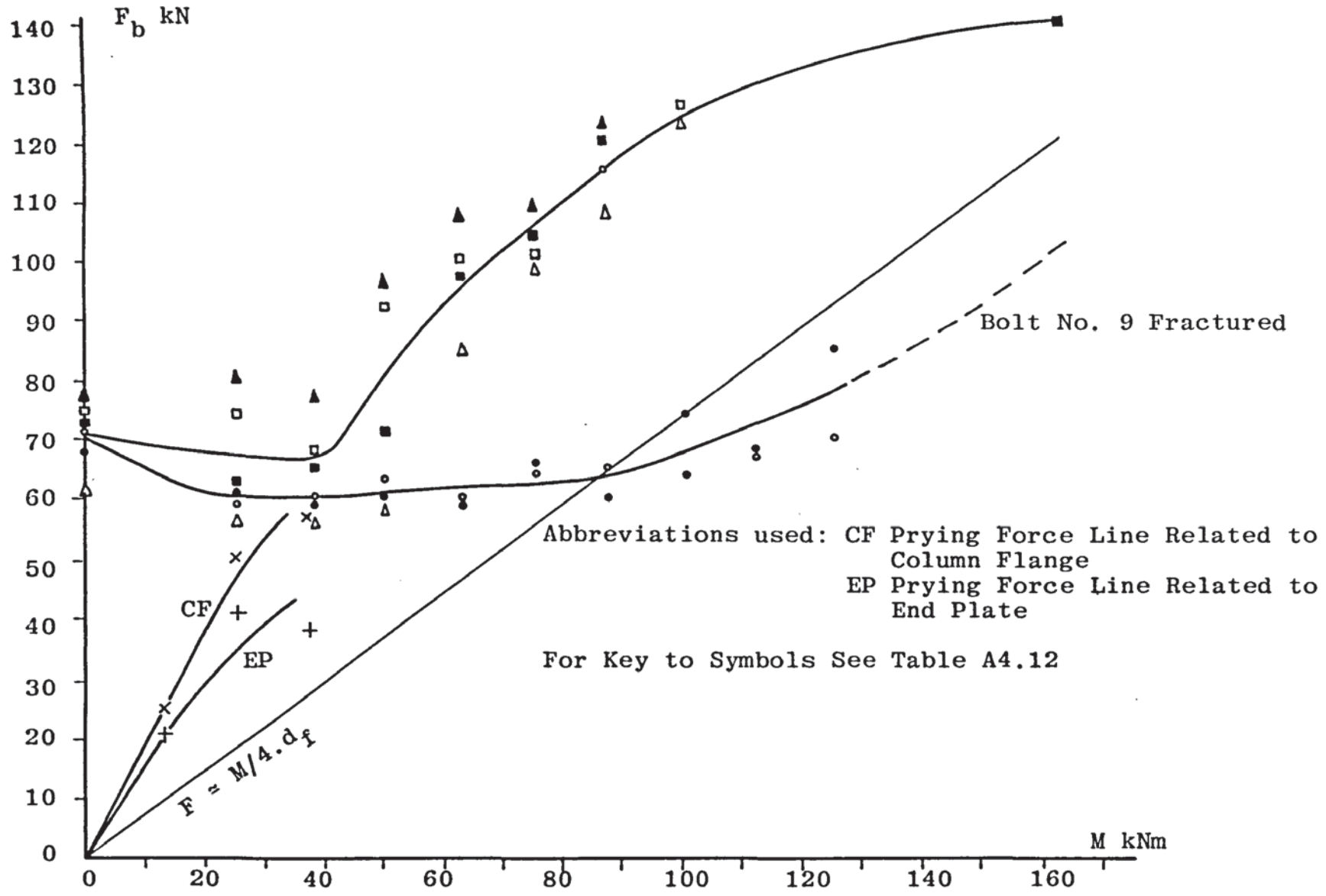

FIGURE 4.8 APPLIED MOMENT - BOLT FORCE RELATIONSHIP FOR TEST CS2-2

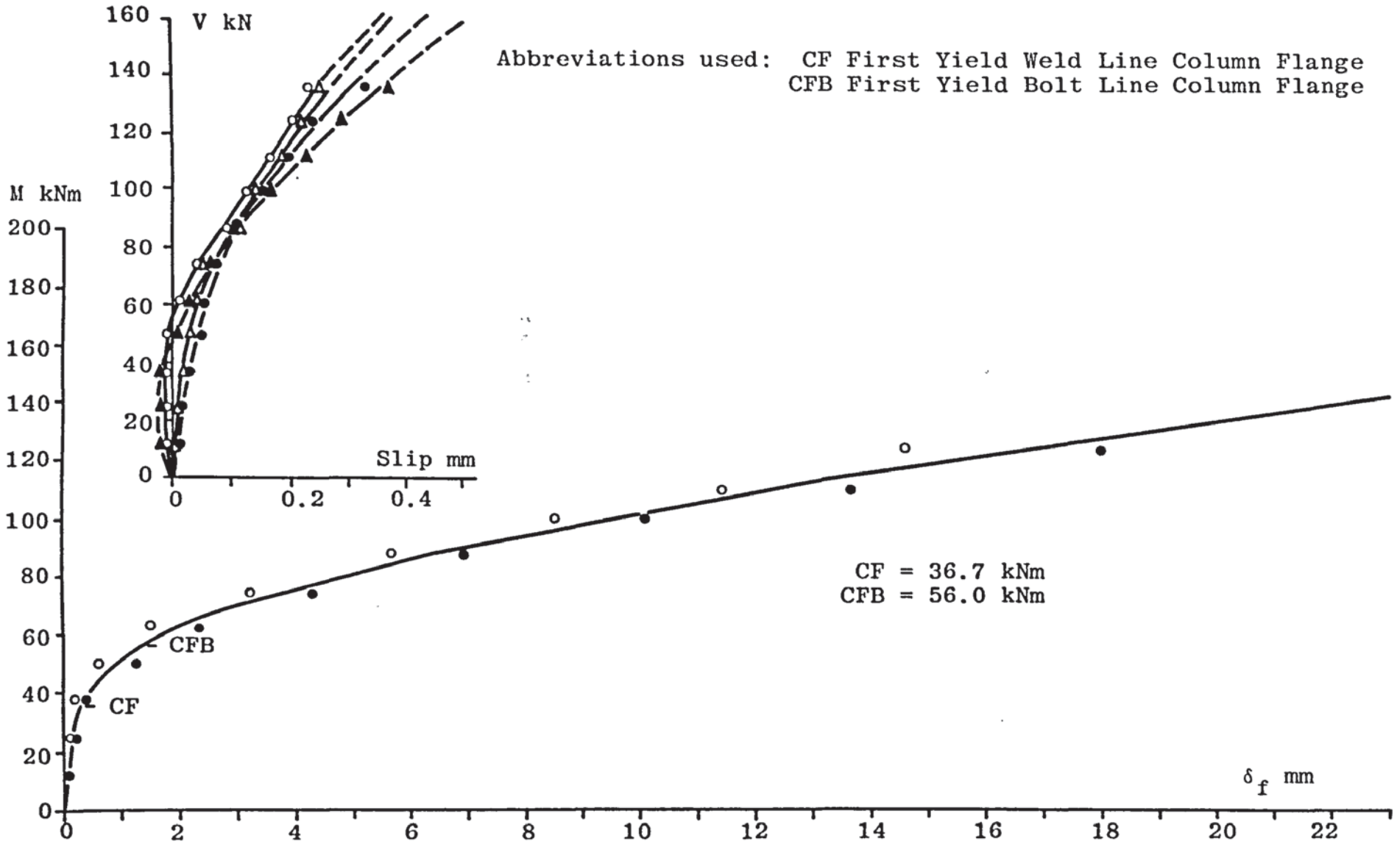

FIGURE 4.9 APPLIED MOMENT - COLUMN FLANGE DEFLECTION RELATIONSHIP AND SHEAR FORCE - SLIP RELATIONSHIP FOR TEST CS2-2

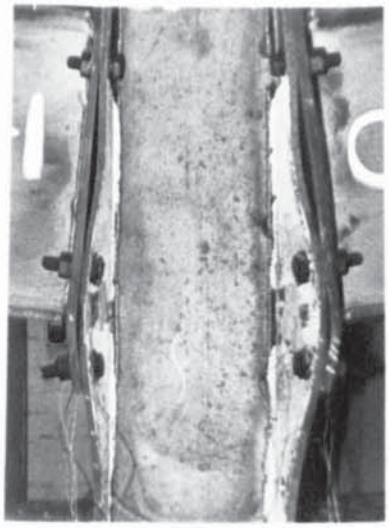

CS2-1

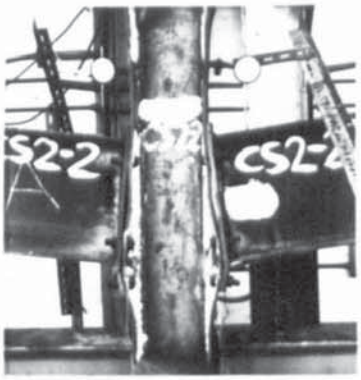

CS2-2

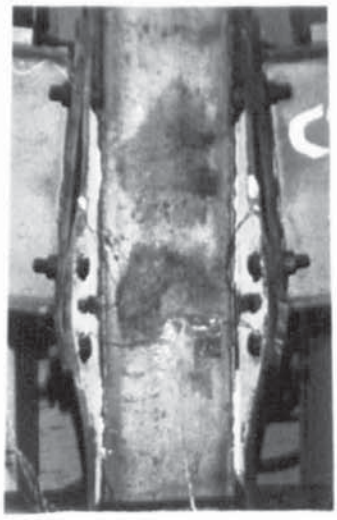

CS2-3

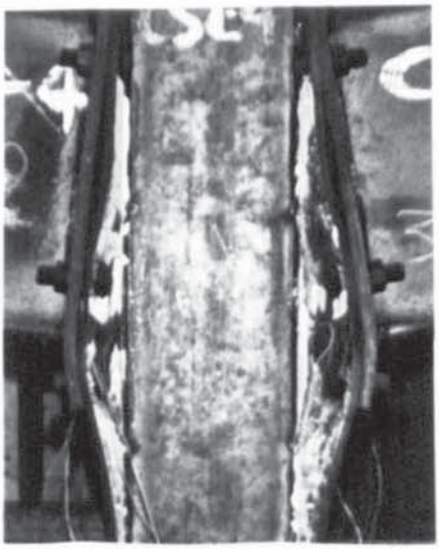

CS2-4

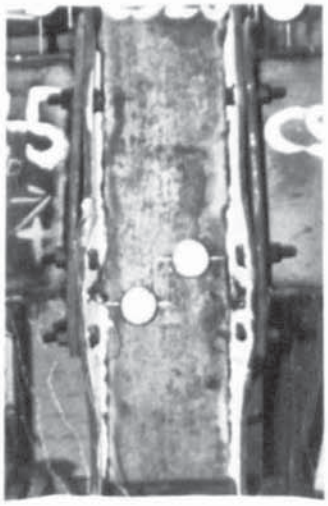

CS2-5

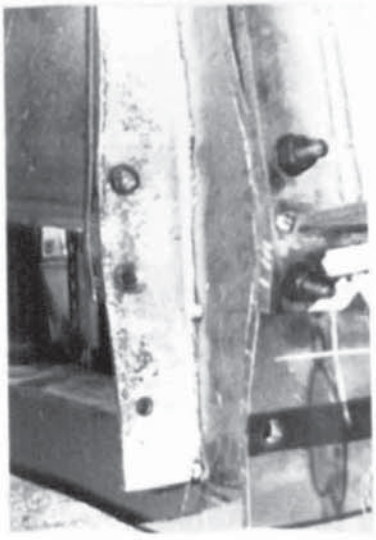

Typical Column Flange
Yield Pattern

PLATE 4.4 TEST SPECIMENS FOR SERIES CS2 AFTER FAILURE

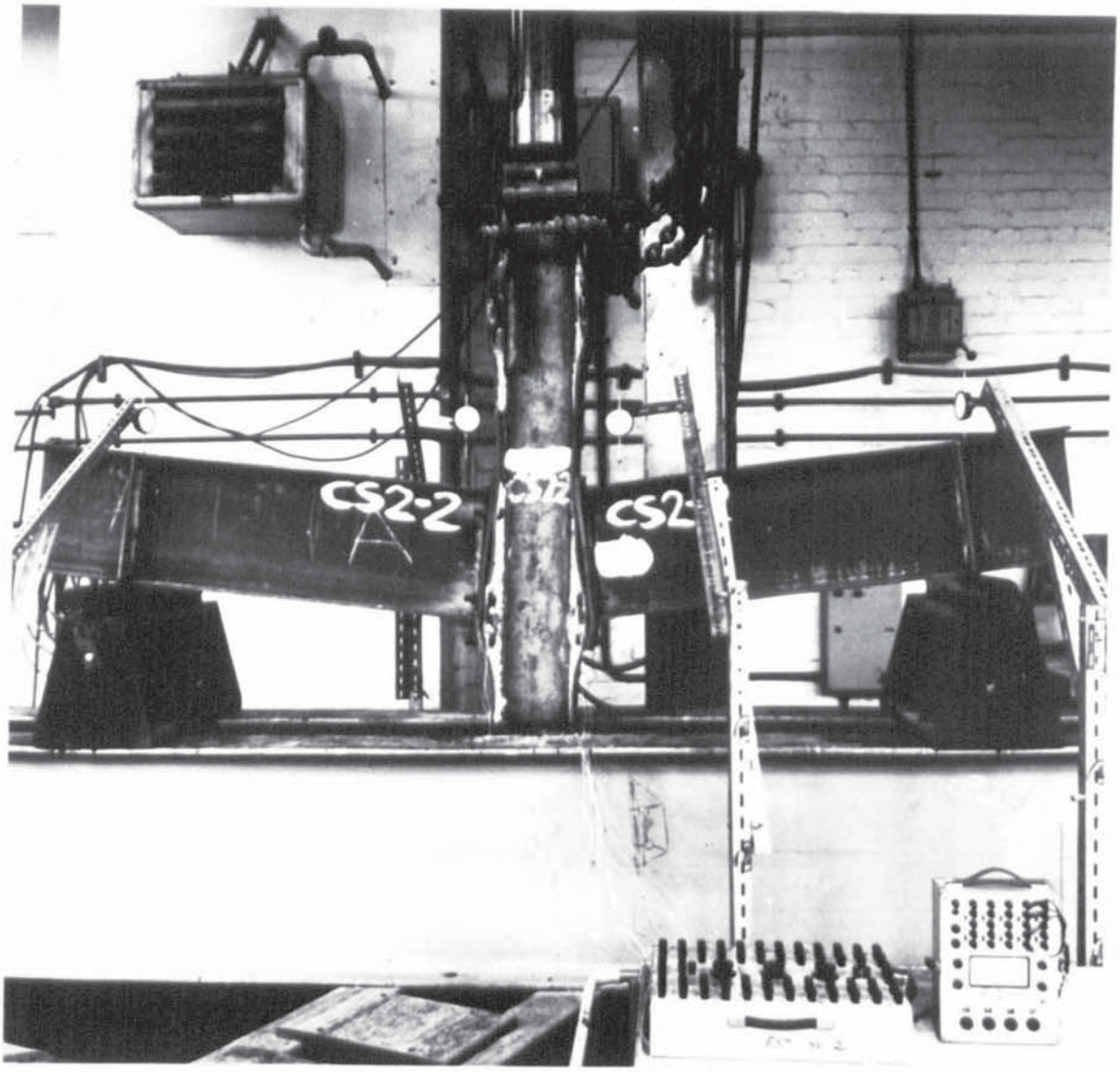

PLATE 4.5 TYPICAL TEST SPECIMEN AFTER FAILURE

CS2-2 TOP

CS2-5 TOP

CS2-2 MIDDLE

CS2-5 MIDDLE

CS2-2 BOTTOM

CS2-5 BOTTOM

PLATE 4.6 TYPICAL BOLT DEFORMATIONS FOR TEST SERIES CS2

inside face of a column flange in this series is also shown in Plate 4.4. Bolt deformations for test CS2-2, a typical joint where slip did not occur, are shown in Plate 4.6. Bolt deformations for test CS2-5 where slip did occur are also shown in Plate 4.6. The bolts in Plate 4.6 are labelled similar to those shown for series CS1.

4.4.4 Connection Series CS3

This series also consisted of five tests with steel of a higher yield stress than that used for the previous two series. The column flange and end plate thickness was 20mm. 6mm fillet welds were used in the fabrication of the column section. 10mm profile fillet welds were used for connecting the end plates to the universal beams. Details of the test specimens are given in Table 4.3 The joints used in series CS3 were similar to test P2 and from the results of that test column flange strain gauges were only attached adjacent to the weld line.

The moment-rotation relationship, moment-column flange deformation relationship and shear force-slip relationship for test CS3-2 are shown in Figure 4.10. The bolt force-applied moment relationship for test CS3-2 is shown in Figure 4.11. The experimental readings for this test are given in Appendix A-4 together with the graphical results of the remaining four tests in this series. The stages during each test at which first yield was obtained from the

Test No	CS3-1	CS3-2	CS3-3	CS3-4	CS3-5
t_p mm	20	20	20	20	20
t_c mm	20	20	20	20	20
L m	1.220	1.015	0.820	0.571	0.326
σ_{py} N/mm^2	328.1	328.1	328.1	328.1	328.1
σ_{cy} N/mm^2	328.1	328.1	328.1	328.1	328.1
LRM Rotation rads $x10^{-3}$	15.31	12.52	11.59	11.48	19.55
LRM Col. Flg. Deform. mm	1.04	1.34	1.16	1.19	0.62
LRM Slip - Deform. mm	0.067	0.142	0.102	2.191	0.683
M_u kNm	197.0	193.1	190.0	194.9	138.1*
V_u kN	161.5	196.0	231.7	341.4	423.6*
Q_u kN	56.2	58.4	71.7	60.8	*
Mode of Failure	BF	BF	BF	BF	*

Abbreviations used: LRM, Last Recorded Mean; BF, Bolt Fracture; *, Test discontinued due to damage to hydraulic ram.

TABLE 4.3 EXPERIMENTAL RESULTS FOR BEAM TO COLUMN CONNECTION SERIES CS3

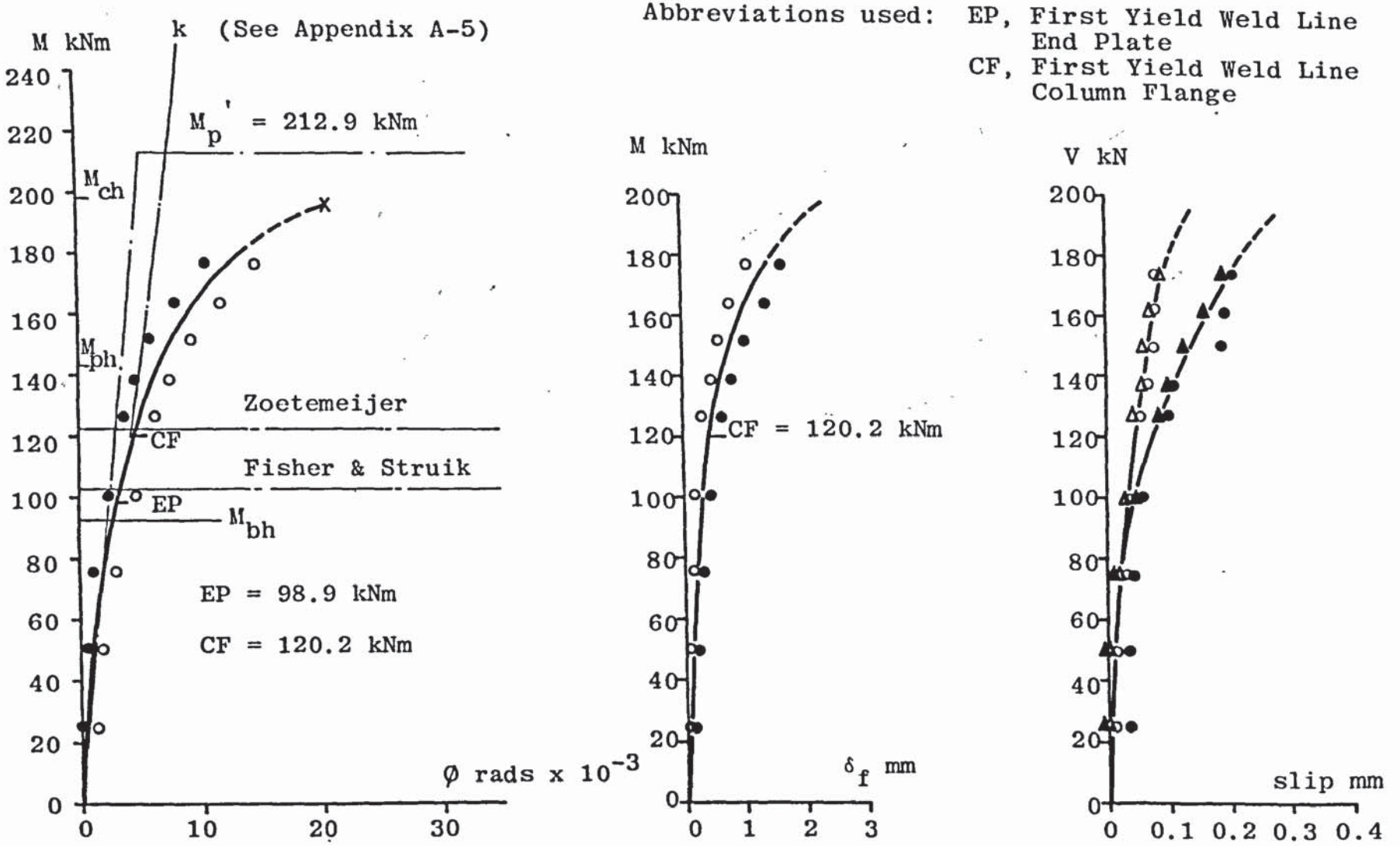

FIGURE 4.10 APPLIED MOMENT - ROTATION RELATIONSHIP, APPLIED MOMENT - COLUMN FLANGE DEFLECTION RELATIONSHIP AND SHEAR FORCE - SLIP RELATIONSHIP FOR TEST CS3-2

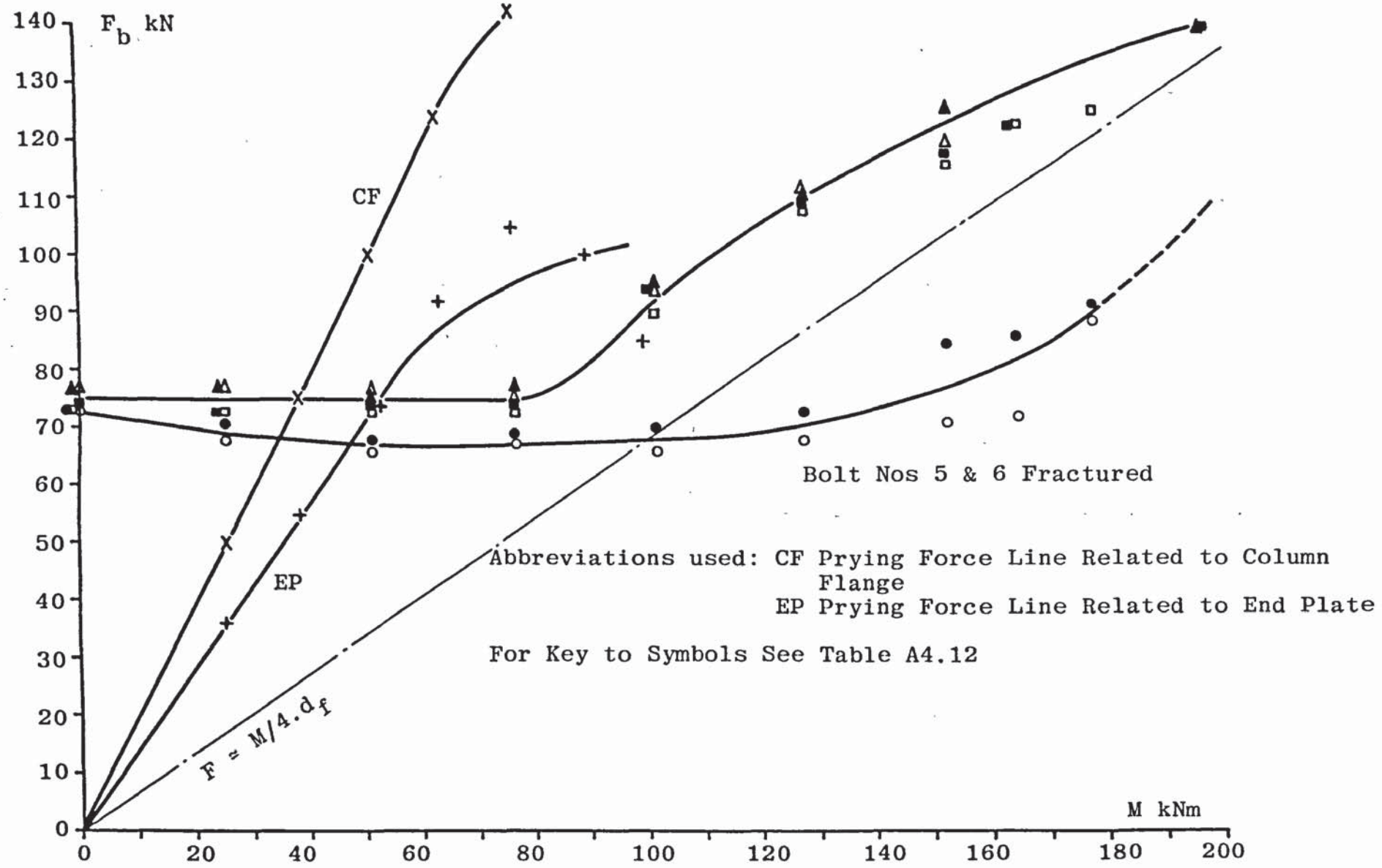

FIGURE 4.11 APPLIED MOMENT - BOLT FORCE RELATIONSHIP FOR TEST CS3-2

strain gauge readings are indicated on these figures.

All tests except for test CS3-5 failed by bolt fracture. During test CS3-4 the bolts of the right hand side connection slipped into bearing with a slight retort. From Figure A4.34 it can be seen that the bolts of the left hand side connection had slipped approximately 1.7mm at the last recorded reading. At this stage the bolts were probably just bearing on the end plate and column flange. Two bolts fractured in the right hand side of this test and although the bolts slipped into bearing there was little difference between the mode of failure and failure load compared with the other connections. The bolts of both joints in test CS3-5 slipped into bearing with a loud retort at approximately the same load. The dial gauges attached to the column flange to measure slip were dislodged when final slip took place and no further readings were possible. Considerable shear deformation occurred in the webs of the beams during test CS3-5, which influenced the moment-rotation characteristics of the specimen as can be seen from Figure A4.35. Similar to tests CS1-5 and CS2-5, test CS3-5 was discontinued before bolt failure occurred due to damage to the hydraulic ram.

The test specimens after failure are shown in Plate 4.7. Bolt deformations for test CS3-1, a typical test where slip did not occur, are shown in Plate 4.8. Bolt deformations for tests CS3-4 and CS3-5 where slip into bearing occurred

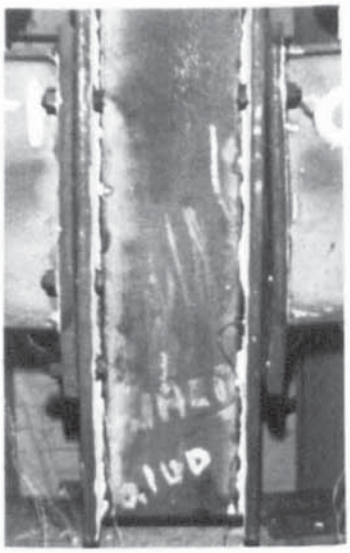

CS3-1

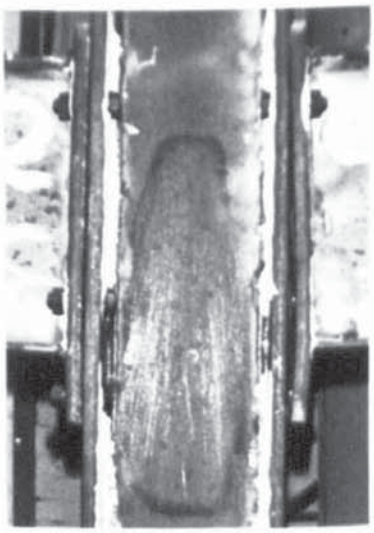

CS3-2

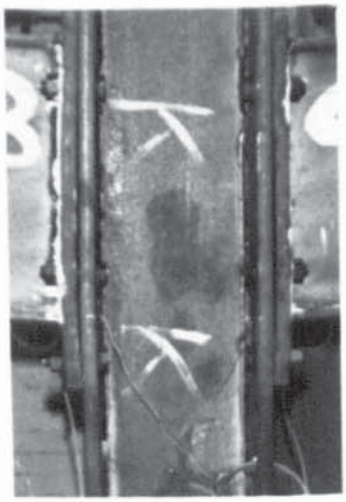

CS3-3

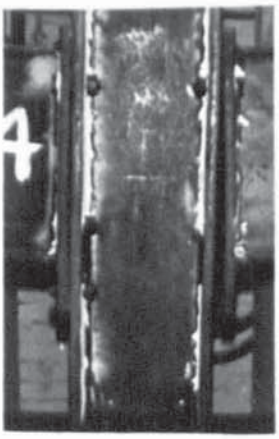

CS3-4

CS3-5

PLATE 4.7 TEST SPECIMENS FOR SERIES CS3 AFTER FAILURE

CS3-1 TOP

CS3-4 TOP

CS3-1 MIDDLE

CS3-4 MIDDLE

CS3-1 BOTTOM

CS3-4 BOTTOM

PLATE 4.8 TYPICAL BOLT DEFORMATIONS FOR TEST SERIES CS3

CS3-5 TOP

CS4-3 TOP

CS3-5 MIDDLE

CS4-3 MIDDLE

CS3-5 BOTTOM

CS4-3 BOTTOM

PLATE 4.9 TYPICAL BOLT DEFORMATIONS FOR TEST SERIES CS3 AND CS4

are shown in Plates 4.8 and 4.9 respectively. The bolts in these plates are labelled similar to those shown for test series CS1.

4.4.5 Connection Series CS4

Two tests were performed in this series with steel from the same batch as connection series CS3. The column flange thickness remained at 20mm while the end plate was machined down to 15mm thick on one side only. The original as received face of the end plate was welded to the beam with an 8mm profile fillet weld. The column welds remained at 6mm fillets. Details of the test specimens are given in Table 4.4. Column flange strain gauges were attached adjacent to the weld line opposite the beam tension flange.

The moment-rotation relationship, moment-column flange deformation relationship and shear force-slip relationship for test CS4-1 are shown in Figure 4.12. The bolt force-applied moment relationship for test CS4-1 is shown in Figure 4.13. During test CS4-3 loading was discontinued at approximately 180 kN due to a mechanical fault in the hydraulic loading system. After the fault was repaired the test specimen was reloaded to its last recorded value and the test continued in the usual manner until failure occurred. The experimental results for test CS4-3 are shown in Figures A4.38 and A4.39. The average moments at which first yield was obtained from the strain gauge readings

Test No	CS4-1	CS4-3	CS5-1	CS5-2
t_p mm	15.04	14.35	20	20
t_c mm	20	20	17.5	16.92
L m	1.218	0.815	1.023	0.320
σ_{py} N/mm^2	328.1	328.1	328.1	328.1
σ_{cy} N/mm^2	328.1	328.1	328.1	328.1
LRM Rotation rads $x10^{-3}$	12.16	19.57	23.81	38.8
LRM Col. Flg. Deform. mm	1.12	0.95	4.24	1.74
LRM Slip - Deform. mm	0.063	0.104	0.187	2.252
M_u kNm	163.9	166.5	210.3	155.5*
V_u kN	134.6	204.3	205.6	485.9*
Q_u kN	101.0	95.0	26.7	*
Mode of Failure	BF	BF	BF	*

Abbreviations used: LRM, Last Recorded Mean; BF, Bolt Fracture; *, Test discontinued due to damage to hydraulic ram.

TABLE 4.4 EXPERIMENTAL RESULTS FOR BEAM TO COLUMN CONNECTION SERIES CS4 and CS5

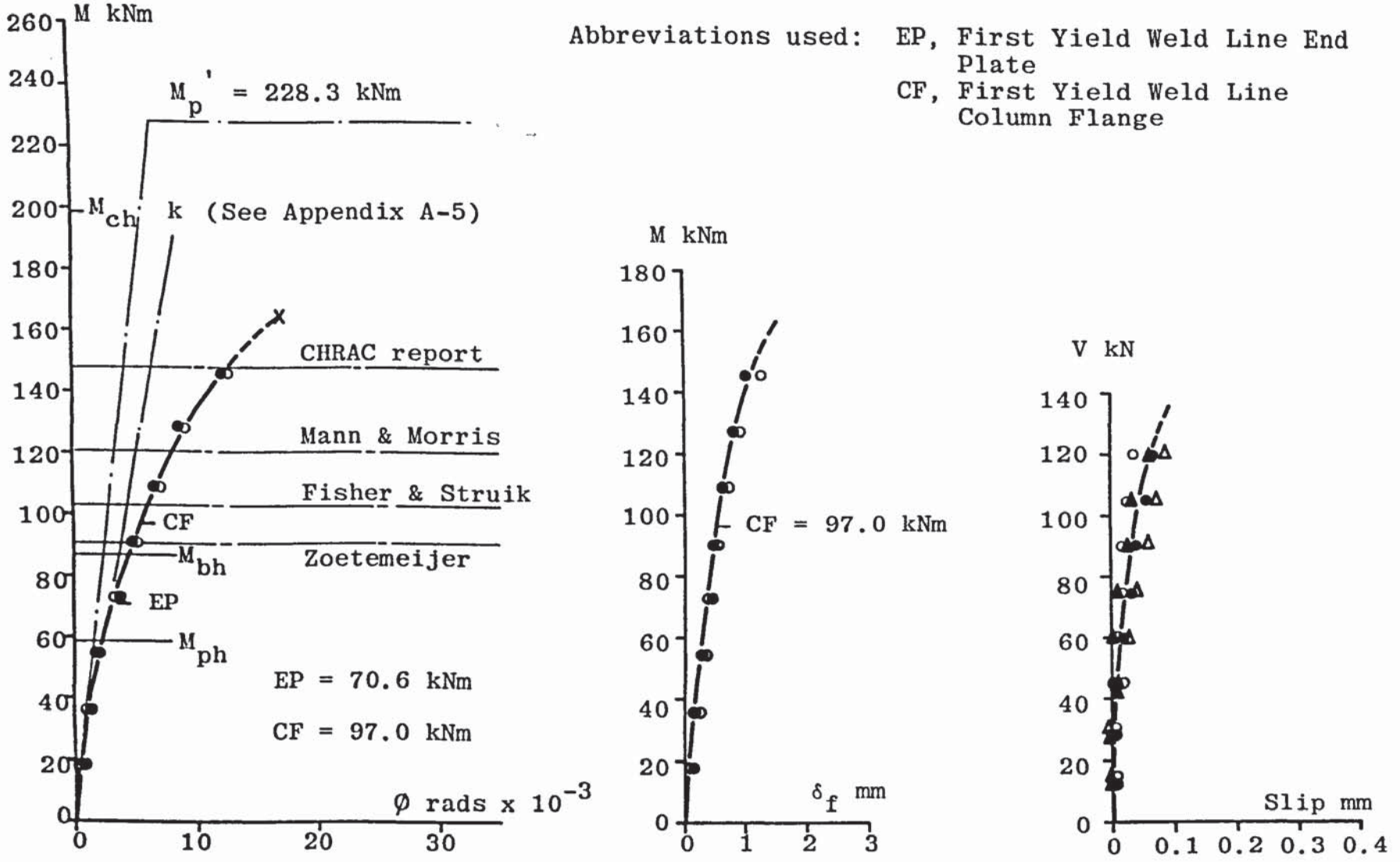

FIGURE 4.12 APPLIED MOMENT - ROTATION RELATIONSHIP, APPLIED MOMENT - COLUMN FLANGE DEFLECTION RELATIONSHIP AND SHEAR FORCE - SLIP RELATIONSHIP FOR TEST CS4-1

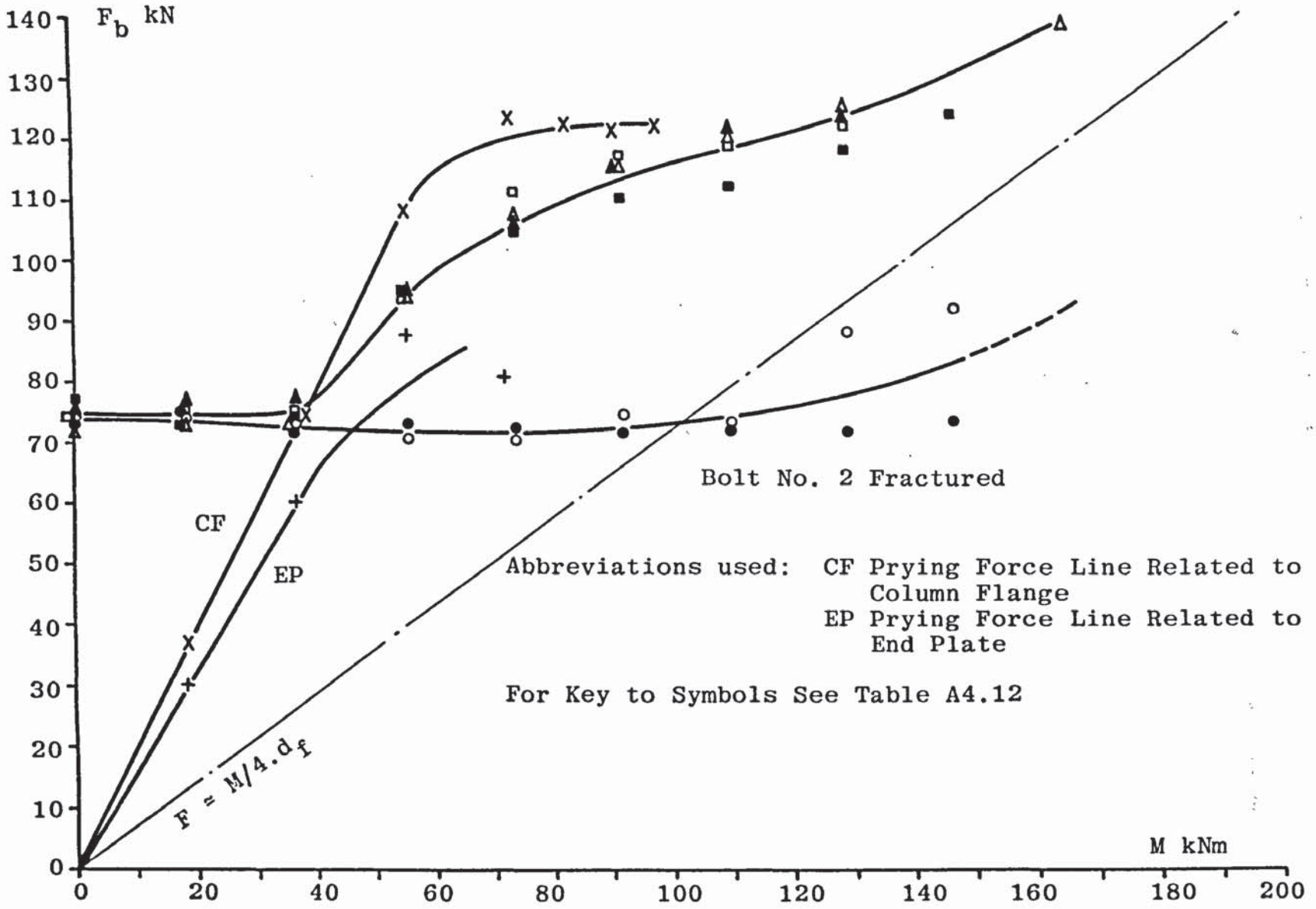

FIGURE 4.13 APPLIED MOMENT - BOLT FORCE REALTIONSHIP FOR TEST CS4-1

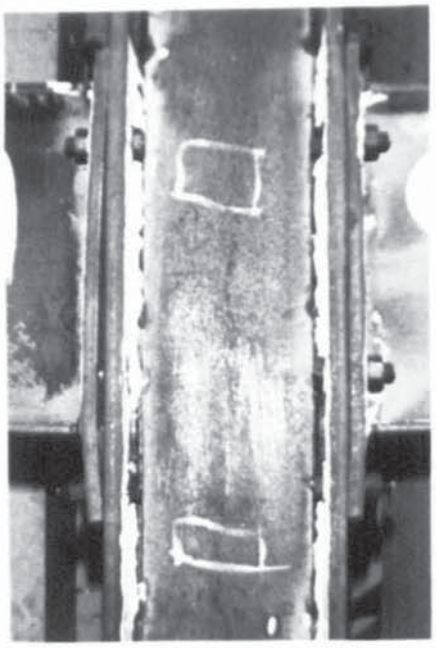

CS4-1

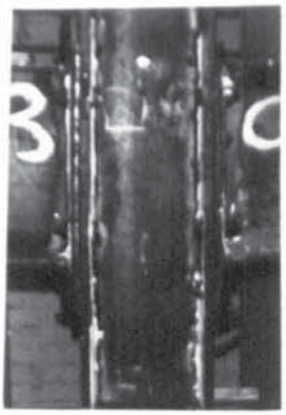

CS4-3

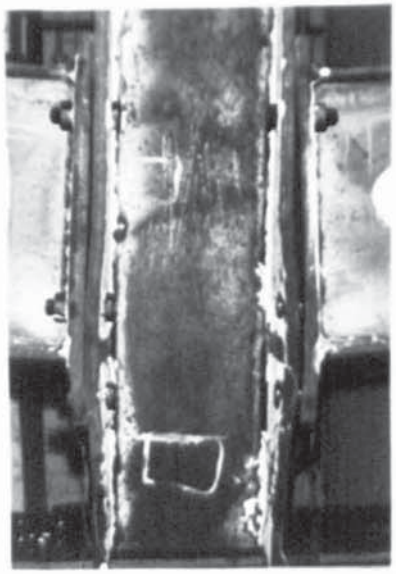

CS5-1

CS5-2

PLATE 4.10 TEST SPECIMENS FOR SERIES CS4 AND CS5 AFTER FAILURE

for tests CS4-1 and CS4-3 are indicated on Figures 4.12 and A4.38 respectively.

Both tests failed by bolt fracture and the test specimens after failure are shown in Plate 4.10. Bolt deformations for test CS4-3, typical for both tests are shown in Plate 4.9 and are labelled similar to those shown for test series CS1.

4.4.6 Connection Series CS5

Two tests were performed in this series. One test specimen had a large moment to shear ratio while the other had a small moment to shear ratio. The steel used was from the same batch as series CS3 and CS4. The end plate thickness remained at 20mm while the outside faces of the column flanges were machined down to approximately 17mm. The column welds were 6mm fillets while the end plate was connected to the beam with a 10mm fillet weld. Details of the test specimens are given in Table 4.4. Column flange strain gauges were attached adjacent to the weld line and at the bolt line opposite the beam tension flange.

The moment-rotation relationship for test CS5-1 is shown in Figure 4.14. The moment-column flange deformation relationship and shear force-slip relationship for test CS5-1 are shown in Figure 4.15. The bolt force - applied moment relationship for test CS5-1 is shown in Figure 4.16.

Abbreviations used: EP, First Yield Weld Line End Plate
CF, First Yield Weld Line Column Flange

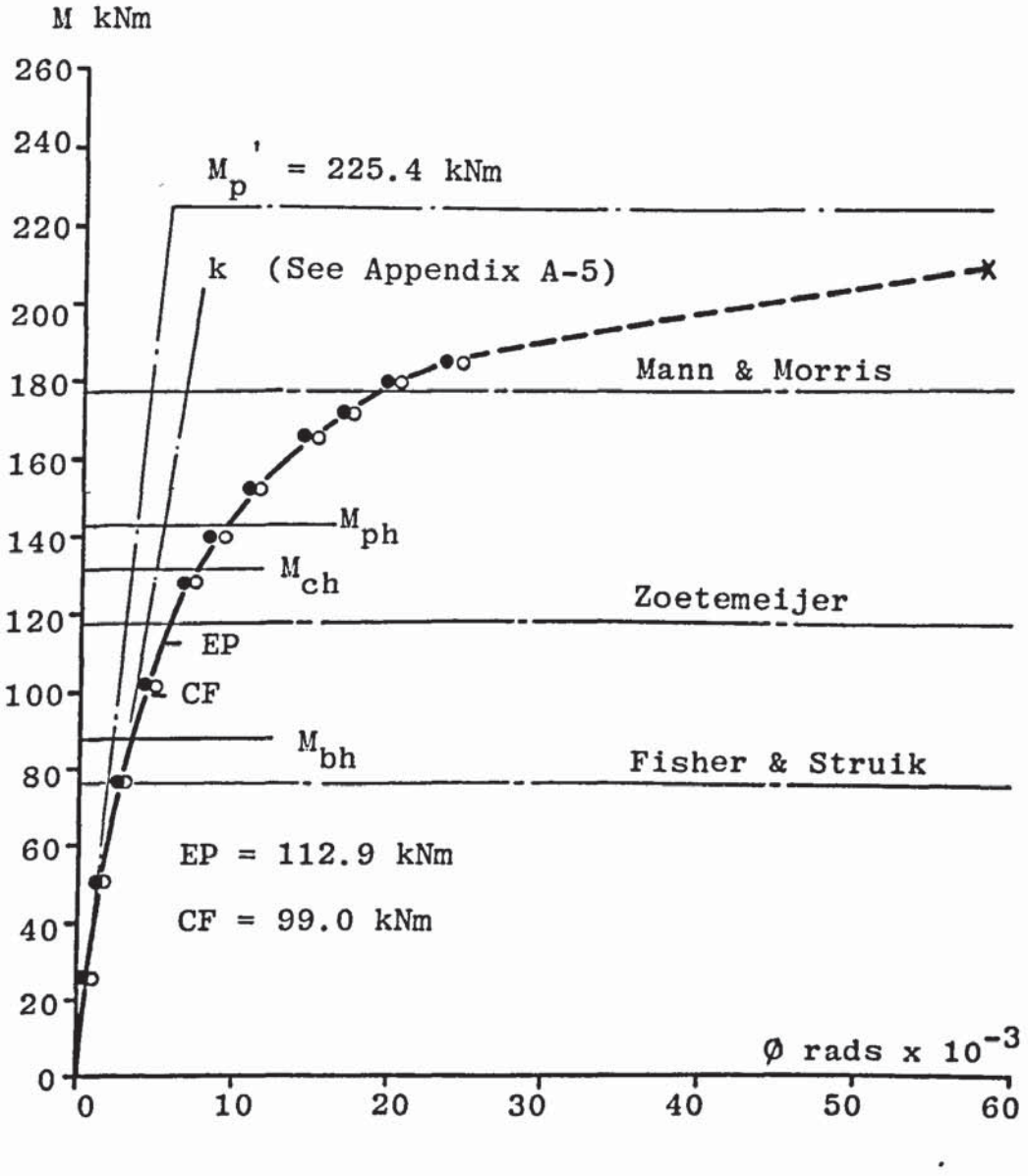

FIGURE 4.14 APPLIED MOMENT - ROTATION RELATIONSHIP FOR TEST CS5-1

Abbreviations used: CF First Yield Weld Line Column Flange

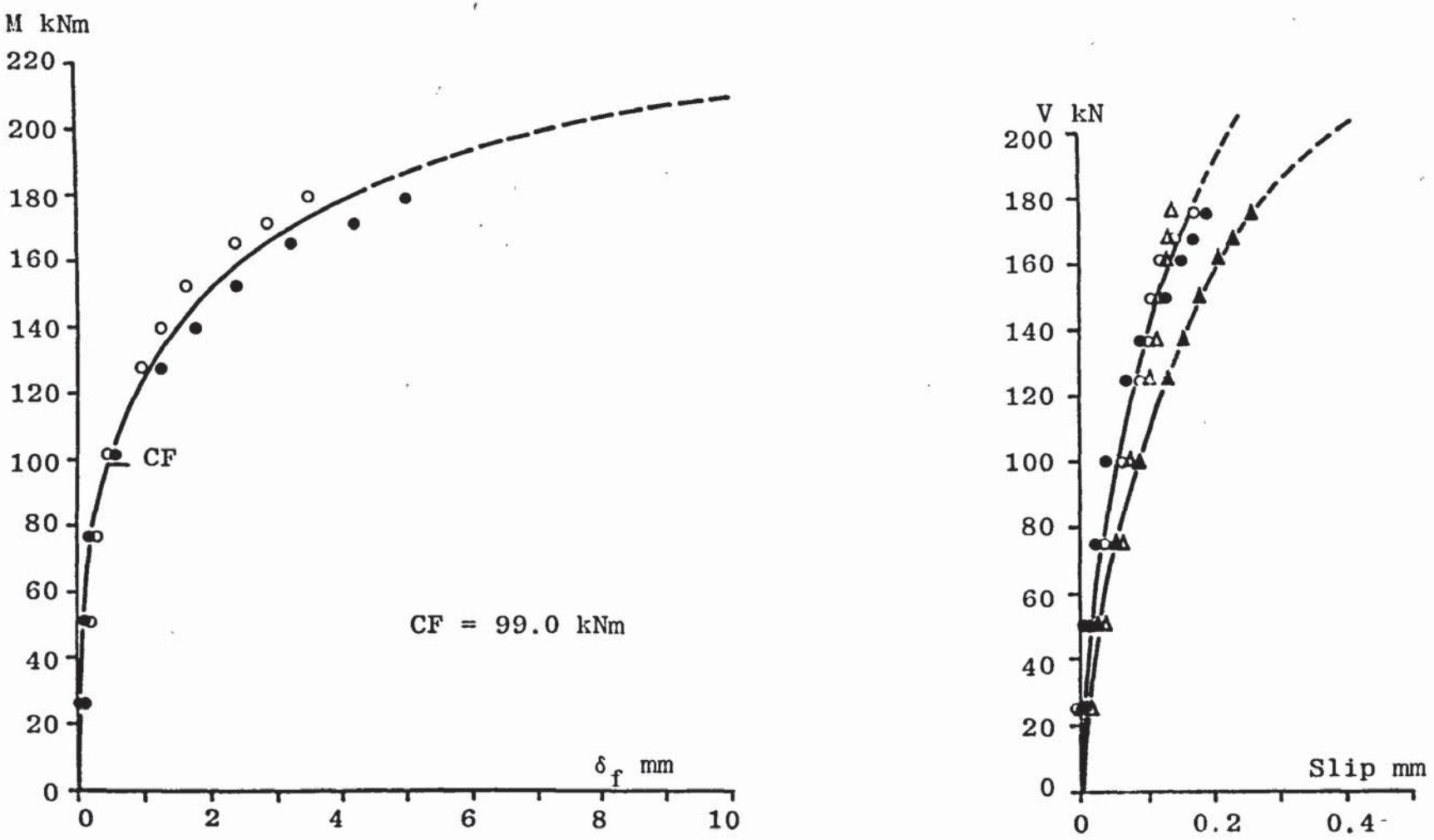

FIGURE 4.15 APPLIED MOMENT - COLUMN FLANGE DEFLECTION RELATIONSHIP AND SHEAR FORCE - SLIP RELATIONSHIP FOR TEST CS5-1

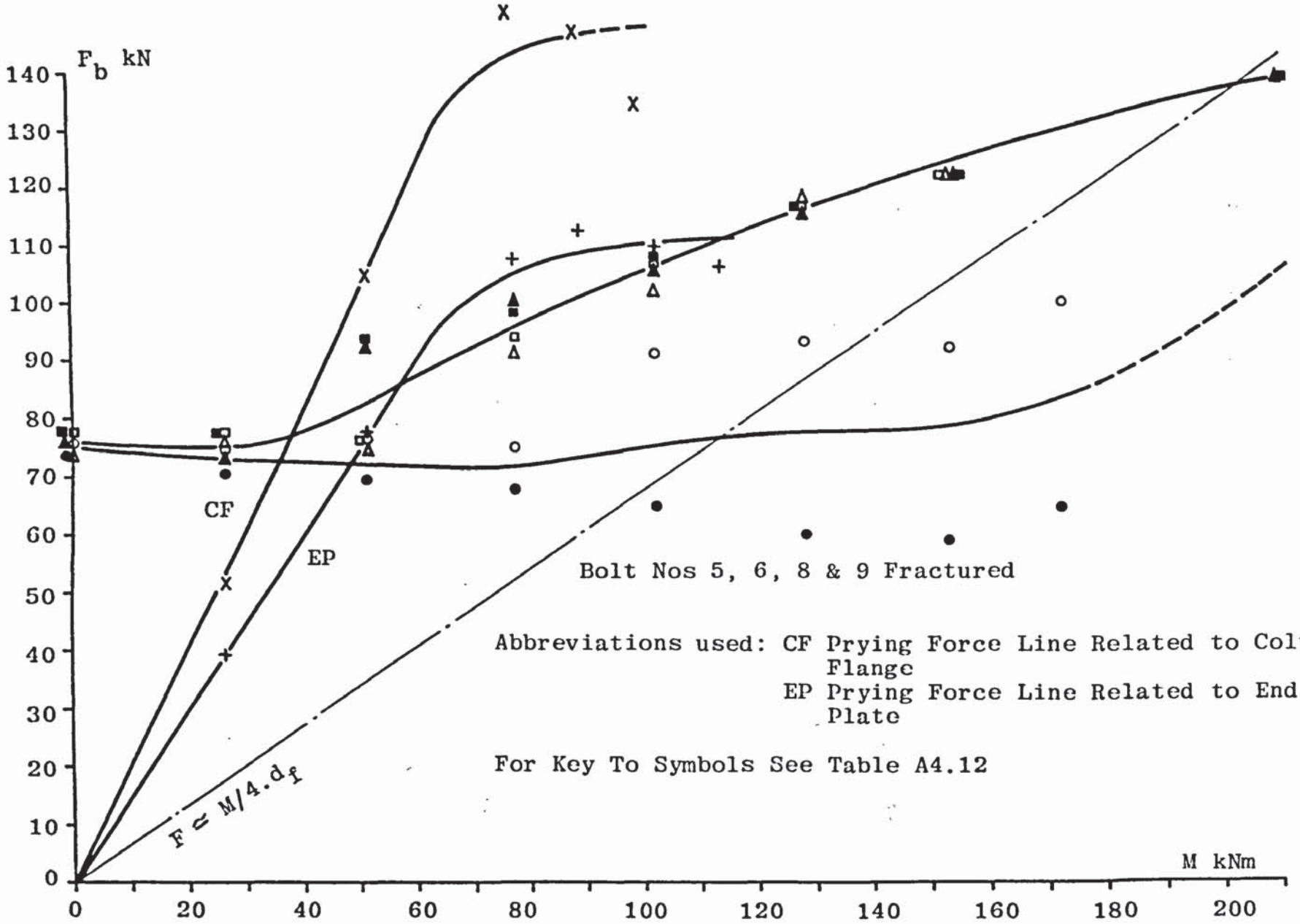

FIGURE 4.16 APPLIED MOMENT - BOLT FORCE RELATIONSHIP FOR TEST CS5-1

CS5-1 TOP

CS5-2 TOP

CS5-1 MIDDLE

CS5-2 MIDDLE

CS5-1 BOTTOM

CS5-2 BOTTOM

PLATE 4.11 TYPICAL BOLT DEFORMATIONS FOR TEST SERIES CS5

Similar relationships for test CS5-2 are shown in Figures A4.40, A4.41 and A4.42. The average moments at which first yield was obtained from the strain gauges for tests CS5-1 and CS5-2 are indicated on Figures 4.14 and A4.40 respectively.

In test CS5-1 failure was due to bolt fracture. During test CS5-2 the bolts of the right hand side connection slipped into bearing with a loud retort. The bolts of the left hand side connection slipped at a greater load and it would appear from Figure A4.42 that bearing did not occur. The effect of the right hand side connection slipping on the moment - rotation characteristics of the joints can be seen from Figure A4.40. Large shear deformation and some buckling occurred in the webs of the beams during test CS5-2, which influenced the moment - rotation relationship of the specimen. This can also be seen from Figure A4.40. Test CS5-2 was discontinued, before bolt failure occurred, at an applied load of 975 kN which was the maximum available from the loading system.

The test specimens after each test are shown in Plate 4.10. Bolt deformations for each test are shown in Plate 4.11 and are labelled similar to those shown for test series CS1.

4.5 Discussion of Experimental Results

During the early stages of loading up to approximately the

elastic limit of either the end plate or column flange, each test, except those with plastic shear deformation in the beams, behaved in a rigid manner. The moment - rotation curves for these tests up to first yield, were almost identical to the theoretical elastic behaviour of these joints.

Each test in series CS1 and CS2, except test CS1-5, experienced a considerable amount of rotation due to plastic deformation of both the end plate and column flange before failure occurred. The failure moments in test series CS1 and CS2 were approximately the same even though the column flange thickness was reduced in test series CS2. A decrease in the column flange thickness however increased the column flange deformation and connection rotation although the maximum extrapolated rotation was approximately constant for both test series. The elastic range of test series CS1 was however larger than that of test series CS2. The last recorded rotation for each other test, except tests CS3-5 and CS5-2, was small in comparison with those obtained for test series CS1 and CS2. Plastic shear deformation occurred in the beam webs of tests CS1-5, CS3-5 and CS5-2 which influenced their moment - rotation characteristics. The connection details for test P2 and test series CS3 were similar, however the yield stress of the end plate and column flange was higher in test series CS3. The higher yield stress steel increased the elastic range but decreased the

maximum rotation capacity of the joints in series CS3 although the failure loads were similar. The difference between the rotation capacities of test P2 and test series CS3 increased when the moment - rotation curves were extrapolated up to failure. The end plate thickness for test series CS4 was approximately 15mm and the failure moments were similar to those for test series CS1 and CS2 where the end plate thickness was also 15mm. The maximum recorded rotation however was similar to that of test series CS3. The moment - column flange deformation relationship for the tests in series CS3 and CS4 were also similar. Decreasing the thickness of the column flange for test CS5-1 slightly increased the failure moment and column flange deformation. The last recorded rotation of test CS5-1 was similar to that obtained for test series CS3 and CS4. Extrapolating the moment - rotation curve of test CS5-1 up to failure increased the rotation capacity by quite an extent. The deflections of the end plates and column flanges for all tests at failure, when compared with those obtained in the strip beam tests in Chapter Three indicated that significant work hardening had occurred.

In general it may be stated that the failure loads for these connections are independent of the column flange thickness. However, it would appear that their rotation capacity is dependent on the column flange thickness. The yield strength of the plates has not only an effect on the

elastic range of the joints but also their rotation capacity. Furthermore considerable rotation capacity is achieved before failure occurs when the bolt diameter is larger than the thickness of both the end plate and column flange.

During test series CS2 and CS4 mean values of slip increased as the applied shear force increased. During test CS2-5 where $L/d_f = 1$ approximately the bolts slipped into bearing. During test series CS1, CS3 and CS5 mean values of slip increased as the applied shear force increased, except in cases where slip into bearing occurred. In tests where slip into bearing occurred, namely CS1-5, CS3-5 and CS5-2, $L/d_f = 1$ approximately and in test CS3-4, $L/d_f = 1.6$ approximately. The experimental results at final slip are shown in Table 4.5 and it should be noted that when final slip into bearing took place tensile bolt separation had occurred. The effect of gradual slip on the moment - rotation characteristics of the joints tested was negligible. When sudden slip occurred however there was a noticeable deviation in the moment - rotation curves. When both joints of an experiment suddenly slipped into bearing it was at slightly different stages of loading. This resulted in an apparent decrease in the rotation of the connection that slipped, with an apparent increase in the rotation of the other joint. When the bolts of the other joint suddenly slipped into bearing the reverse procedure occurred resulting in the apparent rotations being approximately equal to the values at which the first sudden slip began. Good examples

Test No.	L m	V_s kN	Q_{bs} kN	Surface Treatment
CS1-5	0.315	112.1	69	clean dry AR
CS2-5	0.317	286.6	56	FP clean dry m/c EP clean dry AR
CS3-4	0.571	211.8	31	clean dry AR
CS3-5	0.326	209.3	33	clean dry AR
CS5-2	0.320	137.1	60	FP clean dry m/c EP clean dry AR

Abbreviations used: AR, As received; EP, End Plate; FP, Flange Plate; m/c, Machined.

TABLE 4.5 EXPERIMENTAL RESULTS AT FINAL SLIP

of this are tests CS1-5 and CS3-5. When one joint only of an experiment suddenly slipped into bearing there was an apparent decrease in its rotation and an apparent increase in the other joint. Good examples of this are tests CS2-5 and CS5-2. During test CS3-4 only one joint suddenly slipped into bearing. From Figure A4.34 it can be seem that the amount of final slip was small and from Figure A4.32 it can also be seen that this resulted in little variation in the moment-rotation curve.

In each test the tensile forces in the bottom four bolts were approximately equal at all stages of loading. The average last recorded tensile force in these bolts was approximately 90% of the full tensile strength at approximately 70% of the failure moment. It therefore appears that the full tensile strength of the bolts were developed at failure. Bolt fracture was always in the threaded portion of the bolt. The compression zone tensile bolt force - applied moment relationship was extrapolated up to failure. This produced an average maximum tensile bolt force of approximately 110 kN. After each test the bolts were removed from the test specimens and those from test series CS2 had the greatest amount of deformation. Although the bolts of five tests slipped into bearing mainly in the early stages of loading they had negligible shear deformation. This may be seen from Plates 4.3, 4.6, 4.8, 4.9 and 4.11. There was also negligible bearing deformation in the bolt holes of the end plates

and column flanges for these tests. In test CS3-4 the bolts slipped into bearing at approximately half the maximum shear force at failure. The failure moment and failure mode for this test was approximately the same as the other tests in this series. Therefore bearing of the bolts had no influence on the failure moment and failure mode of this experiment.

At failure of each test, there appeared to be contact points at the extreme edge of the extended portion of the end plate. The total prying force at the bottom of the end plate shown in Tables 4.1, 4.2, 4.3 and 4.4 was obtained from taking moments of all forces obtained in the experiments about the line of rotation. Rotation was seen to occur in the vicinity of the beam compression flange. Therefore rotation was considered about the outer edge of this flange for test P1, test series CS1, CS2 and CS4. For the remaining tests the line of rotation was assumed to be 19mm above the top flange because of the stiffer end plate. Except for test CS5-1 the prying force just after separation of the end plate and column flange was approximately twice the value at failure.

In Appendix A-3 it is shown that the prying force, assumed acting at the extreme edge of a tee stub, can be determined using the strains obtained at the weld line at any loading stage within the elastic range. Assuming a tee stub analogy, prying force related to the end plate may be determined in

a similar manner. This method may also be applied in determining the prying force related to the column flange. Prying force lines related to the end plate and column flange from equation A3.1 are shown in the bolt force - applied moment relationship for each test. From these figures it can be seen that the assumed prying force related to either the end plate or column flange increased approximately linearly until separation occurred.

CHAPTER FIVE

THEORETICAL INVESTIGATION

5.1 Introduction

Theoretical analyses for the elastic and ultimate strength of tee stub connections and beam to column connections are developed in this chapter. Emphasis is on the determination of the magnitude of prying force at bolt failure. The elastic analysis for beam to column connections is valid as long as the rotation of the joint is within the linear-elastic range.

5.2 Tee Stub Connections

A check on the equilibrium of moments about the web for the tee stub model shown in Figure 3.8, assuming a plastic hinge at the web and the tensile strength of the bolt and prying forces deduced in each test showed an out of balance moment. The results for each tee stub test can be seen from Table 5.1 from which the possibility of work hardening was inferred. This was confirmed by the strip steel beam test results from which similar moments of resistance as those shown in Table 5.1 were found for the tee stubs. The beam test results shown in Figures 3.9, 3.10 and 3.11 may be summarized by stating that the load-deformation relationship is approximately bi-linear and the moment of resistance at the plastic hinge depends on the deflection.

Test No	t_p mm	Q_{bu} kN	m_p kNm	Moment of Resistance at Web kNm
TS1	20.1	21.0	2.57	1.84 m_p
TS2	12.5	52.8	0.99	2.36 m_p
TS3	15.9	42.3	1.61	1.95 m_p
TS4	12.7	45.3	1.02	2.83 m_p
TS5	15.4	35.3	1.64	2.23 m_p

TABLE 5.1 MOMENTS OF RESISTANCE FOR TEE STUBS

Specimen	W at m_p kN	W at m_{ph} kN	$\frac{m_{ph}}{m_p}$	$\frac{l}{t}$
B1	6.5	7.6	1.17	5.33
B2	4.2	3.8	0.90	6.50
B3	10.3	19.3	1.87	3.33
B4	6.2	10.7	1.73	4.17
B5	17.1	29.8	1.74	1.99
B6	11.4	21.2	1.86	2.46
B7*	11.3	12.7	1.13	3.31
B8*	7.0	9.0	1.29	4.20
B9	9.7	8.0	0.83	4.07
B10	14.7	19.8	1.34	3.34
B11	26.5	39.0	1.47	2.48
B12*	10.4	8.5	0.82	4.12
B13*	15.9	20.0	1.26	3.34
B14*	28.8	40.5	1.41	2.48
B15*	11.6	15.8	1.36	3.65

Note: σ_y (B1 to B8) 229 N/mm^2, σ_y(B9 to B14) 328.1 N/mm^2, σ_y (B15) 277.3 N/mm^2

Specimens marked thus * had a partial UDL, otherwise specimens loaded via a knife edge.

TABLE 5.2 m_{ph}/m_p VALUES FOR STEEL STRIP TESTS

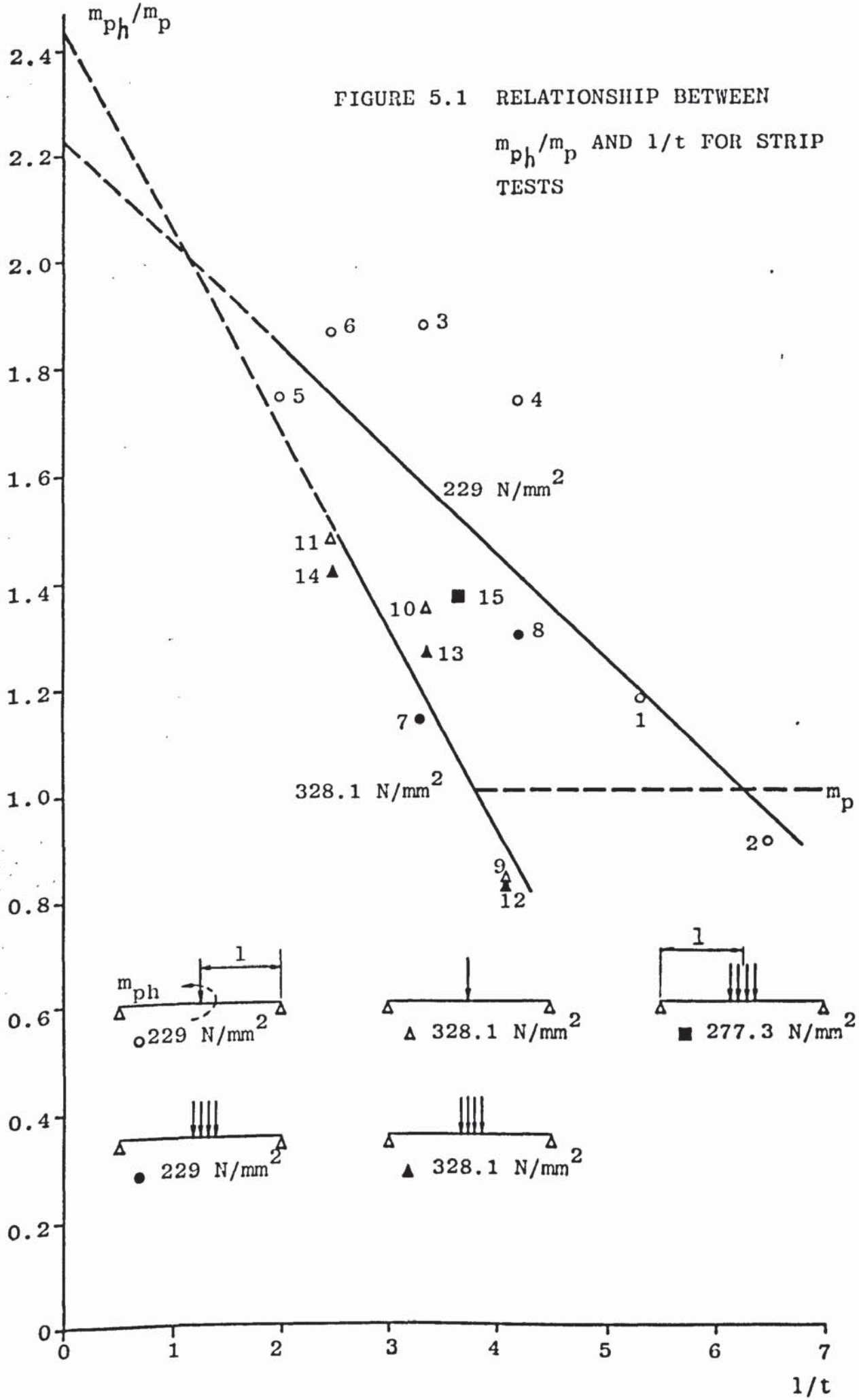

FIGURE 5.1 RELATIONSHIP BETWEEN m_{ph}/m_p AND 1/t FOR STRIP TESTS

The ratio of the moment of resistance at the first discontinuity, i.e. at the intersection of the two slopes, to the theoretical plastic moment of resistance for the steel strips are given in Table 5.2. The relationship between m_{ph}/m_p and 1/t for the strip tests are shown in Figure 5.1. From a linear regression analysis of these values for 229 N/mm^2 and 328.1 N/mm^2 steel the following empirical equations were found

229 N/mm^2

$$m_{ph}/m_p = 2.225 - 0.195\ (1/t) \qquad 5.1$$

for $2 < (1/t) < 6.3$

$r = 0.76$

328.1 N/mm^2

$$m_{ph}/m_p = 2.430 - 0.376\ (1/t) \qquad 5.2$$

for $2.5 < (1/t) < 3.8$

$r = 0.94$

The absolute value of the correlation coefficient, r, for equation 5.1 is reduced due to the difference between the load deflection relationships for the two types of loading system used. Further investigation is needed if the value of r is to be improved. Equations 5.1 and 5.2 will however be used in the following theory to determine the discontinuity limits.

5.2.1 Elastic Theory

The theoretical model for the tee stub is shown in Figure 3.8.

The free body diagram showing the forces applied to the flange plate per bolt is shown in Figure 5.2. Plate separation at the bolt line is assumed to have occurred.

From elastic principles

$$E_p.I_p.d^2y/dx^2 = - Q_{be}.x + F_{be}\left[x - a_p\right] \qquad 5.3$$

$$E_p.I_p.dy/dx = - Q_{be}.\frac{x^2}{2} + \frac{F_{be}}{2}\left[x - a_p\right]^2 + A \qquad 5.4$$

$$E_p.I_p.y = - Q_{be}.\frac{x^3}{6} + \frac{F_{be}}{6}\left[x - a_p\right]^3 + A.x + B \qquad 5.5$$

Boundary conditions

$dy/dx = 0, \quad x = (a_p + b_p)$ (i)

$y = 0, \quad x = 0$ (ii)

$y = -(e_{be} - e_{bp}) = -\delta, \quad x = a_p$ (iii)

From equation 5.4 using BC(i)

$$A = \frac{Q_{be}}{2}.(a_p + b_p)^2 - F_{be}.\frac{b_p^2}{2}$$

From equation 5.5 using BC(ii)

$B = 0$

From equation 5.5 using BC(iii)

$$-E_p.I_p.\delta = -\frac{Q_{be}}{6}.a_p^3 + \frac{Q_{be}}{2}(a_p + b_p)^2.a_p - \frac{F_{be}}{2}.a_p.b_p^2$$

$$-E_p.I_p.\delta + \frac{F_{be}}{2}.a_p.b_p^2 = Q_{be}\left[\frac{a_p(a_p + b_p)^2}{2} - \frac{a_p^3}{6}\right]$$

$$Q_{be} = \frac{F_{be} - 2.E_p.I_p.\delta/a_p.b_p^2}{1 + 2(a_p/b_p) + (2/3)(a_p/b_p)^2} \qquad 5.6$$

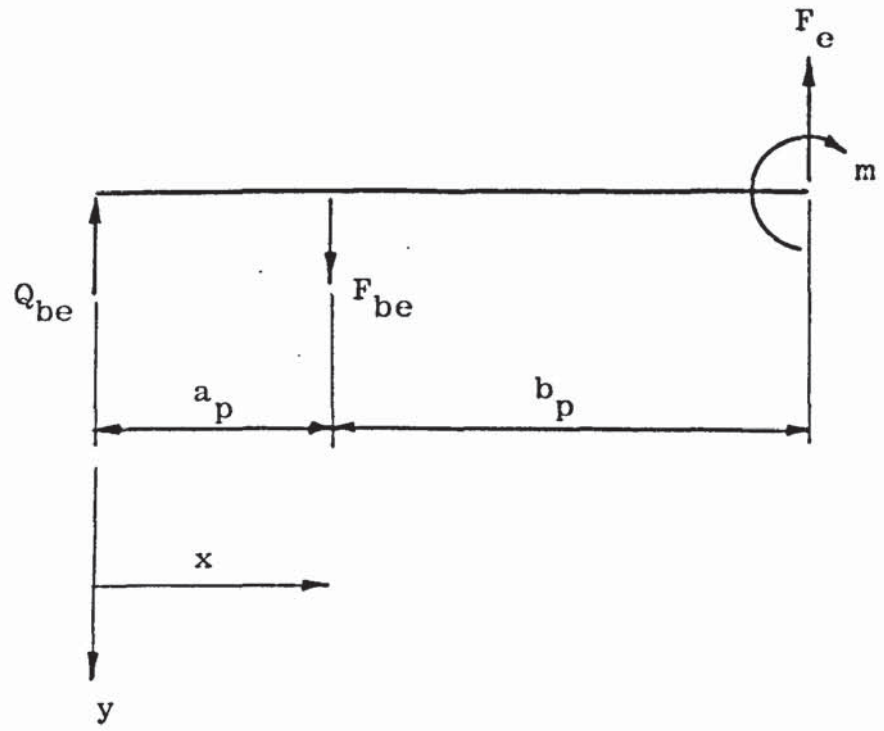

FIGURE 5.2 FREE BODY DIAGRAM FOR A TEE STUB

For simplicity

$$\delta = g_p(F_{be} - F_s)/A_b.E_b$$

$$\delta = g_p(S_{be} - S_{bs}) \qquad 5.7$$

Therefore substituting 5.7 into 5.6 gives

$$Q_{be} = \frac{F_{be} - F_p(S_{be} - S_{bs})}{1 + 2(a_p/b_p) + (2/3)(a_p/b_p)^2} \qquad 5.8$$

where $F_p = (E_p.w_p.t_p^3.g_p)/(6.a_p.b_p^2)$ 5.9

This form of theoretical approach was originally produced by Douty and McGuire[12].

5.2.2 Ultimate Load Theory

The work hardening effect shown in Figure 3.11 for tee stub TS5 suggested that the elastic range of behaviour of the plate associated with E_p could be extended to bolt failure conditions. The strain of the bolt at ultimate load however needed further investigation and was fixed empirically at 1.05%. This value is of the same magnitude as the last recorded results in tests. The expression for the prying force at ultimate load when failure of the bolt occurs is therefore

$$Q_{bu} = \frac{F_{bu} - F_p(S_{bu} - S_{bs})}{1 + 2(a_p/b_p) + (2/3)(a_p/b_p)^2} \qquad 5.10$$

where S_{bu} = 1.05% and F_p is obtained from equation 5.9.

5.3 Beam to Column Connections

The elastic and ultimate load equations for prying force for tee stubs, equations 5.8 and 5.10 respectively, may be similarly applied to the end plate in the beam to column connections. The equations can also be applied to the column flange in beam to column connections but in this situation the effective width of the column flange w_c, per bolt must be defined. The effective width of the column flange is that value which gives the same elastic deflection as the corresponding width of a simple cantilever assumed to be equivalent to the tee stub. In order to obtain an approximate estimate of the effective width a somewhat simplified analysis is made. From Timoshenko and Woinowsky-Krieger[71] the distribution of bending moments at the junction of the web and column flange around the tension zone of a typical beam to column connection tested is shown in Figure 5.3 Prying forces are assumed to act at the toe of the column flange adjacent to the bolt force.

It may be shown from the work by Holmes[73] that the deflection Δ_c may be determined from the standard simple cantilever deflection equations using the bending moments determined from the above method as follows. If prying force does not exist, the maximum bending moment is $0.505\ F_{be}$. Therefore,

$$\Delta_c = 0.505.F_{be}.b_c^2\ (1 + 3.a_c/2.b_c)/\ 3.E_c.I_c$$

assuming that an equivalent moment acts on a cantilever from which

$$\Delta_c = 202.F_{be}.b_c^2\ (1 + 3.a_c/2.b_c)/E_c.t_c^3$$

the same deflection can also be obtained from and equivalent cantilever, therefore,

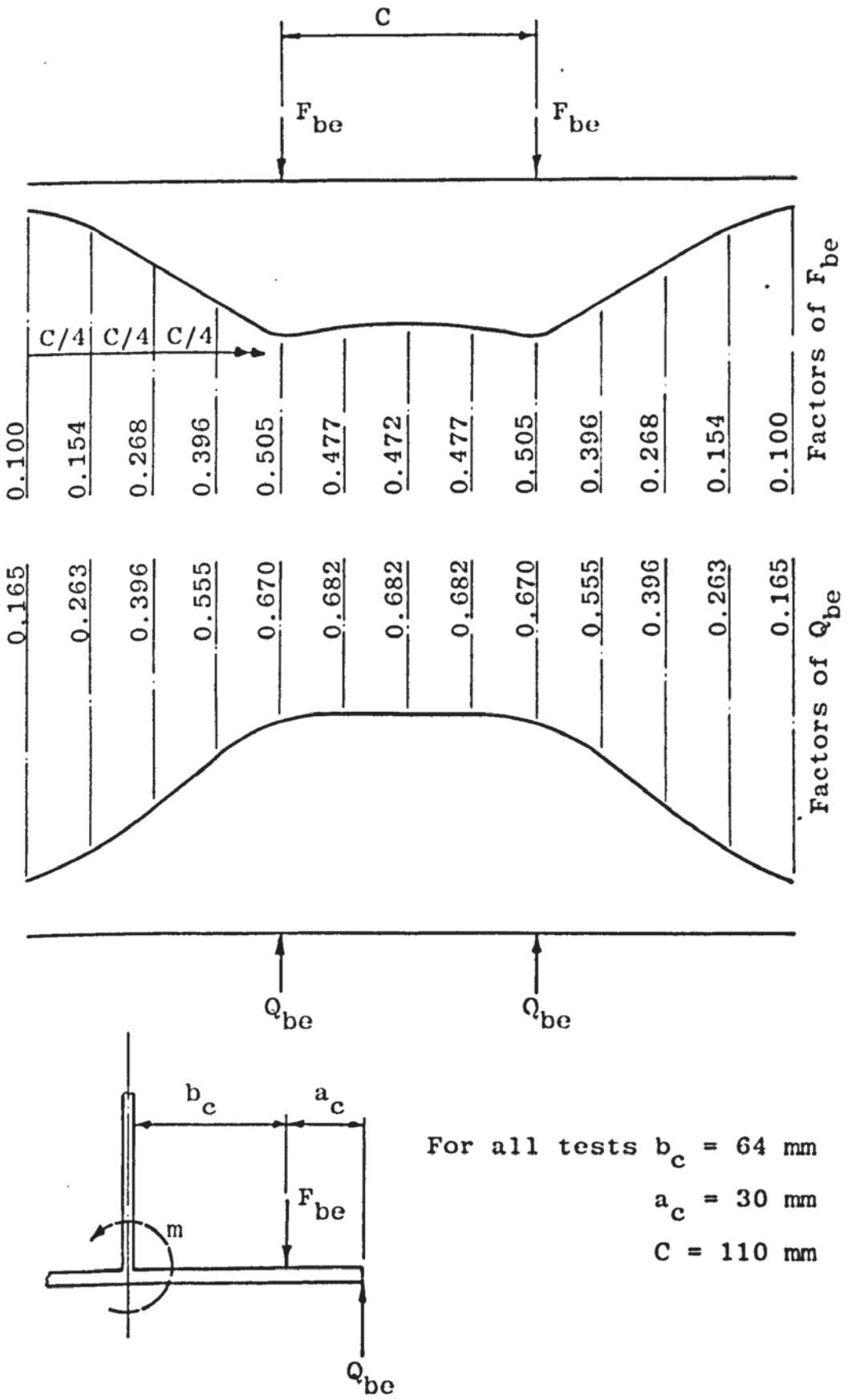

FIGURE 5.3 DISTRIBUTION OF BENDING MOMENTS ALONG THE COLUMN FLANGE

$$\Delta_c = 4.F_{be}.b_c^3\ (1 + 3.a_c/2.b_c)/E_c.w_c\ .t_c^3 \qquad 5.12$$

Equating 5.11 and 5.12 gives

$$w_c \approx 2.b_c \qquad 5.13$$

If prying force does exist the maximum bending moment is $0.505\ F_{be} - 0.670\ Q_{be}$. Therefore

$$\Delta_c = \frac{0.505.F_{be}.b_c^2}{3.E_c.I_c}\ (1 + 3.a_c/2.b_c) - \frac{0.670.Q_{be}}{3.E_c.I_c}\ (a_c + b_c)^2$$

from which

$$\Delta_c = \frac{2.02.F_{be}.b_c^2}{E_c.t_c^3}\ (1 + 3.a_c/2.b_c) - \frac{2.68.Q_{be}}{E_c.t_c^3}\ (a_c + b_c)^2 \qquad 5.14$$

The same deflection can also be obtained from an equivalent cantilever, therefore

$$\Delta_c = \frac{4.F_{be}.b_c^3}{E_c.w_c\ .t_c^3}\ (1 + 3.a_c/2.b_c) - \frac{4.Q_{be}}{E_c.w_c\ .t_c^3}\ (a_c + b_c)^3 \qquad 5.15$$

Equating 5.14 and 5.15 gives

$$w_c = \frac{4.F_{be}.b_c^3(1 + 3.a_c/2.b_c) - 4.Q_{be}(a_c + b_c)^3}{2.02.F_{be}.b_c^2(1 + 3.a_c/2.b_c) - 2.68.Q_{be}(a_c + b_c)^2}$$

$a_c = 30mm$, $b_c = 64mm$ therefore

$$w_c = 126.8\ (F_{be} - 1.861\ Q_{be})/(F_{be} - 1.681Q_{be})$$

therefore for the range of sizes tested

$$w_c = 2.b_c \qquad 5.16$$

The effective width of the column flange per bolt, w_c, may therefore be taken as $2.b_c$ whether prying forces are acting or not.

A similar method was used by Holmes[73] in the preparation of design tables for runway beams. Also an equation given by Timoshenko and Woinowsky-Krieger[71] for the deflection of a semi-infinite cantilever carrying a single load may be used. This method depends on the point of singularity being known, i.e. the point at which any of the stress components become infinitely large. It is difficult to establish the point of singularity for the loading arrangement shown in Figure 5.3 and arbitrary selection of this point along the fixed edge produces vastly varying values of deflection. Another equation given by Timoshenko and Woinowsky-Krieger[71] gives the deflection along the free edge of a very long plate for a concentrated force applied at the free edge. This approach will now be used to examine whether the equivalent cantilever width of $2.b_c$ per bolt is approximately correct.

Consider two examples where 2 point loads P and P_1, of equal value act at the free edge a distance C apart. The width of the plate is (a) b equal to 64mm and (b) b_1 equal to 94mm and in both cases C is equal to 110mm similar to the dimensions in the beam to column connection tests.

(ii) Plate Width b = 64mm which is equal to b_c

Deflection Δ at P due to load P is $\Delta = \alpha Pb^2/D$ 5.1a

where α is an empirical constant based on the geometry of the loading arrangement and where D is the flexural rigidity $E.t^3/12\ (1-v^2)$ where v is poissons ratio assumed to be 0.3 and where t is the plate thickness.

In this case $\alpha = 0.168$ therefore

$\Delta = 0.168.P.b^2.12\ (1-v^2)/E.t^3$ 5.2a

Deflection Δ_1 at P due to load P_1 is $\Delta_1 = \alpha_1 P_1 b^2/D$ 5.3a

where α_1 is an empirical constant based on the geometry of the loading arrangement.

In this case C = 110mm = 1.719b therefore $\alpha_1 = 0.0306$

$\Delta_1 = 0.0306.P_1.b^2.12(1-v^2)/E.t^3$ 5.4a

The total deflection $(\Delta + \Delta_1)$ under P or P_1 as load P is equal to load P_1 is therefore

$\Delta + \Delta_1 = 0.199.P.b^2.12(1-v^2)/E.t^3$ 5.5a

The same deflection from an equivalent cantilever is

$\Delta + \Delta_1 = 12.P.b^3/3.E.w.t^3$ 5.6a

where w is the effective cantilever width.

Equating 5.5a and 5.6a gives

$w = 1.84b = 1.84b_c$

If the width of the plate was 94mm and the two point loads acted a distance of 64mm from the built-in edge and the deflections determined at the free edge then the value of the effective cantilever width for this case would probably be similar to that of 1.84b or $1.84b_c$.

(b) Plate width b_1 = 94mm

Deflection Δ_{11} at P due to load $P\Delta_{11} = \alpha_2 P b_1^2/D$ 5.7a

where α_2 is an empirical constant based on the geometry of the loading arrangement.

In this case $\alpha_2 = 0.168$ therefore

$$\Delta_{11} = 0.168.P.b_1^2.12(1-v^2)/E.t^3 \quad 5.8a$$

Deflection Δ_{111} at P due to load P_1 is $\Delta_{111} = \alpha_3.P_1.b_1^2/D$ 5.9a

where α_3 is an empirical constant based on the geometry of the loading arrangement.

In this case C = 110mm = $1.17.b_1$ therefore $\alpha_3 = 0.0592$

$$\Delta_{111} = 0.0592.P_1.b_1^2.12(1-v^2)/E.t^3 \quad 5.10a$$

The total deflection ($\Delta_{11} + \Delta_{111}$) under P or P_1 as load P is equal to load P_1 is therefore

$$\Delta_{11} + \Delta_{111} = 0.2272.P.b_1^2.12(1-v^2)/E.t^3 \quad 5.11a$$

The same deflection from an equivalent cantilever is

$$\Delta_{11} + \Delta_{111} = 12.P.b_1^3/3.E.w.t^3 \quad 5.12a$$

where w is the effective cantilever width

Equating 5.11a and 5.12a gives

$w = 1.61\ b_1 = 2.37b_c$

If in case (b) two additional point loads were to act at a distance of 64mm from the built-in edge and 110mm apart then the effective width of $2.37b_c$ would probably be reduced, i.e. taking into account the results from cases (a) and (b) the combined loading case would produce a value of w within the limits of $1.84b_c$ and $2.37b_c$. Further work is necessary in order to define more accurately the value of the effective width. However, based on the limited evidence of the method

proposed on page 164 and the preceeding examples it will be assumed in the ensueing analyses that $w = 2.b_c$ within the context of the test geometry.

5.3.1 Distribution of Prying Forces

The distribution of prying forces must be clarified. In the tee stubs the forces are linearly distributed at the toes on either side of the web. In the beam to column connections there is indirect evidence that contact areas adjacent to the four tensile bolts are combinations of pairs as shown in Figure 5.4. De Back and Zoetemeijer[22] suggested similar contact points for tee stub models. The contact areas C develop prying forces related to the column flanges while those labelled P develop prying forces related to the end plate. If the end plate and column flange are 'thick' then there will be no contact areas and therefore no prying forces. If the column flange is 'thin' and the end plate of 'medium' thickness then there will be the maximum of eight contact points and thus two prying forces per bolt. This effect is shown in the experimental results of Packer and Morris[33]. In the experimental results reported in Chapter Four there appear to be four contact areas in the elastic stage and two contact areas at the ultimate load.

5.3.2 Discontinuity Limits

The bending moment applied to a beam to column connection

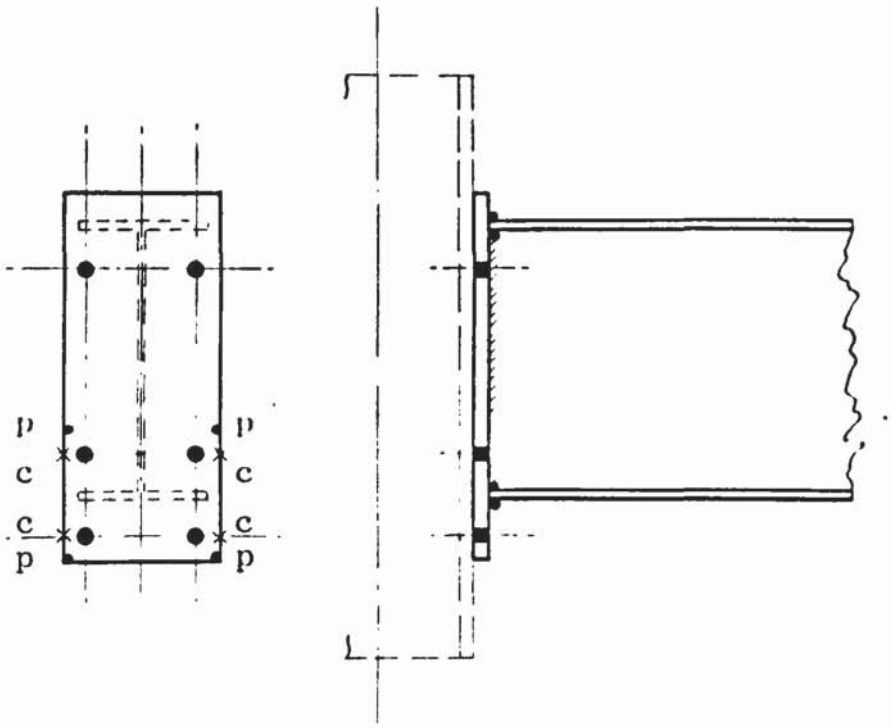

(a) End Plate

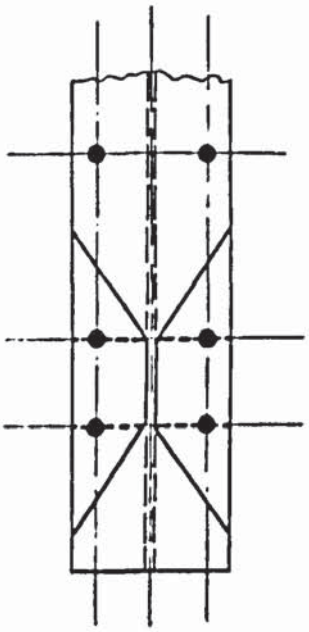

(b) Column Flange

FIGURE 5.4 POSITION OF PRYING FORCES ON THE END PLATE AND YIELD LINE PATTERN FOR THE COLUMN FLANGE

at service load should preferably not exceed the limit of the linear portion of the bending moment - joint rotation relationship. This discontinuity limit may be controlled by the non-linearity of the end plate, or the column flange or the tensile bolts whichever is the most critical. The discontinuity limits for the end plate and the column flange are related to the b/t ratios in equations 5.1 and 5.2 assuming 1 = b. The discontinuity limit for the bolts may be obtained from the load - extension relationship or in the case of high strength bolts may be fixed at approximately 80% of the ultimate tensile strength.

Discontinuity limit bending moment equations are now derived for the end plate, column flange and tensile bolts. Two equations are given for each component. One equation is based on the assumption that the four prying forces are related to the end plate. While the other equation is based on the assumption that the four prying forces are related to the column flange.

5.3.3 End Plate Discontinuity Limit, M_{ph}, Equations

The limiting moment that may be applied to the end plate projection is determined from the first change in direction of the load - deflection relationship in the end plate adjacent to the beam flange.

(a) Prying forces related to the end plate

Taking moments of forces acting on the complete end plate, shown in Figure 5.5 (a), about the centre of rotation gives

$$- M_{ph} + 4(F_{be} - Q_{be})\, d_f = 0 \qquad 5.17$$

This equation assumes that there are four tensile bolts resisting the moment, four prying forces associated with the end plate symmetrically distributed about the centroid of the tensile bolts and that the materials are in the elastic range of behaviour.

Taking moments of forces for the end plate projection about section x-x Figure 5.5 (a) gives

$$- m_{ph} - Q_{be}(a_p + b_p) + F_{be}.b_p = 0 \qquad 5.18$$

Equations 5.17 and 5.18 can be combined to eliminate F_{be} and produce

$$- M_{ph} + 4.d_f(m_{ph}/b_p + Q_{be}.a_p/b_p) = 0 \qquad 5.19$$

Rearranging equation 5.8 gives

$$Q_{be} = \frac{F_{be} - F_{be}(F_p/A_b.E_b) + F_p.S_{bs}}{1 + 2(a_p/b_p) + (2/3)(a_p/b_p)^2} \qquad 5.20$$

Combining equations 5.18 and 5.20 to eliminate F_{be} gives

$$Q_{be} = \frac{(m_{ph}/b_p)\left[1 - (F_p/A_b.E_b)\right] + F_p.S_{bs}}{(a_p/b_p) + (2/3)(a_p/b_p)^2 + F_p\left[1 + (a_p/b_p)\right]/A_b.E_b} \qquad 5.21$$

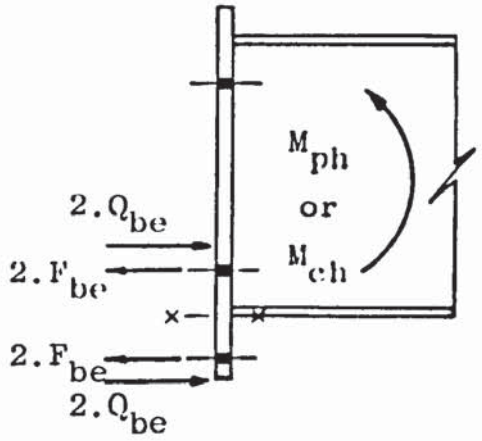

(a) Q_{be} Related to EP

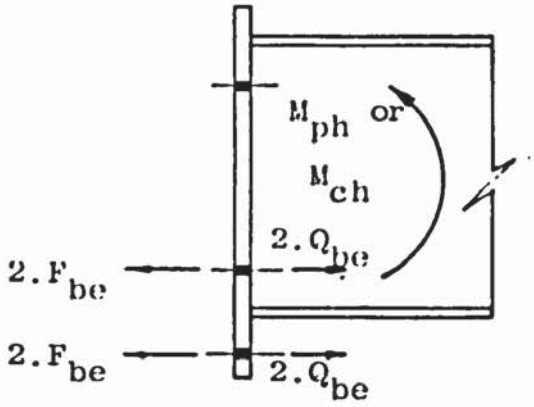

(b) Q_{be} Related to CF

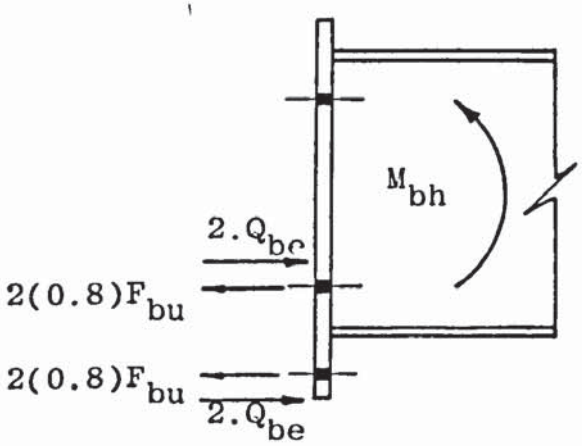

(c) Q_{be} Related to EP

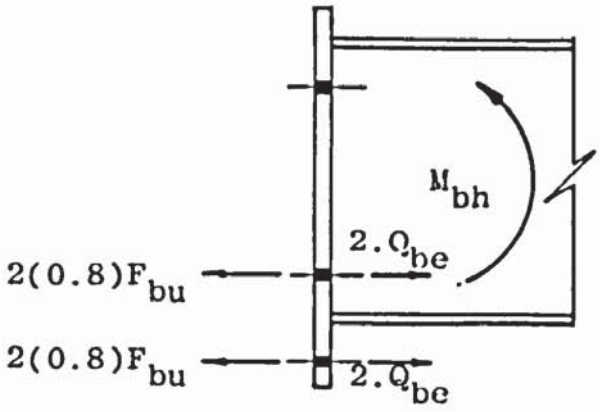

(d) Q_{be} Related to CF

Abbreviations used: EP, End Plate; CF, Column Flange

FIGURE 5.5 FORCES ADJACENT TO THE END PLATE AT THE DISCONTINUITY LIMITS

Substituting equation 5.21 into 5.19 gives

$$M_{ph} = 4.m_{ph}(d_f/b_p)(1 + k_p) \qquad 5.22$$

where

$$k_p = \frac{1 + F_p \left[F_s(b_p/m_{ph}) - 1\right] /A_b.E_b}{1 + (2/3)(d_p/b_p) + F_p \left[1 + (b_p/a_p)\right] /A_b.E_b} \qquad 5.23$$

The value of k_p depends on the prying forces and will be small for a 'thick' end plate. It should be noted that the value of k_p is normally positive and when substituted into equation 5.22 increases the magnitude of M_{ph}.

(b) Prying forces related to the column flange

The forces acting on the end plate when the prying forces are related to the column flange are shown in Figure 5.5 (b). Taking moment of the forces about the centre of rotation and following the same procedure as before gives

$$M_{ph} = 4.m_{ph}(d_f/b_p)(1 + k_p) \qquad 5.22$$

where $k_p = 0$

If the prying forces are related to the column flange then the value of M_{ph} is independent of the column flange stiffness.

5.3.4 Column Flange Discontinuity Limit, M_{ch} and M_{cy} Equations

The moment that is required to be applied to the connection at the non-linear stage in the moment-rotation relationship corresponding to the discontinuity limit in the column flange, m_{ch}, is determined as follows. A lower bound limit for this bending moment, M_{ch}, is assumed to occur when the work hardened plastic moment per unit length, m_h, forms along the effective cantilever width, $2b_c$ per bolt. The total work hardened moment per bolt is therefore $m_h.2b_c$ which is equivalent to m_{ch}.

(a) Prying forces related to the end plate

Taking moments of forces acting on the column flange about the centre of rotation as shown in Figure 5.5 (a) gives

$$- M_{ch} + 4(F_{be} - Q_{be})d_f = 0 \qquad 5.24$$

Q_{be} is determined from equation 5.20 and when combined with equation 5.24 produces

$$M_{ch} = 4.d_f \left[F_{be} - \frac{F_{be}(1 - F_p/A_b.E_b) + F_p.S_{bs}}{1 + 2(a_p/b_p) + (2/3)(a_p/b_p)^2} \right] \qquad 5.25$$

Taking $F_{be} = m_{ch}/b_c$ and neglecting, for simplicity, any effect due to Q_{be}, then equation 5.25 becomes

$$M_{ch} = 4.m_{ch}(d_f/b_c)(1-k_c) \qquad 5.26$$

where

$$k_c = \frac{1 + F_p \left[F_s(b_c/m_{ch}) - 1\right] / A_b.E_b}{1 + 2(a_p/b_p) + (2/3)(a_p/b_p)^2} \qquad 5.27$$

and where the equivalent width per bolt is $2.b_c$ as defined previously. In this case k_c is dependent on both the end plate and column flange properties and when substituted into equation 5.26 will normally decrease the value of M_{ch}.

(b) Prying forces related to the column flange

The forces acting on the end plate when the prying forces are related to the column flange are shown in Figure 5.5 (b). Taking moments of forces about the centre of rotation gives as before equation 5.24

$$- M_{ch} + 4(F_{be} - Q_{be})d_f = 0 \qquad 5.24$$

Q_{be} is determined from equation 5.20a

$$Q_{be} = \frac{F_{be} - F_{be}(F_c/A_b.E_b) + F_c.S_{bs}}{1 + 2(a_c/b_c) + (2/3)(a_c/b_c)^2} \qquad 5.20a$$

where $F_c = (E_c.w_c.t_c^3.g_c)/(6.a_c.b_c^2)$ 5.9a

Combining equations 5.20_a and 5.24 produces

$$M_{ch} = 4.d_f \left[F_{be} - \frac{F_{be}(1-F_c/A_b.E_b) + F_c.S_{bs}}{1 + 2(a_c/b_c) + (2/3)(a_c/b_c)^2}\right] \qquad 5.25a$$

Taking $F_{be}.b_c - Q_{be}(a_c + b_c) = m_{ch}$ 5.28

and combining with the prying force equation 5.20a gives

$$F_{be} = \frac{F_c.S_{bs}(a_c + b_c) + m_{ch}\left[1 + 2(a_c/b_c) + (2/3)(a_c/b_c)^2\right]}{\left[1 + 2(a_c/b_c) + (2/3)(a_c/b_c)^2\right]b_c - (a_c + b_c)(1 - F_c/A_b.E_b)} \quad 5.29$$

Combining equations 5.25 with 5.29 to eliminate F_{be} gives

$$M_{ch} = 4.m_{ch}(d_f/b_c)k_c \quad 5.30$$

where

$$k_c = \left[\frac{1 + F_c.S_{bs}\left[1 + (a_c/b_c)\right](b_c/m_{ch}.X)}{X - \left[1 + (a_c/b_c)\right](1 - F_c/A_b.E_b)}\right]\left[X - 1 + (F_c/A_b.E_b)\right]$$

$$+ F_c.S_{bs}.b_c/X.m_{ch} \quad 5.31$$

where $X = 1 + 2(a_c/b_c) + (2/3)(a_c/b_c)^2$

and where the equivalent width per bolt is $2.b_c$ as defined previously.

An upper bound limit for the bending moment, M_{cy}, at the non-linear stage in the moment-rotation relationship corresponding to the discontinuity limit in the column flange is assumed to occur when the work hardened yield line pattern (m_h per unit length) formed in the column flange adjacent to the tensile flange of the beam is as shown in Figure 5.6. This is produced by the tensile force at the level of the flange of the beam which is M_{cy}/d_f.

(c) Prying forces related to the end plate

The work hardened yield line pattern for this case is shown in Figure 5.6(a). The effect of the prying forces, Q_{be}, on the

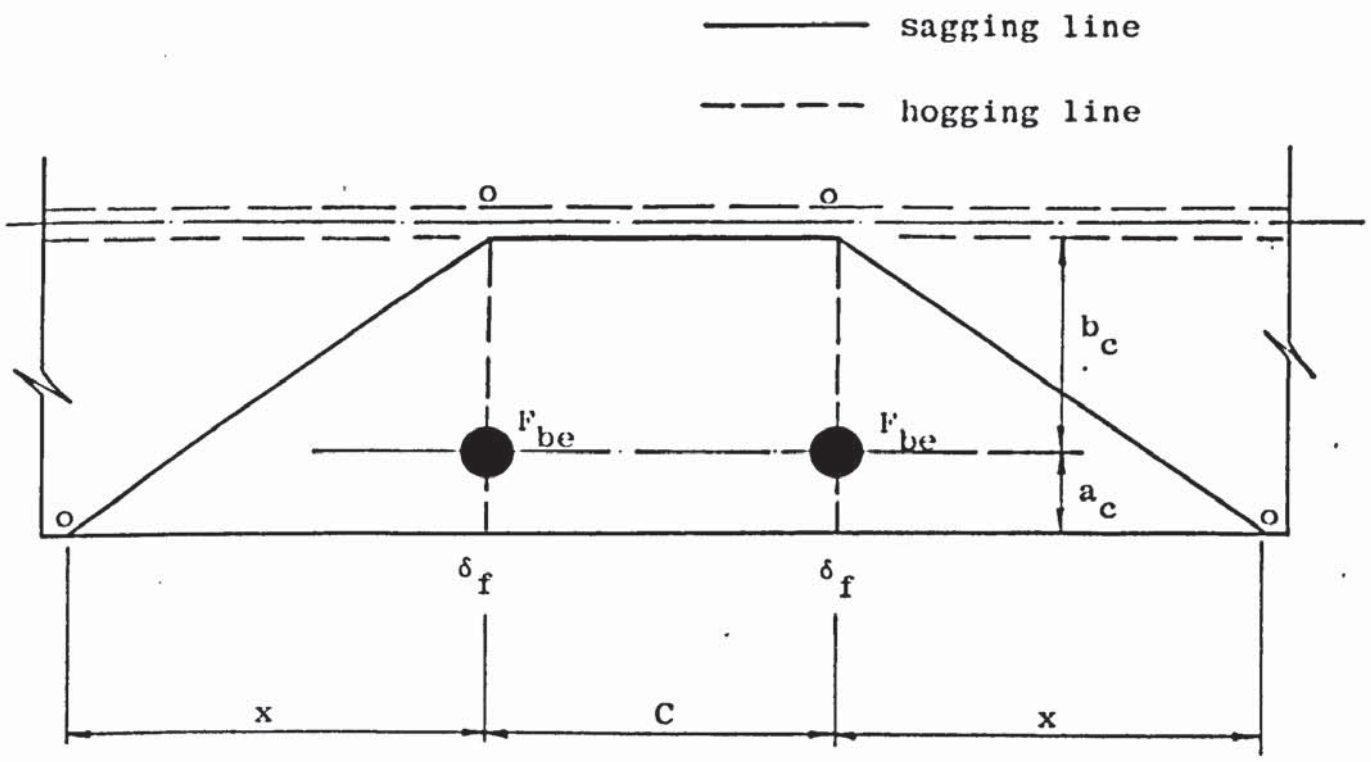

(a) Prying Forces Related to End Plate

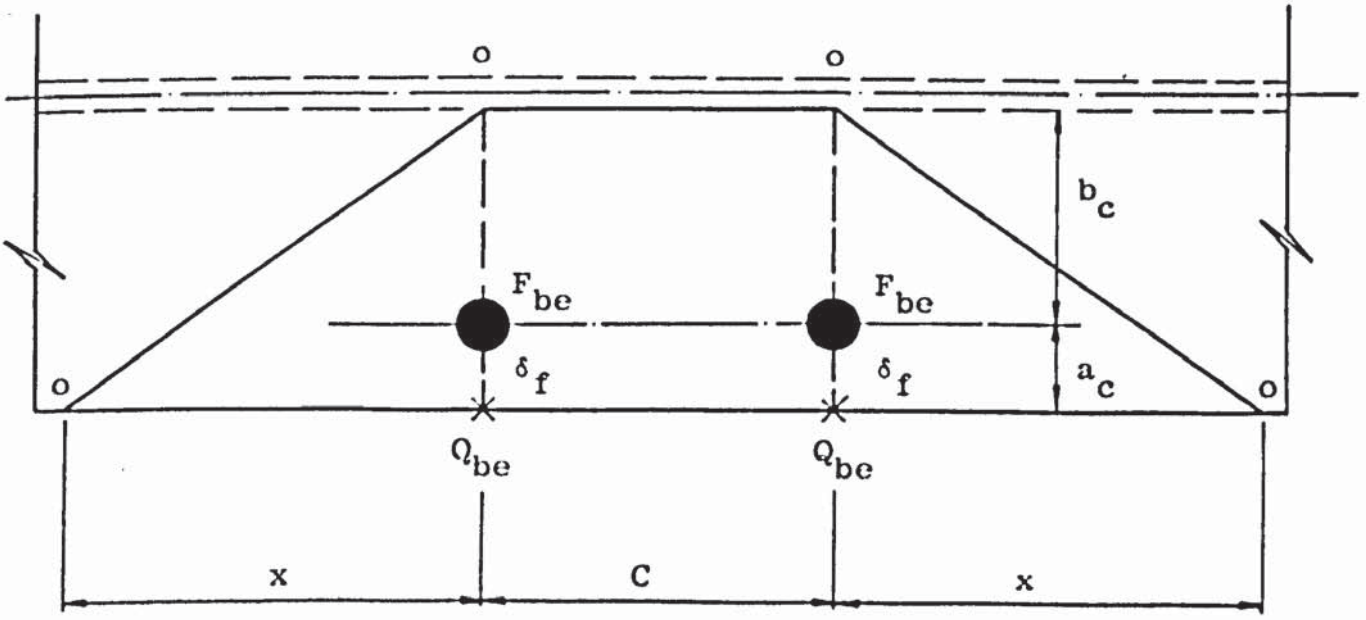

(b) Prying Forces Related To Column Flange

FIGURE 5.6 YIELD LINE PATTERNS FOR THE COLUMN FLANGE

deformation of the column flange is neglected for simplicity. The effect of the elastic bolt force is only considered. Using yield line theory and equating external and internal work done ignoring work done on bolts gives

$$2.F_{be}.b_c.\delta_f/(a_c + b_c) = 4(a_c + b_c)m_h.\delta_f/x + 2.x.m_h.\delta_f/(a_c + b_c) + C.m_h.\delta_f/(a_c + b_c) \qquad 5.32$$

optimising

$$\frac{dF_{be}}{dx} = m_h/b_c - 2(a_c + b_c)^2 m_h/x^2.b_c = 0$$

therefore

$$x = \sqrt{2}\ (a_c + b_c) \qquad 5.33$$

Combining equations 5.32 and 5.33 produces

$$F_{be} = w_{cy}.m_h/b_c \qquad 5.34$$

where

$$w_{cy} = 2.\sqrt{2}\ (a_c + b_c) + C/2 \qquad 5.35$$

M_{cy} can be found in a similar manner to M_{ch} by

$$M_{cy} = 4.m_{ch}(d_f/b_c)(1-k_c) \qquad 5.36$$

where k_c is as defined in equation 5.27 and where the equivalent width per bolt is w_{cy} found from equation 5.35.

(d) Prying forces related to column flange

The work hardened yield line pattern for this case is shown in Figure 5.6(b) and is formed by the elastic bolt forces F_{be} and prying forces Q_{be} acting at the toe of the column flange adjacent to the bolt forces. Using yield line theory and

equating external and internal work ignoring work done on bolts gives

$$2.F_{be}.b_c.\delta_f/(a_c + b_c) - 2.Q_{be}.\delta_f = 4(a_c + b_c)m_h.\delta_f/x$$

$$+ 2.x.m_h.\delta_f/(a_c + b_c) + C.m_h.\delta_f/(a_c + b_c) \qquad 5.37$$

optimising

$$\frac{dF_{be}}{dx} = m_h/b_c - 2(a_c + b_c)^2 m_h/x^2.b_c = 0$$

therefore, as before

$$x = \sqrt{2}\,(a_c + b_c) \qquad 5.33$$

Combining equations 5.33 and 5.37 produces

$$F_{be} - Q_{be}(1 + a_c/b_c) = w_{cy}.m_h/b_c \qquad 5.38$$

where, as before

$$w_{cy} = 2.\sqrt{2}\,(a_c + b_c) + C/2 \qquad 5.35$$

M_{cy} can be found in a similar manner to M_{ch} by

$$M_{cy} = 4.m_{ch}(d_f/b_c).k_c \qquad 5.39$$

where k_c is as defined in equation 5.31 and where the equivalent width per bolt is w_{cy} found from equation 5.35.

These expressions for the column flange are formed ignoring the work done in extending the bolt, assuming that the work hardening moment derived from the strip beam tests also applied to the column flanges and that four prying forces are symmetrically arranged for all four tensile bolts.

It should be noted that the value of k_c when the prying forces are related to the end plate and decreases the magnitude of M_{ch} and M_{cy}. If the prying forces are related to the column flange k_c is positive and the magnitude of M_{ch} and M_{cy} is increased.

5.3.5 Tensile Bolts Discontinuity Limits, M_{bh}, Equations

Discontinuity equations for four tensile bolts which resist the applied moment and four symmetrical prying forces associated with either the end plate or column flange are now determined.

(a) Prying forces related to end plate

The forces acting on the end plate when the prying forces are related to the end plate are shown in Figure 5.5(c). The limiting tensile bolt force is taken as $0.8F_{bu}$ while the remaining materials are assumed to be within the elastic range of behaviour.

Taking moments of forces acting on the end plate about the centre of rotation gives

$$M_{bh} = 4(0.8.F_{bu} - Q_{be})d_f \qquad 5.40$$

Resolving horizontal forces

$$0.8.F_{bu} = M_{bh}/4.d_f + Q_{be} \qquad 5.41$$

Replacing F_{be} by $0.8F_{bu}$ in equation 5.20 then substituting

in equation 5.41 gives

$$Q_{be} = \frac{(M_{bh}/4.d_f)(1 - F_p/A_b.E_b) + F_p.S_{bs}}{2(a_p/b_p) + (2/3)(a_p/b_p)^2 + (F_p/A_b.E_b)} \qquad 5.42$$

Combining equations 5.40 and 5.42 to eliminate Q_{be} gives

$$M_{bh} = 4.d_f(0.8.F_{bu})(1 - k_b) \qquad 5.43$$

where

$$k_b = \frac{1 - (F_p/A_b.E_b)(1 - F_s/0.8.F_{bu})}{1 + 2(a_p/b_p) + (2/3)(a_p/b_p)^2} \qquad 5.44$$

The value of k_b depends largely on the properties of the end plate and will normally be small for a 'thick' end plate. When k_b is substituted into equation 5.43 the magnitude of M_{bh} is decreased.

(b) Prying forces related to column flange

The forces acting on the end plate when the prying forces are related to the column flange are shown in Figure 5.5(d). The limiting tensile bolt force is taken as $0.8F_{bu}$ while the remaining materials are also assumed to be within the elastic range of behaviour. Taking moments of forces acting on the end plate about the centre of rotation and resolving horizontal forces gives as before equations 5.40 and 5.41 respectively. Replacing F_{be} by $0.8F_{bu}$ in equation 5.20(a) and substituting in equation 5.41 gives

$$Q_{be} = \frac{(M_{bh}/4.d_f)(1 - F_c/A_b.E_b) + F_c.S_{bs}}{2(a_c/b_c) + (2/3)(a_c/b_c)^2 + (F_c/A_b.E_b)} \qquad 5.45$$

Combining equations 5.40 and 5.45 to eliminate Q_{be} gives

$$M_{bh} = 4.d_f(0.8.F_{bu})(1 - k_b) \qquad 5.45(a)$$

where

$$k_b = \frac{1 - (F_c/A_b.E_b)(1 - F_s/0.8.F_{bu})}{1 + 2(a_c/b_c) + (2/3)(a_c/b_c)^2} \qquad 5.46$$

The value of k_b depends largely on the properties of the column flange and will normally be small for a thick column flange. When k_b is substituted into equation 5.45(a) the magnitude of M_{bh} is decreased. It is worth noting that the value of k_b is normally positive and reduces the value of M_{bh} whether the prying forces are related to the end plate or column flange.

5.3.6 Theory for Slip

In the beam to column connection tests where $M/V.d_f < 1$ slip occurred prior to failure. In the beam to column connection tests where $M/V.d_f < 1.6$ slip did not occur in every specimen prior to failure.

Slip is resisted by frictional forces between the end plate and the column at the compression flange of the beam and by symmetrical prying forces adjacent to all tensile bolts, see Figure 5.7 (a). It is assumed that the initial pretension in the compression bolts is present when slip occurs and also

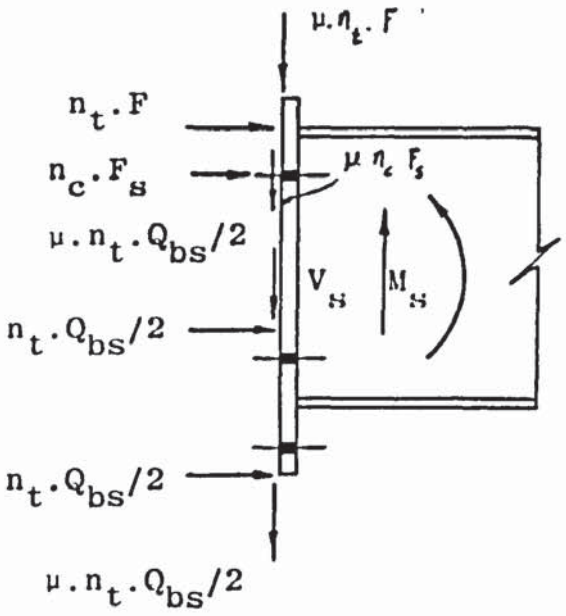

(a) Final Slip

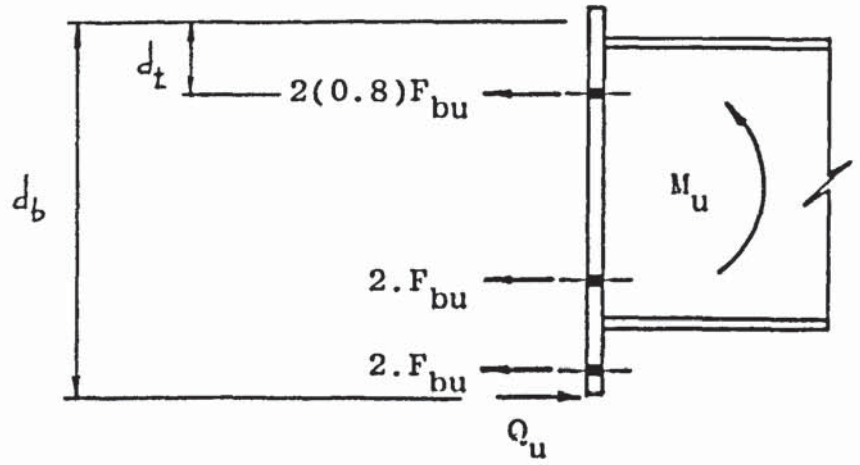

(b) Failure

FIGURE 5.7 FORCES ADJACENT TO THE END PLATE AT FINAL SLIP AND FAILURE

resists slip.

Taking moments about the beam tension flange

$$n_t.F.d_f - M_s = 0 \qquad 5.47$$

resolving vertical forces

$$V_s - \mu.n_t.F - \mu.n_t.Q_{bs} - \mu.n_c.F_s = 0 \qquad 5.48$$

combining equations 5.47 and 5.48 to eliminate F gives

$$\mu = \frac{V_s}{(M_s/d_f + n_t.Q_{bs} + n_c.F_s)} \qquad 5.49$$

This equation assumes that the tensile bolts are placed at equal vertical distances from the tensile flange of the beam.

5.3.7 Ultimate Load Theory

In the beam to column connection tests where $M/V.d_f > 1$ the majority of the test specimens failed by tensile bolt fracture. The forces acting on the end plate at bolt failure are shown in Figure 5.7 (b). Two prying forces are assumed to act at the bottom of the end plate and the full tensile strength of four bolts are also assumed to develop. The maximum tensile force on each compression zone bolt at ultimate load is assumed to be $0.8F_{bu}$. This assumption was taken from the extrapolated applied moment - bolt force experimental relationship, e.g. see page 133.

Therefore taking moments about the centre of rotation gives

$$M_u = 4.F_{bu}(d_f + 0.4.d_t) - Q_u.d_b \qquad 5.50$$

now

$$Q_u = 2.Q_{bu}$$

where

$$Q_{bu} = \frac{F_{bu} - F_p(S_{bu} - S_{bs})}{1 + 2(a_p/b_p) + (2/3)(a_p/b_p)^2} \qquad 5.10$$

where $S_{bu} = 1.05\%$.

CHAPTER SIX

COMPARISON OF EXPERIMENTAL AND THEORETICAL RESULTS

6.1 Introduction

The tee stub and beam to column test results, together with test results by other authors are compared with the theoretical values obtained from methods suggested in the theoretical investigation and by other authors.

6.2 Tee Stubs

The value of prying forces at failure measured in the tee stub tests are compared with the theoretical values in Table 6.1. The proportion of the grip length used to calculate the extension of the bolt per plate is the flange plate thickness, plus one washer. A comparison of experimental and theoretical prying forces for other investigators is shown in Tables 6.2, 6.3, 6.4, 6.5 and 6.7. The comparison has been limited to tests where prying forces definitely existed and also where bolt failure occurred. The test specimens used by other investigators were either similar to those reported in Chapter Three or had an I section placed between the tee stubs. In some cases both types of models were studied. The prying forces at failure, Q_{bu}, were determined from equation 5.10. In tests where I sections were involved, Q_{bu} was determined for both the tee stub

Spec.	Expt.		Theory		F_u	Q_{bu}
	F_u kN	Q_{bu} kN	F_u kN	Q_{bu} kN	$\frac{\text{expt.}}{\text{theory}}$	$\frac{\text{expt.}}{\text{theory}}$
TS1	119.0	21.0	115.7	24.3	0.99	1.05
TS2	87.2	52.8	91.2	48.8	0.95	1.10
TS3	97.7	42.3	98.7	41.3	0.97	1.07
TS4	94.7	45.3	92.6	47.4	1.01	0.97
TS5	104.7	35.3	100.0	40.0	1.05	0.88
	Mean				0.99 ±0.034	1.01 ±0.080
	Coefficient of Variation				3.4%	7.9%

TABLE 6.1 COMPARISON OF EXPERIMENTAL AND THEORETICAL RESULTS FOR TEE STUBS

Spec.	Expt.		Theory Douty & McGuire		Theory Author		Douty & McGuire		Author	
	F_u kips	Q_{bu} kips	F_u kips	Q_{bu} kips	F_u kips	Q_{bu} kips	$\frac{F_u \text{ expt.}}{\text{theory}}$	$\frac{Q_{bu} \text{ expt.}}{\text{theory}}$	$\frac{F_u \text{ expt.}}{\text{theory}}$	$\frac{Q_{bu} \text{ expt.}}{\text{theory}}$
A1	44.0	12.0	38.8	17.3	41.9	14.1	1.14	0.70	1.05	0.85
A1S	40.8	16.7	40.5	17.0	42.9	14.6	1.01	0.98	0.95	1.14
A9	44.3	11.7	40.5	15.5	43.2	12.8	1.09	0.75	1.03	0.91
B1	50.5	13.5	42.8	21.3	47.5	16.5	1.18	0.64	1.06	0.82
B3	57.5	4.5	51.0	11.0	56.9	5.1	1.13	0.41	1.01	0.88
B4	57.0	3.0	50.0	10.0	52.3	4.7	1.14	0.30	1.09	0.63
						Mean	1.12 ±0.054	0.63 ±0.223	1.03 ±0.044	0.87 ±0.150
						Coefficient of Variation	4.8%	35.4%	4.3%	17.2%

TABLE 6.2 COMPARISON OF EXPERIMENTAL RESULTS BY DOUTY AND McGUIRE[6]

Spec.	Expt.		Theory Struik		Theory Author		Struik		Author	
	F_u kN	Q_{bu} kN	F_u kN	Q_{bu} kN	F_u kN	Q_{bu} kN	F_u expt./theory	Q_{bu} expt./theory	F_u expt./theory	Q_{bu} expt./theory
HB-20-1T	161.0	19.0	131.4	48.6	160.2	19.8	1.23	0.39	1.00	0.96
HB-20-2T	157.0	23.0	131.4	48.6	160.2	19.8	1.19	0.47	0.98	1.16
HB-20-3T	159.5	20.5	131.4	48.6	160.2	19.8	1.21	0.42	1.00	1.03
HB-20-4T	160.0	20.0	131.4	48.6	160.2	19.8	1.22	0.41	1.00	1.01
HB-17-1T	146.5	28.8	122.6	52.7	143.0	32.3	1.20	0.55	1.02	0.89
HB-17-2T	144.8	30.6	122.6	52.7	143.0	32.3	1.18	0.58	1.01	0.95
HB-17-NT	147.5	27.8	122.6	52.7	150.3	25.0	1.20	0.53	0.98	1.11
HB-16-1TS	142.0	33.3	113.8	61.5	135.2	40.1	1.25	0.54	1.05	0.83
HB-16-2TS	141.3	34.0	113.8	61.5	135.2	40.1	1.24	0.55	1.05	0.85
B-16-NT	69.0	1.0	64.8	5.2	69.0	1.1	1.06	0.19	1.00	0.95
B-12-NT	59.5	11.5	53.0	17.0	56.8	13.2	1.12	0.68	1.05	0.87
B-10-NT	56.3	13.8	49.3	20.7	53.8	16.2	1.14	0.67	1.05	0.85
						Mean	1.19 ±0.053	0.50 ±0.129	1.02 ±0.026	0.96 ±0.102
						Coefficient of Variation	4.5%	25.8%	2.6%	10.6%

TABLE 6.3 COMPARISON OF EXPERIMENTAL RESULTS BY STRUIK[19]

Spec.	Expt.		Theory De Back & Zoet.		Theory Author		De Back & Zoet.		Author	
	F_u kN	Q_{bu} kN	F_u kN	Q_{bu} kN	F_u kN	Q_{bu} kN	$\frac{F_u \text{ expt.}}{\text{theory}}$	$\frac{Q_{bu} \text{ expt.}}{\text{theory}}$	$\frac{F_u \text{ expt.}}{\text{theory}}$	$\frac{Q_{bu} \text{ expt.}}{\text{theory}}$
t_p = 17	140.0	33.2	129.5	43.7	141.5	31.7	1.08	0.76	0.99	1.05
HE 240B t_p = 17	148.8	24.4	129.5	43.7	141.5	31.7	1.15	0.56	1.05	0.77
HE 160M t_p = 20	170.0	23.6	157.5	36.1	170.1	23.5	1.08	0.65	1.00	1.00
HE 160M t_p = 25	177.3	7.3	165.5	19.0	172.4*	12.1*	1.07	0.38	1.03	0.60
HE 160M t_p = 32	165.0	8.0	164.0	9.0	164.2*	8.9*	1.01	0.89	1.00	0.90
			Mean				1.08 ±0.044	0.65 ±0.174	1.01 ±0.022	0.86 ±0.149
			Coefficient of Variation				4.1%	26.8%	2.2%	17.2%

Note: * Indicates values determined using column flange properties

TABLE 6.4 COMPARISON OF EXPERIMENTAL RESULTS BY DE BACK AND ZOETEMEIJER[22]

Spec.	Expt.		Theory Nair et al		Theory Author		Nair et al		Author	
	F_u kips	Q_{bu} kips	F_u kips	Q_{bu} kips	F_u kips	Q_{bu} kips	$\frac{F_u \text{ expt.}}{\text{theory}}$	$\frac{Q_{bu} \text{ expt.}}{\text{theory}}$	$\frac{F_u \text{ expt.}}{\text{theory}}$	$\frac{Q_{bu} \text{ expt.}}{\text{theory}}$
S(TO)3-1	38.0	4.0	35.1	6.9	38.4	3.6	1.08	0.58	0.99	1.11
U(TO)3-1	38.5	3.5	35.1	6.9	38.4	3.6	1.10	0.51	1.00	0.97
U(TO)3-2	38.5	3.5	35.1	6.9	38.4	3.6	1.10	0.51	1.00	0.97
S(T4)3-1	30.8	11.2	28.7	13.3	31.8	10.2	1.07	0.84	0.97	1.09
U(T4)3-1	30.8	11.2	28.7	13.3	31.8	10.2	1.07	0.84	0.97	1.09
S(TO)4-1	42.8	9.0	39.2	12.6	44.2	7.6	1.09	0.71	0.97	1.18
U(TO)4-1	42.3	9.5	39.2	12.6	44.2	7.6	1.08	0.75	0.96	1.24
U(TO)4-2	42.5	9.3	39.2	12.6	44.2	7.6	1.08	0.74	0.96	1.22
U(T2)4-1	43.5	8.3	40.7	11.1	44.7	7.1	1.07	0.75	0.97	1.17
U(T4)4-1	35.5	16.3	32.3	19.5	37.0	14.8	1.10	0.84	0.96	1.10
U(T4)4-2	35.8	16.0	32.3	19.5	37.0	14.8	1.11	0.82	0.97	1.08
			Mean				1.09 ±0.014	0.72 ±0.122	0.97 ±0.014	1.11 ±0.084
			Coefficient of Variation				1.3%	17.0%	1.5%	7.6%

TABLE 6.5 COMPARISON OF EXPERIMENTAL RESULTS BY NAIR ET AL[30]

Spec.	Expt.		Theory		F_u expt./theory	Q_{bu} expt./theory
	F_u kN	Q_{bu} kN	F_u kN	Q_{bu} kN		
8	150.0	32.9	134.1	48.8	1.12	0.67
9	150	32.9	147.3	35.6	1.02	0.93
11	140	42.9	135.6	47.3	1.03	0.91
20/21	124.2	57.0	133.2	47.9	0.93	1.19
22/23	133.1	32.3	122.4	43.0	1.09	0.75
				Mean	1.04 ±0.066	0.89 ±0.179
	Coefficient of Variation				6.3%	20.1%

TABLE 6.6 COMPARISON OF EXPERIMENTAL RESULTS BY ZOETEMEIJER[31]

Spec.	Expt.		Theory				$\frac{F_u \text{ expt.}}{\text{theory}}$	$\frac{Q_{bu} \text{ expt.}}{\text{theory}}$
	F_u kN	Q_{bu} kN	F_u kN	Q_{bu} EP kN	Q_{bu} CF kN	Q_{bu} Total kN		
T1	70.0	93.3	66.8	42.9	53.6	96.5	1.05	0.97
T2	69.8	93.6	66.2	43.5	53.6	97.1	1.05	0.96
T3	77.0	86.3	66.7	44.0	52.6	96.6	1.15	0.89
T5	115.0	48.3	119.8	42.1	43.5	43.5	0.96	1.11
				Mean			1.05 ±0.067	0.98 ±0.080
				Coefficient of Variation			6.4%	8.1%

Abbreviations used: EP, End Plate; CF, Column Flange

TABLE 6.7 COMPARISON OF EXPERIMENTAL RESULTS BY PACKER AND MORRIS[33]

plate and column flange. In the latter case the effective width per bolt was taken as $2.b_c$. The prying force was related to the column flange only in the experimental results of Zoetemeijer[31], Table 6.6. Packer and Morris[33], Table 6.7, reported results from tee stub models where the column flange thickness in some specimens were thin, 6.8mm, and where the tee stub plates were of medium thickness, 15mm. It has been suggested earlier that in such cases two prying forces per bolt may be induced. One prying force would be related to the end plate and the other related to the column flange. Table 6.7 therefore shows the theoretical prying force for both the end plate and column flange. For simplicity the total theoretical prying force per bolt was taken as the summation of these two forces in the case of very flexible flanges. Table 6.1, 6.2, 6.3, 6.4, 6.5, 6.6 and 6.7 also show the comparison of experimental and theoretical applied forces, which produce lower % coefficients of variation than those associated with Q_{bu}. The method of comparing applied forces was used by many investigators to present their results.

Douty and McGuire[6], Struik[19], De Back and Zoetemeijer[22] and Nair et al[30] suggested methods to determine Q_{bu} and F_u and their results are given in the appropriate table. F_u values obtained from these methods may be considered acceptable, however the values obtained for Q_{bu} are inaccurate. Similar values are determined from the theory suggested in the previous chapter and compare favourably with the experimental values obtained from tee stubs

reported by the author and several other investigators. Apart from one result all values of F_u show a better correlation than those determined by the above authors. Also, values obtained for Q_{bu} are considerably more accurate, with smaller % coefficients of variation than those previously achieved.

6.3 Beam to Column Connections

6.3.1 Discontinuity Limits

The bending moments at the first discontinuity for the end plate, column flange and tensile bolts are shown in Tables 6.8 and 6.9. The values in Table 6.8 were determined assuming four symmetrical prying forces associated with the end plate, while the values in Table 6.9 were determined assuming four symmetrical prying forces associated with the column flange. It should be noted that the values of M_{bh} are similar and from the M-F_b relationship for each test these results give values of F_b in the region of 0.8 F_{bu}. The smallest values from Table 6.8 and 6.9 for each test are the critical moments and should preferably not exceed the limit of the linear portion of the M-ϕ relationship. In the majority of cases the critical moments are very conservative when the prying forces are related to the end plate. The critical moments are near the limit of the linear portion of the M-ϕ relationship however when the prying forces are related to the column flange and are normally within the linear portion of these curves.

Test or Series No.	M_{ph} kNm	M_{ch} kNm	M_{cy} kNm	M_{bh} kNm
P2	177.8	66.2	183.5	102.5
CS1	93.4	27.3	74.1	93.6
CS2	93.4	12.6	37.1	93.6
CS3	207.3	70.5	194.2	102.5
CS4	94.1	66.2	171.1	93.6
CS5	207.3	39.3	116.3	102.5

TABLE 6.8 DISCONTINUITY LIMITS WHEN PRYING FORCES RELATED TO END PLATE

Test or Series No.	M_{ph} kNm	M_{ch} kNm	M_{cy} kNm	M_{bh} kNm
P2	121.3	190.3	400.3	90.6
CS1	56.3	91.3	206.9	82.5
CS2	56.3	48.9	116.5	81.5
CS3	143.1	198.9	418.2	90.6
CS4	56.7	198.9	396.5	85.9
CS5	143.1	131.6	287.5	88.2

TABLE 6.9 DISCONTINUITY LIMITS WHEN PRYING FORCES RELATED TO COLUMN FLANGE

In test series CS2 however the critical moments associated with four prying forces related to the column flange tend to lie outside the linear elastic range of the M-ϕ relationship. This suggests that in test series CS2 more than four prying forces act when the connection is within its elastic stage of behaviour. Nevertheless the method outlined in Chapter Five gives acceptable values of critical discontinuity limits when the prying forces are related to the column flange in test P2 and test series CS1, CS3 and CS5 where the end plate thickness was greater than or equal to that of the column flange. The method developed in Chapter Five also gives acceptable but slightly low values of critical discontinuity limits when the prying forces are related to the end plate in test series CS4, where the column flange was thicker than the end plate. This can be seen from the M-ϕ relationship for each test where the discontinuity limits from Table 6.8 are indicated for test series CS4 and where the discontinuity limits from Table 6.9 are indicated for the remaining tests. It should be noted that in test series CS2 and CS5 mean values of t_c equal to 11.82mm and 17.21mm respectively and a mean value of t_p equal to 14.70mm in test series CS4 were used in determining the discontinuity limits given in Tables 6.8 and 6.9. It should also be noted that the critical discontinuity is controlled by the tensile bolts when t_p and t_c are both larger than the bolt diameter, but only when the prying forces are related to the column flange.

6.3.2 Slip

The values of the slip coefficient μ have been determined using equation 5.49 for the beam to column tests where the beam slipped relative to the column. These values are given in Table 6.10. Similar values have also been determined using the slip equations suggested by Bailey[21] and are also given in Table 6.10. The mean μ value from equation 5.49 is 0.350 compared to quite a high value of 0.622 obtained using Bailey's[21] method. The μ values obtained from equation 5.49 also have a smaller coefficient of variation than that obtained from Bailey[21]. In the theory for slip it was suggested that the initial preload in the compression zone bolts remained when slip occurred. Variation in the compression force between the end plate and column flange at these bolt positions may account for the variation in the μ values obtained. Bahia[74] also obtained μ values of approximately 0.350 ± 0.036 from six single bolt tests and seven two bolt tests where the faying surfaces were similar to those used in the beam to column connection tests.

Test No.	L m	V_s kN	Q_{bs} kN	μ Author	μ Bailey
CS1-5	0.315	112.1	69	0.212	0.323
CS2-5	0.317	286.6	56	0.451	0.955
CS3-4	0.517	211.8	31	0.370	0.706
CS3-5	0.326	209.3	33	0.447	0.698
CS5-2	0.320	137.1	60	0.269	0.426
			Mean	0.350 ±0.096	0.622 ±0.224
			Coefficient of Variation	27.3%	36.1%

TABLE 6.10 COEFFICIENT OF SLIP

6.3.3 Ultimate Load

The values of the total prying force acting at the bottom of the end plate at failure measured in the beam to column tests are compared with the theoretical values in Table 6.11. The ratio of the experimental and theoretical applied bending moments are also compared in Table 6.11. Q_u was determined from equation 5.10 and the values obtained are quite favourable with the experimental results for the range of sizes tested. Test series CS5 however consisted of only one test, CS5-1, and the theoretical Q_u value is low compared to the actual value. More tests on specimens of this type are required to provide a better comparison between experimental and theoretical results. M_u was determined from equation 5.50 and the results obtained are compatible with the experimental failure loads for all the test specimens reported.

From the available literature it was found that only one test specimen reported by Packer and Morris[33] failed by tensile bolt fracture. This connection consisted of a 15mm end plate and a 6.5mm column flange with four bolts symmetrically placed about the beam tension flange. It has been suggested earlier that in such connections two prying forces per bolt may exist. One prying force would be related to the column flange and the other related to the end plate. Consider that two prying forces per bolt

Spec.	Expt.		Theory		M_u	Q_u
	M_u kNm	Q_u kN	M_u kNm	Q_u kN	$\frac{\text{expt.}}{\text{theory}}$	$\frac{\text{expt.}}{\text{theory}}$
P2	196.0	58.4	202.0	56.9	0.97	1.03
CS1-1	176.3	72.3	171.1	95.6	1.03	0.76
CS1-2	164.4	99.8	171.1	95.6	0.96	1.04
CS1-3	160.5	108.8	171.1	95.6	0.94	1.14
CS1-4	167.5	92.6	171.1	95.6	0.98	0.97
CS2-1	163.9	101.0	171.1	95.6	0.96	1.06
CS2-2	163.6	101.7	171.1	95.6	0.96	1.06
CS2-3	164.5	99.6	171.1	95.6	0.96	1.04
CS2-4	159.1	112.1	171.1	95.6	0.93	1.17
CS3-1	197.0	56.2	202.0	56.9	0.98	0.99
CS3-2	193.1	58.4	202.0	56.9	0.96	1.03
CS3-3	190.0	71.7	202.0	56.9	0.94	1.26
CS3-4	194.9	60.8	202.0	56.9	0.96	1.07
CS4-1	163.9	101.0	171.2	95.4	0.96	1.06
CS4-3	166.5	95.0	169.8	98.6	0.98	0.96
CS5-1	210.3	26.7	202.0	56.9	1.04	0.47
				Mean	0.97 ±0.028	1.01 ±0.173
				Coefficient of Variation	2.9%	17.2%

TABLE 6.11 COMPARISON OF EXPERIMENTAL AND THEORETICAL RESULTS FOR BEAM TO COLUMN CONNECTIONS

Spec.	Expt.		Theory				$\frac{M_u \text{ expt.}}{M_u \text{ theory}}$	$\frac{4.Q_{bu} \text{ expt.}}{4.Q_{bu} \text{ theory}}$
	M_u kNm	$4.Q_{bu}$ kN	M_u kNm	$4.Q_{bu}$ EP kN	$4.Q_{bu}$ CF kN	$4.Q_{bu}$ Total kN		
J5	82.6	386.4	82.4	172.2	215.0	387.2	1.00	1.00

Abbreviations used: EP, End Plate; CF, Column Flange

TABLE 6.12 COMPARISON OF EXPERIMENTAL RESULTS BY PACKER AND MORRIS[33]

act at failure and that each value can be determined from equation 5.10. Also consider that the compression zone bolts resist a tensile force equal to 0.8 F_{bu}. Therefore taking moments about the outer edge of the top flange gives prying force and failure moment values approximately equal to those obtained experimentally. This can be seen from Table 6.12.

6.3.4 Theoretical Results from Other Investigators

Plastic moment capacities of the end plates and column flanges for the specimens tested from methods suggested by other investigators are shown in Table 6.13. Fisher and Struik[20] recommended that the end plate be designed as an equivalent tee stub with Mechanisms A, B and C, as shown in Figure 1.3, able to form. An effective length was recommended for the design of the column flange. Zoetemeijer[31] and Mann and Morris[35] also suggested that the end plate be designed as an equivalent tee stub. Separate equations were recommended for each Mechanism A, B and C, however Mann and Morris[35] recommended Mechanism C as the failure mode. Both authors also suggested equations for the plastic moment capacity of the column flange based on complete yield line patterns. A comparable value from the theory in Chapter Five is the upper bound value for work hardened yield lines in the column flange, M_{cy}, given in Tables 6.8 and 6.9.

Test or Series No.	Fisher & Struik[20]		Zoetemeijer[31]				Mann and Morris[35]			CIRAC Report[46]		(35) & (46)
	M_p End Plt kNm	M_p Col. Flg. kNm	M_p End Plt Mech B kNm	M_p End Plt Mech C kNm	M_p Col. Flg. Mech I kNm	M_p Col. Flg. Mech II kNm	M_p End Plt Mech C kNm	M_p Col. Flg. Mech I kNm	M_p Col. Flg. Mech II kNm	M_p End Plt kNm	t_c mm	$M_p=3.F_{bu}.d_f$ Bolts kNm
P2	129.9	74.6	104.1	148.5	118.6	219.7	163.2	178.6	194.4	198.5	19.7	153.7
CS1	100.4	40.3	82.7	80.2	83.8	115.4	88.1	118.7	101.6	107.3	14.8	145.7
CS2	94.4	25.0	80.4	76.4	69.4	71.7	84.0	93.5	63.1	-	14.8	145.7
CS3	147.4	102.7	121.7	204.4	142.6	293.9	224.6	225.2	267.5	273.2	19.7	153.7
CS4	114.1	102.7	89.6	105.2	142.6	293.9	120.3	225.2	267.5	147.6	14.5	145.7
CS5	147.4	76.0	121.7	204.4	117.4	217.4	224.6	177.3	191.4	-	19.7	153.7

TABLE 6.13 COMPARISON OF THEORETICAL RESULTS BY OTHER INVESTIGATORS

The rotations associated with these values of M_{cy} are normally outside the linear-elastic range of behaviour for the joints tested, especially if the prying force is related to the column flange. M_{cy} values, however, for test series CS2, when the prying force is related to the end plate produces rotations that lie just within the linear-elastic range.

The CHRAC Report[46] recommended an equation for end plate thickness valid only if the column flange thickness was suitable. An equation for minimum flange thickness was given. The calculated flange thicknesses for test series CS2 and CS5 were greater than those actually used therefore plastic moment capacities for the end plates by this method are not included in Table 6.13. The least value of M_p for each test series by each author is shown on the moment-connection rotation diagrams.

It should be emphasised that the design methods suggested by Mann and Morris[35] and the CHRAC Report[46] have been used in determining M_p values in Table 6.13 ignoring the recommended end plate geometry that is included in their design procedure. The end plate geometry suggested by both[35, 46] is

$B \approx 9d, \quad A \approx 5d, \quad C \approx 6d, \quad a \geq 2.5d$

where B is the width of the end plate, A is the horizontal cross-centres of bolt holes, C is the vertical cross-centres of the tensile bolt holes, a is the end plate edge distance

and d is the nominal bolt diameter. The end plate geometry of the beam to column connections tested is

$B \simeq 12.5d$, $A \simeq 8d$, $C \simeq 7d$, $a \simeq 2d$

and therefore the design methods suggested by Mann and Morris[35] and the CIRAC Report[46] are not applicable to the joints tested. Despite the disparity in the geometry a comparison of these design methods with the experimental results will be made bearing in mind that Mann and Morris's[35] and CIRAC Report[46] recommendations would effectively have produced smaller deformations than those actually recorded in the experiments. Mann and Morris[35] suggested their end plate design method as a lower bound solution which limited connection deformation, and also suggested the CIRAC Report[46] end plate design method as an upper bound solution which limited connection deformation. A similar equation was given by both Mann and Morris[35] and the CIRAC Report[46] for the design of the tensile bolts and by rearranging this equation gives an alternative lower bound solution for the plastic moment capacity of the connection where 'thick' end plates are used, i.e. $M_p = 3.F_{bu}.d_f$. M_p values based on this lower bound bolt equation are also given in Table 6.13.

According to Horne[72] the joints of rigidly designed structures can have a certain amount of flexibility at ultimate load. The degree the rigidity however must be sufficient to ensure that for a reasonable range of deformation of the structure as a whole, the bending moments can become redistributed in accordance with the assumptions of plastic theory. He

suggested that the relative joint rotation at M_p be within the region of two or three times the relative rotation that would arise owing to elastic deformation in the structure if the joint was rigid. Therefore from the moment-rotation diagrams the method suggested by Fisher and Struik[20.] may be considered in the majority of cases very conservative. The method recommended in the CIRAC Report[46] when valid produced M_p values sometimes greater than M_u. In test series CS1 the rotation associated with M_p from this method is beyond that suggested by Horne[72]. However, in test series CS4 the rotation associated with M_p is acceptable but the value of M_p is close to failure. Zoetemeijer's[31] results are conservative for the majority of the tests although in test series CS1 the rotations produced may be considered just acceptable. In test series CS2 the rotations associated with M_p are excessive. Mann and Morris[35] considered that their design procedure would produce limited distortions in beam to column connections. In fact the values of moment capacity obtained for test series CS3 were greater than M_u and the rotation associated with P2 excessive. However similar values obtained for test series CS5 may be considered just within the limits specified by Horne[72]. M_p values obtained from this method for test series CS1 and CS2 are similar to those determined from Zoetemeijer's[31] method and although similar conclusions may be drawn for series CS2 the rotations obtained for series CS1 are on the whole slightly excessive. However the results obtained from Mann and Morris's[35] method are acceptable for test series CS4.

M_p values obtained from the equation $M_p = 3.F_{bu}.d_f$ are lower than the alternative lower bound end plate method when the end plate was 20mm thick i.e. in test P2 and test series CS3 and CS5. The rotations associated with these values of M_p are therefore smaller and although these rotations are within the limits specified by Horne[72] for test series CS3 and CS5 the rotation associated with test P2 is slightly excessive.

In general it may be stated that rigid connections designed by the equations given by Zoetemeijer[31], Mann and Morris[35] and the CHRAC Report[46] may have excessive deformations at M_p within the context of the test end plate geometry. However if the restrictions on end plate geometry stipulated by Mann and Morris[35] and the CHRAC Report[46] were complied with then the resulting deformations at M_p may well have come within the limitations suggested by Horne[72]. Similar connections designed by Fisher and Struik's[20] method may have thick column flanges and little deformation at M_p. If these connections were designed using equations 5.22 and 5.31 with M_p equal to M_{ph} and M_{ch} then the rotation at the design moment would be within that recommended by Horne[72]. This approach would still result in practical end plate and column flange sizes, although equation 5.31 may be somewhat arduous for use in a design office. However, for a range of practical joint dimensions equation 5.31 may be simplified to produce a fairly straightforward method for the design of rigid connections. It is suggested that the bolt diameter

be greater than the thickness of both the end plate and column flange. M_{bh} would therefore not be critical and brittle bolt failure would be avoided before ample joint ductility was achieved. Nevertheless M_{bh} should be calculated to ensure that it is greater than M_p.

CHAPTER SEVEN

CONCLUSIONS AND RECOMMENDATIONS FOR FURTHER RESEARCH

7.1 Conclusions

The following conclusions are drawn from the experiments and theory developed in this thesis.

7.1.1 Bolt Tightening Control

1) 'Coronet' load indicating washers placed under the nut of M16 high strength friction grip bolts and flattened to the recommended average measured gap of 0.25 mm, induced an average bolt preload of 90.0 kN with a coefficient of variation of 3.5%.

2) The average measured gap of 'Coronet' load indicating washers, placed under the nut of M16 HSFG bolts, at the specified minimum shank tension of 92 kN was 0.215 mm with a coefficient of variation of 26.8%.

3) 'Coronet' load indicating washers placed under the nut of M20 HSFG bolts and flattened to the recommended average gap of 0.25 mm, induced an average bolt preload of 117.8 kN with a coefficient of variation of 7.2%.

4) The average measured gap of 'Coronet' load indicating washers, placed under the nut of M20 HSFG bolts, at the specified minimum shank tension of 144 kN was 0.036 mm with a coefficient of variation of 100.3%.

5) The torques required to induce the specified minimum shank tension in M16 and M20 HSFG bolts were consistent for each bolt type and had a coefficient of variation in both cases of approximately 6%.

7.1.2 Tee Stubs

1) At failure the bolts developed the full tensile strength *approx.*, despite bending distortions.

2) In the majority of the tests the prying force remained approximately constant or increased slightly after separation of the flange plates.

3) The prying force appears to increase approximately linearly until separation of the flange plates.

4) Within the elastic limit of the flange plate, the prying force may be determined approximately using equation A3.1

5) At failure the moment of resistance of the flange plate at the web was greater than $w_p.t_p^2.\sigma_{py}/4$ and depended on the deflection of the plate and associated work hardening.

6) The prying force at failure may be determined with a reasonable degree of accuracy using equation 5.10.

7.1.3 Beam to Column Connections

1) The connections behaved in a rigid manner up to the elastic limit of either the end plate or column flange.

2) For values of $M/V.d_f < 1$ the bolts slipped into bearing.

3) For values of $M/V.d_f > 1$ tensile bolt failure occurred in the majority of tests.

4) For values of $1.6 > M/V.d_f > 1$ the bolts of one test specimen slipped into bearing with no adverse effect on the failure load or failure mode of the connection.

5) The coefficient of slip between the beam and column when final slip occurred was about 0.350.

6) Gradual slip into bearing had negligible effect on the moment - rotation characteristics of the joints.

7) Sudden slip into bearing of both joints of a test specimen had only an initial effect on the moment - rotation characteristics of the connections.

8) Sudden slip into bearing of only one joint of a test specimen resulted in a large discrepancy between the moment - rotation characteristics of both joints.

9) Tensile bolt separation occurred before slip into bearing took place.

10) Rotation occurred in the vicinity of the beam compression flange.

11) At bolt failure the bolts developed the full tensile strength, similar to the tee stub tests, despite bending and shear distortions at earlier loading stages.

12) Bolt failure loads were independent of the column flange thickness.

13) Column flange thickness had a considerable influence on the rotation capacity of the connections.

14) The yield strength of the plates not only affected the elastic range of behaviour of the joints, but also their rotation capacity.

15) Considerable rotation capacity was achieved before bolt failure occurred, when the bolt diameter was larger than the thickness of both the end plate and column flange.

16) The prying force in the tensile bolts at separation was approximately twice the value that occurred at failure.

17) The tensile forces in the bottom four bolts for each test were approximately equal at ultimate load.

18) At failure, prying force acted at the extreme edge of the end plate and may be determined with a reasonable degree of accuracy using equation 5.10. The failure moment may therefore be obtained from equation 5.50.

19) The moment - rotation relationship for a connection is non-linear when the moment applied to the joint reaches the discontinuity limit of either the end plate, column flange or tensile bolts, whichever is the least value. Discontinuity limit equations are developed for each component, based on prying force being related to either the end plate or column flange. The magnitude of the prying forces at any stage in the loading depends on the areas of contact between the column flange and end plate. The prying forces are calculated based on either the end plate or column flange properties.

7.2 Recommendations for Further Research

It is evident from the results of this investigation that load indicating washers when used in practice will probably cause shank tensions to be below those recommended. The

present study was limited to LIW's placed beneath the nut. For a better overall understanding of this type of tightening control it is recommended that these washers be studied when placed under the head of high strength bolts. It is also recommended that the load indicating washers be obtained from different batchs.

The tee stub tests reported in Chapter Three were symmetrical about both the vertical and horizontal axis and the investigation is by no means conclusive. It is suggested that further work is required not only on asymmetrical tee stubs but also in obtaining information on joint behaviour when t_p, b_p and a_p vary.

The beam to column connections reported represent internal joints of a single storey building. The effect of axial load is therefore negligible, however it may have a significant influence on the behaviour of these joints when used in low-rise or multi-storey frames. The effects of axial load therefore requires investigation. It is also suggested that further work be carried out on joints subjected to small moment to shear ratios, where the bolts not only slip into bearing but also fail in shear. Special attention should be given to the behaviour of the compression zone bolts and surrounding area. Furthermore, practical rigid connections are not limited to the type reported in this thesis

and may in some cases have more bolts within the beam depth. Little information exists on the behaviour of these connections, especially those with unstiffened column flanges and the results of an in depth study into the behaviour of these joints would prove most useful. More immediate however, is the problem of prying force location in the elastic range of the beam to column connections, two alternatives have been suggested and clarification is necessary.

APPENDIX A-2

Test No	20mm Dia. Washer Thickness mm	Sleeve or 16mm Dia. Washer* Thickness mm mm	Nut Thickness mm	No. of Strain Gauges
16.DT.1	3.64	3.03 3.08	14.98	2
16.DT.2	3.70	3.03 3.08	15.02	2
16.DT.3	3.64	3.03 3.08	14.96	2
16.DT.4	3.64	3.03 3.08	14.88	2
16.DT.5	3.69	3.39*	15.50	3
16.DT.6	3.65	3.20*	15.00	3

Note: Bolt Diameter 16.3mm, Base Plate Thickness 20.39mm and 20.27mm. Unthreaded Length of Bolt 30mm.

TABLE A2.1 MEAN DIMENSIONS AND DETAILS FOR DIRECT TENSION TESTS M16 BOLTS

Test No.	24mm Dia. Washer Thickness mm	20mm Dia. Washer Thickness mm	Nut Thickness mm	No. of Strain Gauges
20.DT.1	3.93	3.64	17.95	2
20.DT.2	3.89	3.59	18.17	2
20.DT.3	3.91	3.64	18.02	2
20.DT.4	3.99	3.65	18.05	2
20.DT.5	3.93	3.70	18.08	2

Note: Bolt Diameter 19.72mm, Base Plate Thickness 20.39mm and 20.27 mm. Unthreaded Length of Bolt 17mm.

TABLE A2.2 MEAN DIMENSIONS AND DETAILS FOR DIRECT TENSION TESTS M20 BOLTS

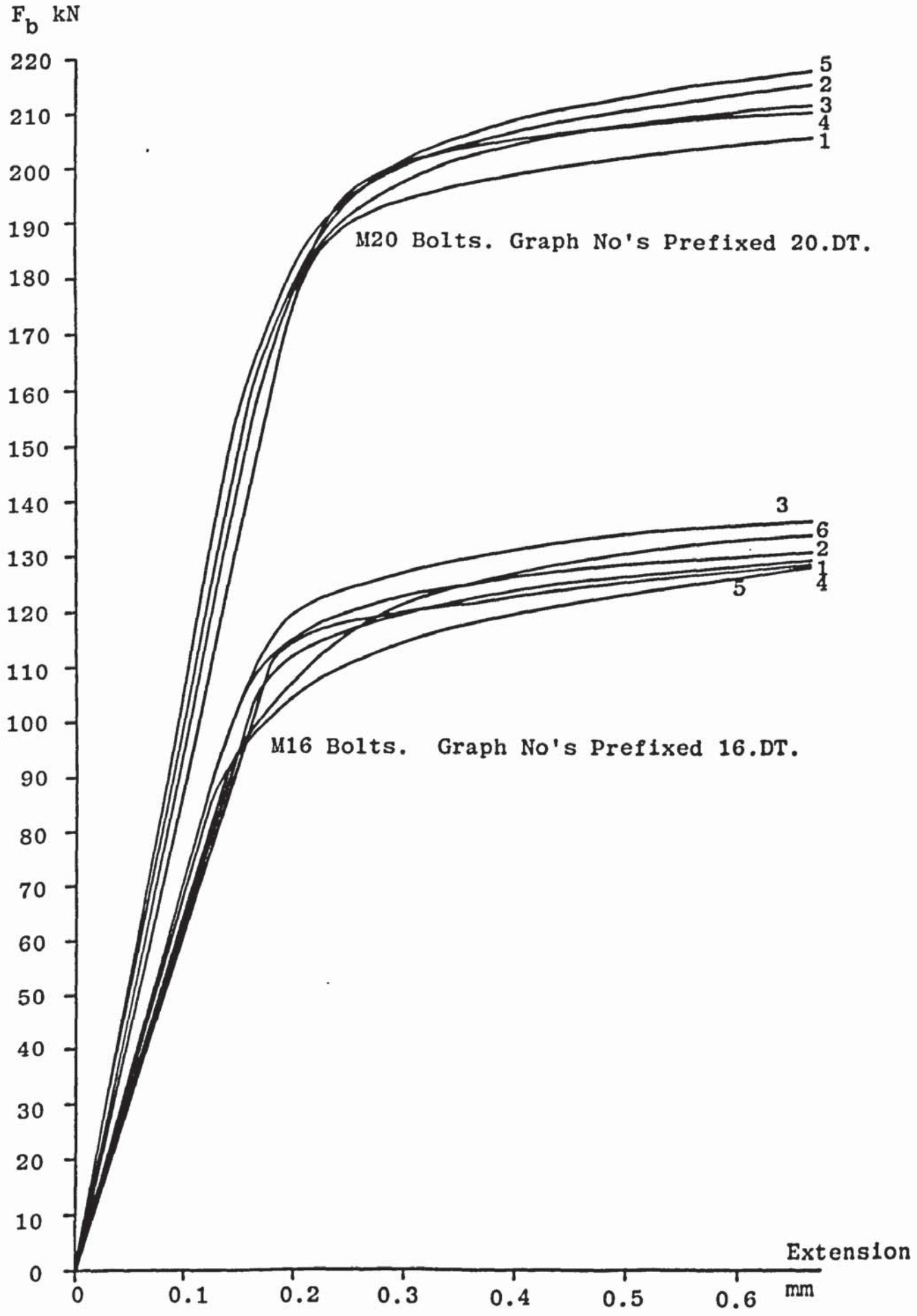

FIGURE A2.1 RELATIONSHIP BETWEEN TENSILE BOLT FORCE AND EXTENSION FOR DIRECT TENSION M16 and M20 BOLTS

M16 Bolts			M20 Bolts		
Test No	Extension at 90 kN mm	E_b kN/mm^2	Test No	Extension at 155 kN mm	E_b kN/mm^2
16.DT.1	0.143	212.5	20.DT.1	0.170	238.9
16.DT.2	0.126	215.0	20.DT.2	0.163	232.7
16.DT.3	0.126	210.0	20.DT.3	0.148	240.0
16.DT.4	0.140	210.0	20.DT.4	0.170	229.1
16.DT.5	0.135	220.0	20.DT.5	0.158	226.8
16.DT.6	0.137	205.0			
Mean	0.135 ±0.007	212.1 ±4.7		0.162 ±0.008	233.5 ±5.2
Coeff. of Var.	4.8%	2.2%		5.1%	2.2%

TABLE A2.3 E_b VALUES FOR DIRECT TENSION TESTS M16 AND M20 BOLTS

M16 Bolts			M20 Bolts		
Test No	Reduced Diameter mm	E_b kN/mm^2	Test No	Reduced Diameter mm	E_b kN/mm^2
R16.DT.1	13.29	217.5	R20.DT.1	16.50	215.7
R16.DT.2	13.15	211.0	R20.DT.2	16.50	213.4
R16.DT.3	13.00	211.0	R20.DT.3	16.30	217.1
			R20.DT.4	16.15	218.60
Mean		213.2 ±3.1			216.2 ±1.9
Coeff. of Var.		1.4%			0.9%

TABLE A2.4 E_b VALUES FOR DIRECT TENSION TESTS REDUCED M16 AND M20 BOLTS

FIGURE A2.2 RELATIONSHIP BETWEEN STRESS AND STRAIN FOR A TYPICAL DIRECT TENSION M16 AND M20 BOLT

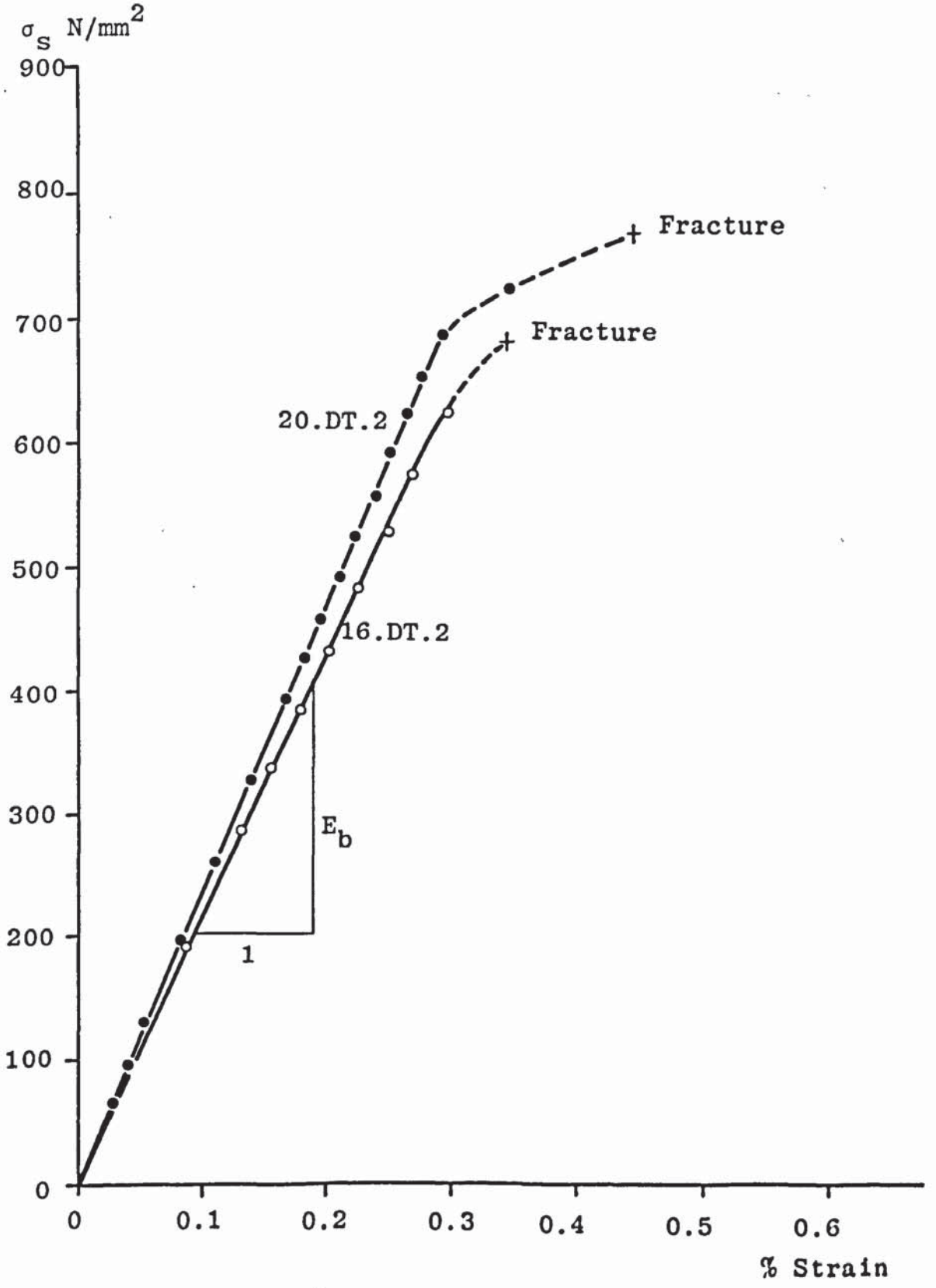

M16 Bolts		M20 Bolts	
Test No.	Ultimate Load kN	Test No.	Ultimate Load kN
16.DT.1	139.6	20.DT.1	220.3
16.DT.2	140.8	20.DT.2	234.2
16.DT.3	145.0	20.DT.3	231.7
16.DT.4	138.6	20.DT.4	228.3
16.DT.5	133.7	20.DT.5	236.2
16.DT.6	140.5	1	233.2
1	144.7	2	225.3
2	139.6	3	221.3
3	140.2	4	234.2
4	132.9	5	244.2
5	145.3	6	229.3
6	140.9	7	233.2
7	137.6	8	233.2
8	140.4	9	229.3
9	138.9	10	224.3
10	139.5	11	228.3
11	142.9	12	230.2
12	138.5	13	230.2
13	136.2	14	226.3
14	143.6	15	236.2
15	140.6	16	219.3
16	139.5	17	233.2
		18	224.3
		19	230.2
		20	224.3
		21	211.3
Mean	140.0 ±3.1		228.9 ±6.5
Coefficient of Variation	2.2%		2.8%

TABLE A2.5 ULTIMATE TENSILE STRENGTH OF M16 AND M20 BOLTS

Test No.	20mm Dia. Washer Thickness mm	Nut face Washer Thickness mm	LIW Thickness With Protru-sions mm	LIW Thickness Without Protru-sions mm	Nut Thickness mm	Flange Thickness mm	Plate Thickness mm	No. of Strain Gauges
16.TT.1	3.80	3.10	5.06	3.37	15.03	15.33	20.09	3
16.TT.2	3.84	3.19	4.98	3.33	14.79	15.29	20.10	3
16.TT.3	3.70	3.20	5.01	3.30	15.57	15.23	20.17	3
16.TT.4	3.65	3.11	5.01	3.33	14.91	16.26	20.14	3
16.TT.5	3.70	3.15	4.88	3.28	15.13	16.31	20.12	3
16.TT.6	3.72	3.28	5.01	3.38	15.13	16.12	20.16	3

Note: Bolt Diameter 16.3mm, Unthreaded Length of Bolt 30mm

TABLE A2.6 MEAN DIMENSIONS AND DETAILS FOR TORQUE TENSION TESTS M16 BOLTS

FIGURE A2.3 RELATIONSHIP BETWEEN TENSILE BOLT FORCE AND EXTENSION, TORQUE AND AVERAGE LIW GAP FOR TORQUE TENSION M16 BOLTS

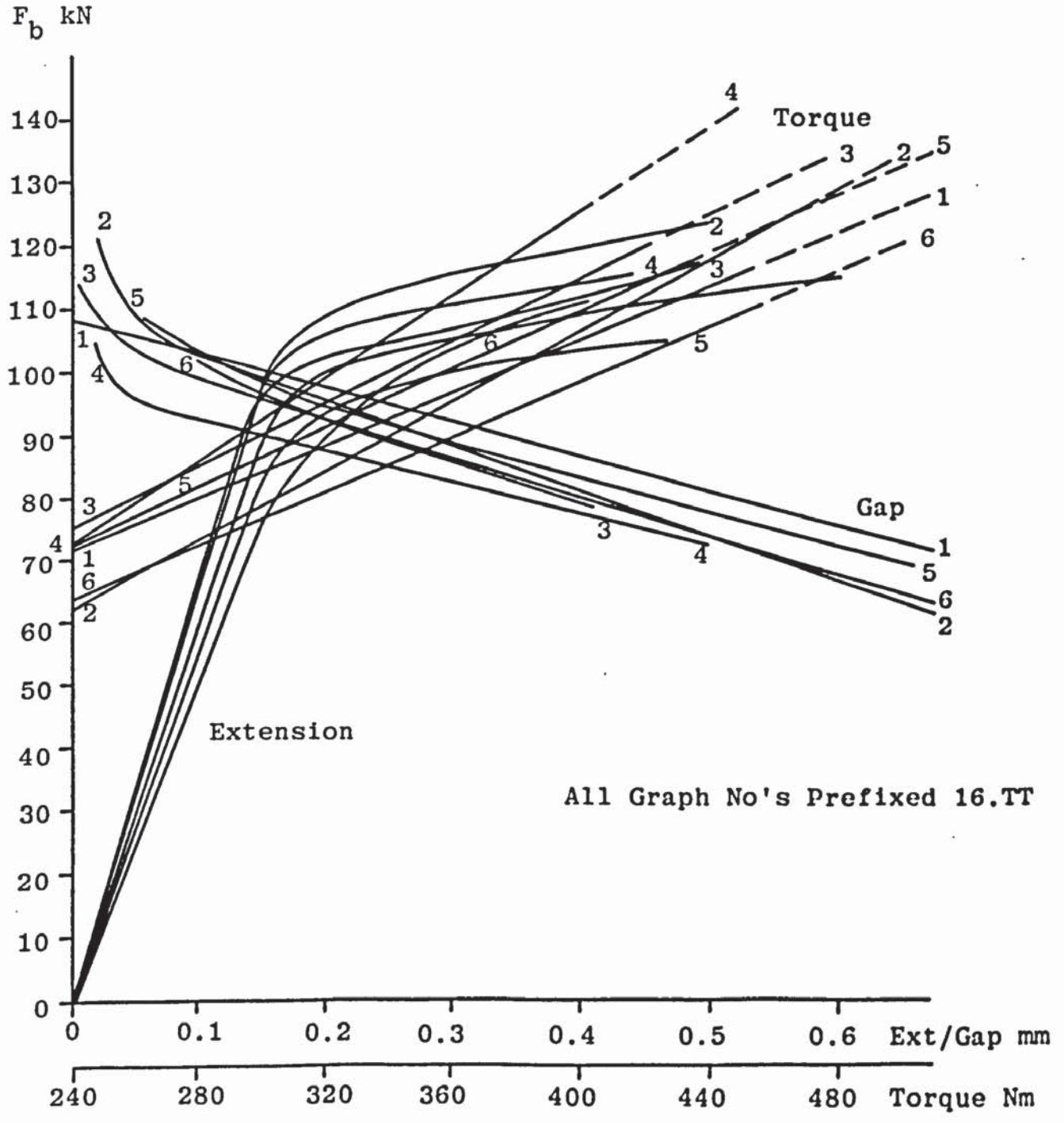

Test No	24 mm Dia Washer Thick-ness mm	Nut Face Washer Thick-ness mm	LIW Thickness With Protrusions mm	LIW Thickness Without Protrusions mm	Nut Thick-ness mm	Flange Thick-ness mm	Plate Thick-ness mm	No. of Strain Gauges	
20.TT.1	3.93	3.69	5.51	3.78	17.81	16.15	20.04	2	Series 1
20.TT.2	4.00	3.66	5.47	3.73	18.01	16.34	20.04	2	
20.TT.3	3.90	3.68	5.58	3.78	18.09	16.41	20.02	2	
20.TT.4	3.90	3.66	5.60	3.84	17.85	15.33	20.02	2	
20.TT.5	3.91	3.60	5.53	3.77	18.28	15.43	20.03	2	
20.TT.6	3.96	3.64	5.55	3.77	18.08	15.27	20.21	3	
20.TT.7	3.88	3.64	5.59	3.81	17.92	16.25	20.16	3	
20.TT.8	3.90	3.66	5.51	3.72	18.24	16.42	20.19	3	
20.TT.9	3.88	3.71	5.52	3.76	18.03	16.35	20.20	3	
20.TT.10	3.95	3.65	5.58	3.77	17.64	15.26	20.15	3	
20.TT.11	3.78	3.63	5.49	3.79	17.79	15.36	20.23	3	
20.TT.12	3.91	3.62*	5.53	3.79	18.04	15.22	20.16	3	
20.TT.13	3.95	3.68*	5.45	3.76	17.86	16.25	20.01	3	
20.TT.14	3.90	3.60	5.57	3.82	17.99	15.25	25.02	3	Series 2
20.TT.15	3.94	3.69	5.45	3.77	17.84	15.23	25.14	3	
20.TT.16	3.91	3.64	5.53	3.82	17.99	16.15	25.05	3	
20.TT.17	3.93	3.73	5.39	3.73	18.13	15.19	25.05	3	
20.TT.18	4.08	3.67	5.62	3.85	18.15	16.16	25.0	3	
20.TT.19	3.92	3.64	5.57	3.79	17.98	16.24	24.98	3	

Note: * Indicates 20 mm Diameter Washer Thickness, Bolt Diameter 19.72 mm, Unthreaded Length of Bolt 17 mm

TABLE A2.7 MEAN DIMENSIONS AND DETAILS FOR TORQUE TENSION TESTS M20 BOLTS

FIGURE A2.4 RELATIONSHIP BETWEEN TENSILE BOLT FORCE AND EXTENSION, TORQUE AND AVERAGE LIW GAP FOR TORQUE TENSION M20 BOLTS SERIES 1

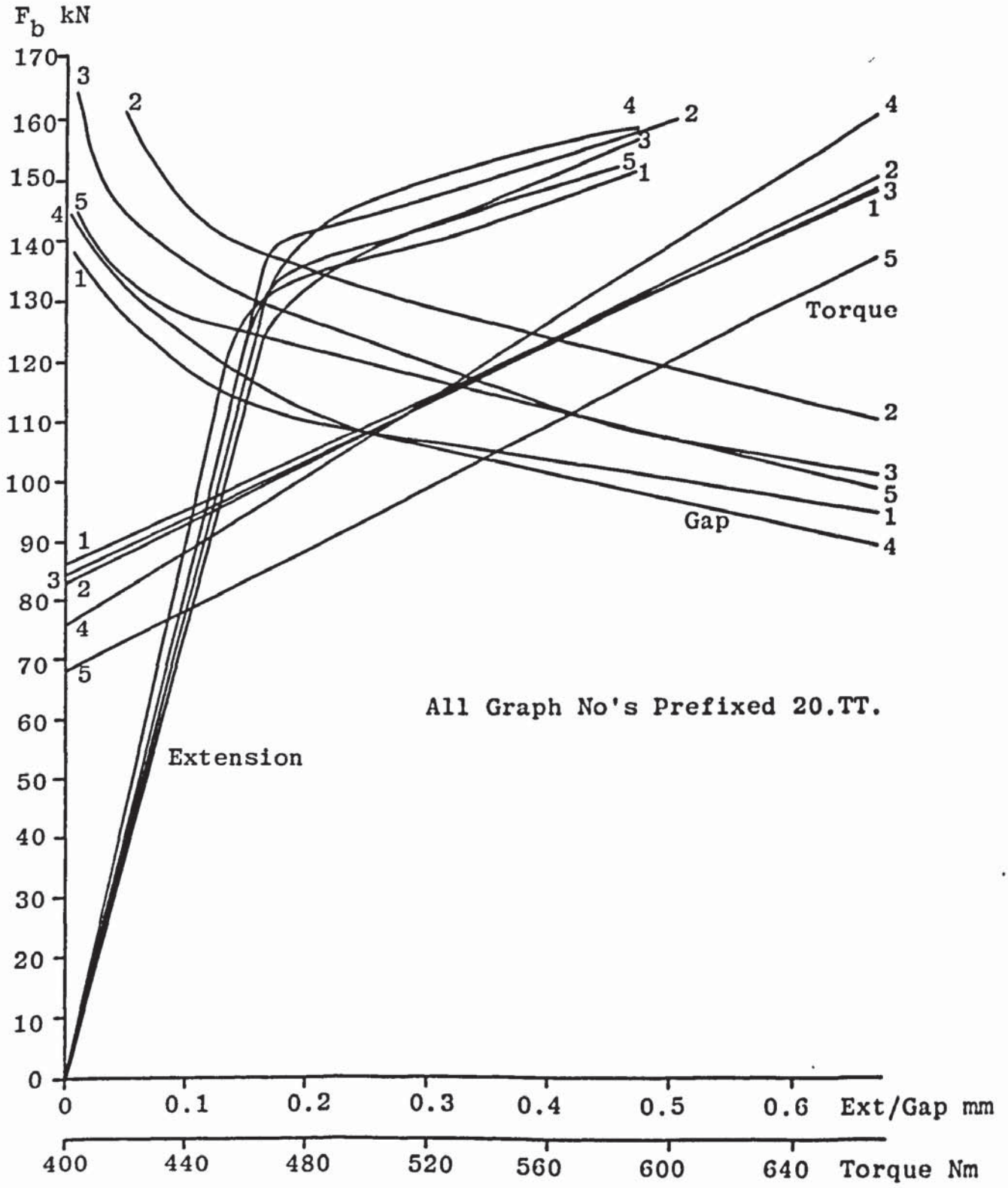

FIGURE A2.5 RELATIONSHIP BETWEEN TENSILE BOLT FORCE AND EXTENSION, TORQUE AND AVERAGE LIW GAP FOR TORQUE TENSION M20 BOLTS SERIES 1

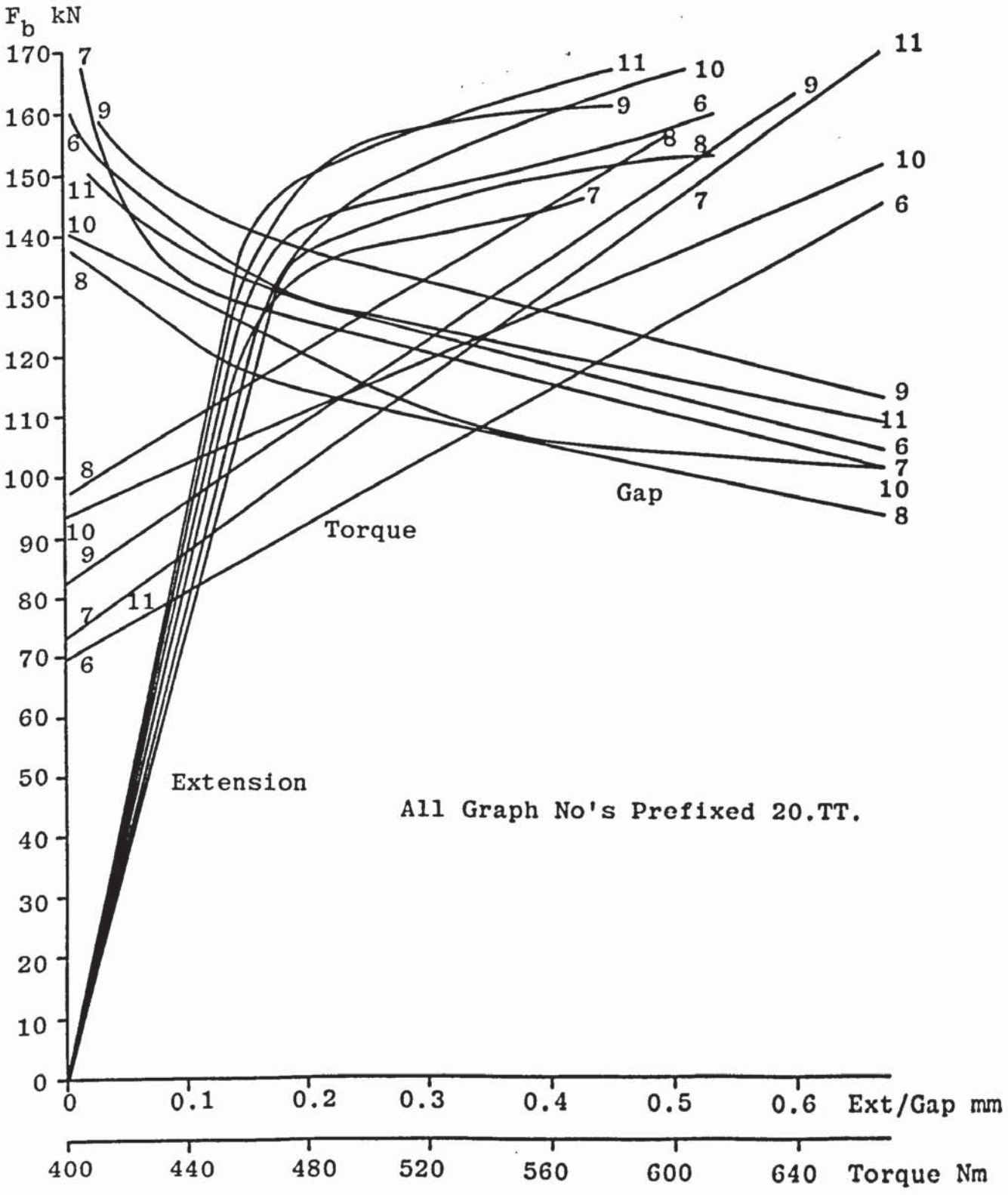

FIGURE A2.6 RELATIONSHIP BETWEEN TENSILE BOLT FORCE AND EXTENSION AND TORQUE FOR TORQUE TENSION M20 BOLTS SERIES 1

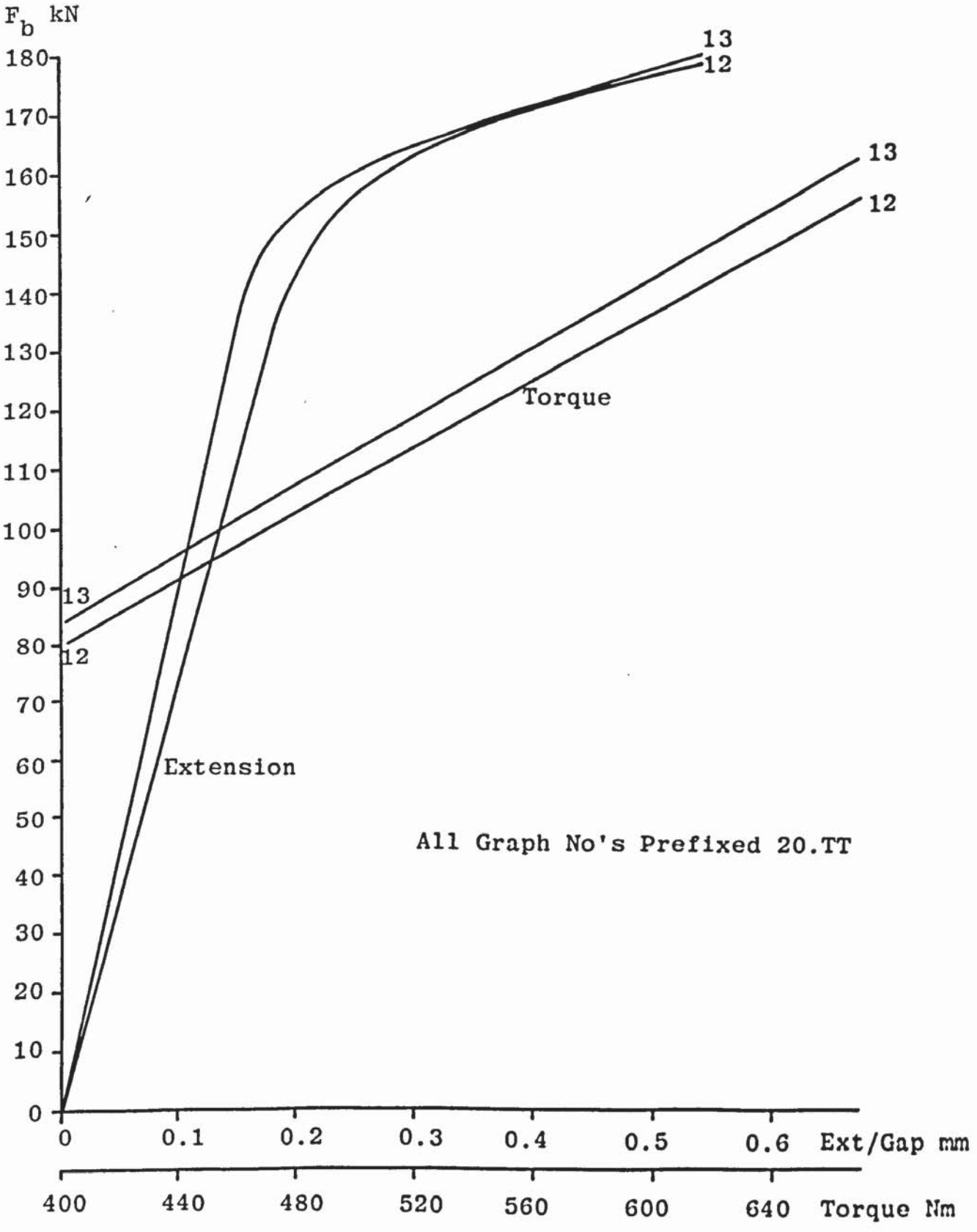

FIGURE A2.7 RELATIONSHIP BETWEEN TENSILE BOLT FORCE AND EXTENSION, TORQUE AND AVERAGE LIW GAP FOR TORQUE TENSION M20 BOLTS SERIES 2

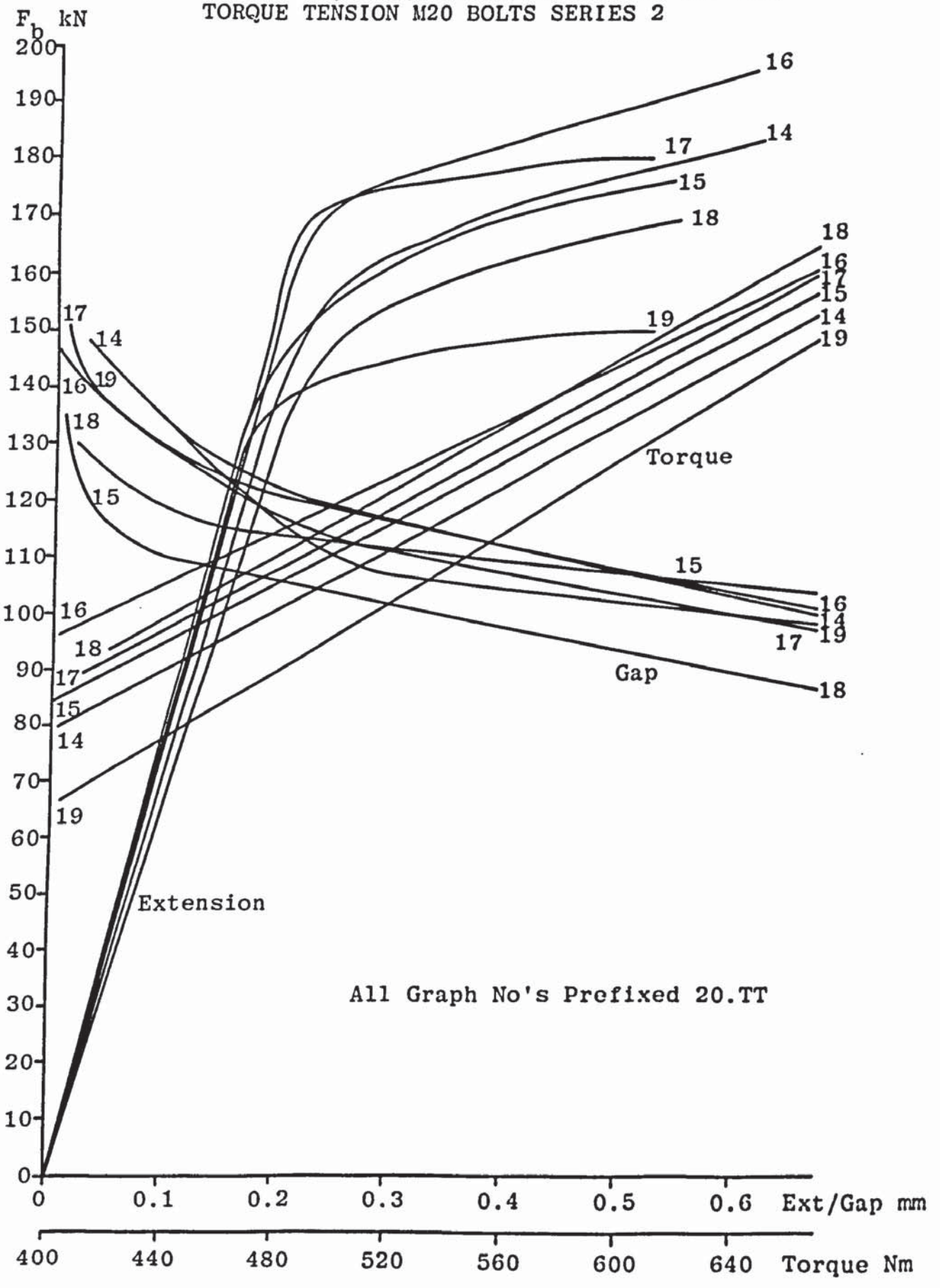

Lot	$T + t_w$ ins	L_1 ins	e Direct Tension ins	e Torque Tension ins	F_b cal. Direct Tension kips	F_b cal. Torque Tension kips	$\frac{F_b \text{ test}}{F_b \text{ cal. Direct}}$	$\frac{F_b \text{ test}}{F_b \text{ cal. Torque}}$
B	4.25	3.50	0.010	0.009	35.83	29.02	1.01	1.24
C	8.25	7.25	0.023	0.034	45.54	63.43	0.79	0.57
D	4.25	3.50	0.010	0.010	35.83	32.35	1.01	1.12
D	3.80	3.50	-	0.009	-	32.42	-	1.11
Z	4.25	3.50	0.010	0.009	35.83	29.02	1.01	1.24
Q	4.25	3.25	0.012	0.014	42.36	44.54	0.85	0.81
R	4.25	2.25	0.010	0.026	33.33	78.55	1.08	0.46
S	4.25	0	0.021	0.033	62.20	89.52	0.58	0.40
T	5.00	4.25	0.014	0.015	43.66	42.65	0.83	0.85
U	5.50	4.75	0.015	0.015	43.05	39.54	0.84	0.91
V	6.25	5.25	0.016	0.017	41.03	40.38	0.88	0.89
W	7.00	6.25	0.017	0.018	39.39	38.91	0.92	0.93
H	8.125	7.75	0.018	0.019	36.91	36.63	0.98	0.98
E	4.25	4.00	0.011	0.012	40.63	39.77	0.89	0.91
E	4.125	4.00	0.010	0.011	38.21	37.58	0.94	0.96
8A	4.00	3.75	0.010	0.010	38.93	34.74	0.93	1.04
8A	4.50	3.75	-	0.010	-	30.87	-	1.17
8B	4.125	4.00	0.010	0.012	38.21	41.00	0.94	0.88
8B	4.25	4.00	0.011	0.013	40.63	43.08	0.89	0.84
						Mean	0.90 ±0.11	0.91 ±0.23
						Coefficient of Variation	12.2%	25.1%

1) All bolts are 7/8 ins diameter A325
2) $l_n = 0.859$ ins, $A_b = 0.462$ ins^2, F_b test = 36.05 kips

TABLE A2.8 COMPARISON OF EXPERIMENTAL RESULTS BY RUMPF AND FISHER[59]

Lot	$T + t_w$ ins	L_1 ins	e Direct Tension ins	e Torque Tension ins	F_b cal. Direct Tension kips	F_b cal. Torque Tension kips	$\frac{F_b \text{ test}}{F_b \text{ cal}}$ Direct	$\frac{F_b \text{ test}}{F_b \text{ cal}}$ Torque
LI	4.125	4.00	0.0147	0.015	56.16	51.24	0.99	1.08
LI	4.125	4.00	0.0154	0.016	58.84	54.66	0.94	1.01
LI	4.563	4.00	0.0160	0.018	54.54	55.50	1.02	1.00
LI	4.563	4.00	0.0171	0.018	58.29	55.50	0.95	1.00
AB	8.250	8.125	0.0280	0.028	57.10	53.70	0.97	1.03
AB	8.250	8.125	0.0282	0.028	57.50	53.70	0.96	1.03
AB	8.688	8.125	0.0297	0.033	56.90	59.68	0.97	0.93
AB	8.688	8.125	0.0302	0.031	57.85	56.06	0.96	0.99
						Mean	0.97 ±0.02	1.01 ±0.04
						Coefficient of Variation	2.4%	3.9%

1) All bolts are 7/8 ins. diameter A490

2) l_n = 0.859 ins., A_b = 0.462 ins.^{2}, F_b test = 55.45 kips.

TABLE A2.9 COMPARISON OF EXPERIMENTAL RESULTS BY STERLING ET AL[61]

Direct Tension				Torque Tension					
Test No	$\sigma_{y0.2}$ N/mm^2	Test No	$\sigma_{y0.2}$ N/mm^2	Test No	$\sigma_{yt0.2}$ N/mm^2	Test No	$\sigma_{yt0.2}$ N/mm^2	Test No	$\sigma_{yt0.2}$ N/mm^2
16.DT.1	758	20.DT.1	800	16.TT.1	665	20.TT.1	575	20.TT.14	705
16.DT.2	770	20.DT.2	830	16.TT.2	737	20.TT.2	603	20.TT.15	684
16.DT.3	810	20.DT.3	815	16.TT.3	680	20.TT.3	579	20.TT.16	743
16.DT.4	763	20.DT.4	830	16.TT.4	702	20.TT.4	610	20.TT.17	725
16.DT.5	723	20.DT.5	835	16.TT.5	625	20.TT.5	580	20.TT.18	665
16.DT.6	774			16.TT.6	643	20.TT.6	600	20.TT.19	595
						20.TT.7	557		
						20.TT.8	580		
						20.TT.9	645		
						20.TT.10	623		
						20.TT.11	640		
						20.TT.12	671		
						20.TT.13	690		
Mean	766.3 ±25.6		822.0 ±12.9		675.3 ±37.0		611.8 ±38.5		686.2 ±48.1
Coeff. of Var.	3.3%		1.6%		5.5%		6.3%		7.0%

TABLE A2.10 0.2% YIELD STRESSES FOR BOLTS TESTED IN DIRECT AND TORQUE TENSION

Load	SG Reading 1	SG Reading 2	Mean Strain	σ_s	σ_b	e	$\frac{e}{g - 7.44}$
kN	$x10^{-6}$	$x10^{-6}$	%	N/mm^2	N/mm^2	mm	%
0	52819	52536	0	0	0	0	0
19.9	53037	53105	0.039	95.4	126.8	0.027	0.054
39.9	53473	53576	0.085	190.8	254.1	0.057	0.113
59.8	53947	54009	0.130	286.2	380.9	0.083	0.165
69.8	54177	54215	0.152	334.5	444.6	0.096	0.190
79.7	54426	54439	0.176	381.9	507.6	0.111	0.220
89.7	54679	54650	0.199	429.9	571.3	0.125	0.248
99.7	54945	54840	0.222	477.8	635.0	0.146	0.289
109.6	55225	54992	0.243	525.2	698.1	0.167	0.331
119.6	55586	55169	0.270	573.1	761.8	0.247	0.489
129.6	55850	55447	0.297	621.1	825.5	0.648	1.284
141.34	Fracture			677.3	900.3		

TABLE A2.11 EXPERIMENTAL RESULTS FOR TEST 16.DT.2

Load	SG Reading 1	SG Reading 2	Mean Strain	σ_s	σ_b	e	$\frac{e}{g - 7.44}$
kN	$x10^{-6}$	$x10^{-6}$	%	N/mm^2	N/mm^2	mm	%
0	54000	53655	0	0	0	0	0
19.9	54255	53951	0.028	65.3	81.2	0.025	0.046
39.9	54528	54206	0.054	130.5	162.9	0.043	0.078
59.8	54872	54450	0.083	195.8	244.1	0.068	0.126
79.7	55174	54625	0.112	261.1	325.3	0.086	0.160
99.7	55418	55028	0.140	326.3	406.9	0.103	0.191
119.6	55668	55344	0.168	391.6	488.2	0.124	0.230
129.6	55792	55500	0.182	424.3	529.0	0.137	0.254
139.5	55913	55649	0.195	456.9	569.4	0.146	0.271
149.5	56043	55813	0.210	489.5	610.2	0.160	0.297
159.5	56164	55966	0.224	522.2	651.0	0.174	0.323
169.4	56288	56129	0.238	554.6	691.4	0.188	0.349
179.4	56407	56265	0.251	587.4	732.2	0.204	0.379
189.4	56515	56440	0.265	619.8	772.7	0.224	0.416
199.3	56630	56550	0.276	652.7	813.5	0.278	0.516
209.3	56809	56720	0.294	685.3	854.3	0.465	0.863
219.3	57290	57278	0.346	718.0	895.1	0.925	1.716
234.2	Fracture			766.8	955.9		

TABLE A2.12 EXPERIMENTAL RESULTS FOR TEST 20.DT.2

Load	SG Reading 1	SG Reading 2	Mean Strain	σ_b
kN	$x10^{-6}$	$x10^{-6}$	%	N/mm^2
0	53631	52545	0	0
9.9	53496	53331	0.033	71.9
19.9	53550	53960	0.067	143.7
29.9	53839	54345	0.100	215.6
39.9	54158	54666	0.132	287.4
49.8	54496	54983	0.165	359.3
59.8	54840	55304	0.198	431.1
69.8	55200	55612	0.232	503.0
74.8	55368	55768	0.248	538.9
79.7	55536	55925	0.264	574.8
84.7	55725	56057	0.280	610.8
89.7	55900	56168	0.295	646.7
94.7	56056	56295	0.309	682.6
99.7	56290	57342	0.373	718.5
104.6	56943	59170	0.497	754.5
125.6	Fracture			905.3

TABLE A2.13 EXPERIMENTAL RESULTS FOR TEST R16.DT.1

Load	SG Reading 1	SG Reading 2	Mean Strain	σ_b
kN	$x10^{-6}$	$x10^{-6}$	%	N/mm^2
0	52525	52940	0	0
19.9	53229	53155	0.046	95.5
39.9	53625	53624	0.089	191.1
59.8	54046	54104	0.134	286.6
79.7	54416	54331	0.174	382.1
99.7	54796	55056	0.219	477.7
109.6	54971	55311	0.241	525.4
114.6	55082	55428	0.252	549.3
119.6	55167	55551	0.263	573.2
124.6	55253	55687	0.274	597.1
129.6	55348	55802	0.284	621.0
134.6	55452	55960	0.297	644.8
139.5	55520	56081	0.307	668.7
144.5	55616	56191	0.317	692.6
149.5	55722	56311	0.328	716.5
154.4	55836	56464	0.342	740.4
159.5	55939	56615	0.354	764.3
164.5	56027	56780	0.367	788.1
169.4	56335	57067	0.397	812.0
174.4	58285	59596	0.621	835.9
179.4	69746	72412	1.835	859.8
199.3	Fracture			

TABLE A2.14 EXPERIMENTAL RESULTS FOR TEST R20.DT.3

Torque	SG Reading 1	SG Reading 2	SG Reading 3	Mean Strain	F_b	σ_b	LIW Gap	e	$\frac{e}{g - 7.44}$
Nm	$x10^{-6}$	$x10^{-6}$	$x10^{-6}$	%	kN	N/mm^2	mm	mm	%
0	50847	51083	51761	0	0	0	-	0	0
50	51266	51408	51909	0.030	13.0	82.8	-	0.032	0.059
75	51283	51642	52313	0.052	22.6	143.9	1.700	0.043	0.079
150	52262	51988	52778	0.111	48.7	310.4	0.938	0.084	0.155
-	52765	52226	52815	0.137	60.1	382.9	0.825	0.096	0.177
260	53068	52548	53189	0.171	74.7	475.9	0.600	0.126	0.233
300	53460	52739	53320	0.194	85.1	542.3	0.450	0.141	0.260
360	53506	52980	53678	0.216	94.6	602.4	0.263	0.169	0.312
380	53458	53187	53772	0.224	98.3	625.8	0.180	0.187	0.345
400	53193	53752	54015	0.242	106.2	676.3	0.025	0.369	0.682
420	53272	53818	54043	0.248	108.7	692.5	0	0.390	0.720
440	53402	53851	54231	0.260	113.9	752.2	0	0.606	1.120

TABLE A2.15 EXPERIMENTAL RESULTS FOR TEST 16.TT.1

Torque	SG Reading 1	SG Reading 2	SG Reading 3	Mean Strain	F_b	σ_b	LIW Gap	e	$\frac{e}{g - 3.367}$
Nm	$x10^{-6}$	$x10^{-6}$	$x10^{-6}$	%	kN	N/mm^2	mm	mm	%
0	45050	51538	44657	0	0	0	-	0	0
400	46464	52520	46864	0.153	98.4	401.6	0.720	0.123	0.199
440	46625	52410	47002	0.160	102.4	418.1	0.650	0.130	0.210
480	46741	52502	47126	0.171	109.6	447.1	0.325	0.140	0.226
520	46972	52863	46914	0.183	117.6	480.1	0.230	0.150	0.242
540	47060	53040	46783	0.188	120.5	491.9	0.200	0.154	0.249
560	47251	53332	46600	0.198	126.9	518.1	0.120	0.166	0.268
580	47400	53550	46461	0.206	131.8	538.0	0.080	0.176	0.284
600	47485	53733	46380	0.212	135.8	554.2	0.040	0.189	0.305
620	47508	53886	46473	0.221	141.6	577.8	0	0.216	0.349
640	47540	53942	46530	0.226	144.6	590.3	0	0.232	0.374
660	47589	54042	46895	0.243	155.7	635.4	0	0.366	0.591
680	47723	54157	47164	0.260	167.0	681.6	0	0.515	0.831

TABLE A2.16 EXPERIMENTAL RESULTS FOR TEST 20.TT.10

Torque	SG Reading			Mean Strain	F_b	σ_b	LIW Gap	e	$\frac{e}{g - 3.367}$
	1	2	3						
Nm	$x10^{-6}$	$x10^{-6}$	$x10^{-6}$	%	kN	N/mm^2	mm	mm	%
0	48351	43319	45697	0	0	0	-	0	0
400	49341	44822	47647	0.148	95.0	387.8	0.790	0.121	0.178
440	49403	44891	47841	0.159	101.9	415.9	0.650	0.130	0.191
480	49590	45153	48150	0.184	118.1	482.0	0.260	0.147	0.216
520	50018	45193	48150	0.200	128.1	522.9	0.150	0.167	0.245
540	50262	45206	48132	0.208	133.3	544.1	0.070	0.172	0.253
560	50262	45206	48132	0.208	133.3	544.1	0.070	0.172	0.253
580	50262	45206	48132	0.208	133.3	544.1	0.070	0.172	0.253
600	50545	45331	48116	0.221	141.6	578.0	0.020	0.184	0.270
620	50747	45400	48133	0.230	147.8	603.3	0	0.187	0.275
640	50917	45513	48178	0.241	154.8	631.8	0	0.200	0.294
660	50917	45513	48171	0.241	154.8	631.8	0	0.200	0.294
680	51115	45766	48287	0.260	166.8	680.8	0	0.224	0.329
700	51115	45766	48287	0.260	166.8	680.8	0	0.224	0.329
720	51166	45950	48347	0.270	173.1	706.5	0	0.254	0.373
740	51345	46107	48443	0.284	182.3	744.1	0	0.400	0.588
760	51575	46300	48712	0.307	197.1	804.5	0	0.624	0.917

TABLE A2.17 EXPERIMENTAL RESULTS FOR TEST 20.TT.16

APPENDIX A-3

Test No	Specimen Size		Surface Preparation		Yield Stress	Ultimate Stress	E
	Width mm	Thickness mm	Width one side	Thickness both sides	N/mm^2	N/mm^2	kN/mm^2
1	12.49	19.94	n	s	266.1	484.2	207.9
2	12.46	19.93	n	s	259.0	485.9	221.8
3	20.03	19.97	n	s	259.2	484.7	206.5
4	20.02	19.96	n	s	257.8	485.3	206.6
5	25.01	19.93	n	s	257.5	486.7	193.9
6	25.01	19.95	n	s	259.8	484.5	197.9
7	15.06	19.94	n	dm	258.9	483.9	213.2
8	15.00	19.92	n	dm	262.9	485.1	190.4
9	20.00	19.90	n	wm	263.0	489.1	202.0
10	19.98	19.95	n	wm	264.1	489.5	200.0
11	12.46	12.98	s	s	271.2	488.2	201.8
12	12.85	13.16	s	s	265.3	489.3	205.8
13	19.99	12.93	s	s	266.1	490.1	203.8
14	19.92	12.94	s	s	263.0	491.2	197.2
15	25.03	12.95	s	s	253.9	490.6	201.0
16	24.88	13.00	s	s	268.3	500.1	206.2
17	20.00	12.86	s	wm	267.5	495.3	202.6
18	20.02	12.80	s	wm	270.3	504.8	200.2
19	12.43	9.95	s	s	261.9	481.8	212.8
20	12.44	9.99	s	s	257.4	472.6	194.7
21	20.04	10.02	s	s	263.2	482.3	202.5
22	19.91	10.00	s	s	267.9	484.7	206.5
23	25.03	9.78	s	s	281.9	518.1	204.2
24	24.99	10.04	s	s	270.3	496.0	196.3
25	9.94	9.97	s	s	256.7	477.1	200.0
26	14.99	10.03	s	dm	260.0	483.5	192.0
27	15.00	10.04	s	dm	250.4	486.8	205.3
28	20.03	9.97	s	wm	272.1	507.3	210.5
29	20.00	9.98	s	wm	274.7	504.9	193.7
				Mean	263.8 ±6.6	489.8 ±9.4	202.7 ±6.8
				Coefficient of Variation	2.5%	1.9%	3.4%

Note: n = none; s = shaped; dm = dry milled; wm = wet milled

TABLE A3.1 YIELD STRESS, ULTIMATE STRESS AND YOUNG'S MODULUS FOR MACHINED MILD STEEL

Test No	Flange Yield Stress N/mm^2	Flange Ultimate Stress N/mm^2
1	244.5	460.5
2	252.7	459.1
3	262.8	463.0
4	258.7	476.6
5	251.6	462.5
Mean	254.1 ±6.3	462.5 ±2.9
Coeff., of Var.	2.5%	0.6%

TABLE A3.2 TENSILE TEST SPECIMEN RESULTS FOR TEE STUBS TS1, TS2, TS3 AND TS4

Test No	Flange Yield Stress N/mm^2	Flange Ultimate Stress N/mm^2
1	273.5	473.3
2	281.1	472.6
Mean	277.3 ±3.8	473.0 ±0.35
Coeff., of Var.	1.4%	0.1%

TABLE A3.3 TENSILE TEST SPECIMEN RESULTS FOR TEE STUB TS5

	Dial Gauge Number (see Figure 3.2)		Mean Deflection
Load kN	1 mm	2 mm	mm
0	24.24	22.01	0
24.9	24.23	21.98	0.020
49.8	24.22	21.97	0.030
74.8	24.20	21.95	0.050
99.7	24.17	21.92	0.080
124.6	24.13	21.88	0.120
149.5	24.10	21.85	0.150
174.4	24.05	21.81	0.195
199.3	24.01	21.76	0.240
224.3	23.96	21.71	0.290
249.2	23.91	21.64	0.350
274.1	23.86	21.56	0.415
299.0	23.79	21.45	0.505
323.9	23.68	21.29	0.640
348.9	23.45	20.99	0.905
373.8	22.96	20.43	1.430
398.7	22.24	19.63	2.190
413.6	21.10	18.40	3.375

TABLE A3.4 DIAL GAUGE READINGS FOR TEST TS5

	Weld Line		Bolt Line			
Load kN	1 x 10^{-6}	2 x 10^{-6}	3 x 10^{-6}	4 x 10^{-6}	5 x 10^{-6}	6 x 10^{-6}
	(0)	(0)	(0)	(0)	(0)	(0)
0	20330	20020	20470	20420	21740	20900
	(7.4)	(6.3)	(-4.2)	(-8.4)	(-5.3)	(-4.2)
24.9	20365	20050	20450	20380	21715	20880
	(21.0)	(21.0)	(-10.5)	(-17.9)	(-16.8)	(-15.8)
49.8	20430	20120	20420	20335	21660	20825
	(37.8)	(35.7)	(-17.9)	(-27.3)	(-32.6)	(-28.4)
74.8	20510	20190	20385	20290	21585	20765
	(58.8)	(54.6)	(-25.2)	(-33.6)	(-46.2)	(-42.0)
99.7	20610	20280	20350	20260	21520	20700
	(83.0)	(78.8)	(-28.4)	(-42.0)	(-54.6)	(-52.5)
124.6	20725	20395	20335	20220	21480	20650
	(109.2)	(104.0)	(-32.6)	(-50.4)	(-57.8)	(-62.0)
149.5	20850	20515	20315	20180	21465	20605
	(140.7)	(134.4)	(-37.8)	(-63.0)	(-57.8)	(-72.5)
174.4	21000	20660	20290	20120	21465	20555
	(175.4)	(170.1)	(-38.9)	(-75.6)	(-57.8)	(-84.0)
199.3	21165	20830	20285	20060	21465	20500
	(216.3)	(213.2)	(-44.1)	(-91.4)	(-55.7)	(-100.0)
224.3	21360	21035	20260	19985	21475	20425
	(270.4)	(264.6)	(-50.9)	(-116.1)	(-63.0)	(-118.7)
249.2	21618	21280	20228	19868	21440	20335
	(324.5)	(332.9)	(-57.8)	(-140.7)	(-69.3)	(-147.0)
274.1	21875	21605	20195	19750	21410	20200
	(401.1)	(425.3)	(-71.4)	(-177.5)	(-85.1)	(-181.7)
299.0	22240	22045	20130	19575	21335	20035
			(-98.7)	(-228.9)	(-113.4)	(-226.8)
323.9	22785	22830	20000	19330	21200	19820
			(-153.3)	(-265.7)	(-160.7)	(-274.1)
348.9	23695	24605	19740	19155	20975	19595
			(-261.5)	(-308.7)	(-194.3)	(-393.8)
373.8	25295	27800	19225	18950	20815	19025
*	252.4 kN	253.8 kN	377.4 kN	355.6 kN	435.2 kN	349.5 kN

Note: The Number in Brackets Indicates the Corresponding Stress in N/mm^2.

* Refers to the Load at Which First Yield Occurs

TABLE A3.5 STRAIN GAUGE READINGS FOR TEST TS5

	Bolt Number			
Load kN	1 x 10^{-6}	2 x 10^{-6}	3 x 10^{-6}	4 x 10^{-6}
	(0)	(0)	(0)	(0)
0	20765	20065	19290	19010
	(46.4)	(47.7)	(47.5)	(41.5)
PRELOAD	21850	21180	20400	19980
	(46.0)	(48.1)	(47.5)	(41.5)
24.9	21840	21190	20400	19980
	(45.1)	(47.7)	(47.1)	(41.5)
49.8	21820	21180	20390	19980
	(46.4)	(48.6)	(48.4)	(42.4)
74.8	21850	21200	20420	20000
	(48.8)	(50.7)	(52.2)	(44.9)
99.7	21905	21250	20510	20060
	(52.2)	(55.8)	(57.6)	(49.2)
124.6	21985	21370	20635	20160
	(56.3)	(61.6)	(63.5)	(53.9)
149.5	22080	21505	20775	20270
	(62.7)	(69.5)	(70.4)	(60.1)
174.4	22230	21690	20935	20415
	(69.1)	(78.5)	(77.9)	(66.3)
199.3	22380	21900	21110	20560
	(77.9)	(88.6)	(87.1)	(74.2)
224.3	22585	22135	21335	20745
	(87.0)	(98.3)	(96.6)	(82.8)
249.2	22798	22363	21548	20945
	(96.1)	(108.0	(106.1)	(91.4)
274.1	23010	22590	21770	21145
	(108.3)	(119.0)	(116.8)	(101.4)
299.0	23295	22845	22020	21380
418.6	Bolts 1 and 2 Fractured			

Note: The Number in Brackets Indicates the Corresponding Force in kN.

TABLE A3.6 BOLT STRAIN GAUGE READINGS FOR TEST TS5

A3.1 DETERMINATION OF Q_b FROM EXPERIMENTAL RESULTS FOR TEE STUBS

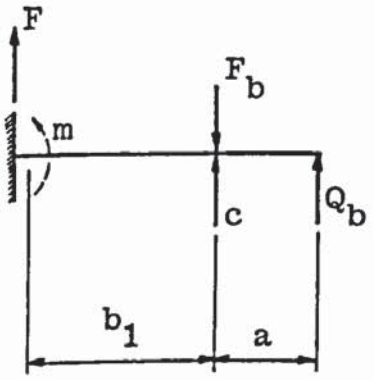

Resolving forces vertically

$$F + Q_b = F_b - c$$

Taking moments

$$m + c.b_1 + Q_b (a + b_1) - F_b.b_1 = 0$$

$$m + Q_b (a + b_1) - (F + Q_b)b_1 = 0$$

$$Q_b = (F.b_1 - m)/a$$

Therefore within the elastic range

$$Q_b = (F.b_1 - w.\sigma.t_p^2/6)/a \qquad \text{A3.1}$$

Load kN	Mean σ Weld Line N/mm^2	Q_b cal. kN	F kN	F + Q_b cal. kN
24.9	6.9	7.4	6.2	13.6
49.8	21.0	13.9	12.5	26.4
74.8	36.8	20.1	18.7	38.8
99.7	56.7	25.8	24.9	50.7
124.6	80.9	30.9	31.1	62.0
149.5	106.6	35.9	37.4	73.3
174.4	137.6	40.1	43.6	83.7
199.3	172.8	43.8	49.8	93.6
224.3	214.8	46.6	56.1	102.7
249.2	267.5	48.0	62.3	110.3
253.1	277.3	48.1	63.3	111.4

Note: Q_b determined from equation A3.1 with b_1 = 40mm

TABLE A3.7 PRYING FORCE VALUES FOR TEST TS5

APPENDIX A-4

Test No.	Component	Yield Stress N/mm^2	Ultimate Stress N/mm^2
P1	End Plate	346.0	491.0
		349.2	492.2
	Mean	347.6 ±1.6	491.6 ±0.6
P1 & P2	End Plate P2	237.0	419.4
	Column Flange P1 & P2	239.8	415.2
	Mean	238.4 ±1.4	417.3 ±2.1
P1 & P2	Beam Flange	309.2	489.9
		321.2	490.6
	Mean	315.2 ±6.0	490.3 ±0.4
P1 & P2	Beam Web	355.8	541.2
		374.0	550.0
		355.0	543.1
	Mean	361.6 ±8.8	544.8 ±3.8

TABLE A4.1 TENSILE TEST SPECIMEN RESULTS FOR TESTS P1 AND P2

Test No.	Component	Yield Stress N/mm^2	Ultimate Stress N/mm^2
Test Series CS1 & CS2	End Plate and Column Flange	234.7	404.8
		224.6	394.3
		226.7	401.8
		226.0	384.5
		229.0	409.5
		230.0	392.0
		227.1	391.7
		229.4	402.7
		223.8	396.7
		239.7	409.6
		221.5	402.6
		240.6	405.6
		235.2	400.2
		217.2	388.4
		229.8	391.7
	Mean	229.0 ±6.2	398.4 ±7.5

TABLE A4.2 TENSILE TEST SPECIMEN RESULTS FOR TEST SERIES CS1 AND CS2

Test No.	Component	Yield Stress N/mm^2	Ultimate Stress N/mm^2
Test Series CS3, CS4 & CS5	End Plate and Column Flange	334.9	497.7
		327.7	509.5
		321.4	509.2
		345.1	514.1
		338.3	508.7
		349.2	514.6
		321.1	512.5
		324.2	509.0
		341.3	512.6
		314.0	478.4
		300.3	478.2
		311.0	480.8
		332.4	506.8
		338.1	506.3
		322.4	508.8
Mean		328.1 ±13.1	503.1 ±12.6

TABLE A4.3 TENSILE TEST SPECIMEN RESULTS FOR TEST SERIES CS3, CS4 AND CS5

Test No.	Component	Yield Stress N/mm^2	Ultimate Stress N/mm^2
Test Series CS1, CS2 & CS3	Beam Flange	286.5 289.1 295.0 292.1	477.5 481.3 473.7 470.3
	Mean	290.7 ±3.2	475.7 ±4.1
Test Series CS1, CS2 & CS3	Beam Web	289.0 276.6 323.8 280.3 282.9	461.4 463.4 468.1 464.8 466.2
	Mean	290.5 ±17.1	464.8 ±2.3
Test Series CS4 & CS5	Beam Flange	309.2 302.5 300.6 306.4 297.9 303.2 308.7 305.3	460.5 461.4 456.3 464.2 464.5 459.4 458.0 462.9
	Mean	304.2 ±3.7	460.9 ±2.7
Test Series CS4 & CS5	Beam Web	307.4 303.1 334.9	461.2 464.0 478.6
	Mean	315.1 ±14.1	467.9 ±7.6

TABLE A4.4 TENSILE TEST SPECIMEN RESULTS FOR TEST SERIES CS1, CS2, CS3, CS4 & CS5

	Dial Gauge Number (see Figure 4.1)									
Load kN	1 mm	2 mm	3 mm	4 mm	5 mm	6 mm	7 mm.	8 mm	9 mm	10 mm
49.8	1.46	2.40	2.52	2.82	0.02	0.13	0.004	0	-0.01	0.036
99.7	2.28	3.89	3.92	3.51	0.06	0.20	0.014	0	-0.006	0.036
149.5	2.73	5.32	5.17	4.15	0.12	0.29	0.032	0.022	0.02	0.042
199.3	3.12	7.17	6.83	4.77	0.17	0.41	0.04	0.034	0.046	0.06
249.2	3.38	9.16	8.94	5.58	0.30	0.64	0.056	0.048	0.082	0.098
274.1	3.38	10.11	10.23	6.11	0.46	0.80	0.066	0.054	0.102	0.106
299.0	3.44	11.87	11.73	6.44	0.58	1.02	0.078	0.06	0.124	0.186
323.9	3.49	14.13	14.06	6.84	0.78	1.36	0.080	0.072	0.158	0.190
348.9	3.49	16.78	16.81	7.20	1.07	1.61	0.086	0.088	0.192	0.202

TABLE A4.5 DIAL GAUGE READINGS FOR TEST CS3-2

Load kN	V kN	M kNm	LHS Ø rads x 10^{-3}	RHS Ø rads x 10^{-3}
49.8	24.9	25.3	1.033	-0.326
99.7	49.8	50.6	1.769	0.446
149.5	74.8	75.9	2.846	1.109
199.3	99.7	101.2	4.451	2.239
249.2	124.6	126.5	6.352	3.652
274.1	137.1	139.1	7.396	4.478
299.0	149.5	151.8	9.264	5.750
323.9	162.0	164.4	11.692	7.848
348.9	174.4	177.0	14.603	10.445

Note: LHS Ø Obtained from Dial Gauges 1 and 2

RHS Ø Obtained from Dial Gauges 3 and 4.

TABLE A4.6 ROTATION VALUES FOR TEST CS3-2

	End Plate Bolt Line				End Plate Weld Line		Column Flange Weld Line	
Load kN	1 x10^{-6}	2 x10^{-6}	3 x10^{-6}	4 x10^{-6}	5 x10^{-6}	6 x10^{-6}	7 x10^{-6}	8 x10^{-6}
	(0)	(0)	(0)	(0)	(0)	(0)	(0)	(0)
0	52767	53245	53085	52300	53017	52270	54037	54812
	(5.7)	(2.3)	(6.1)	(5.5)	(25.0)	(9.9)	(-1.7)	(6.3)
49.8	52794	53256	53114	52326	53136	52317	54029	54842
	(5.0)	(2.1)	(6.9)	(5.9)	(34.0)	(12.8)	(-1.3)	(8.60
74.8	52795	53255	53118	52328	53179	52331	54031	54853
	(8.2)	(4.6)	(9.9)	(7.6)	(44.3)	(17.9)	(0.4)	(12.4)
99.7	52806	53267	53132	52336	53228	52355	54039	54871
	(8.4)	(4.4)	(9.2)	(10.3)	(51.5)	(24.8)	(3.2)	(21.0)
124.6	52807	53266	53129	52349	53262	52388	54052	54912
	(17.4)	(12.8)	(15.1)	(13.9)	(96.4)	(46.0)	(36.5)	(45.4)
149.5	52850	53306	53157	52366	53476	52489	54211	55028
	(25.0)	(17.4)	(21.6)	(18.9)	(214.8)	(155.4)	(115.1)	(102.9)
174.4	52886	53328	53188	52390	54040	53010	54585	55302
	(31.9)	(23.7)	(30.2)	(25.4)	(418.1)	(318.6)	(207.1)	(159.6)
199.3	52919	53358	53229	52421	55008	53787	55023	55572
	(36.8)	(29.6)	(36.1)	(31.5)	(531.9)	(423.6)	(357.2)	(207.1)
224.3	52942	53386	53257	52450	55550	54287	55738	55798
	(35.5)	(38.0)	(40.7)	(37.8)			(585.3)	(302.4)
249.2	52936	53426	53279	52480			56824	56252
	(26.3)	(39.7)	(43.1)	(43.3)				(430.7)
274.1	52892	53434	53290	52506				56863
	(18.4)	(31.3)	(35.7)	(39.1)				
299.0	52855	53394	53255	52486				
	(9.0)	(15.3)	(31.1)	(28.8)				
323.9	52810	53318	53233	52437				
	(-6.5)	(0)	(26.7)	(16.8)				
348.9	52736	53245	53212	52380				
Load at which first yield occurs					188.3kN	219.5kN	201.6kN	254.2kN

Note: The Number in Brackets Indicates the Corresponding Stress in N/mm^2

TABLE A4.7 STRAIN GAUGE READINGS FOR TEST CS3-2

Load kN	Bolt Number (see Figure 4.1) 1 mm	2 mm	3 mm	4 mm	5 mm	6 mm	7 mm	8 mm	9 mm	10 mm	11 mm	12 mm
Pre-Load	0.120	0.130	0.120	0.118	0.130	0.118	0.124	0.127	0.128	0.122	0.126	0.124
49.8	0.116	0.130	0.118	0.112	0.128	0.114	0.124	0.128	0.128	0.110	0.126	0.124
99.7	0.110	0.130	0.118	0.110	0.126	0.116	0.118	0.126	0.130	0.108	0.128	0.124
149.5	0.114	0.128	0.120	0.114	0.130	0.116	0.118	0.126	0.130	0.110	0.124	0.122
199.3	0.110	0.134	0.126	0.116	0.132	0.128	0.118	0.136	0.138	0.112	0.134	0.130
249.2	0.114	0.158	0.148	0.112	0.182	0.154	0.130	0.168	0.188	0.114	0.204	0.178
299.0	0.122	0.214	0.188	0.120	0.356	0.208	0.124	0.356	0.238	0.114	0.280	0.228
323.9	0.122	0.424	0.274	0.122	0.742	0.262	0.124	0.636	0.298	0.118	0.434	0.308
348.9	0.130	0.636	0.358	0.122	1.116	0.436	0.140	1.142	0.438	0.124	0.734	0.368
386.2	Bolts 5 and 6 Fractured											

TABLE A4.8 BOLT EXTENSION READINGS FOR TEST CS3-2

		Bolts 1 and 10			Bolts 2 and 11			Bolts 3 and 12		
Load kN	M kNm	e mm	ε %	F_b kN	e mm	ε %	F_b kN	e mm	ε %	F_b kN
0	0	0.121	0.222	73.0	0.128	0.235	76.9	0.122	0.224	73.2
49.8	25.3	0.113	0.207	67.8	0.128	0.235	76.9	0.121	0.222	73.0
99.7	50.6	0.109	0.200	65.9	0.129	0.236	77.1	0.121	0.222	73.0
149.5	75.9	0.112	0.205	67.5	0.126	0.231	75.5	0.121	0.222	73.0
199.3	101.2	0.111	0.203	66.3	0.134	0.286	94.2	0.128	0.273	89.5
249.2	126.5	0.114	0.209	68.1	0.181	0.387	112.3	0.163	0.348	108.3
299.0	151.8	0.118	0.216	71.0	0.247	0.528	120.1	0.208	0.444	115.7
323.9	164.4	0.120	0.220	72.2	0.429	0.916	-	0.291	0.622	123.2
348.9	177.0	0.127	0.271	88.9	0.685	1.463	-	0.363	0.775	126.4

Note: ε obtained from equation 2.10 where $g = T + t_w + 1n.\alpha$. $\alpha = 0.5$ when extensions are less than or equal to that due to initial preload.

$\alpha = 1$ when extensions are greater than that due to initial period.

$t_w/2$ was taken as 3.25mm and l_n was taken as 15.5mm.

TABLE A4.9 BOLT FORCE VALUES FOR TEST CS3-2

		Bolts 4 and 7			Bolts 5 and 8			Bolts 6 and 9		
Load kN	M kNm	e mm	ε %	F_b kN	e mm	ε %	F_b kN	e mm	ε %	F_b kN
0	0	0.121	0.222	73.0	0.1285	0.236	77.1	0.123	0.225	73.9
49.8	25.3	0.118	0.216	71.0	0.128	0.235	76.9	0.121	0.222	73.0
99.7	50.6	0.114	0.209	68.1	0.126	0.231	75.5	0.123	0.225	73.9
149.5	75.9	0.116	0.213	69.4	0.128	0.235	76.9	0.123	0.225	73.9
199.3	101.2	0.117	0.214	70.3	0.134	0.286	94.5	0.133	0.284	93.6
249.2	126.5	0.121	0.222	73.0	0.175	0.374	111.5	0.171	0.365	109.9
299.0	151.8	0.122	0.261	85.1	0.356	0.761	125.9	0.223	0.476	117.8
323.9	164.4	0.123	0.263	86.4	0.689	1.472	-	0.280	0.598	122.8
348.9	177.0	0.131	0.280	91.8	1.129	2.412	-	0.437	0.934	-

Note: ε obtained from equation 2.10 where $g = T + t_w + l_n.\alpha$. $\alpha = 0.5$ when extensions are less than or equal to that due to initial preload.

$\alpha = 1$ when extensions are greater than that due to initial preload.

$t_w/2$ was taken as 3.25mm and l_n was taken as 15.5mm.

TABLE A4.10 BOLT FORCE VALUES FOR TEST CS3-2

Load kN	M kNm	Mean σ Weld Line EP N/mm^2	Mean σ Weld Line CF N/mm^2	Q_b cal End Plate N/mm^2	F + Q_b cal EP kN	Q_b cal Column Flange kN	F + Q_b cal CF kN
49.8	25.3	17.5	2.3	19.2	36.4	32.8	50.1
74.8	37.9	23.4	3.7	29.3	55.2	49.1	75.0
99.7	50.6	31.1	6.4	39.2	73.7	65.2	99.8
124.6	63.2	38.2	12.1	49.1	92.3	80.4	123.6
149.5	75.9	71.2	41.0	53.3	105.1	89.9	141.8
174.4	88.5	185.1	109.0	39.5	99.9	89.5	150.0
194.9	98.9	328.1		17.2	84.7		
199.3	101.2		183.4			87.6	156.7
224.3	113.8		282.2			79.4	157.2
236.8	120.2		328.1			76.3	158.4

Abbreviations used: EP End Plate; CF Column Flange

Note: Q_b determined from equation A3.1 with b_1 = 40mm when Q_b related to the end plate and b_1 = 58mm together with $w = 2b_1$ when Q_b related to the column flange.

TABLE A4.11 PRYING FORCE VALUES FOR TEST CS3-2

○ Left Hand Side Joint

● Right Hand Side Joint

Applied Moment-Rotation Relationship and Applied Moment - Column Flange Deflection Relationship

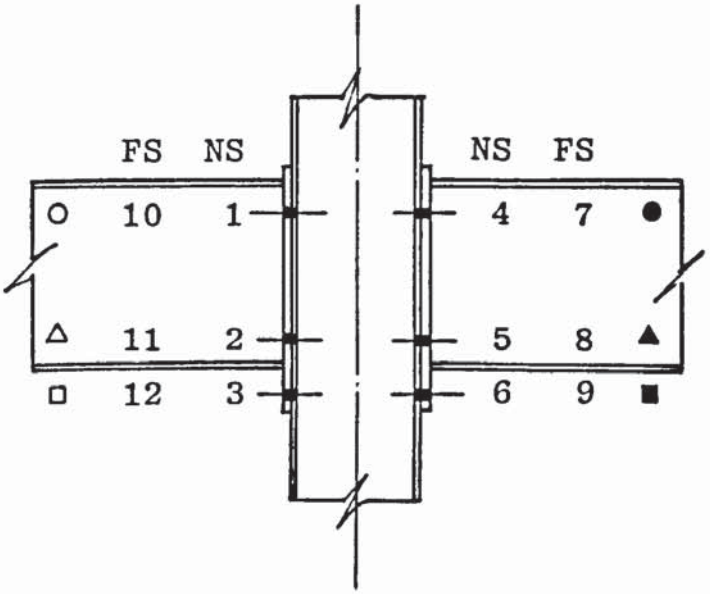

Applied Moment - Bolt Force Relationship

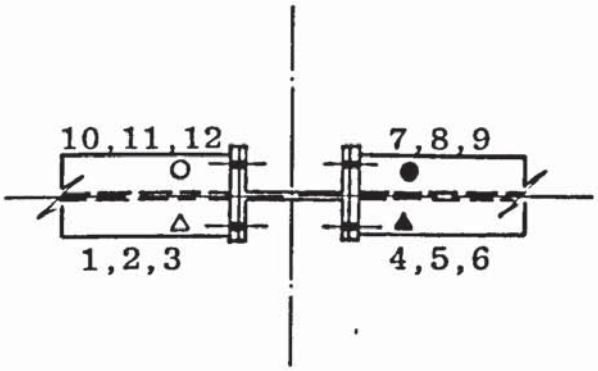

Shear Force - Slip Relationship

Abbreviations used: NS, Near Side; FS, Far Side

Individual Bolt Numbers are Shown Adjacent to Each End Plate

TABLE A4.12 KEY TO SYMBOLS

Abbreviations used: EP, First Yield Weld Line End Plate; CF, First Yield Weld Line Column Flange

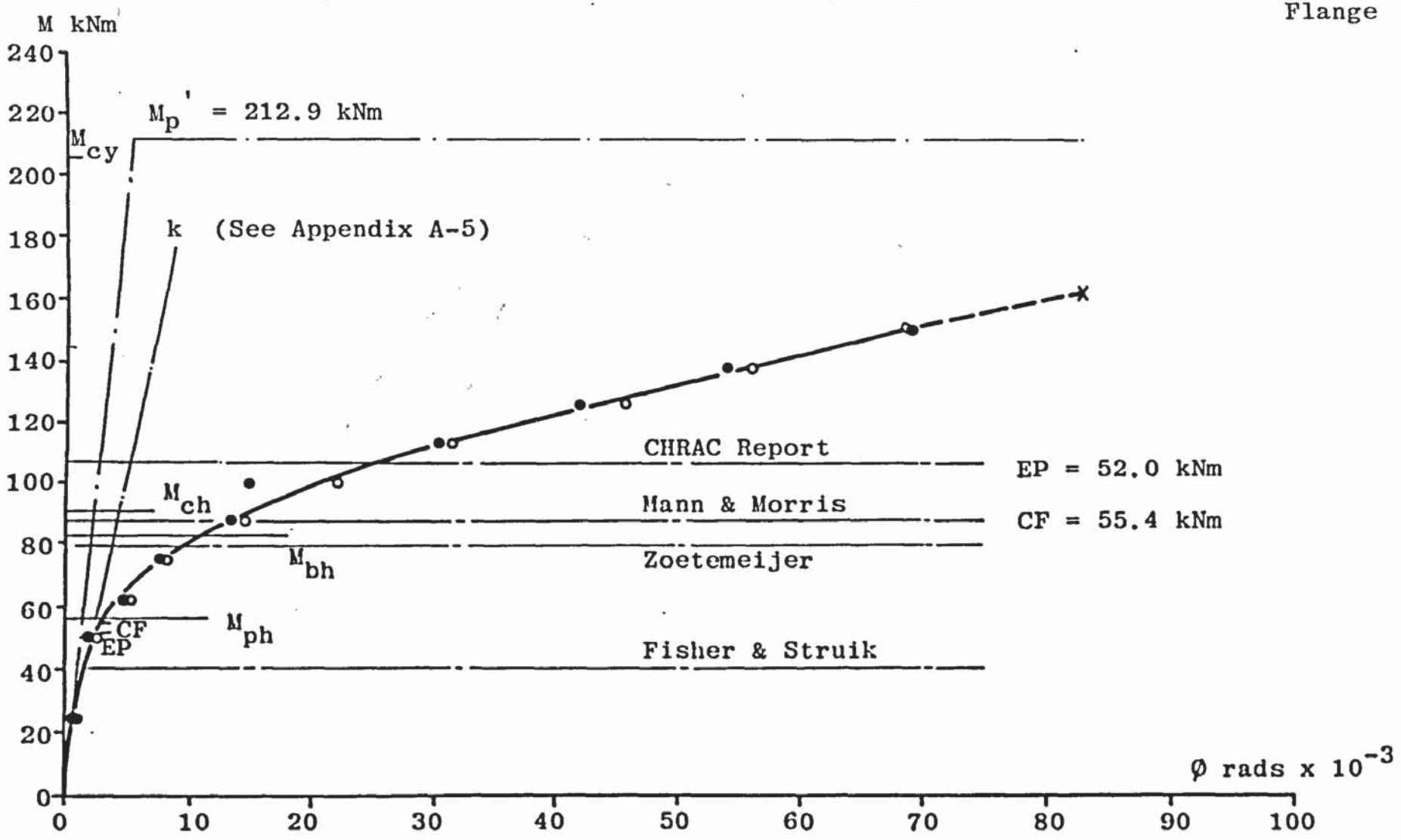

FIGURE A4.1 APPLIED MOMENT - ROTATION RELATIONSHIP FOR TEST CS1-2

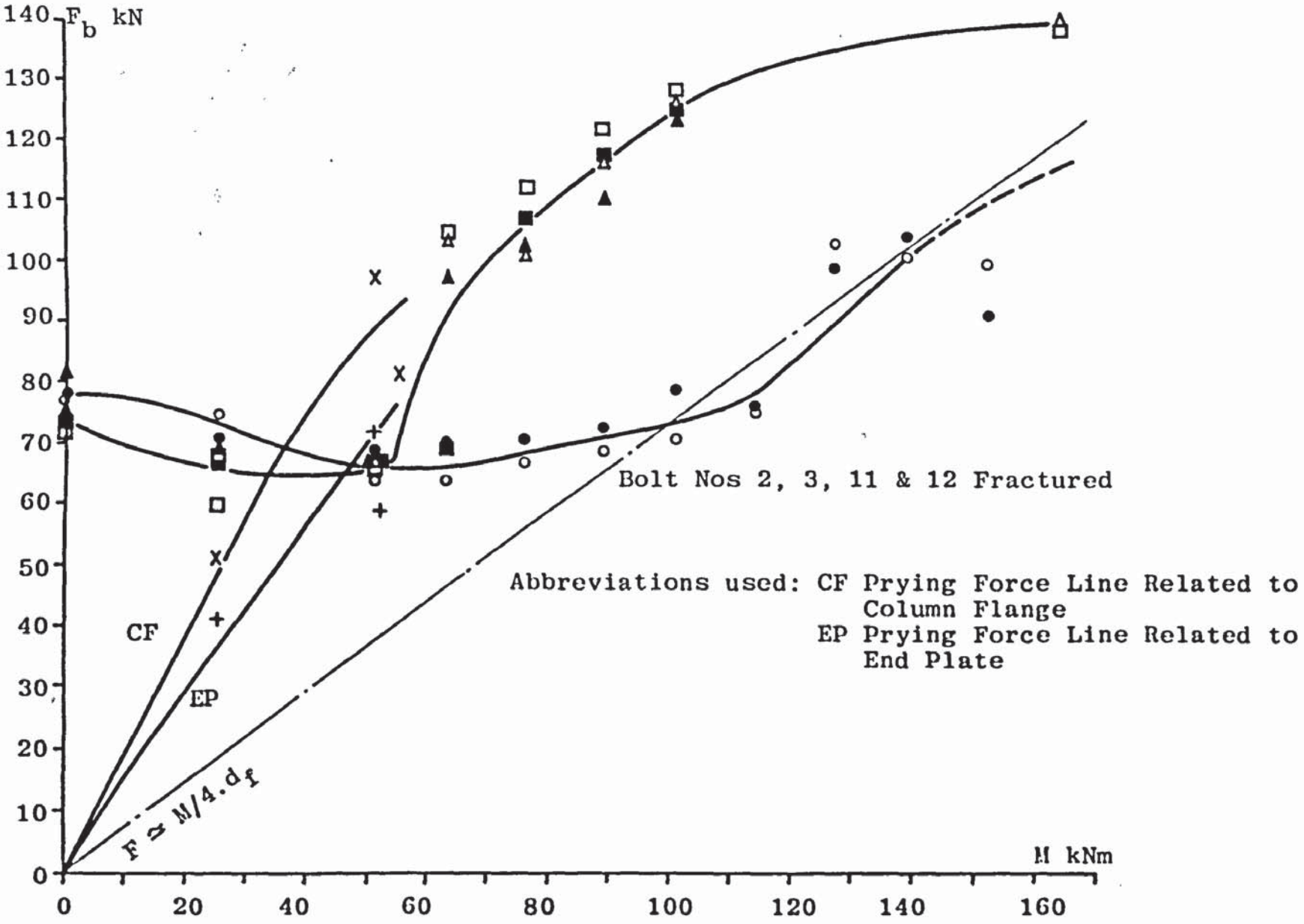

FIGURE A4.2 APPLIED MOMENT - BOLT FORCE RELATIONSHIP FOR TEST CS1-2

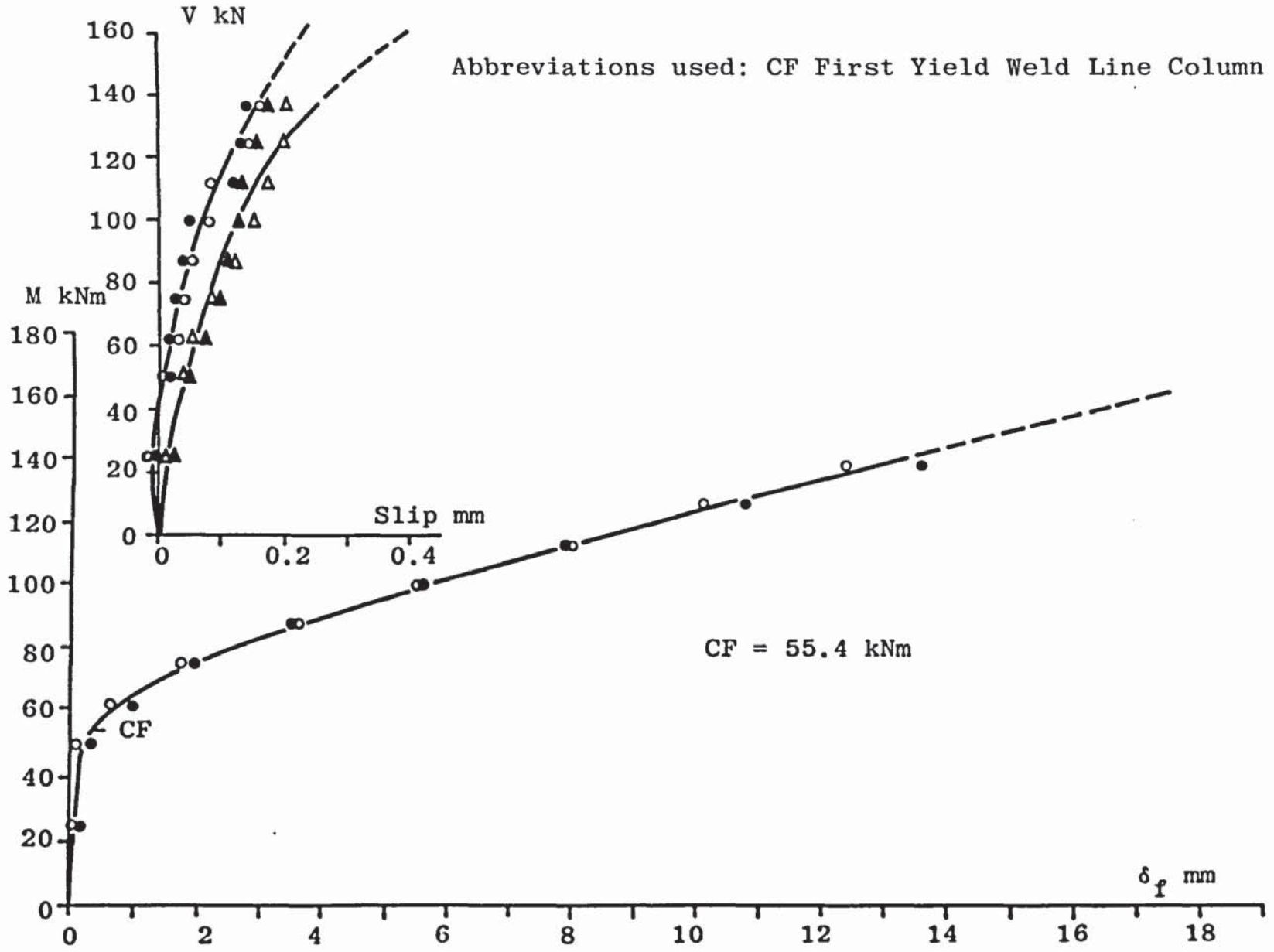

FIGURE A4.3 APPLIED MOMENT - COLUMN FLANGE DEFLECTION RELATIONSHIP AND SHEAR FORCE - SLIP RELATIONSHIP FOR TEST CS1-2

Abbreviations used: EP, First Yield Weld Line End Plate; CF, First Yield Weld Line Column Flange

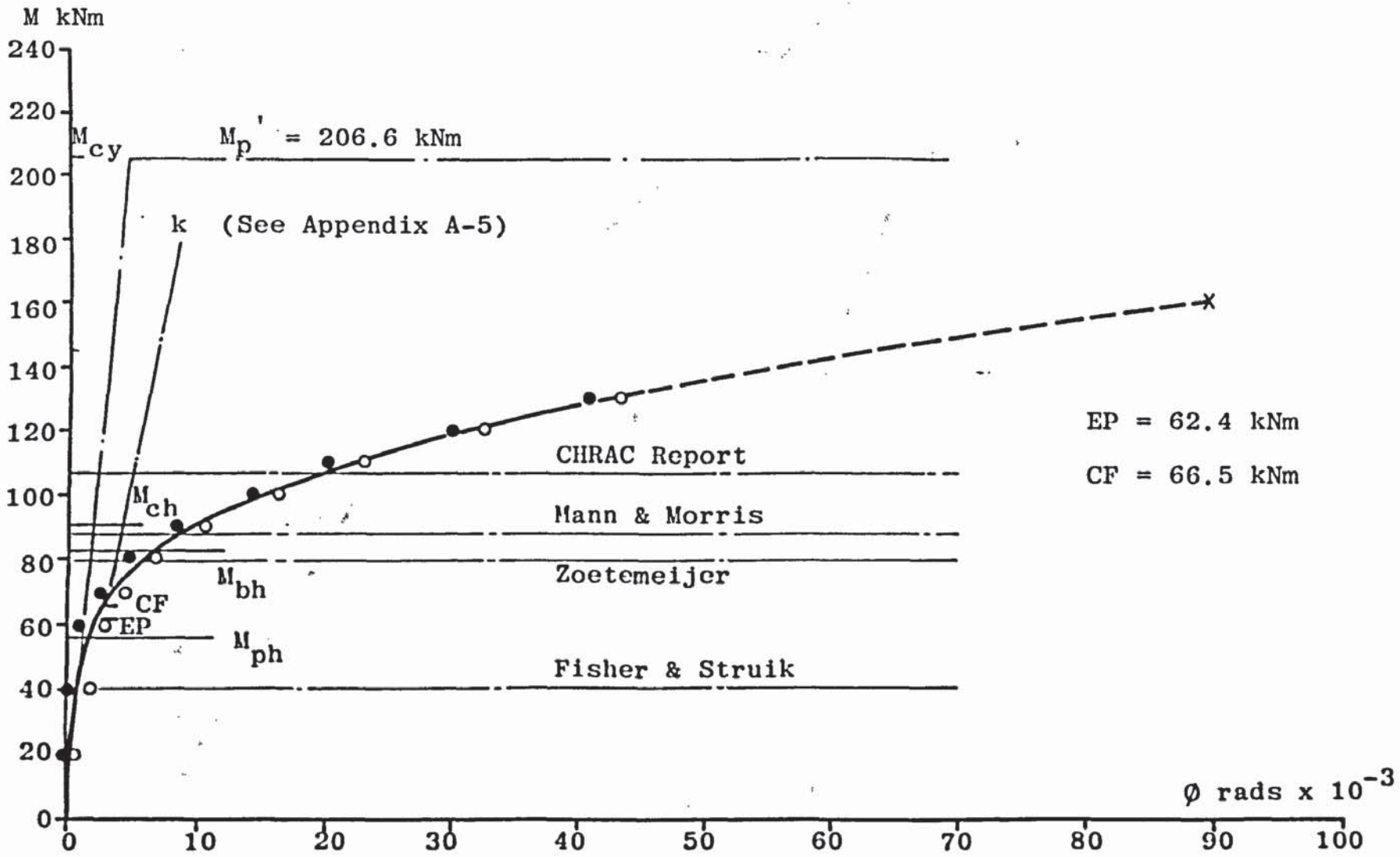

FIGURE A4.4 APPLIED MOMENT - ROTATION RELATIONSHIP FOR TEST CS1-3

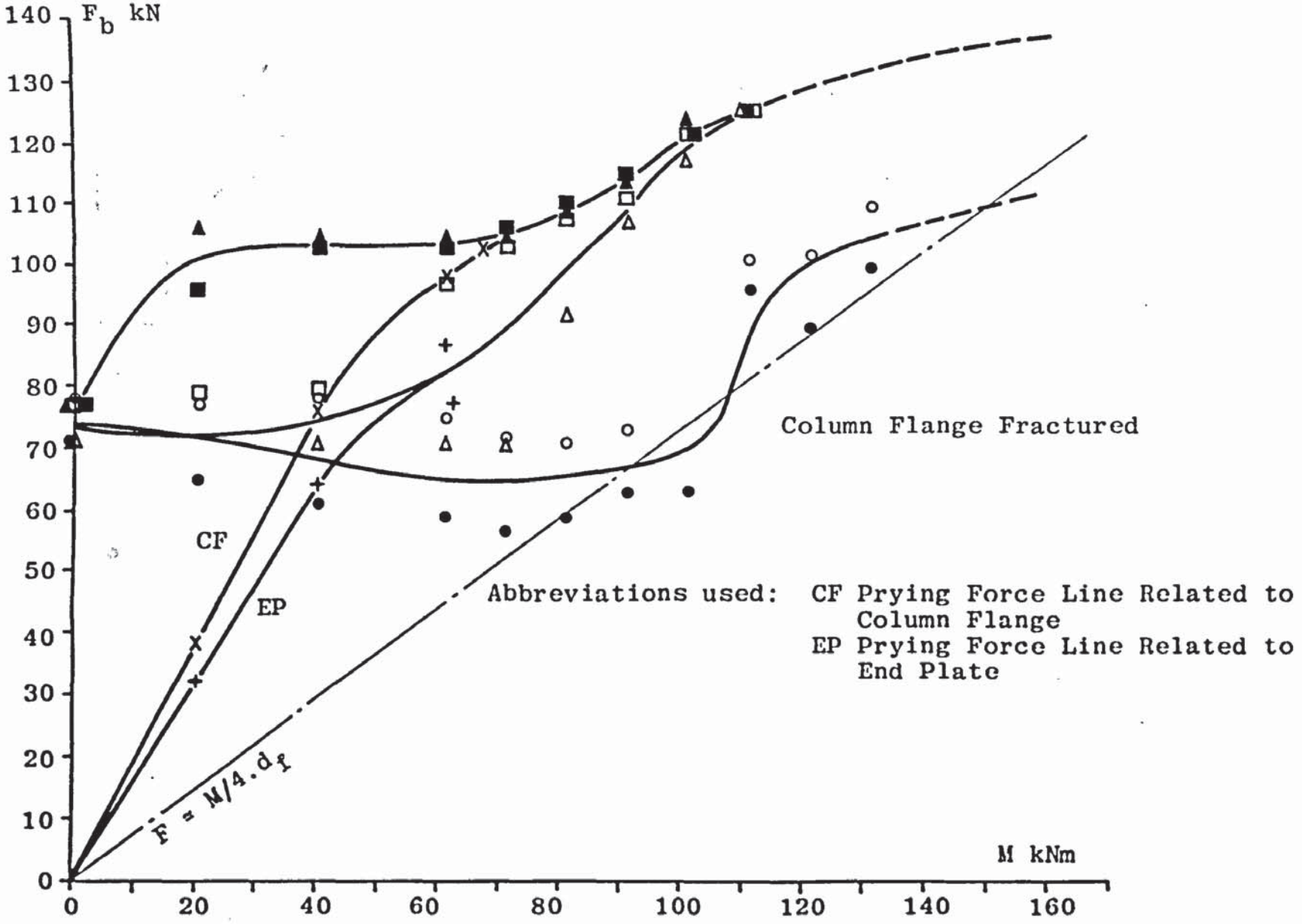

FIGURE A4.5 APPLIED MOMENT - BOLT FORCE RELATIONSHIP FOR TEST CS1-3

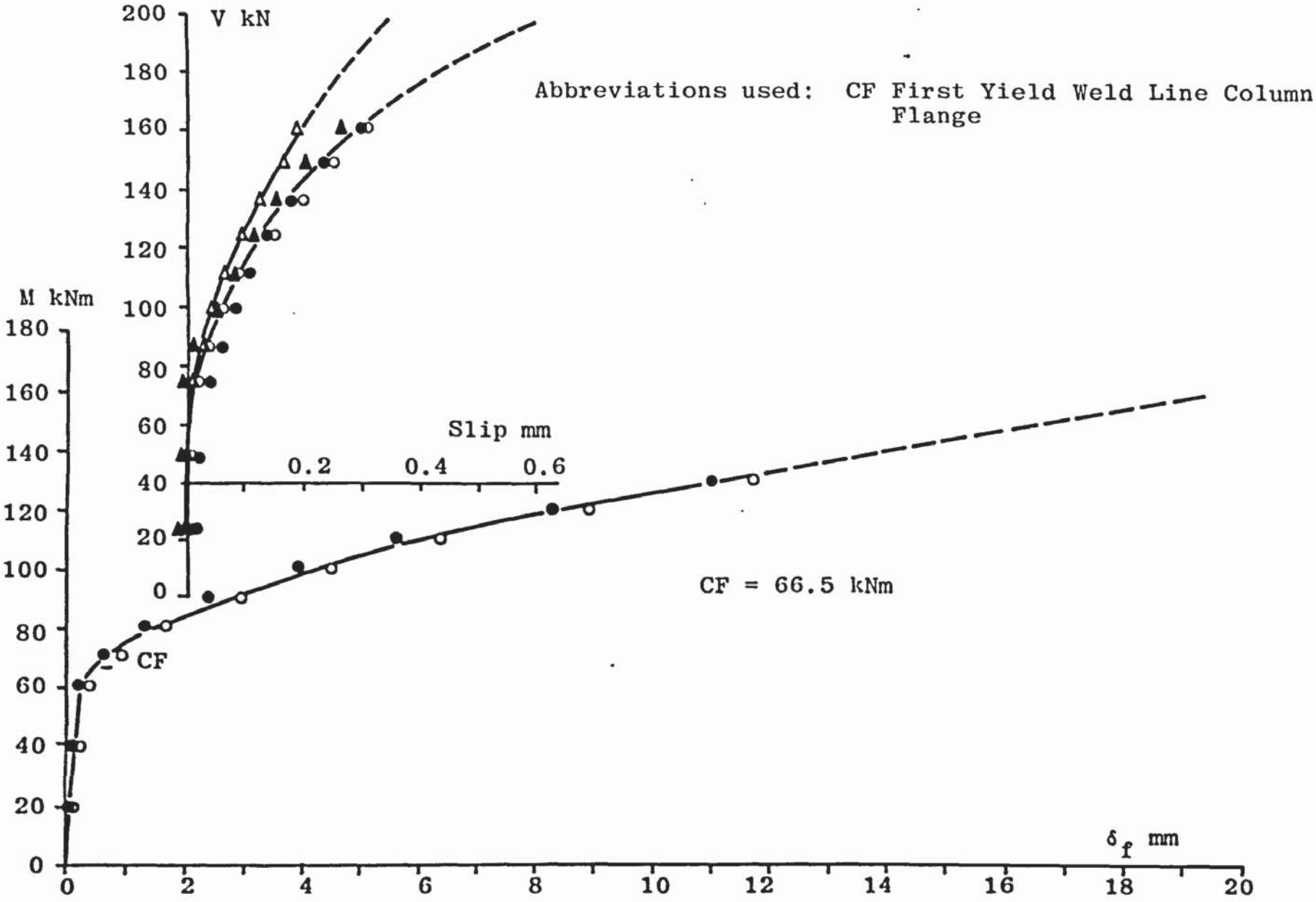

FIGURE A4.6 APPLIED MOMENT - COLUMN FLANGE DEFLECTION RELATIONSHIP AND SHEAR FORCE - SLIP RELATIONSHIP FOR TEST CS1-3

Abbreviations used: EP, First Yield Weld Line End Plate; CF, First Yield Weld Line Column Flange

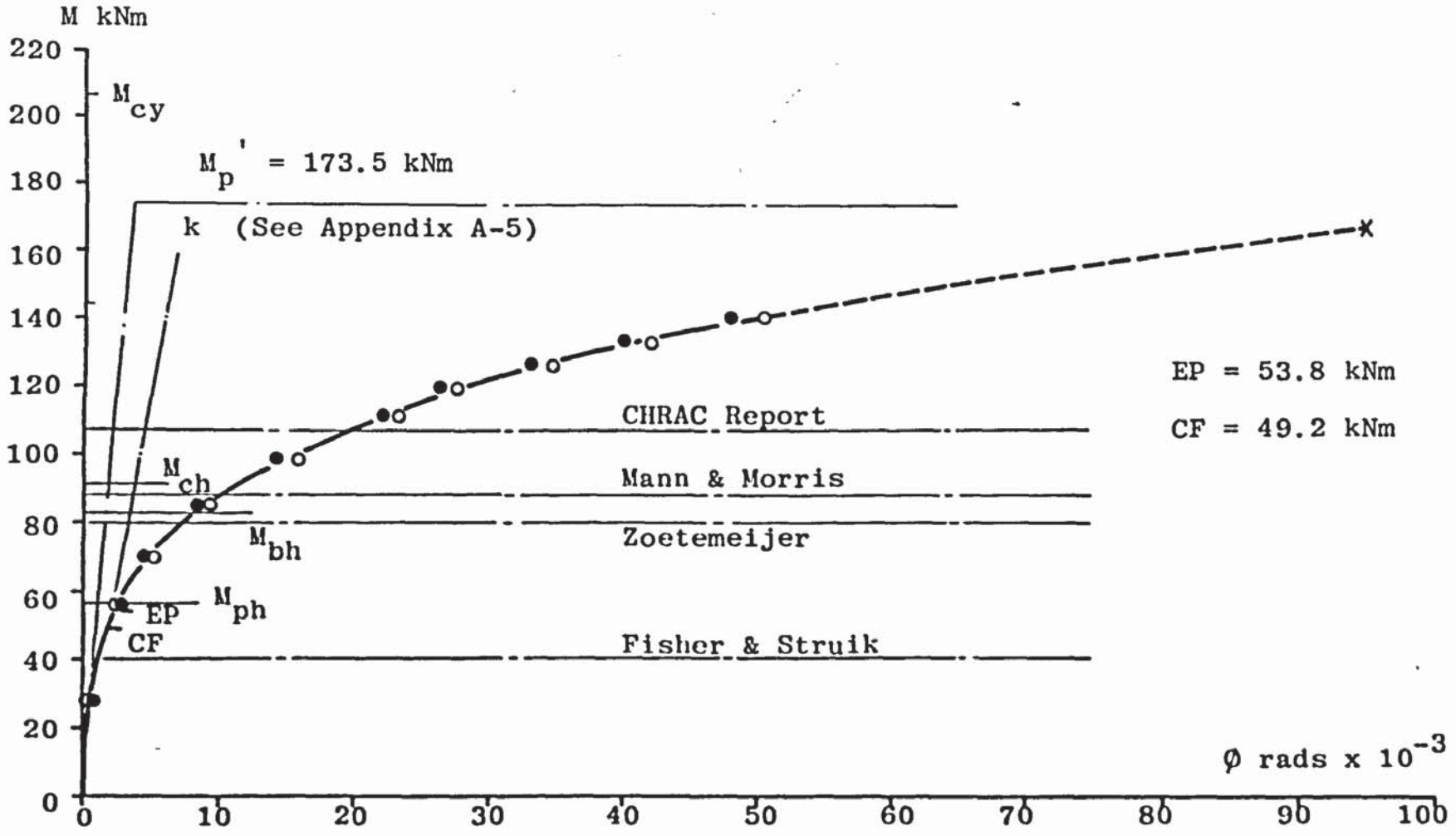

FIGURE A4.7 APPLIED MOMENT - ROTATION RELATIONSHIP FOR TEST CS1-4

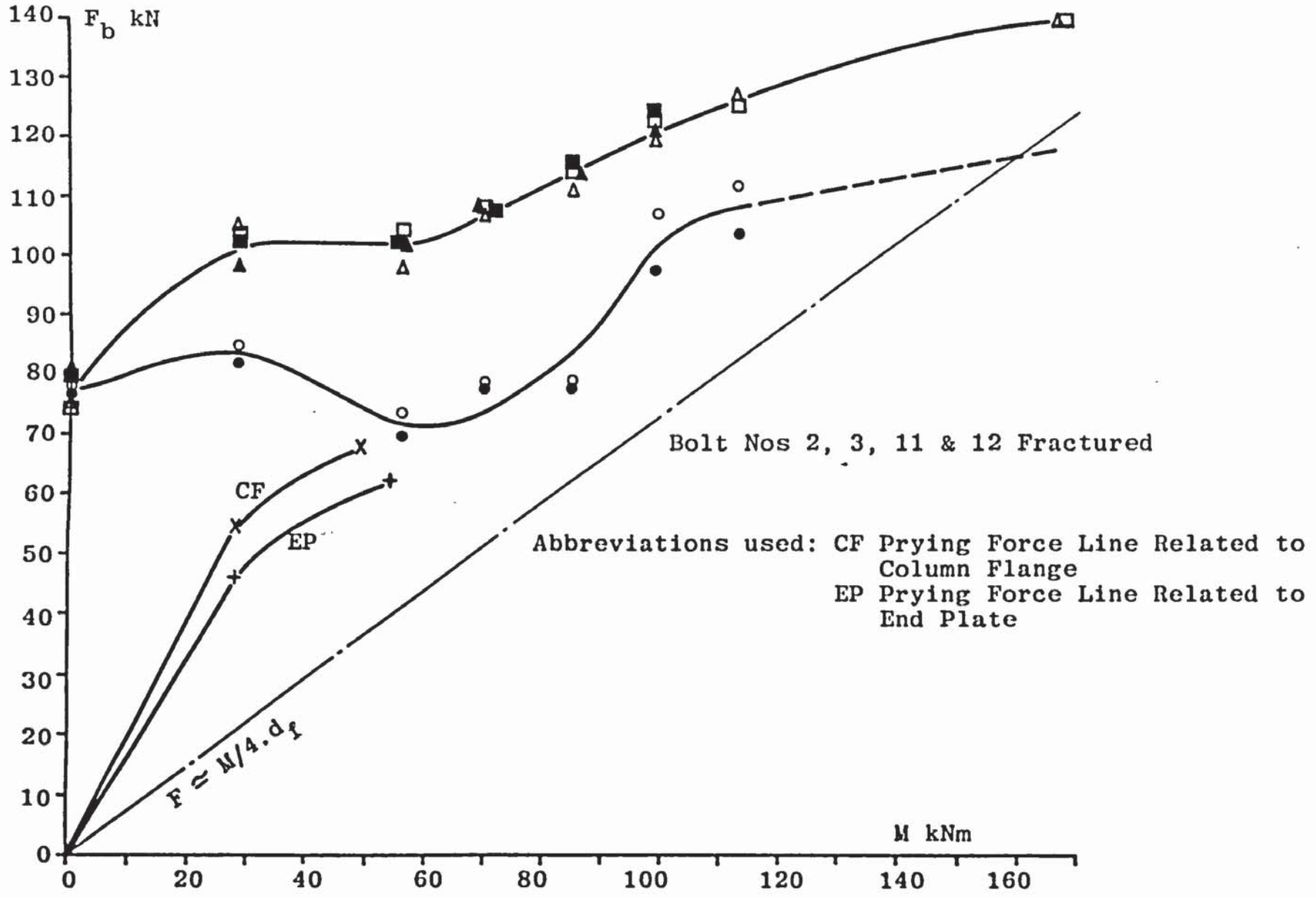

FIGURE A4.8 APPLIED MOMENT - BOLT FORCE RELATIONSHIP FOR TEST CS1-4

Abbreviations used: CF First Yield Weld Line Column Flange

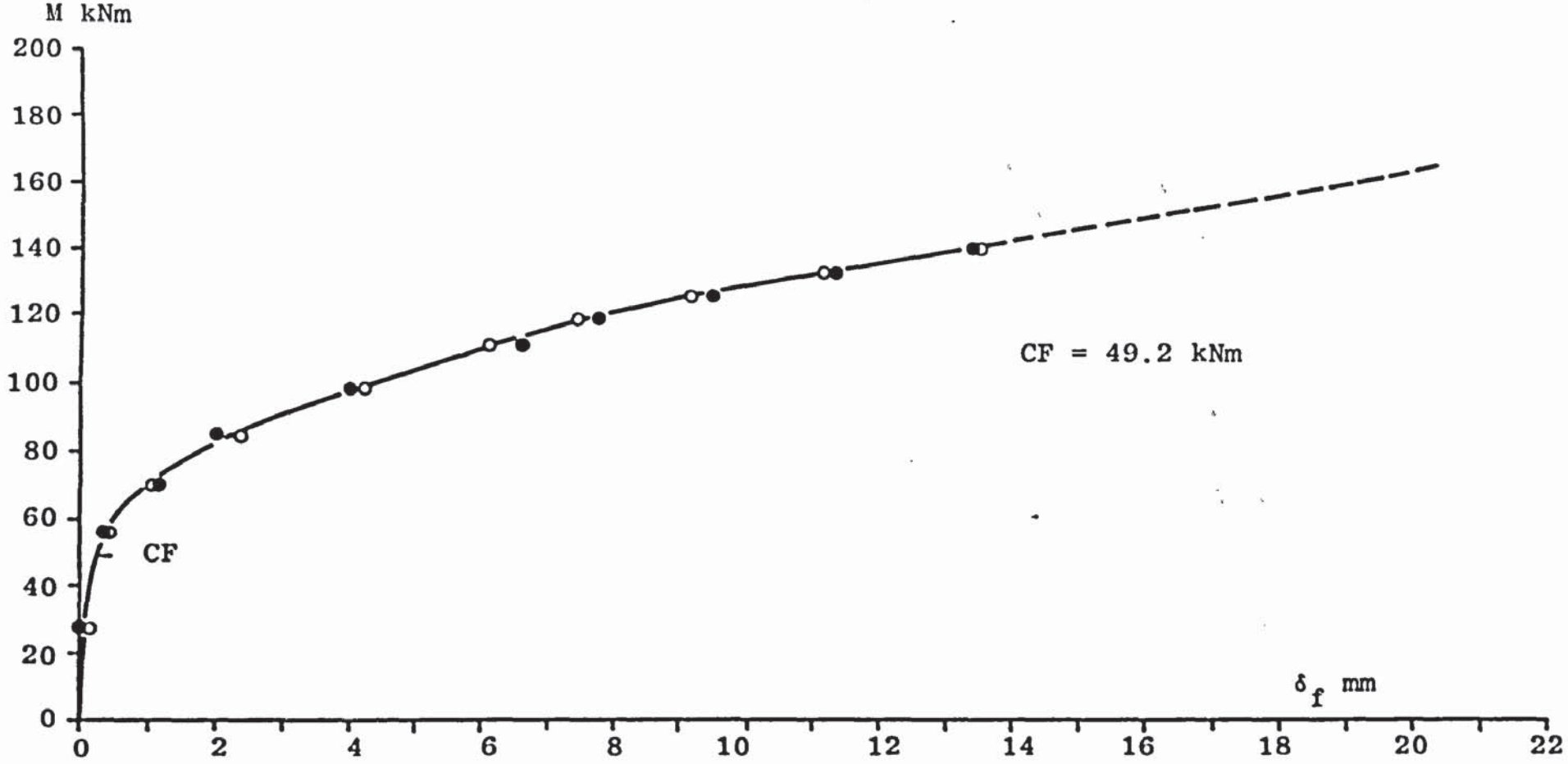

FIGURE A4.9 APPLIED MOMENT - COLUMN FLANGE DEFLECTION RELATIONSHIP FOR TEST CS1-4

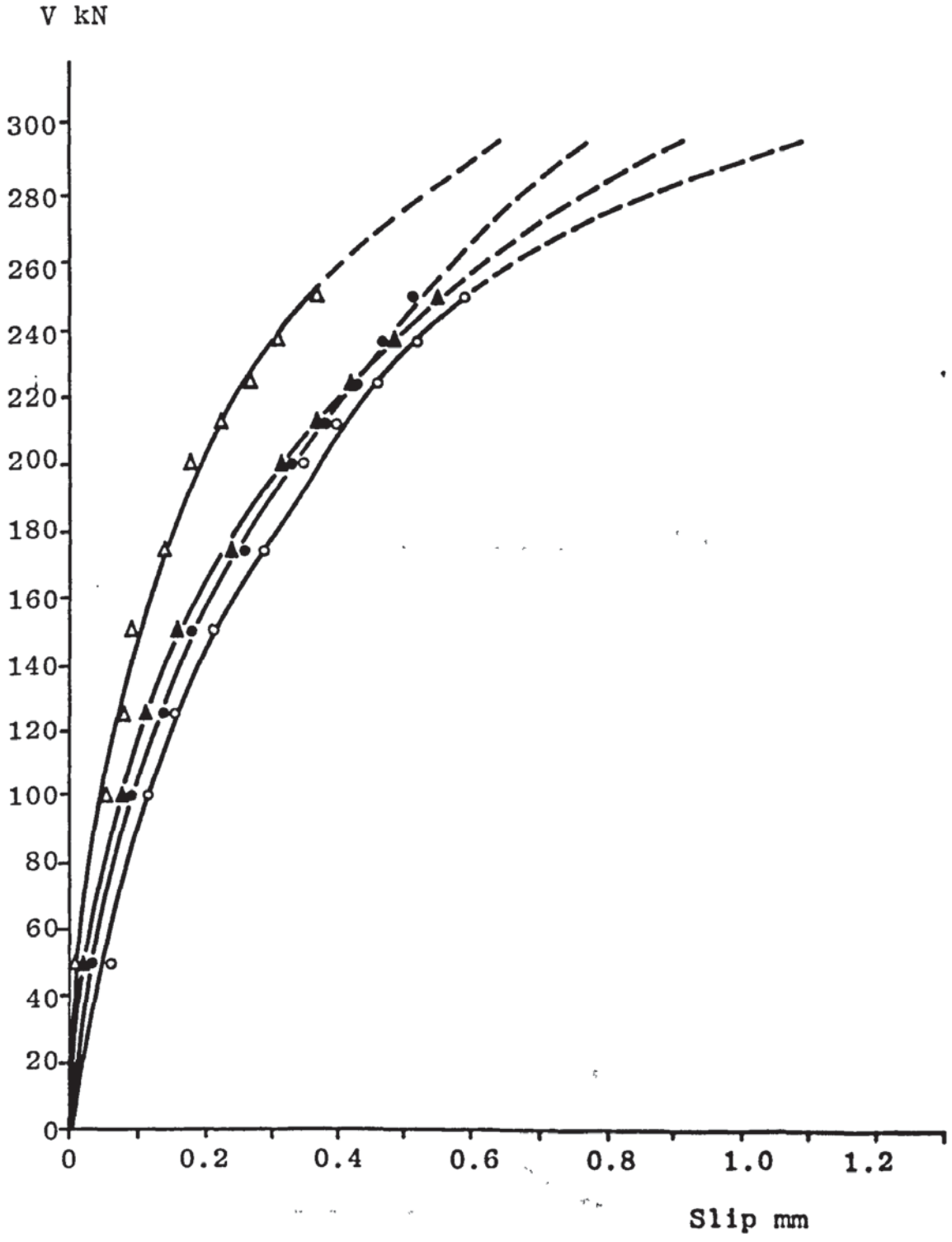

FIGURE A4.10 SHEAR FORCE - SLIP RELATIONSHIP FOR TEST CS1-4

Abbreviations used: EP, First Yield Weld Line End Plate; CF, First Yield Weld Line Column Flange

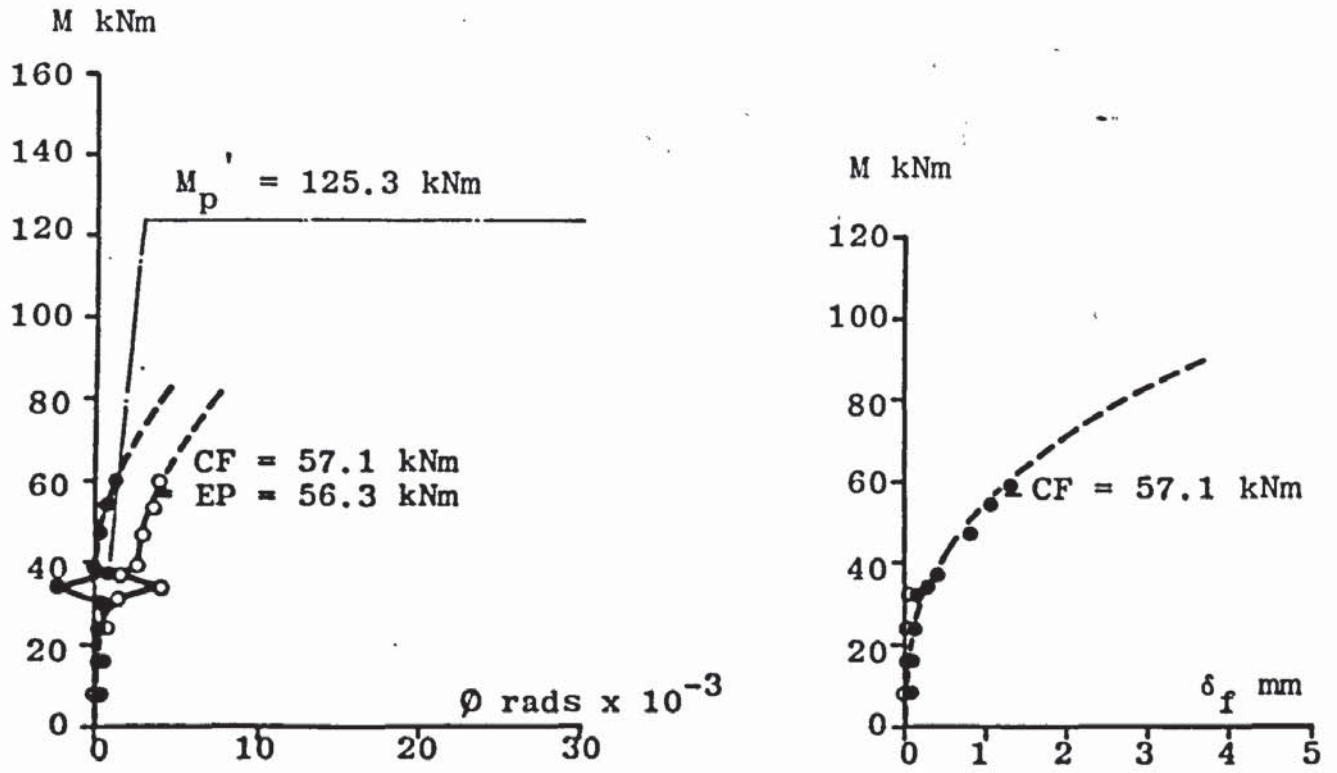

FIGURE A4.11 APPLIED MOMENT - ROTATION RELATIONSHIP AND APPLIED MOMENT - COLUMN FLANGE DEFLECTION RELATIONSHIP FOR TEST CS1-5

Abbreviations used: CF Prying Force Line Related to Column Flange
EP Prying Force Line Related to End Plate

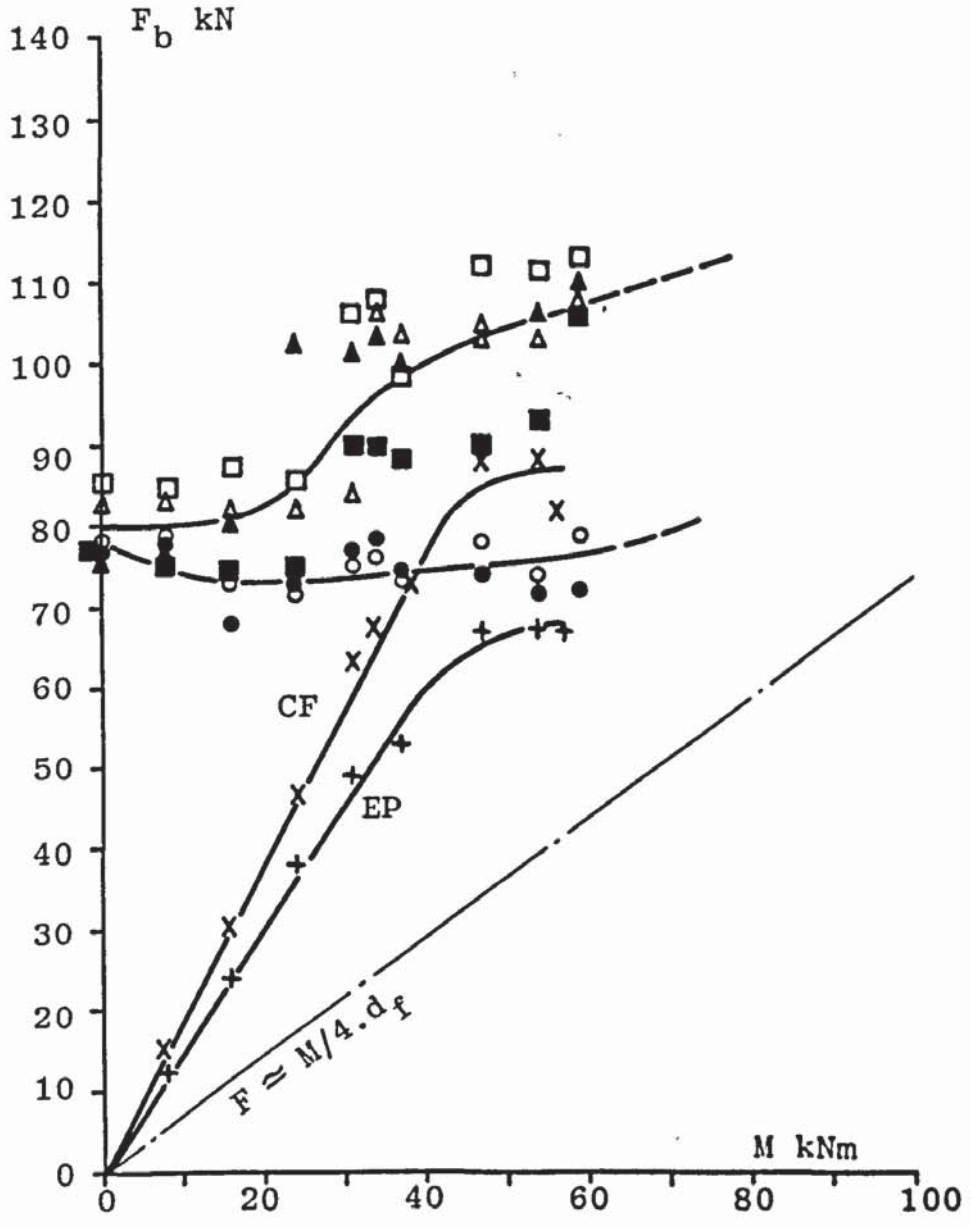

FIGURE A4.12 APPLIED MOMENT - BOLT FORCE RELATIONSHIP FOR TEST CS1-5

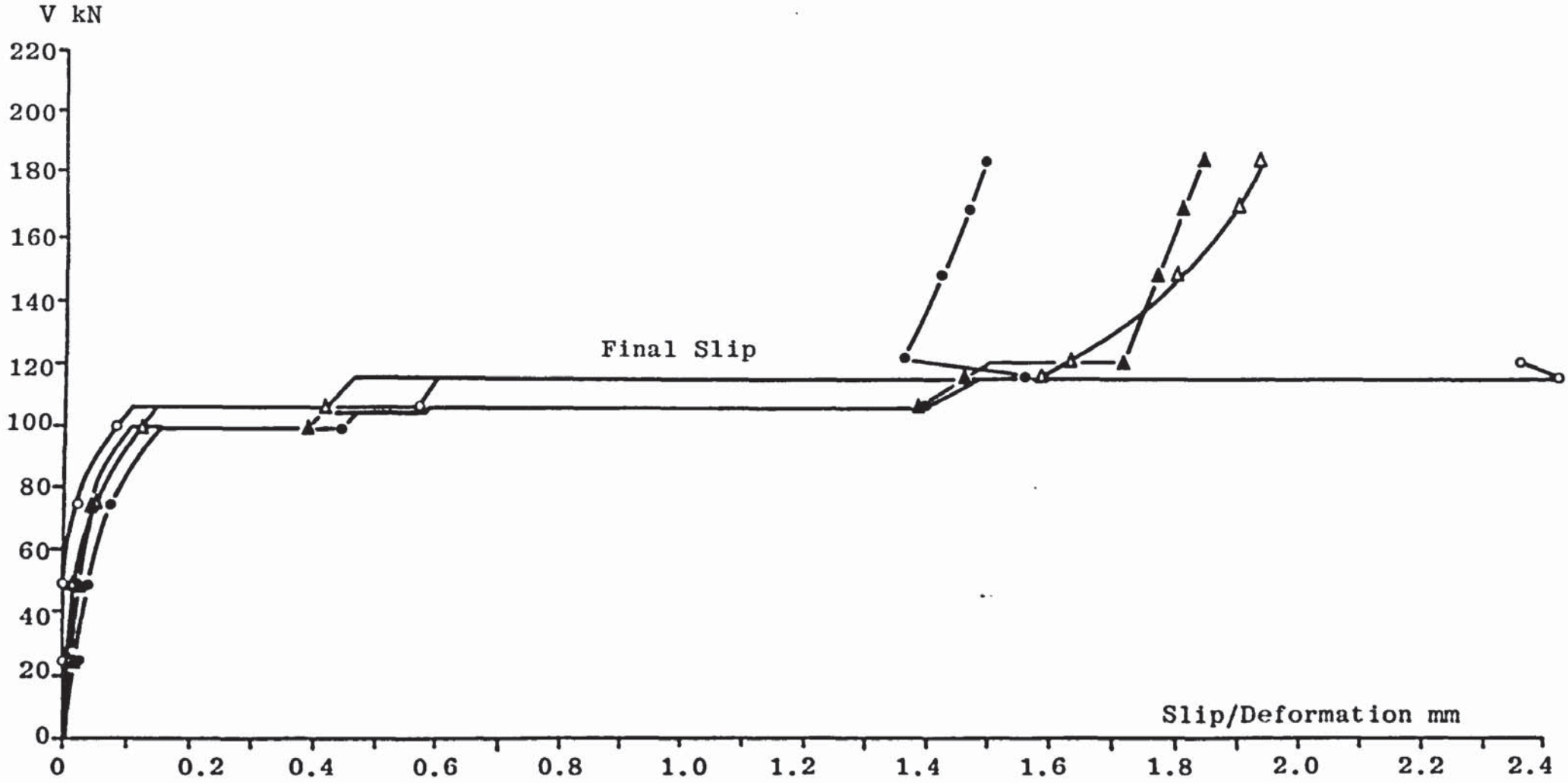

FIGURE A4.13 SHEAR FORCE - SLIP/DEFORMATION RELATIONSHIP FOR TEST CS1-5

Abbreviations used: EP, First Yield Weld Line End Plate; CF, First Yield Weld Line Column Flange; CFB, First Yield Bolt Line Column Flange

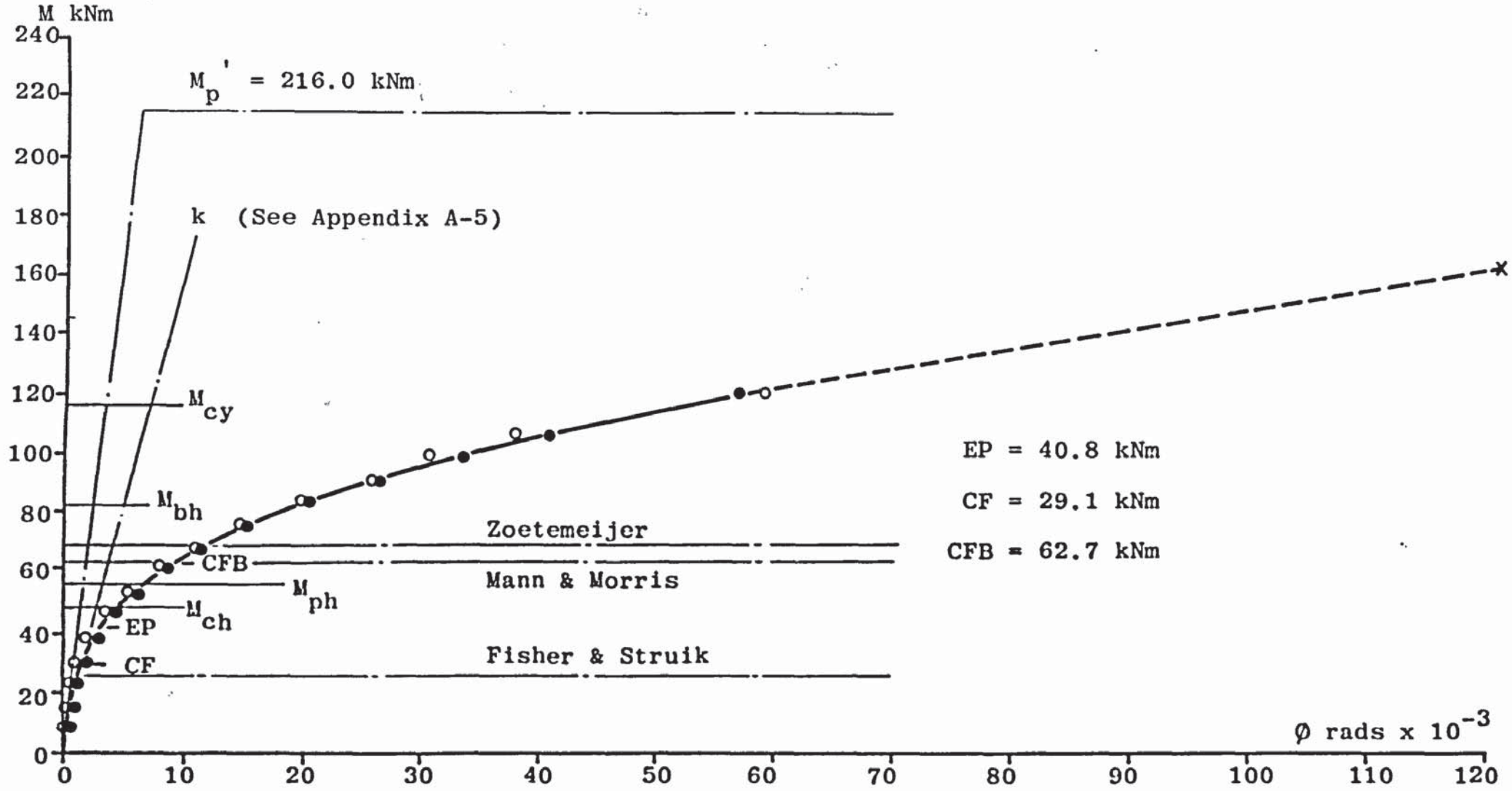

FIGURE A4.14 APPLIED MOMENT - ROTATION RELATIONSHIP FOR TEST CS2-1

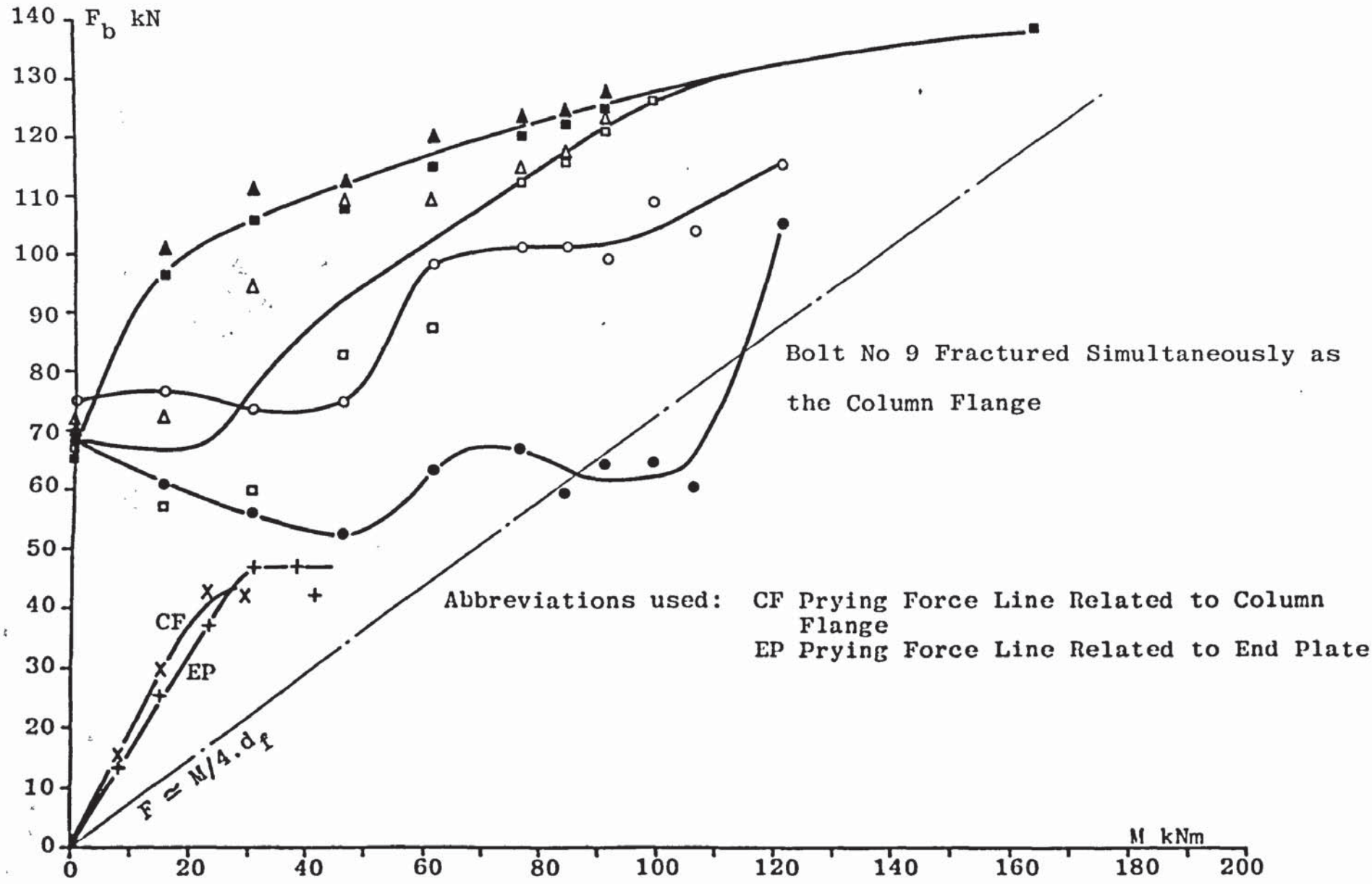

FIGURE A4.15 APPLIED MOMENT - BOLT FORCE RELATIONSHIP FOR TEST CS2-1

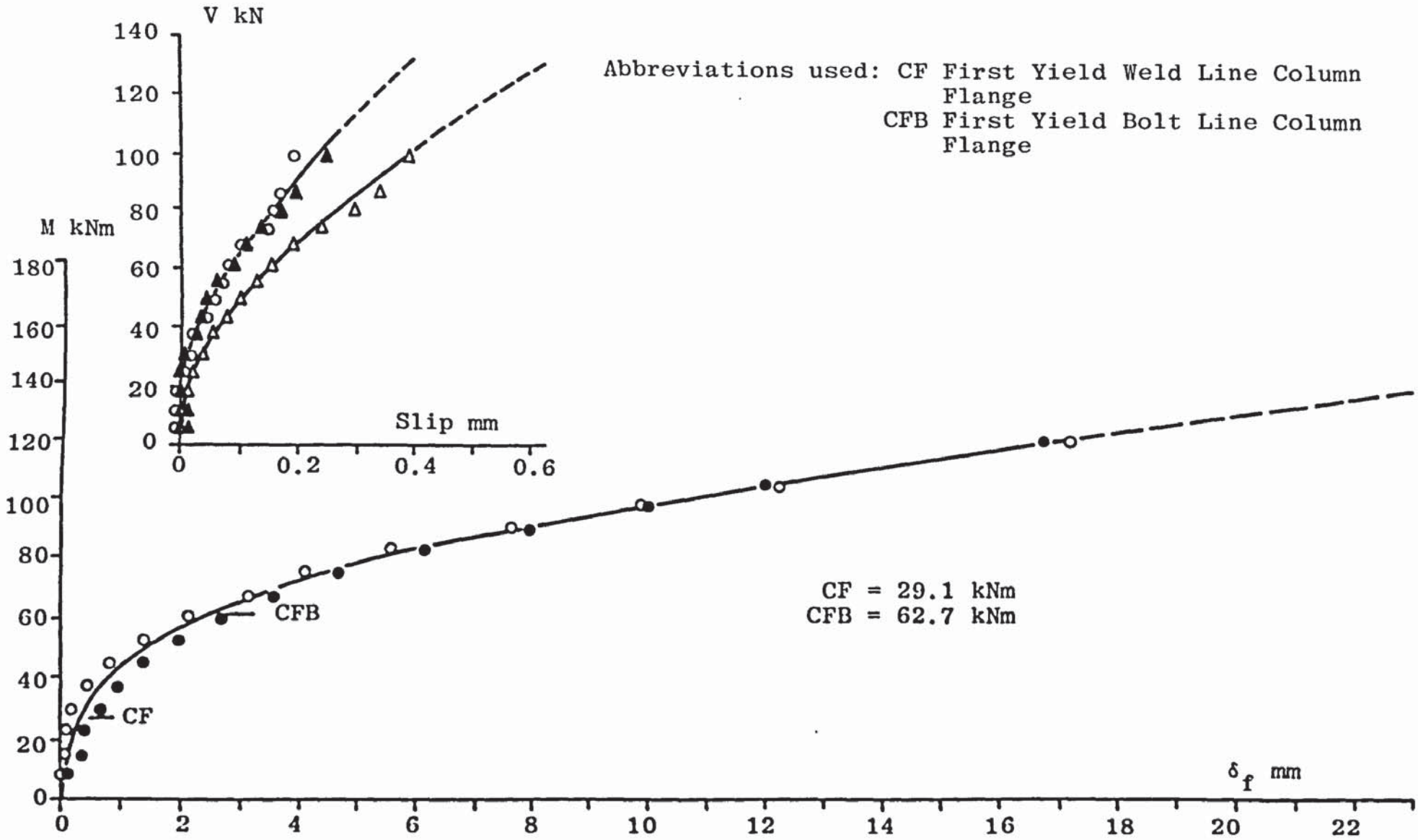

FIGURE A4.16 APPLIED MOMENT - COLUMN FLANGE DEFLECTION RELATIONSHIP AND SHEAR FORCE - SLIP RELATIONSHIP FOR TEST CS2-1

Abbreviations used: EP, First Yield Weld Line End Plate; CF, First Yield Weld Line Column Flange; CFB, First Yield Bolt Line Column Flange

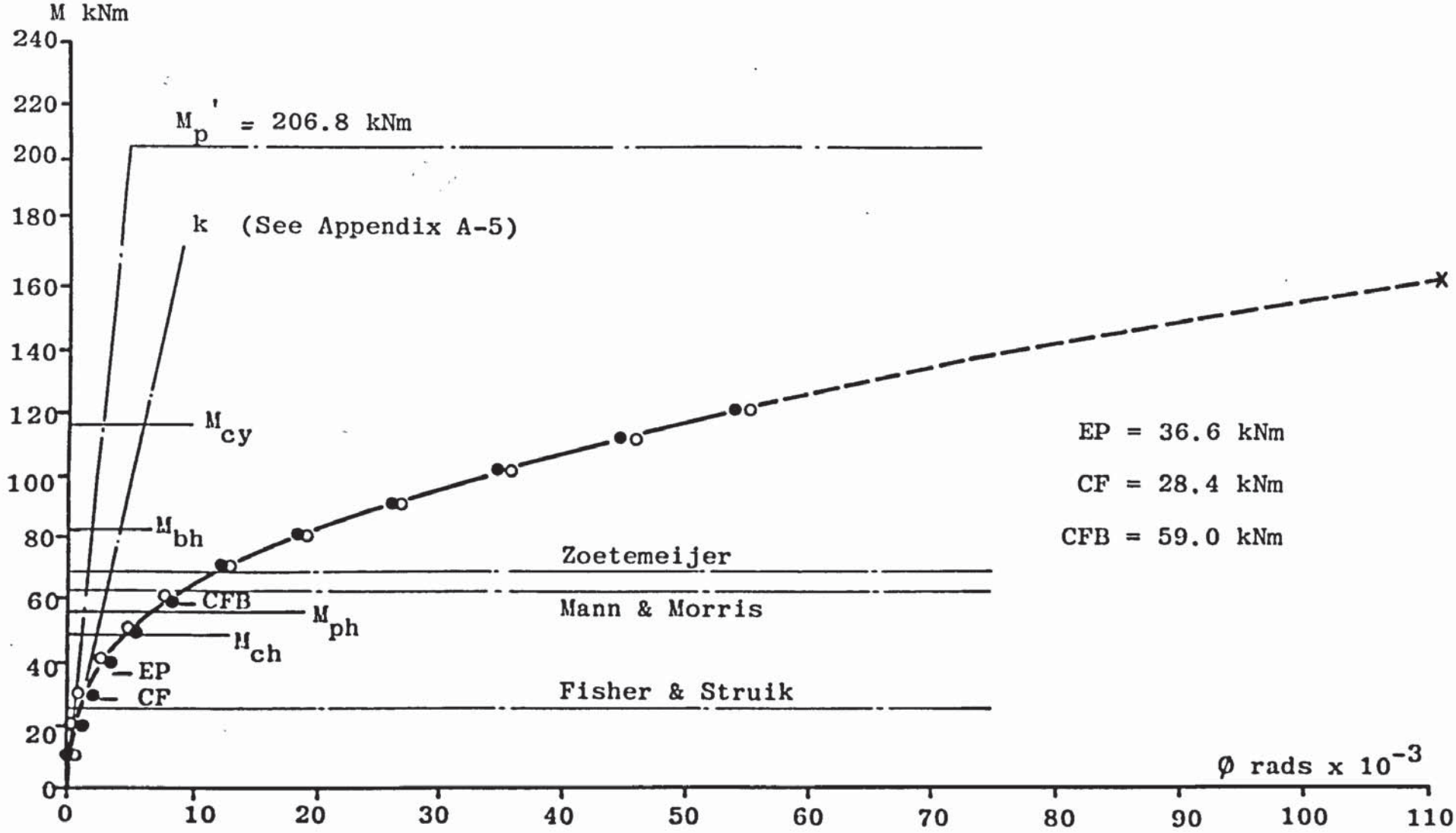

FIGURE A4.17 APPLIED MOMENT - ROTATION RELATIONSHIP FOR TEST CS2-3

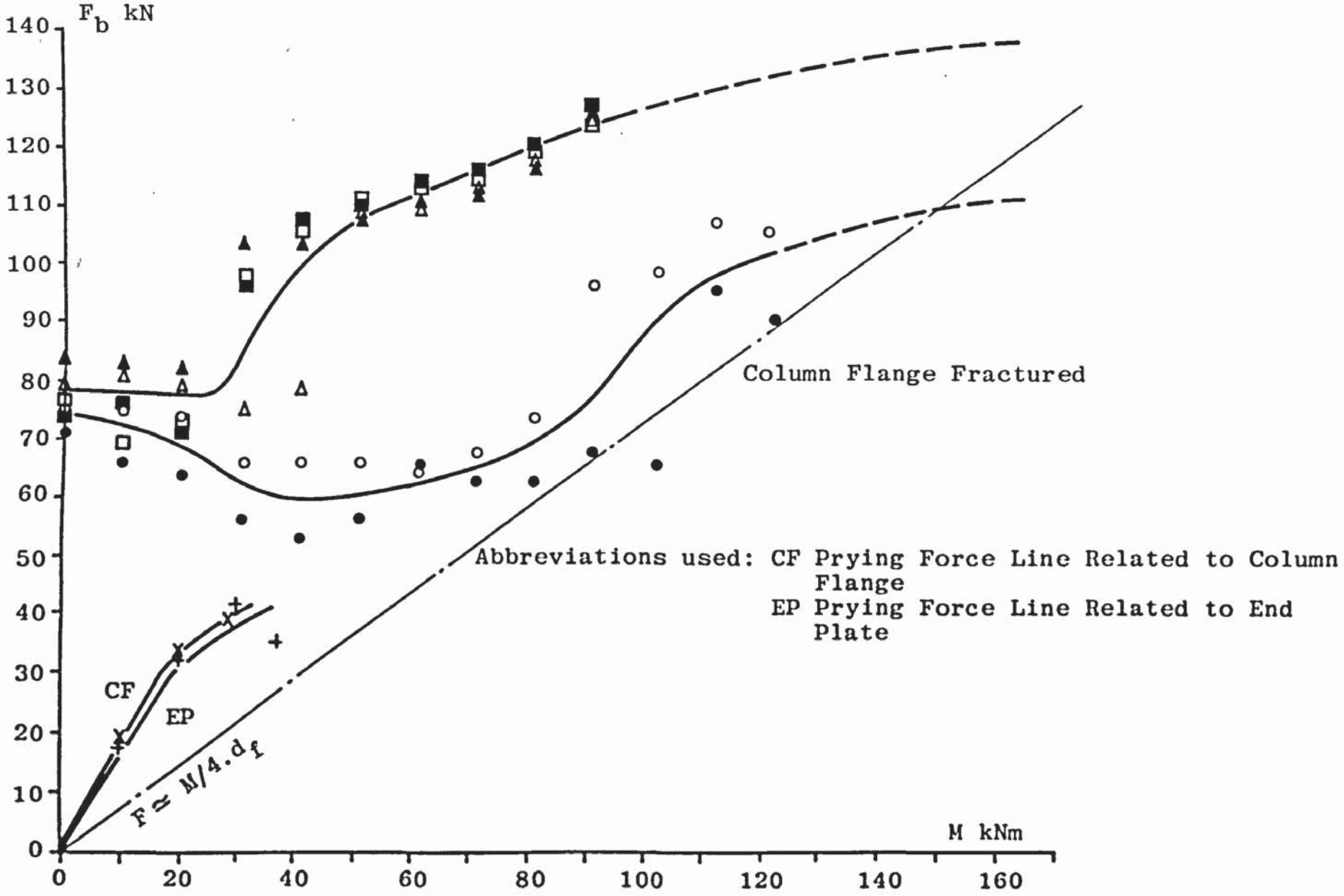

FIGURE A4.18 APPLIED MOMENT - BOLT FORCE RELATIONSHIP FOR TEST CS2-3

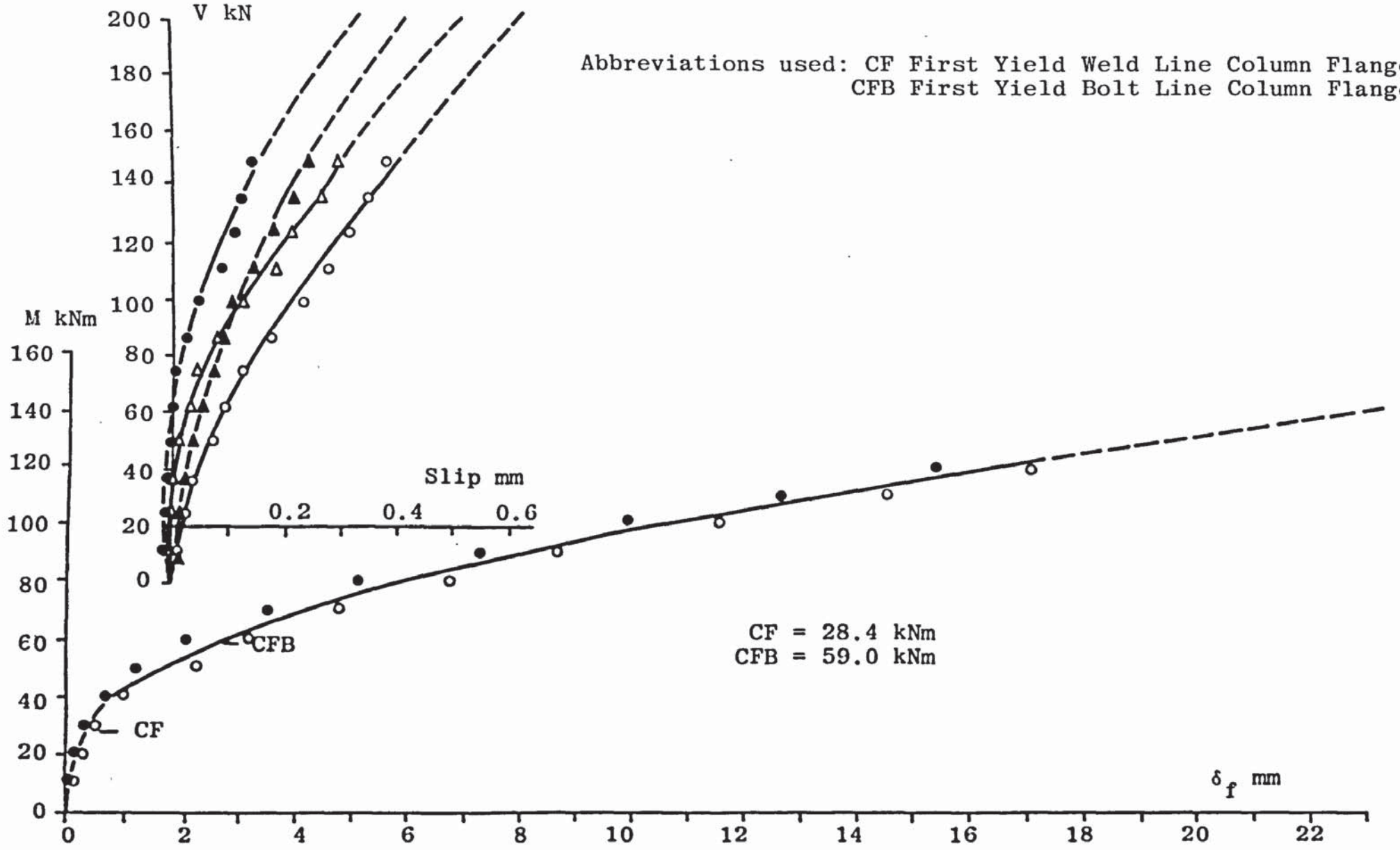

FIGURE A4.19 APPLIED MOMENT - COLUMN FLANGE DEFLECTION RELATIONSHIP AND SHEAR FORCE - SLIP RELATIONSHIP FOR TEST CS2-3

Abbreviations used: EP, First Yield Weld Line End Plate; CF, First Yield Weld Line Column Flange; CFB, First Yield Bolt Line Column Flange

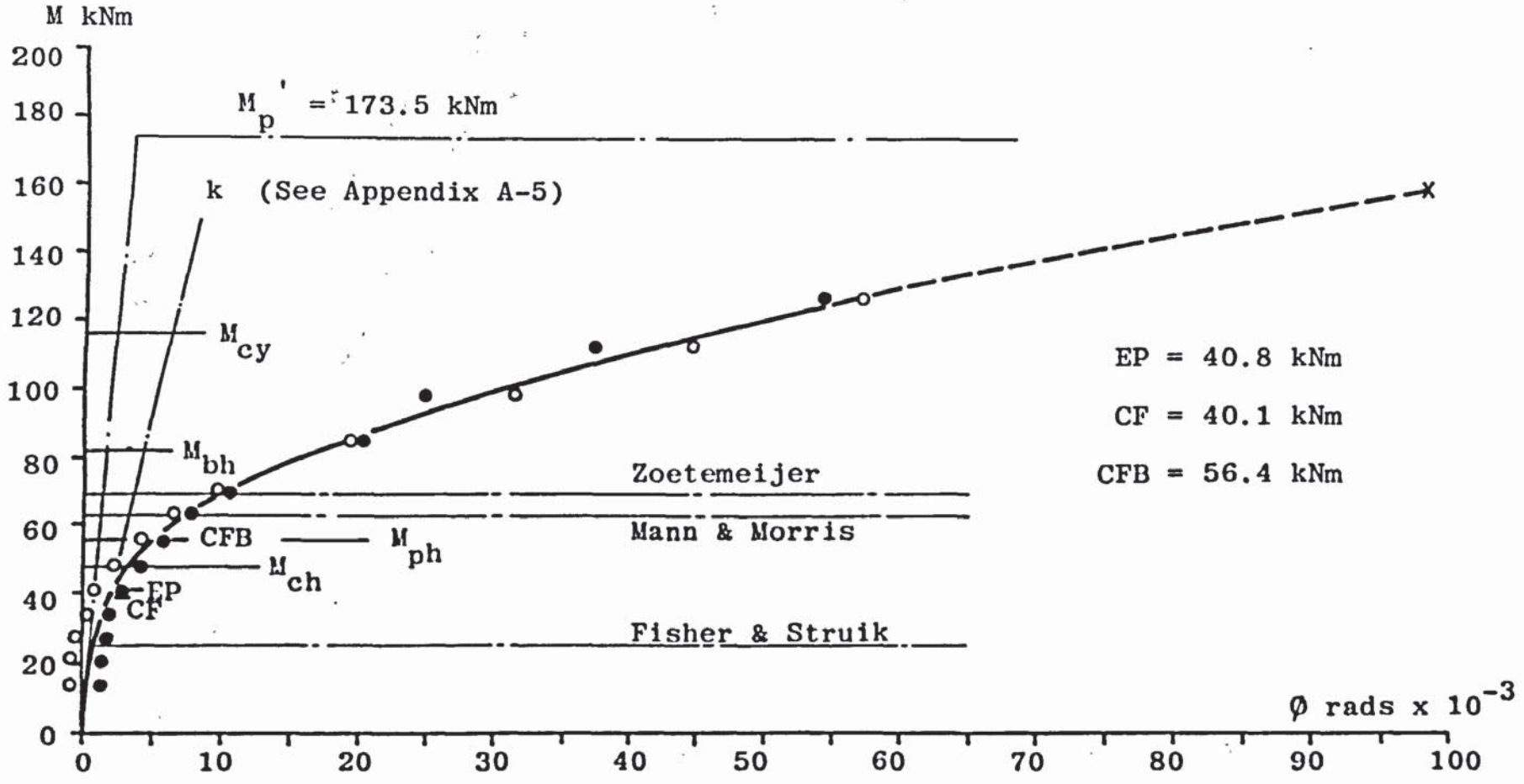

FIGURE A4.20 APPLIED MOMENT - ROTATION RELATIONSHIP FOR TEST CS2-4

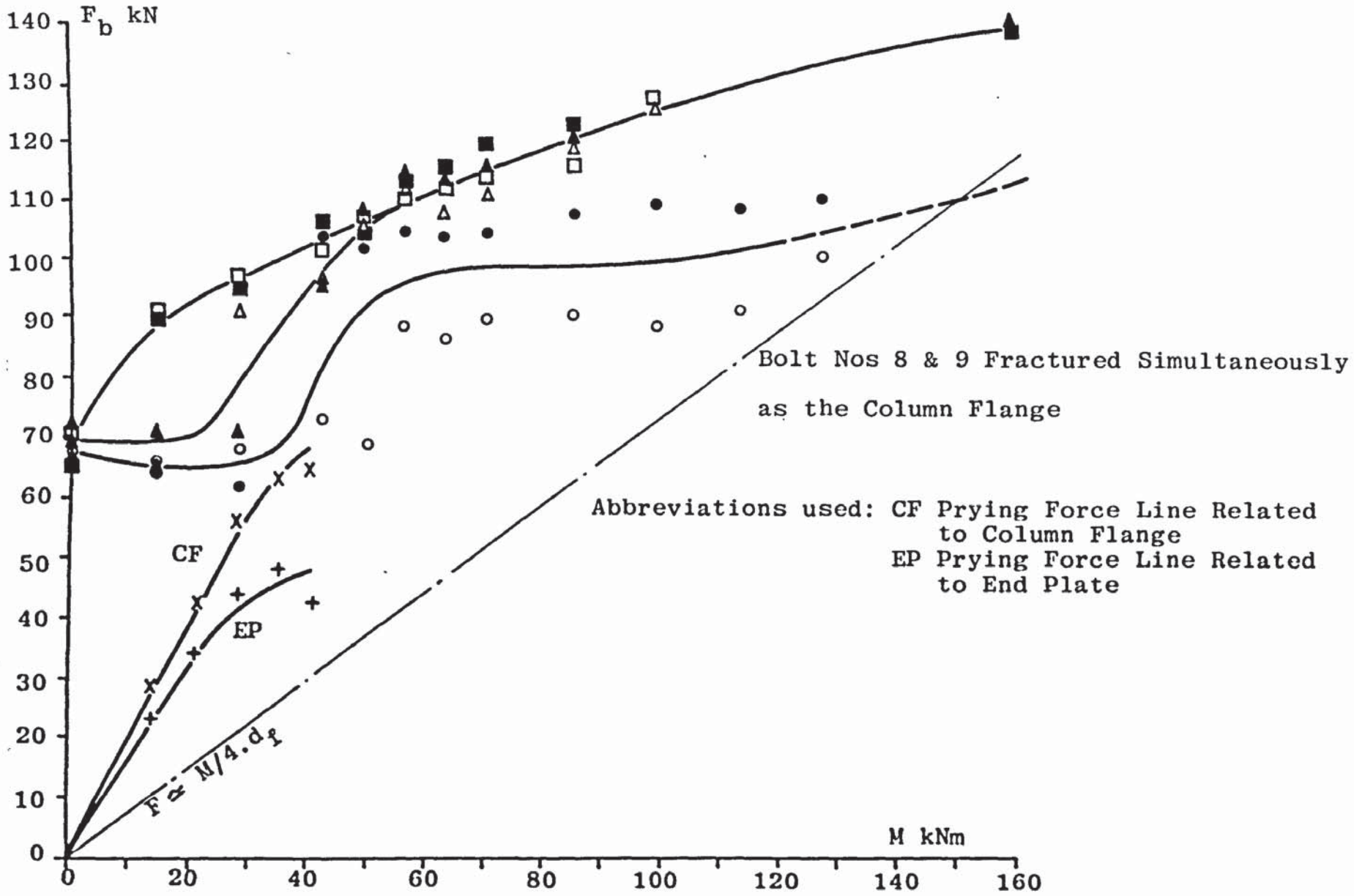

FIGURE A4.21 APPLIED MOMENT - BOLT FORCE RELATIONSHIP FOR TEST CS2-4

Abbreviations used: CF First Yield Weld Line Column Flange
CFB First Yield Bolt Line Column Flange

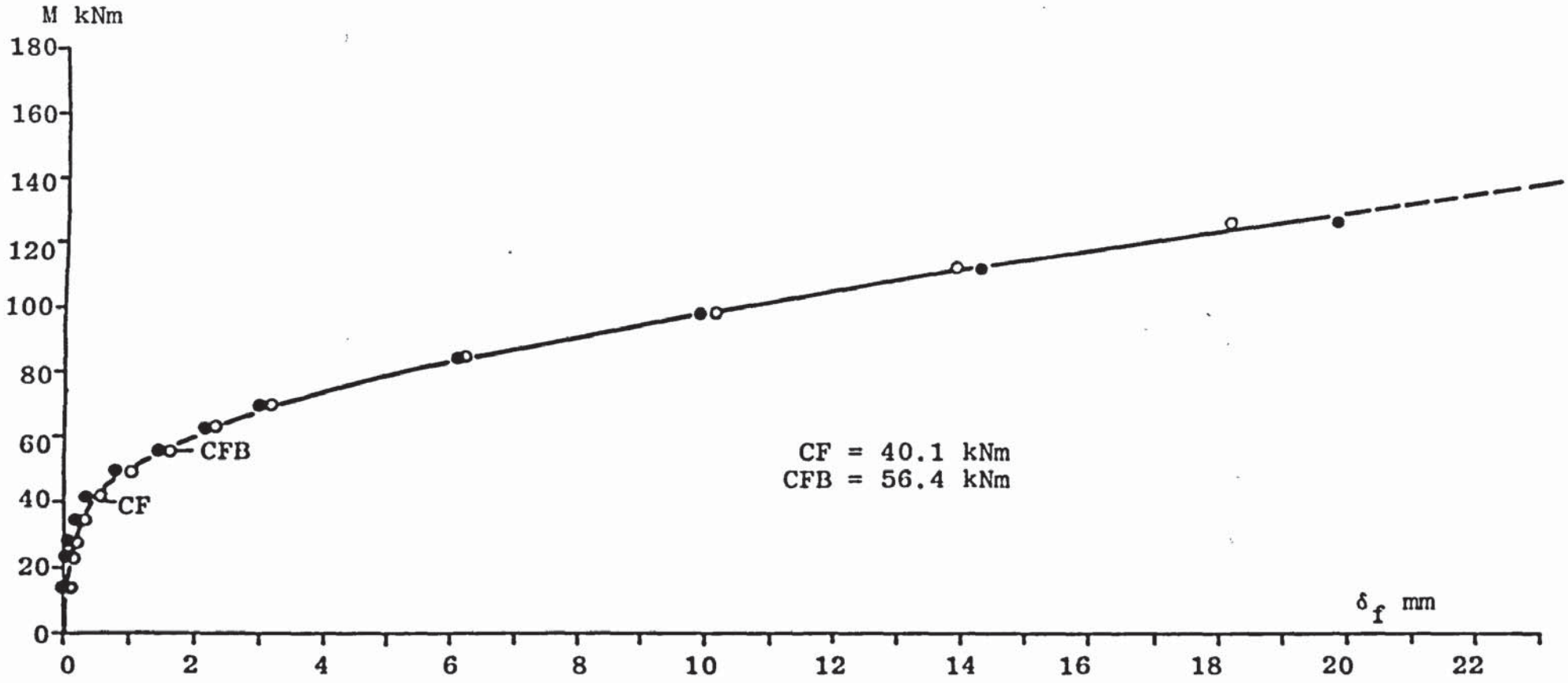

FIGURE A4.22 APPLIED MOMENT - COLUMN FLANGE DEFLECTION RELATIONSHIP FOR TEST CS2-4

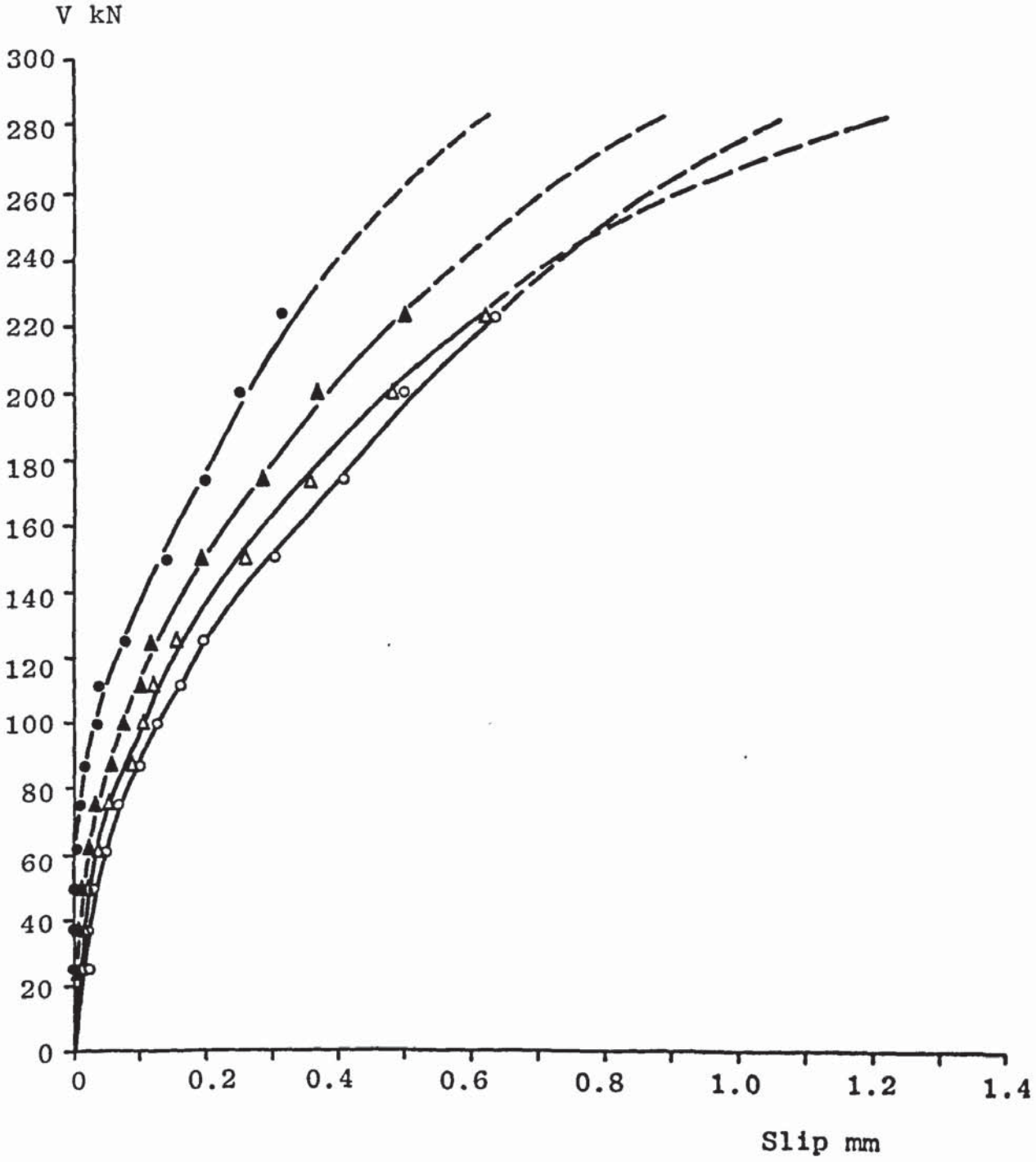

FIGURE A4.23 SHEAR FORCE - SLIP RELATIONSHIP FOR TEST CS2-4

Abbreviations used: EP, First Yield Weld Line End Plate
CF, First Yield Weld Line Column Flange
CFB, First Yield Bolt Line Column Flange

EP = 34.8 kNm, CF = 34.1 kNm, CFB = 60.4 kNm

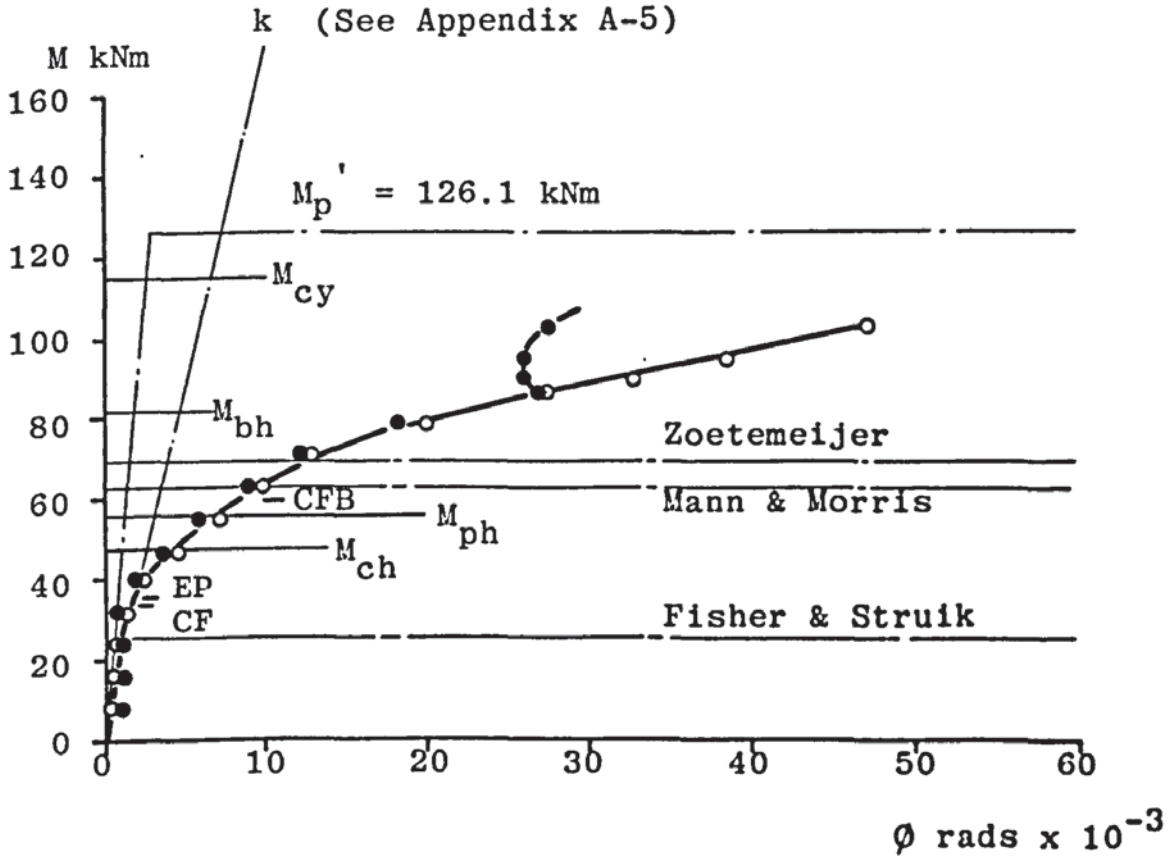

FIGURE A4.24 APPLIED MOMENT - ROTATION RELATIONSHIP FOR TEST CS2-5

Abbreviations used: CF Prying Force Line Related to Column Flange
EP Prying Force Line Related to End Plate

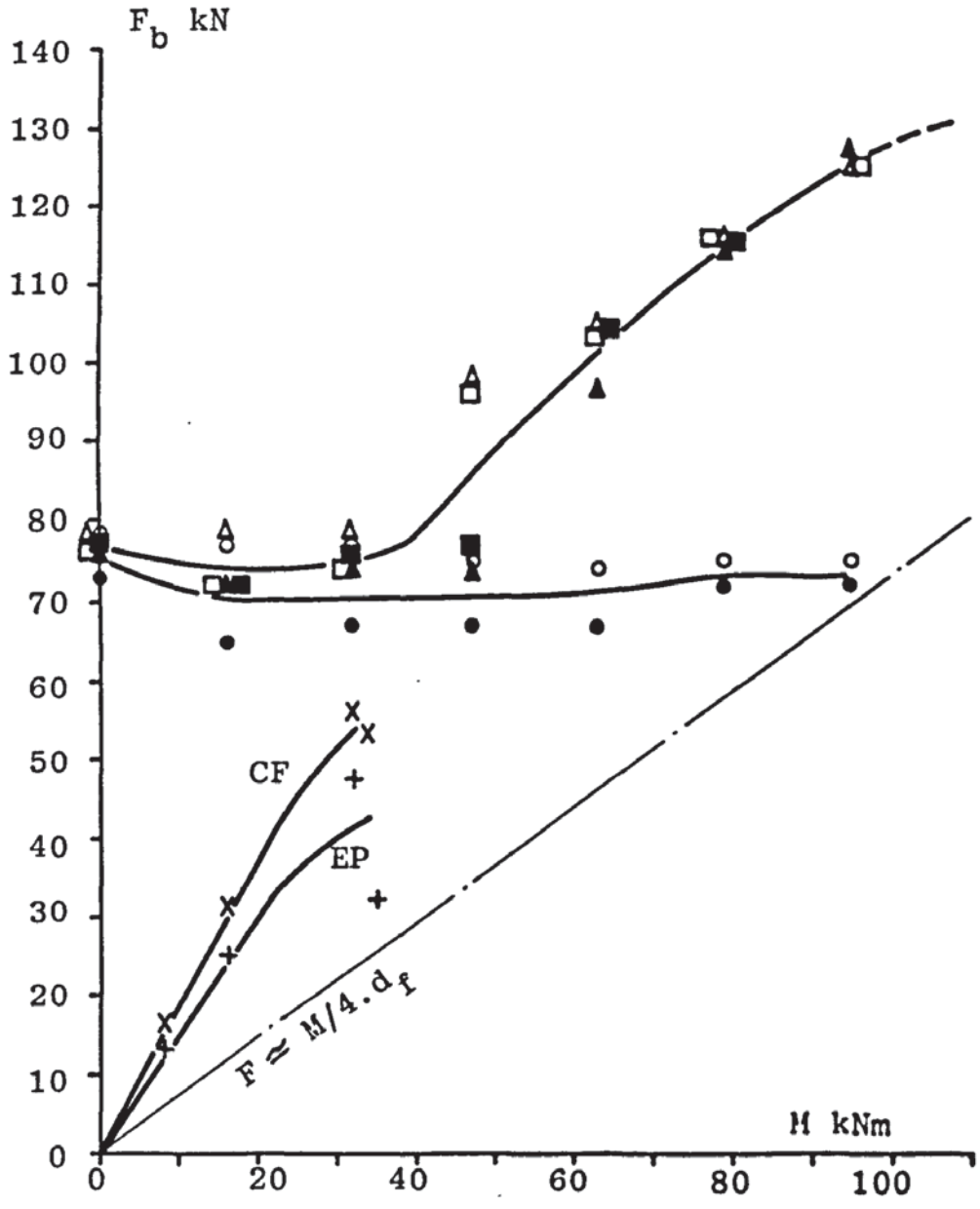

FIGURE A4.25 APPLIED MOMENT - BOLT FORCE RELATIONSHIP FOR TEST CS2-5

Abbreviations used: CF First Yield Weld Line Column Flange
CFB First Yield Bolt Line Column Flange

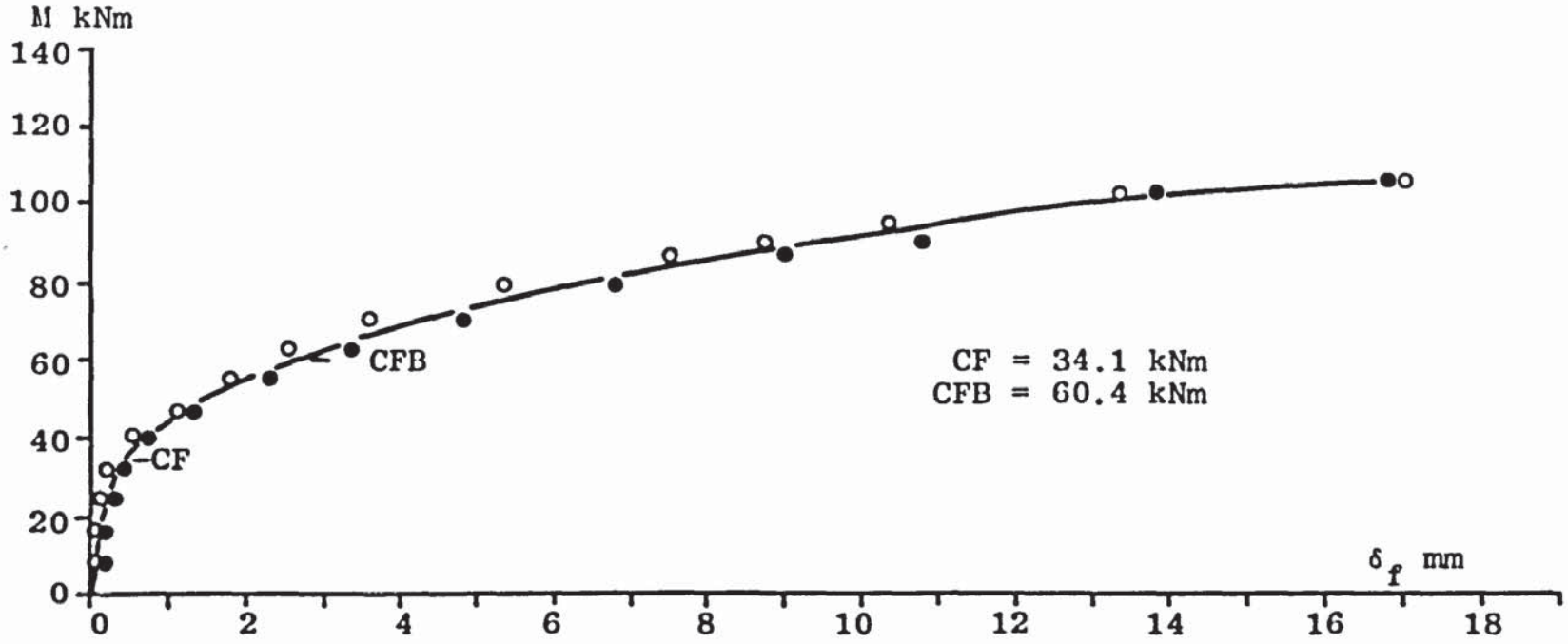

FIGURE A4.26 APPLIED MOMENT - COLUMN FLANGE DEFLECTION RELATIONSHIP FOR TEST CS2-5

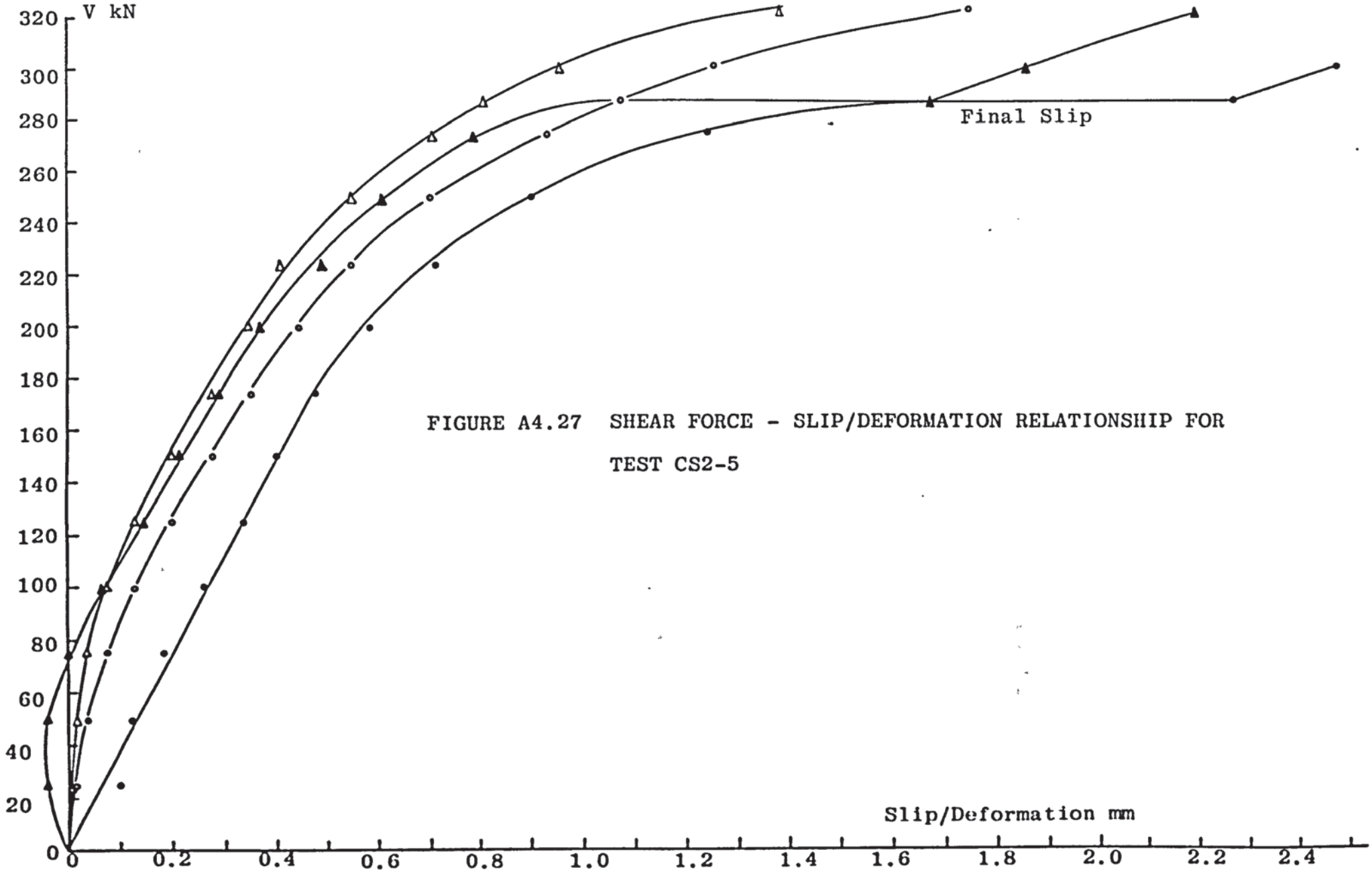

FIGURE A4.27 SHEAR FORCE - SLIP/DEFORMATION RELATIONSHIP FOR TEST CS2-5

Abbreviations used: EP, First Yield Weld Line End Plate
CF, First Yield Weld Line Column Flange

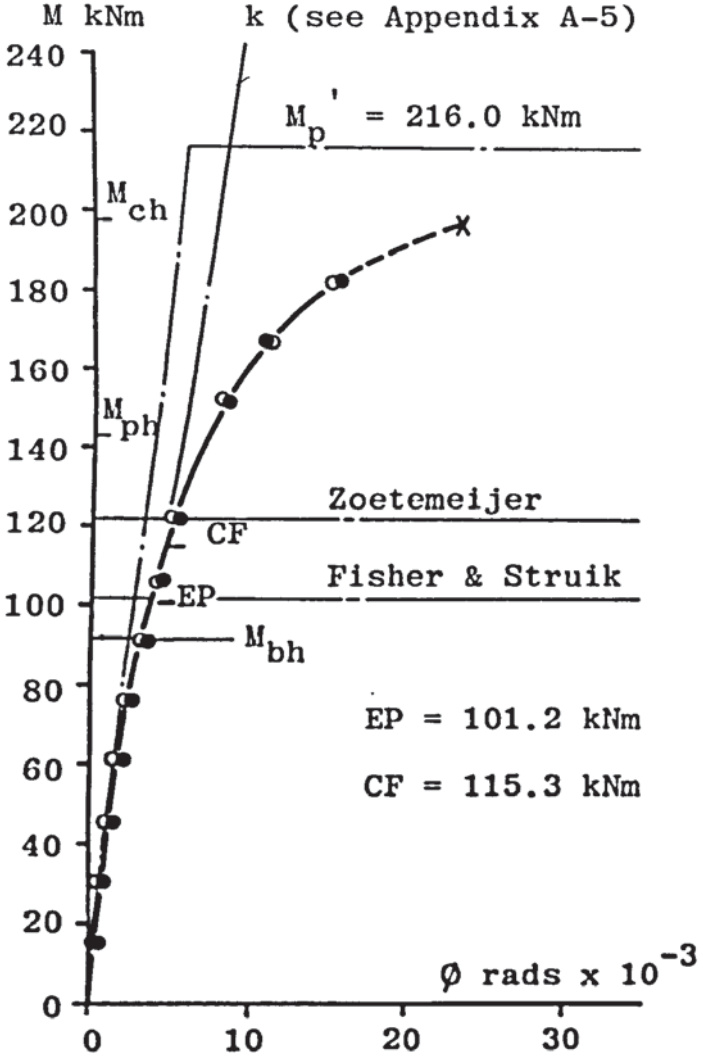

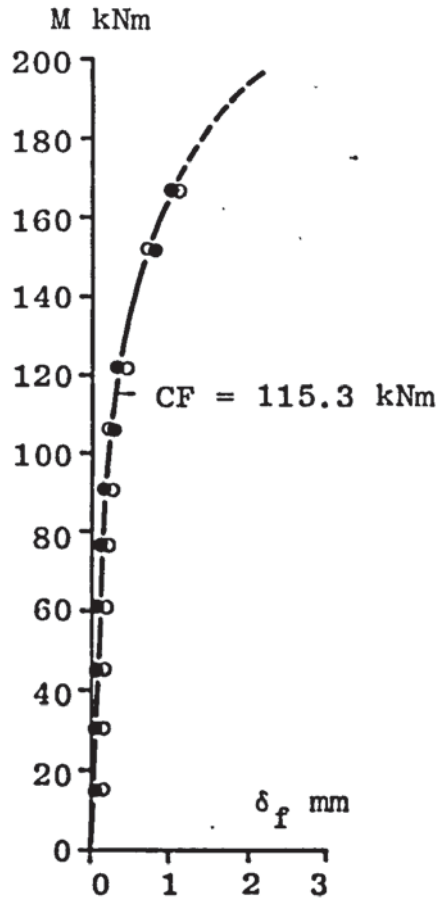

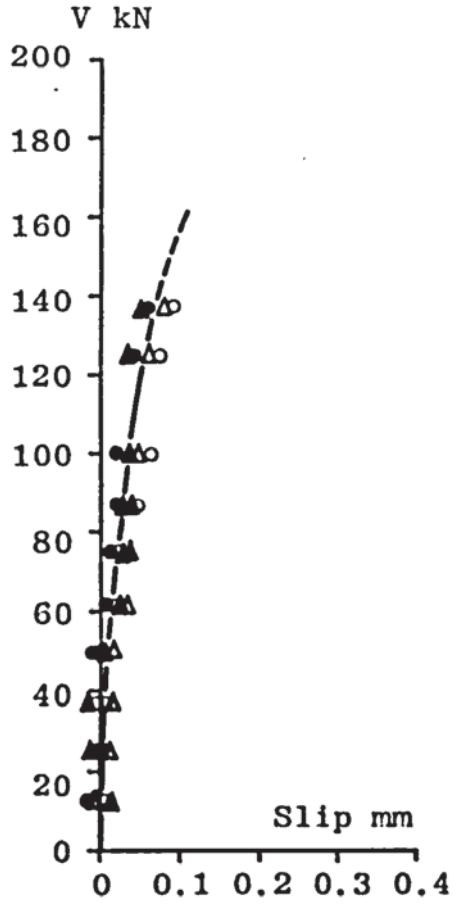

TABLE A4.28 APPLIED MOMENT - ROTATION RELATIONSHIP, APPLIED MOMENT - COLUMN FLANGE DEFLECTION RELATIONSHIP AND SHEAR FORCE - SLIP RELATIONSHIP FOR TEST CS3-1

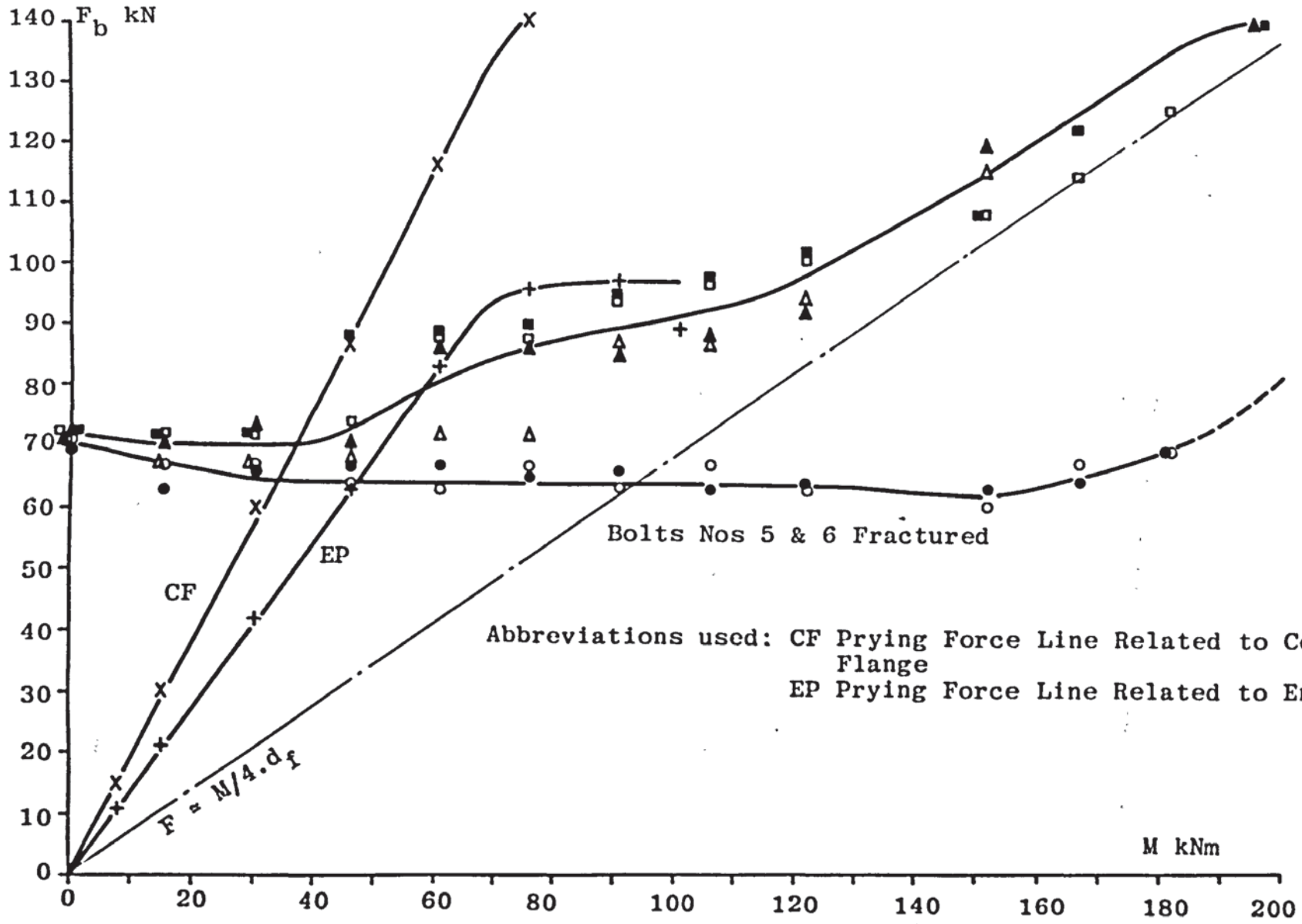

FIGURE A4.29 APPLIED MOMENT - BOLT FORCE RELATIONSHIP FOR TEST CS3-1

Abbreviations used: EP, First Yield Weld Line End Plate; CF, First Yield Weld Line Column Flange (see Appendix A-5)

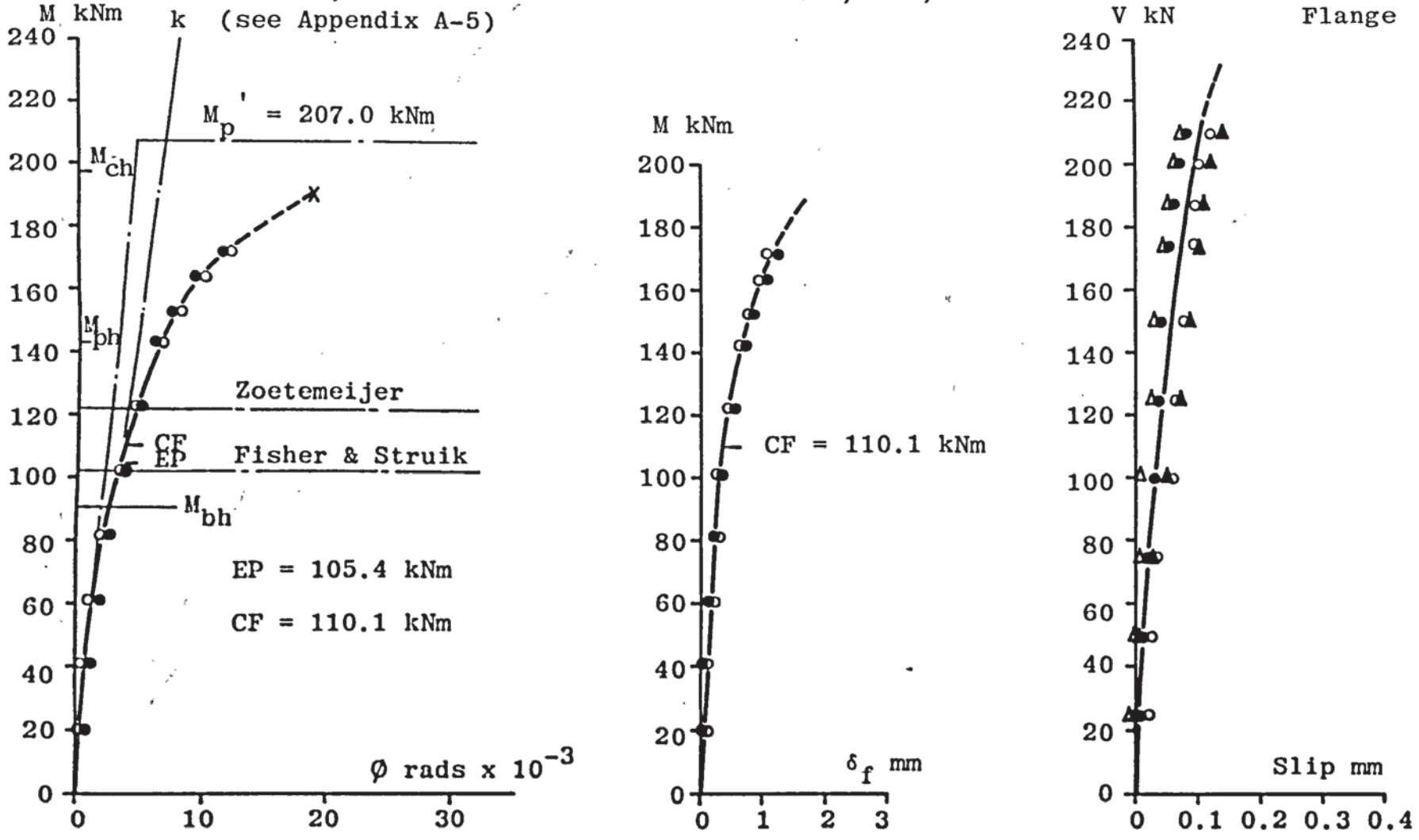

FIGURE A4.30 APPLIED MOMENT - ROTATION RELATIONSHIP, APPLIED MOMENT - COLUMN FLANGE DEFLECTION RELATIONSHIP AND SHEAR FORCE - SLIP RELATIONSHIP FOR TEST CS3-3

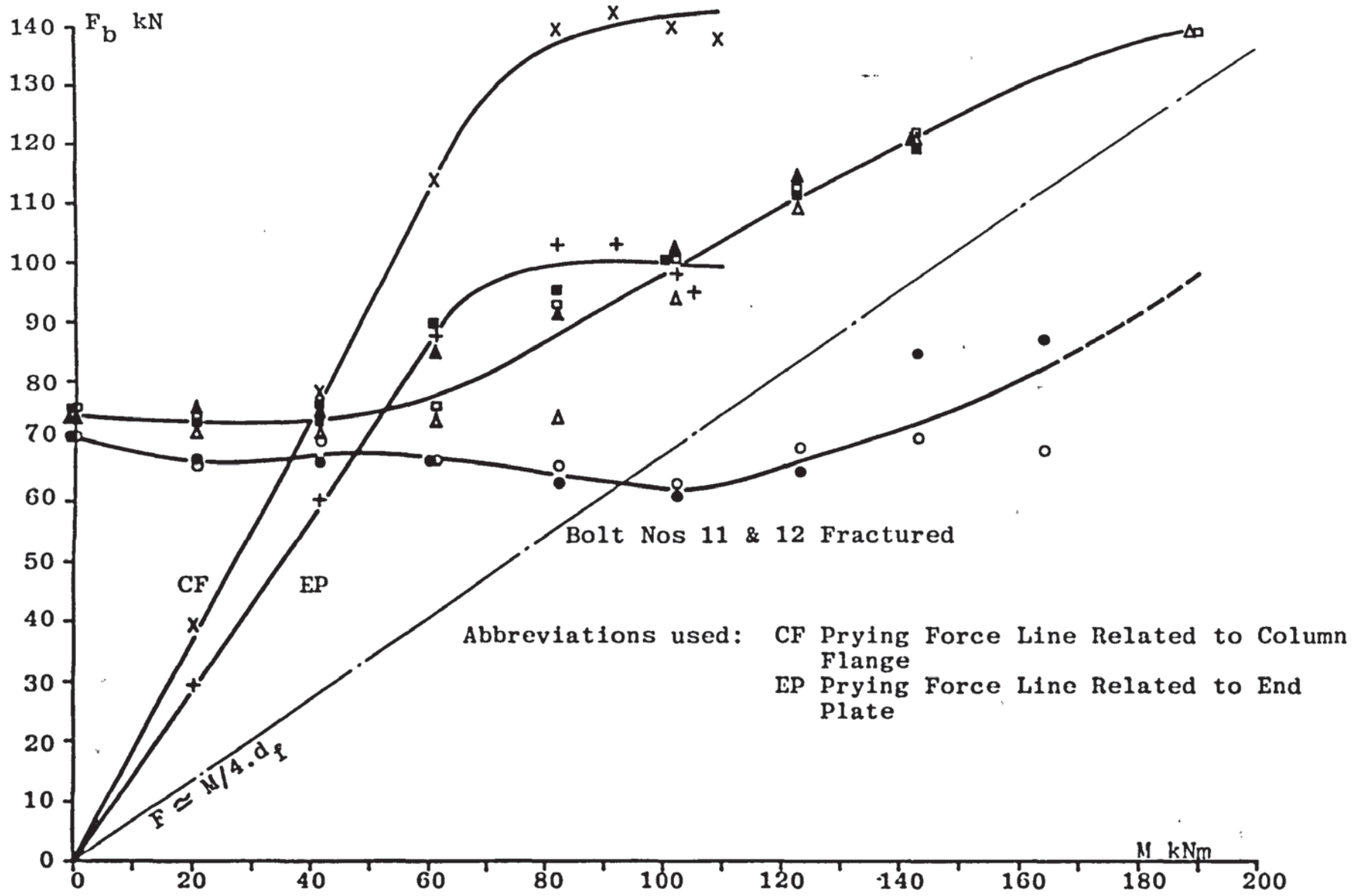

FIGURE A4.31 APPLIED MOMENT - BOLT FORCE RELATIONSHIP FOR TEST CS3-3

Abbreviations used: EP, First Yield Weld Line End Plate; CF, First Yield Weld Line Column Flange

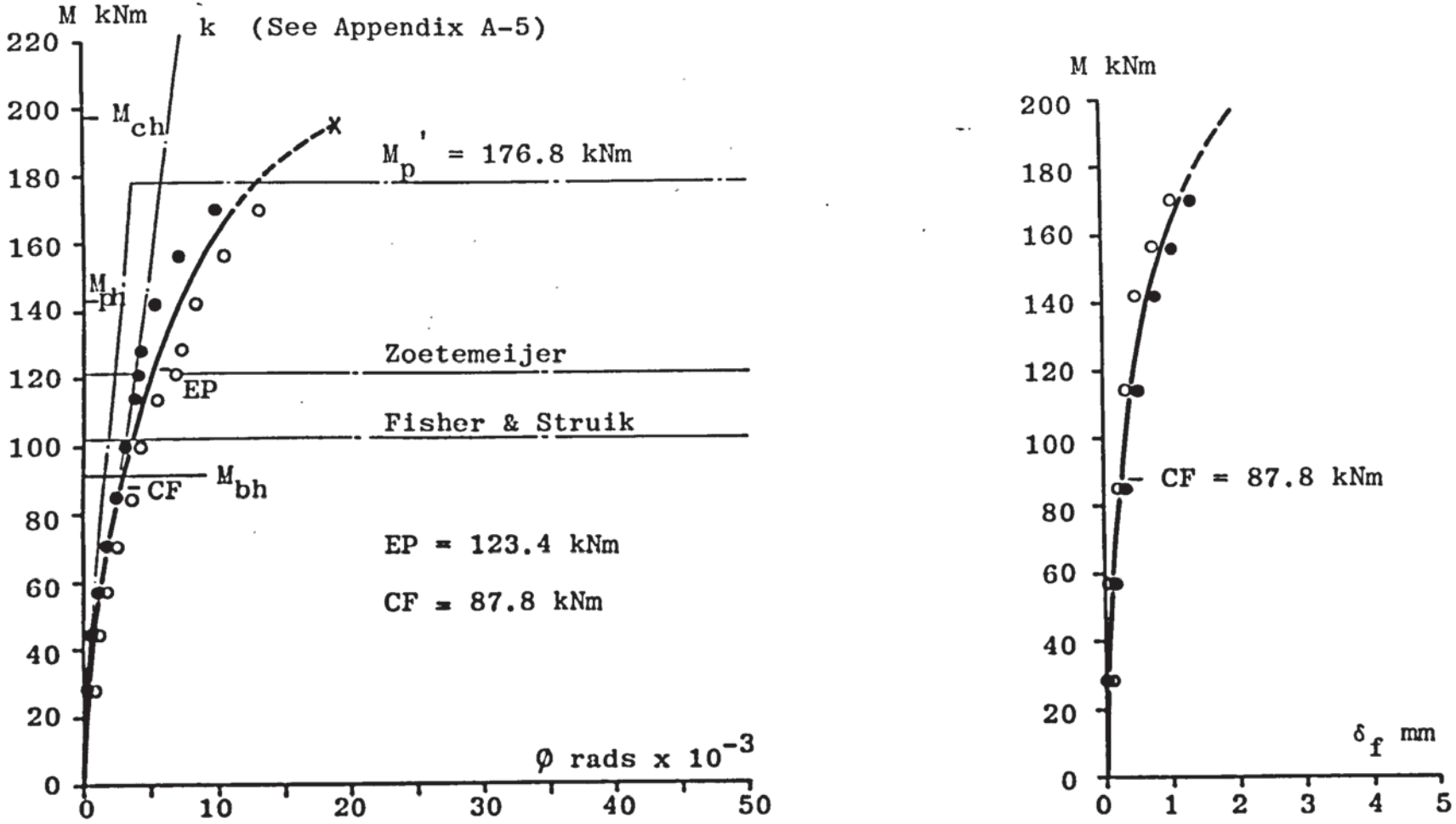

FIGURE A4.32 APPLIED MOMENT - ROTATION RELATIONSHIP AND APPLIED MOMENT - COLUMN FLANGE DEFLECTION RELATIONSHIP FOR TEST CS3-4

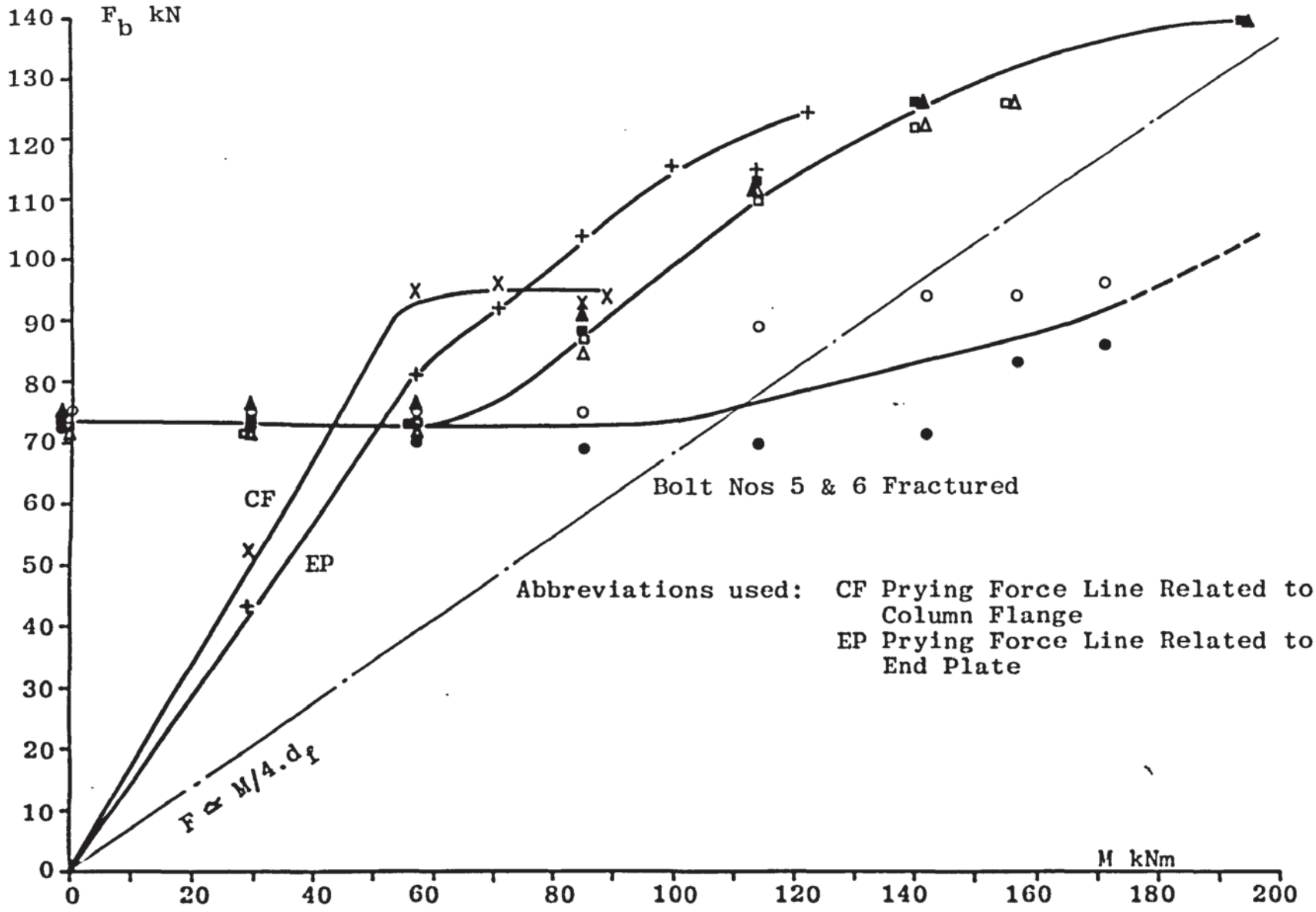

FIGURE A4.33 APPLIED MOMENT - BOLT FORCE RELATIONSHIP FOR TEST CS3-4

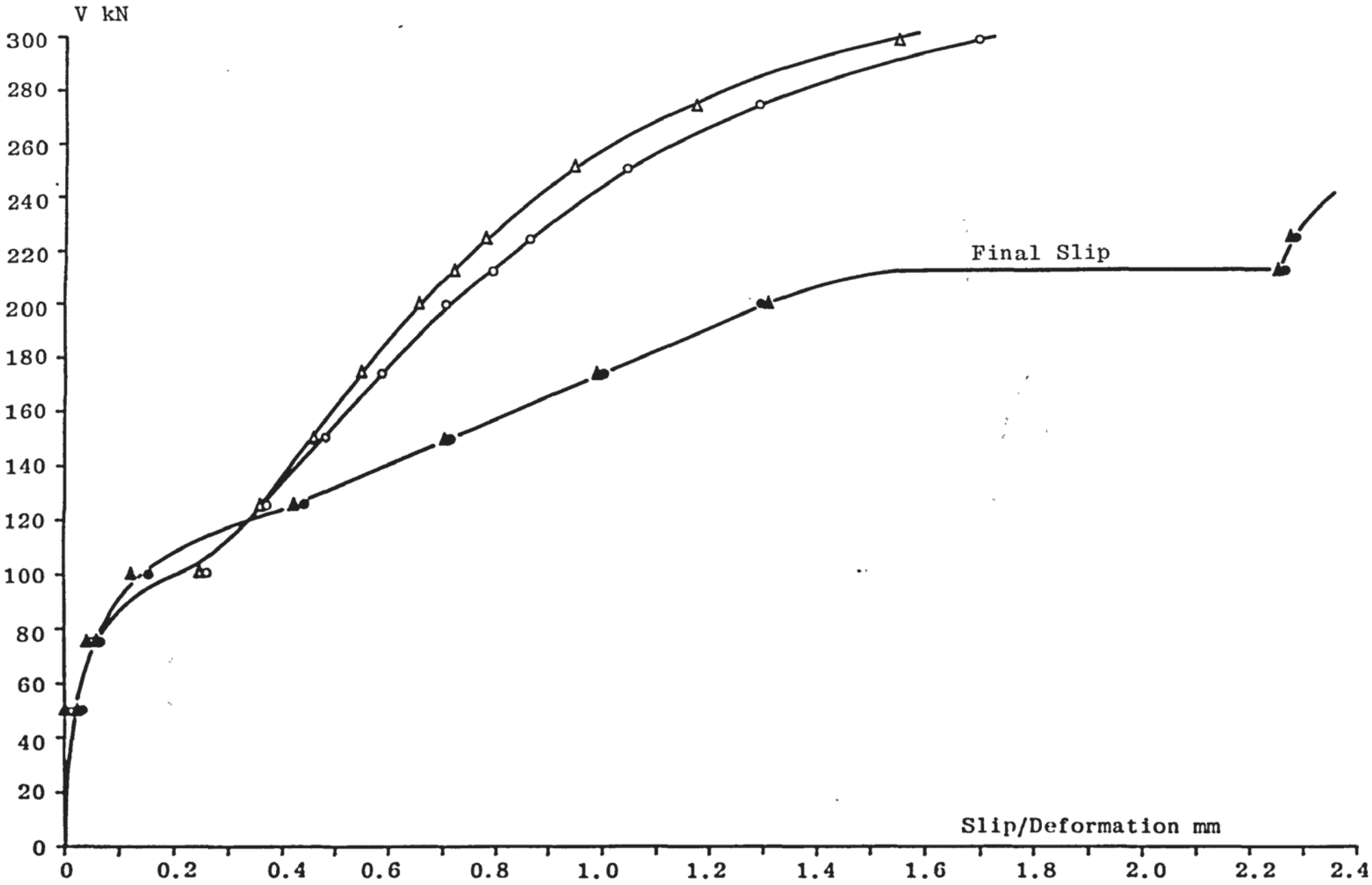

FIGURE A4.34 SHEAR FORCE - SLIP/DEFORMATION RELATIONSHIP FOR TEST CS3-4

Abbreviations used: EP, First Yield Weld Line End Plate; CF, First Yield Weld Line Column Flange

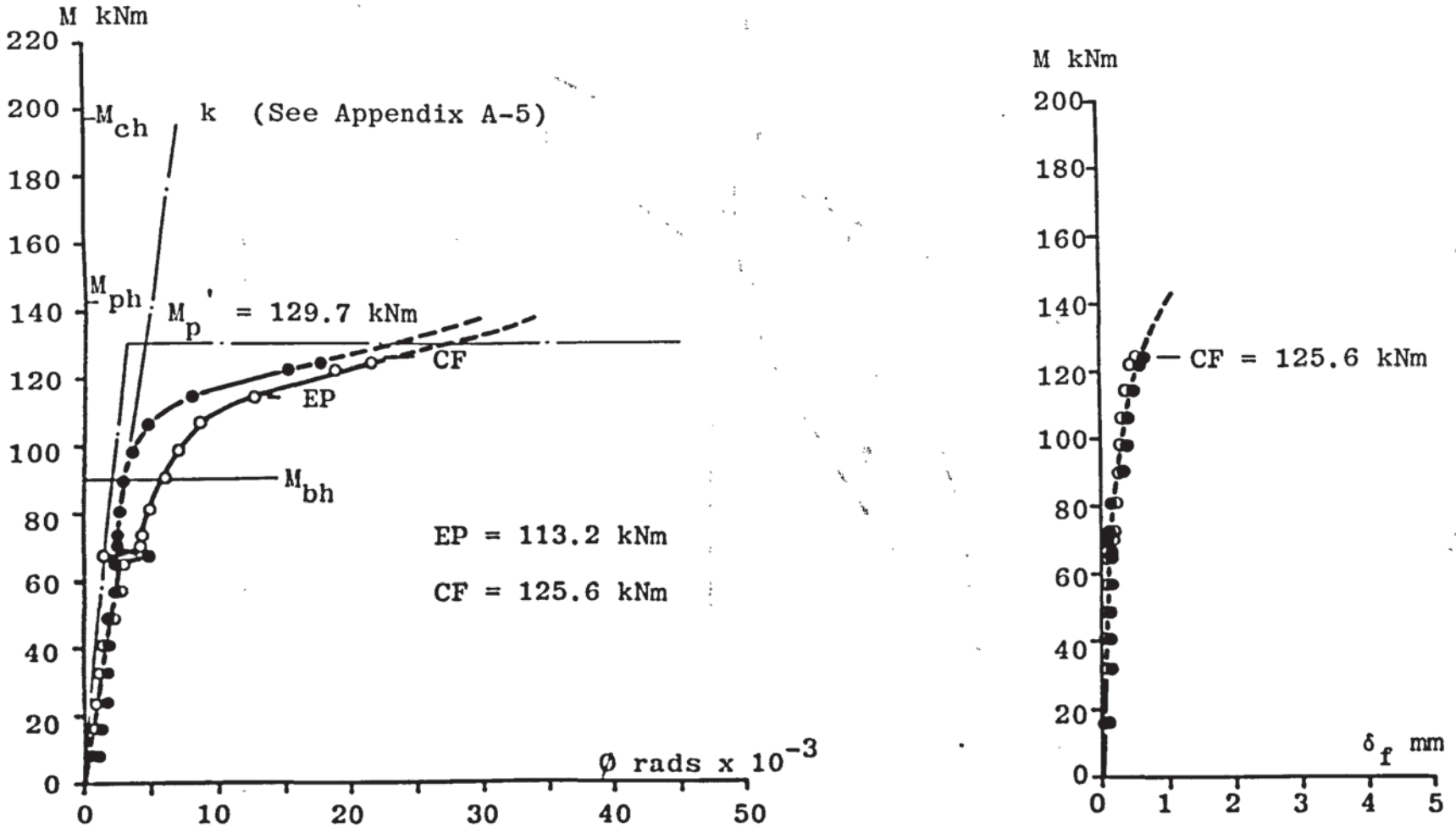

FIGURE A4.35 APPLIED MOMENT - ROTATION RELATIONSHIP AND APPLIED MOMENT - COLUMN FLANGE DEFLECTION RELATIONSHIP FOR TEST CS3-5

Abbreviations used: CF Prying Force Line Related to Column Flange
EP Prying Force Line Related to End Plate

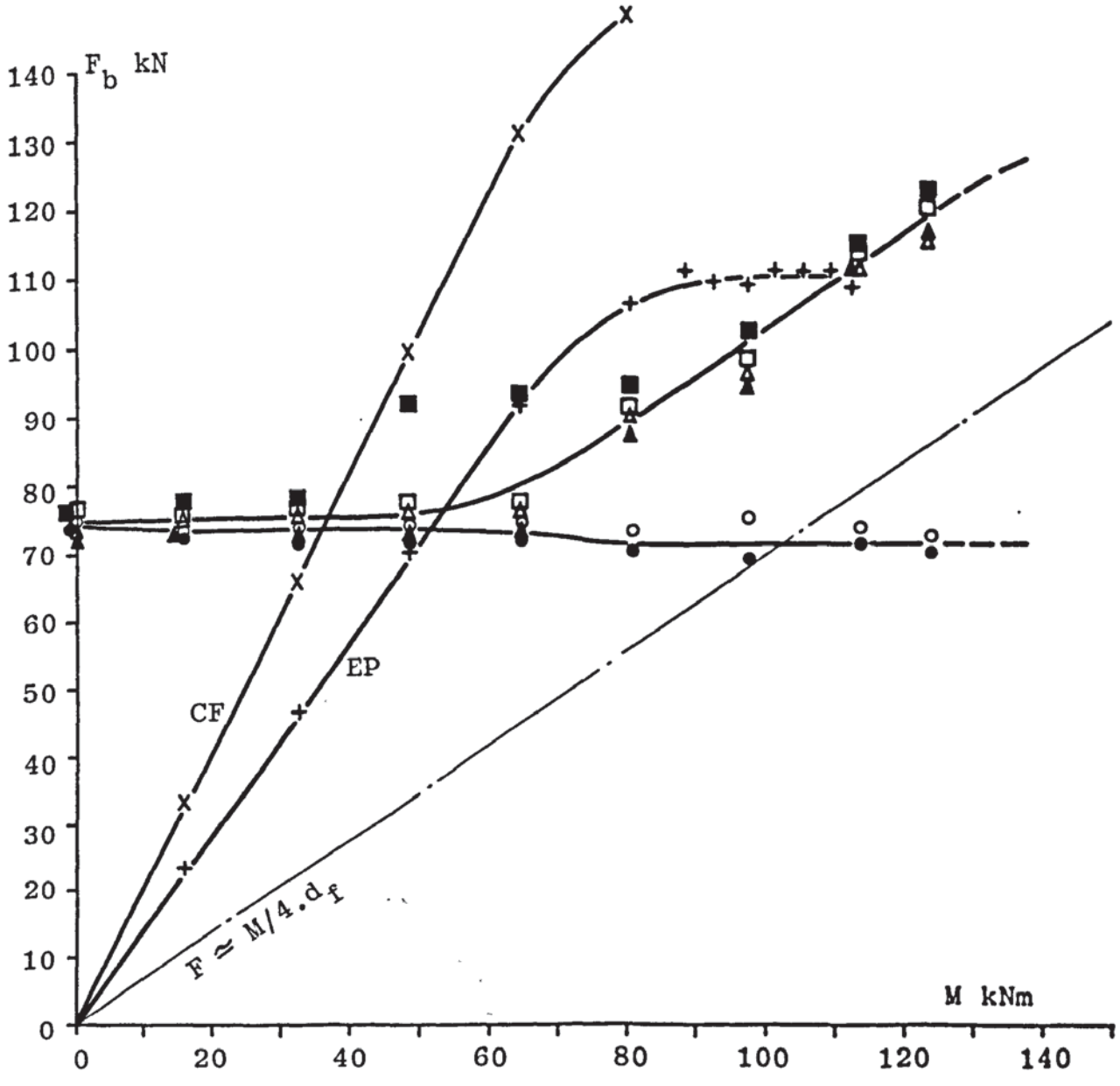

FIGURE A4.36 APPLIED MOMENT - BOLT FORCE RELATIONSHIP FOR TEST CS3-5

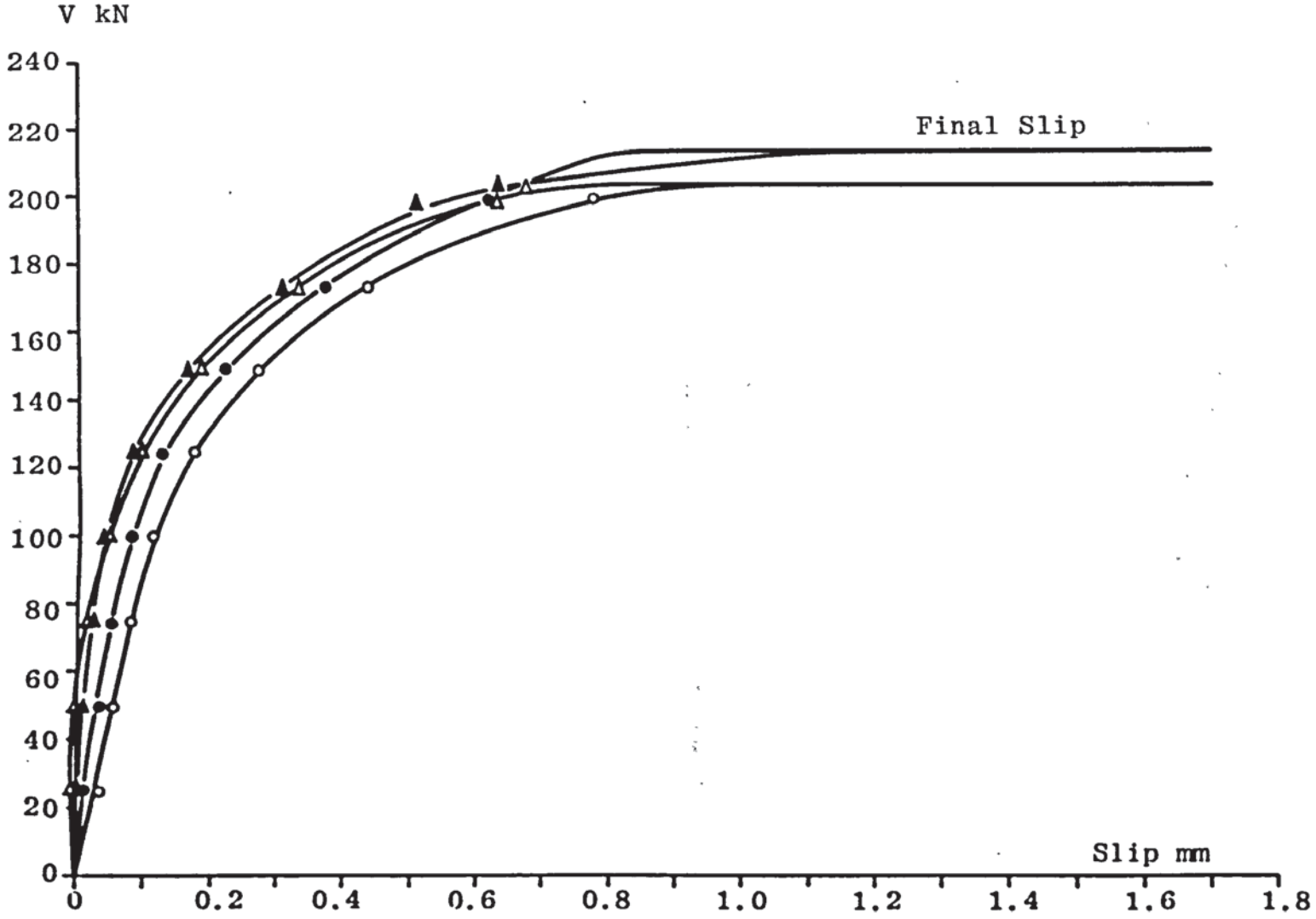

FIGURE A4.37 SHEAR FORCE - SLIP RELATIONSHIP FOR TEST CS3-5

Abbreviations used: EP, First Yield Weld Line End Plate; CF, First Yield Weld Line Column Flange

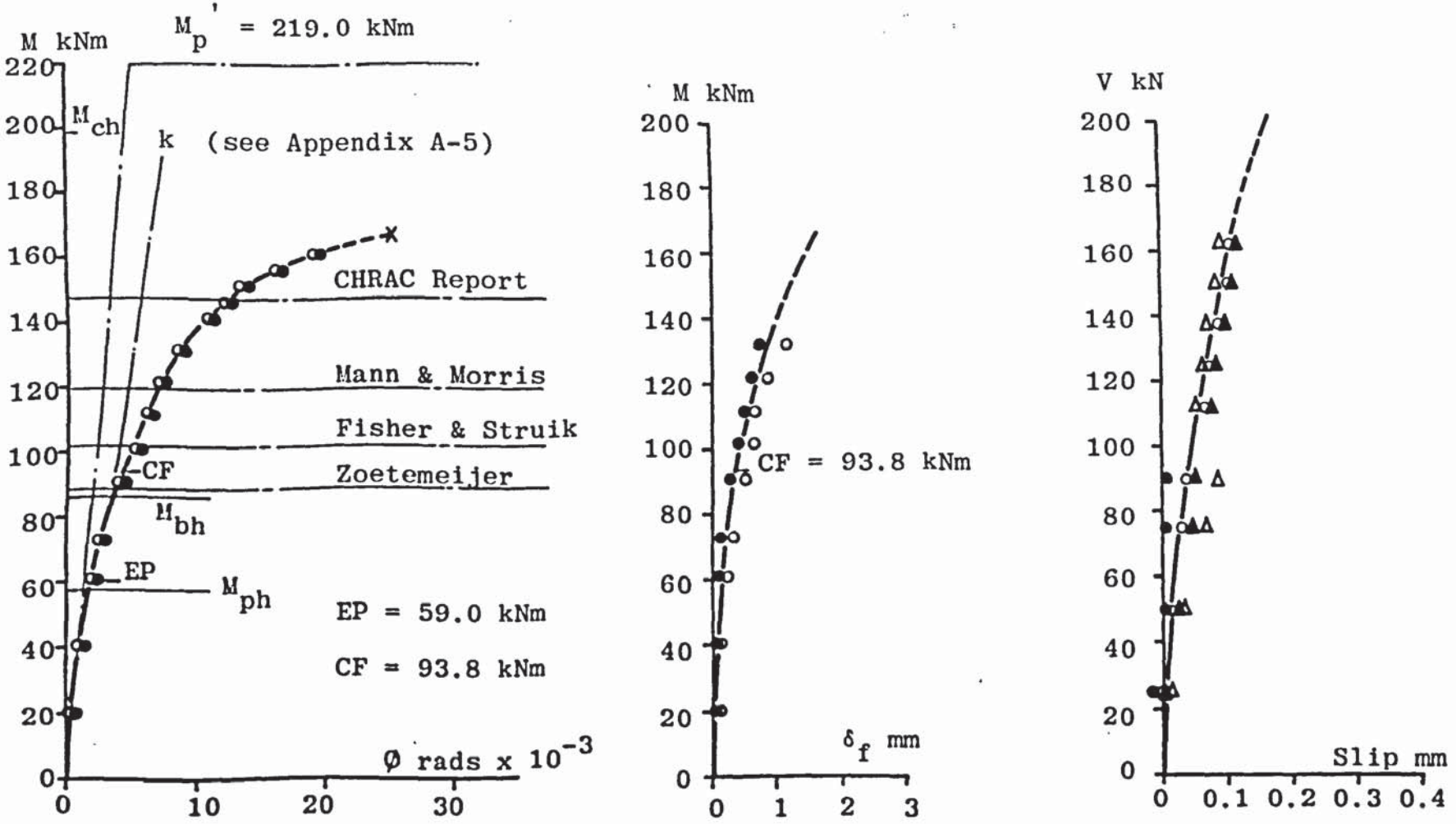

FIGURE A4.38 APPLIED MOMENT - ROTATION RELATIONSHIP, APPLIED MOMENT - COLUMN FLANGE DEFLECTION RELATIONSHIP AND SHEAR FORCE - SLIP RELATIONSHIP FOR TEST CS4-3

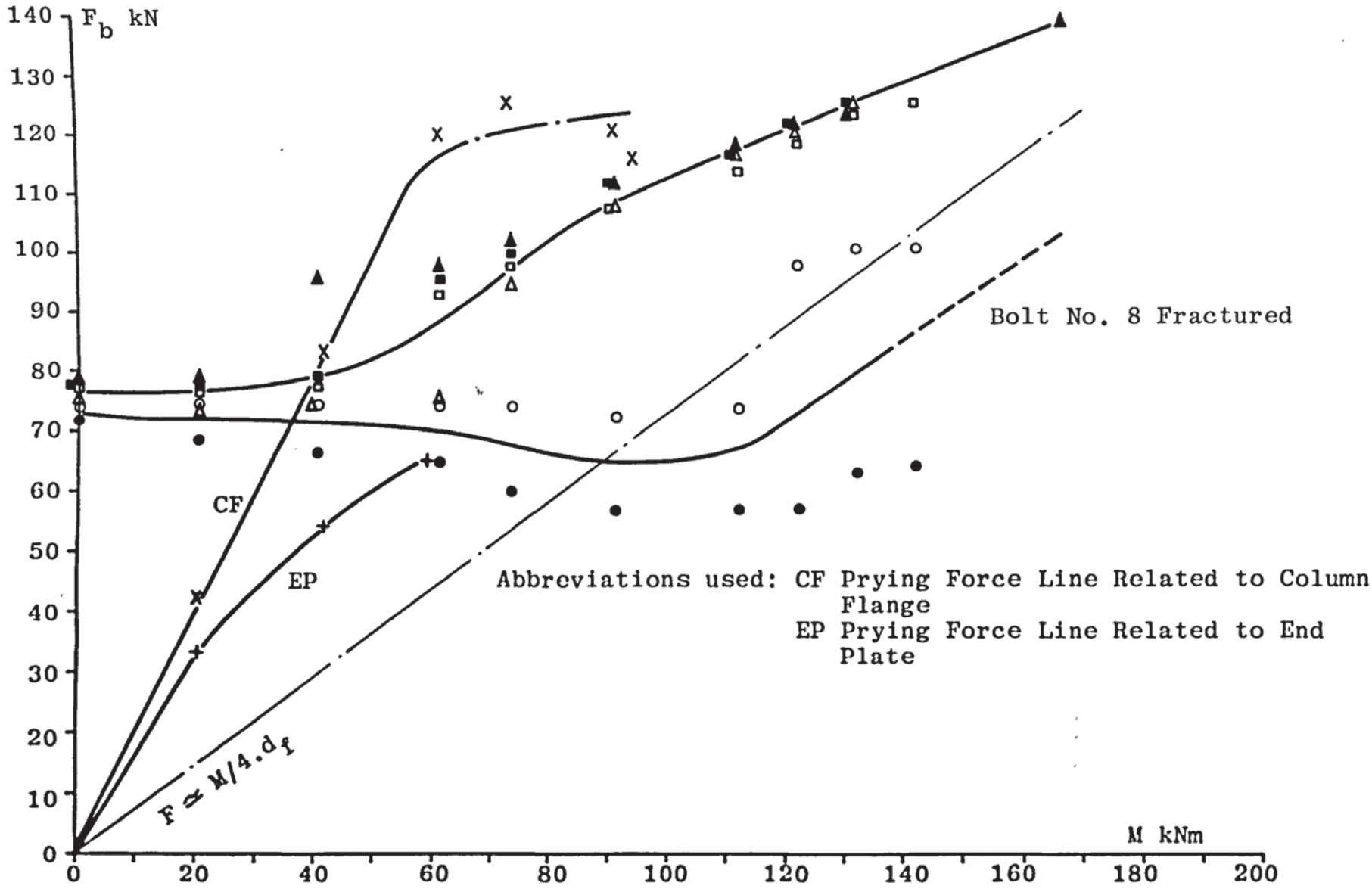

FIGURE A4.39 APPLIED MOMENT - BOLT FORCE RELATIONSHIP FOR TEST CS4-3

Abbreviations used: EP, First Yield Weld Line End Plate; CF, First Yield Weld Line Column Flange

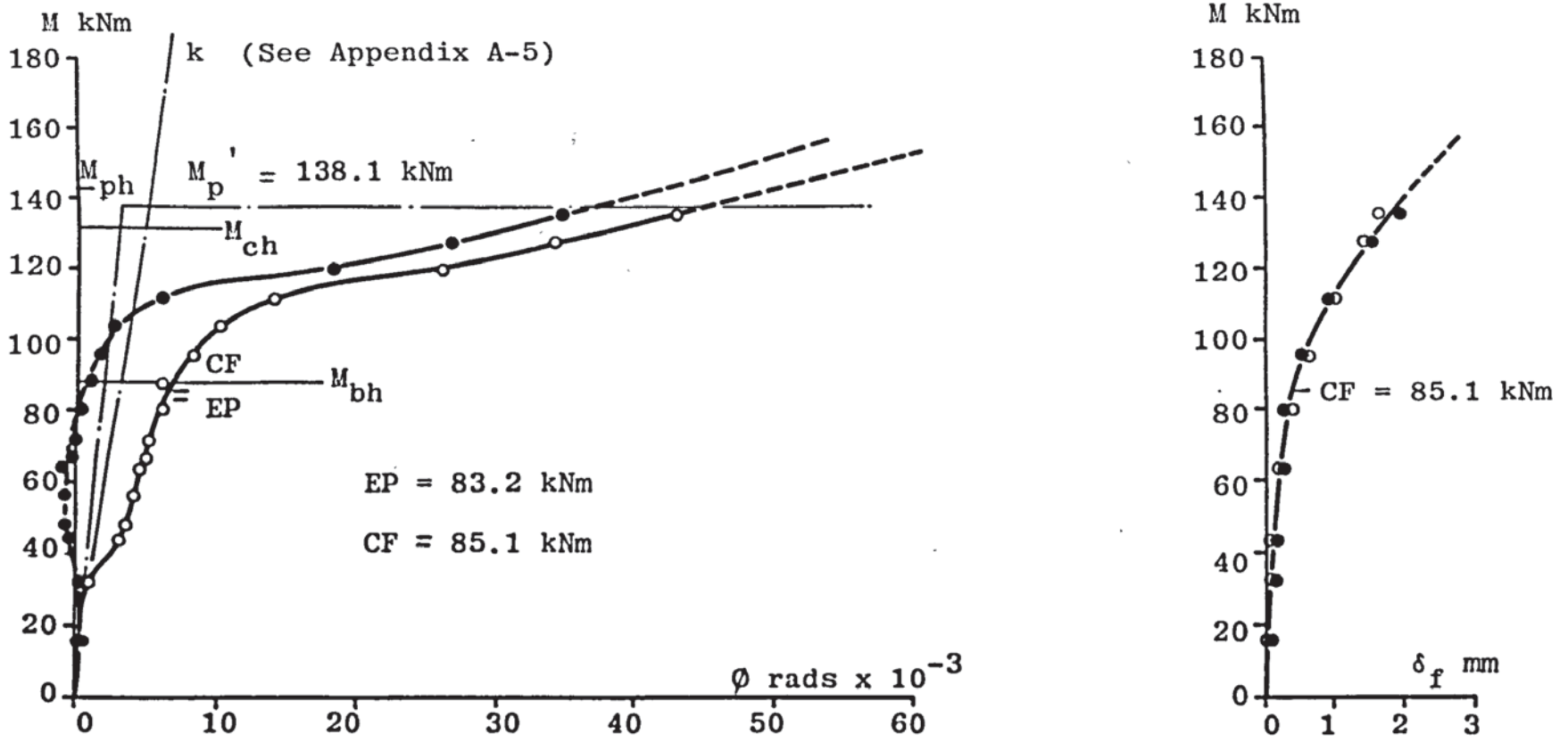

FIGURE A4.40 APPLIED MOMENT - ROTATION RELATIONSHIP AND APPLIED MOMENT - COLUMN FLANGE DEFLECTION RELATIONSHIP FOR TEST CS5-2

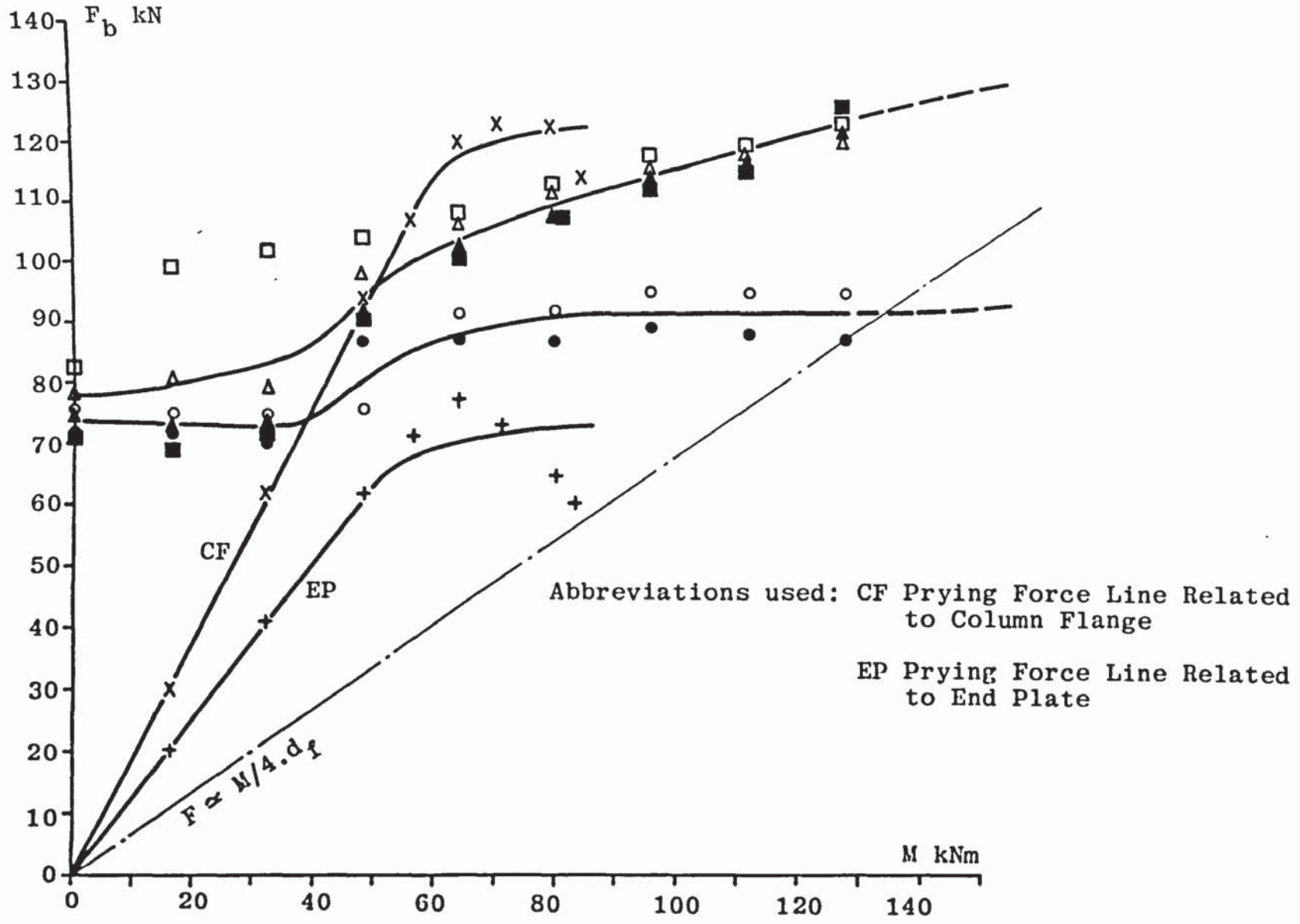

FIGURE A4.41 APPLIED MOMENT - BOLT FORCE RELATIONSHIP FOR TEST CS5-2

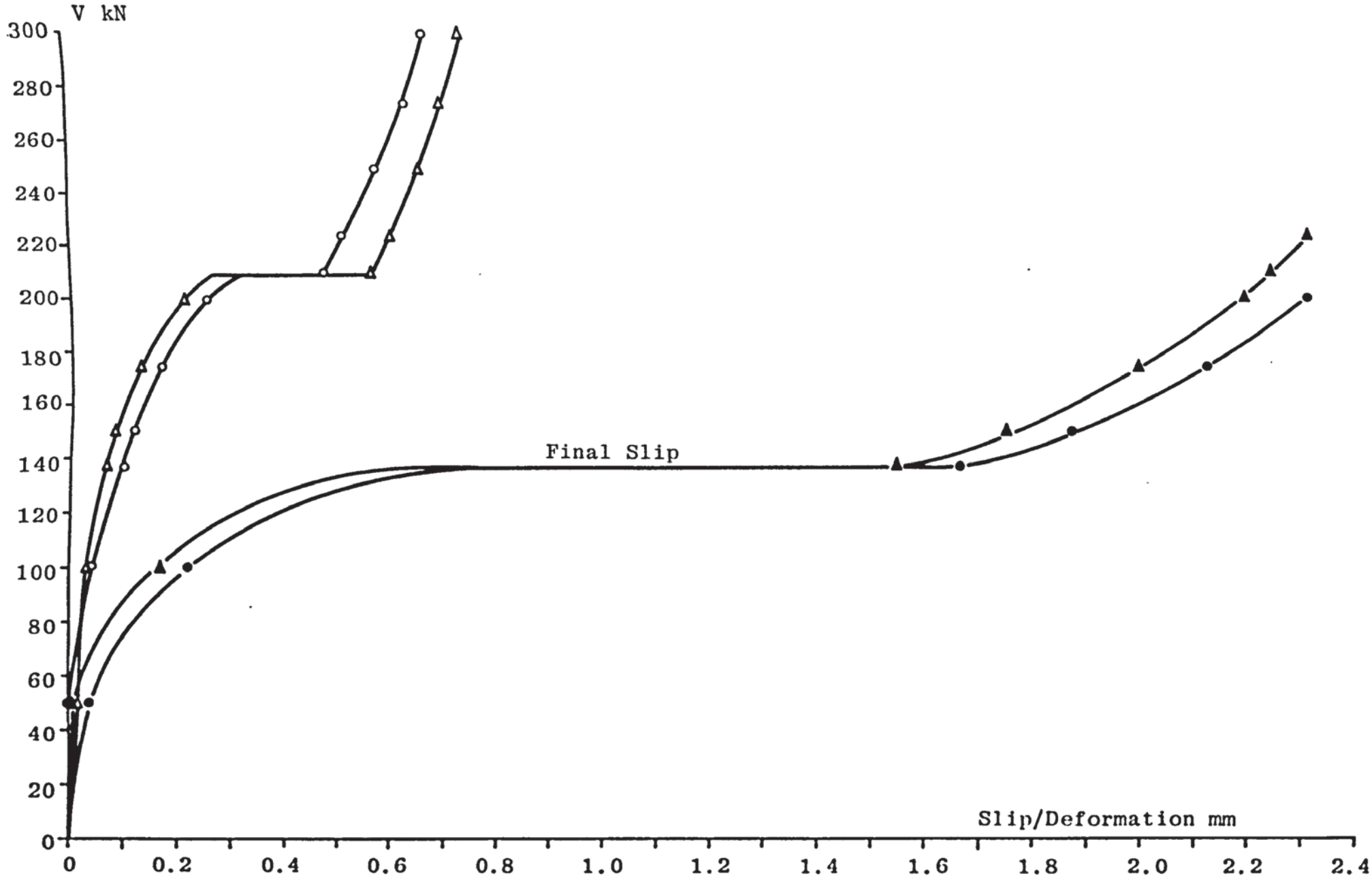

FIGURE A4.42 SHEAR FORCE - SLIP/DEFORMATION RELATIONSHIP FOR TEST CS5-2

APPENDIX A-5

A5.1 CONNECTION STIFFNESS

The elastic rotation of a connection may be considered to be

$$\phi_j = (\Delta_p + \Delta_c)/d_f \qquad \text{A5.1}$$

where

$$\phi_j = k.M \qquad \text{A5.2}$$

The deformed shape of the end plate when the prying forces are related to the end plate and column flange, can be seen from Figures A5.1 (b) and A5.1 (d) respectively. The deformed shape of the column flange is shown in Figure A5.1 (c).

Mann[17] suggested an equation to determine local column web deformations based on the principal of a point load resting on an elastic foundation. It is suggested that this method over-estimates these deformations and that they can be neglected in determining the connection stiffness. Mann[17] also suggested a method to determine the stiffness of a beam to column connection in which column flange deformation and prying forces were neglected. The deflection of the end plate was obtained by assuming the plate simply supported between the bolts. The values obtained from this method tend to underestimate the stiffness of connections.

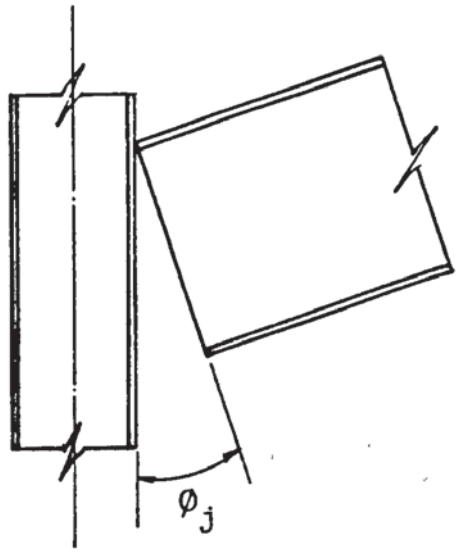

(a) Idealized

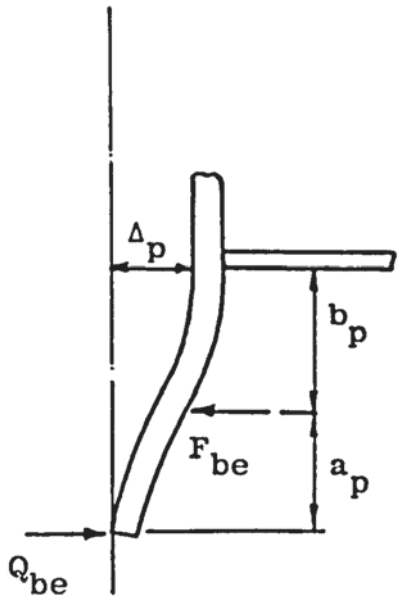

(b) End Plate Deformation

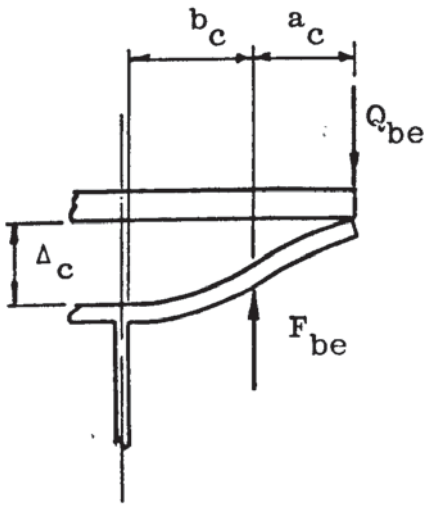

(c) Column Flange Deformation

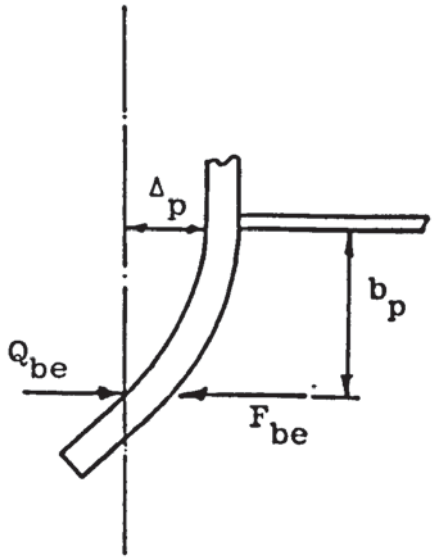

(d) End Plate Deformation

FIGURE A5.1 CONNECTION ROTATION DETAILS

A5.1.1 Prying Force Related to End Plate

Combining equation 5.8 and

$F_e + Q_{be} = F_{be}$

gives

$$Q_{be} = \frac{F_e(1 - F_p/A_b.E_b) + F_p.F_s/A_b.E_b}{2(a_p/b_p) + (2/3)(a_p/b_p)^2 + F_p/A_b.E_b} \qquad \text{A5.3}$$

The forces acting on the extended portion of the end plate may be represented by Figure A5.1 (b). The elastic deflection of the end plate at the tension flange is therefore

$$\Delta_p = \left[(F_e + Q_{be})(1 + 3_{ap}/2b_p)b_p^3 - Q_{be}(a_p + b_p)^3\right]/3E_p.I_p \qquad \text{A5.4}$$

where Q_{be} is obtained from A5.3.

The forces acting on the column flange may be represented by Figure A5.1 (c). The elastic deflection of the column flange at the beam tension flange is therefore

$$\Delta_c = \left[(F_e + Q_{be})(1 + 3a_c/2b_c)b_c^3 - Q_{be}(a_c + b_c)^3\right]/3E_c.I_c \qquad \text{A5.5}$$

where Q_{be} is obtained from A5.3.

Substituting the values of Δ_p and Δ_c into equation A5.1 gives ϕ_j hence the connection stiffness k. Applying these equations to the connections tested gave the approximate k values shown in Table A5.1.

Test or Series No.	k Related To End Plate rads/kNm x 10^{-6}	k Related To Column Flange rads/kNm x 10^{-6}
P2	12.799	11.642
CS1	26.399	25.956
CS2	46.194	34.437
CS3	12.799	11.642
CS4	15.543	21.492
CS5	17.707	13.315

TABLE A5.1 APPROXIMATE k VALUES

A5.1.2 Prying Force Related to Column Flange

Combining equation 5.8 and

$F_e + Q_{be} = F_{be}$

gives

$$Q_{be} = \frac{F_e(1 - F_c/A_b.E_b) + F_c.F_s/A_b.E_b}{2(a_c/b_c) + (2/3)(a_c/b_c)^2 + F_c/A_b.E_b} \qquad \text{A5.6}$$

The forces acting on the extended portion of the end plate may be represented by Figure 5.1 (d). The elastic deflection of the end plate at the tension flange is therefore

$$\Delta_p = F_e.b_p^3/3E_p.I_p \qquad \text{A5.7}$$

The forces acting on the column flange may be represented by Figure A5.1 (c). The elastic deflection of the column flange at the beam tension flange is therefore

$$\Delta_c = \left[(F_e + Q_{be})(1 + 3a_c/2b_c)b_c^3 - Q_{be}(a_c + b_c)^3\right]/3E_c.I_c \qquad \text{A5.5}$$

where Q_{be} is obtained from A5.6.

Substituting the values of Δ_p and Δ_c into equation A5.1 gives ϕ_j hence the connection stiffness k. Applying these equations to the connections tested gave the approximate k values shown in Table A5.1.

The least value of k for each test, from Table A5.1, compares reasonably well with the slope of the elastic portion of the moment - rotation curves obtained experimentally. It should be noted that the governing or least value of k for all the test series, except CS4, occurs when the prying force is related to the column flange. In test series CS4 the end plate thickness was smaller than that of the column flange. In this case the governing value of k occurs when the prying force is related to the end plate.

REFERENCES

1 Batho C. and Bateman E.H. Investigations on Bolts and Bolted Joints with Brief Suggestions for the Use of Black Bolts under Controlled Torque in Steel Frame Construction, Steel Structures Research Committee, Second Report, Department of Scientific and Industrial Research, HMSO, London, 1934.

2 Batho C. and Rowan H.C. Investigations on Beam and Stanchion Connections, Steel Structures Research Committee, Second Report, Department of Scientific and Industrial Research, HMSO, London, 1934.

3 Steel Structures Research Committee, Final Report, Department of Scientific and Industrial Research, HMSO, London, 1936.

4 British Standard 449, Specification for the Use of Structural Steel in Building, Part 2, 1969.

5 British Standards Institution, Draft Standard Specification for the Structural Use of Steelwork in Building, Part 1, November 1977.

6 Munse W.H. Research on Bolted Connections, Transactions, ASCE, Vol. 121, 1956.

7 Munse W.H. Petersen K.S. and Chesson E. Strength of Rivets and Bolts in Tension, Journal of the Structural Division, ASCE, Vol. 85, No. ST3, March 1959.

8 Schutz F.W. Strength of Moment Connections Using High Tensile Strength Bolts, AISC National Engineering Conference, Proceedings, 1959.

9 Ranger, B.E.S. Development of a Moment Connexion for Rigid Frames, Proceedings of the Jubilee Symposium on High Strength Bolts, Institution of Structural Engineers, London, June 1959.

10 Johnson L.G. Cannon J.C. and Spooner L.A. Joints in High Tensile Preloaded Bolts - Tests on Joints Designed to Develop Full Plastic Moments of Connected Members, Proceedings of the Jubilee Symposium on High Strength Bolts, Institution of Structural Engineers, London, June 1959.

11 Sherbourne A.N. Bolted Beam to Column Connections, The Structural Engineer, Vol. 39, London, June 1961.

12 Douty R.T. and McGuire W. High Strength Bolted Moment Connections, Journal of the Structural Division, ASCE, Vol. 91, No. ST2, April 1965.

13 Bannister A. Behaviour of Certain Connections Incorporating High Strength Friction Grip Bolts, Civil Engineering and Public Works Review, Oct./Nov. 1965.

14 Bannister A. Moment-Angle Change Relationships for Certain Connections Incorporating Friction Grip Bolts, Civil Engineering and Public Works Review, June/July 1966.

15 Naka T. Kato B. Tanaka A. and Morita K. Experimental Study on High Strength Bolted Moment Connections, Proceedings of the Symposium on High Strength Steel and its Joints, Japan, Sept., 1966.

16 Konishi I. and Yamakawa S. Behaviour of High Strength Bolted End Plate Connections, Proceedings of the Symposium on High Strength Steel and its Joints, Japan, Sept., 1966.

17 Mann A.P. End Plate Connections in Plastically Designed Structures, PhD Thesis, University of Leeds, 1968.

18 Surtees J.O. and Mann A.P. End Plate Connections in Plastically Designed Structures, Conference on Joints in Structures, University of Sheffield, July 1970.

19 Struik J.H.A. Tests on Bolted T-Stubs with Respect to Bolted Beam-to-Column Connections, Report 6-69-13, Stevin Laboratory, Delft University of Technology, Delft, Netherlands, 1969.

20 Fisher J.W. and Struik J.H.A. Guide to Design Criteria for Bolted and Riveted Joints, New York, N.Y., Wiley-Interscience, 1974.

21 Bailey J.R. Strength and Rigidity of Bolted Beam to Column Connections, Conference on Joints in Structures, University of Sheffield, July 1970.

22 De Back J. and Zoetemeijer P. High Strength Bolted Beam to Column Connections, The Computation of Bolts, T-Stub Flanges and Column Flanges, Report 6-72-13, Stevin Laboratory, Delft University of Technology, Delft, Netherlands, March 1972.

23 Agerskov H. and Thomsen K. Behaviour of Butt Plate Joints in Rolled Beams Assmebled with Prestressed High Tensile Bolts, Report No. R29, Structural Research Laboratory, Technical University of Denmark, Nov., 1972.

24 Agerskov H. Behaviour of Connections Using Prestressed High Strength Bolts Loaded in Tension, Report No. R55, Structural Research Laboratory, Technical University of Denmark, Sept., 1974.

25 Agerskov H. Analysis of High Strength Bolted Connections Subject to Prying. A Simplified Approach, Report No. R68, Structural Research Laboratory, Technical University of Denmark, Dec., 1975.

26 Manual of Steel Construction, American Institute of Steel Construction, 7th Edition, New York, NY, 1970.

27 Agerskov H. High Strength Bolted Connections Subject to Prying, Journal of the Structural Division, ASCE, Vol. 102, No. ST1, Jan., 1976.

28 Agerskov, H. Analysis of Bolted Connections Subject to Prying, Journal of the Structural Division, ASCE, Vol. 103, No. ST2, Nov., 1977.

29 Kato B. and McGuire W. Analysis of T-Stub Flange-to-Column Connections, Journal of the Structural Division, ASCE, Vol. 99, No. ST5, May 1973.

30 Nair R.S., Birkemoe P.C. and Munse W.H. High Strength Bolts Subject to Tension and Prying, Journal of the Structural Division, ASCE, Vol. 100, No. ST2, Feb., 1974.

31 Zoetemeijer P. A Design Method for the Tension Side of Statically Loaded, Bolted Beam to Column Connections, Heron 20, No. 1, Delft University, Delft, The Netherlands, 1974.

32 Packer J.A. A Study of the Tension Region of Plastically Designed, Bolted Beam to Column Connections, MSc Thesis, University of Manchester, 1975.

33 Packer J.A. and Morris L.J. A Limit State Design Method for the Tension Region of Bolted Beam to Column Connections, The Structural Engineer, Vol. 55, No. 10, London, Oct., 1977.

34 Packer J.A. and Morris L.J. Correspondence on A Limit State Design Method for the Tension Region of Bolted Beam to Column Connections, The Structural Engineer, Vol. 56A, No. 8, London, Aug., 1978.

35 Mann A.P. and Morris L.J. Limit Design of Extended End Plate Connections, Journal of the Structural Division, ASCE, Vol. 105, No. ST3, March 1979.

36 Krishnamurthy N. A Fresh Look at Bolted End Plate Behaviour and Design, Engineering Journal, AISC, Vol. 15, No. 2, 1978.

37 Krishnamurthy N. Discussion of Analysis of Bolted Connections Subject to Prying by H. Agerskov, Journal of the Structural Division, ASCE, Vol. 104, No. ST12, Dec., 1978.

38 Krishnamurthy N. Huang H.T. Jeffrey P.K. and Avery L.K. Analytical M-Ø Curves for End Plate Connections, Journal of the Structural Division, ASCE, Vol. 105, No. ST1, Jan., 1979.

39 Grundy P. Thomas I.R. and Bennetts I.D. Beam to Column Moment Connections, Journal of the Structural Division, ASCE, Vol. 106, ST1, Jan., 1980.

40 Morris L.J. and Newsome C.P. Bolted Corner Connection Subjected to an Out-of-Balance Moment - The Behaviour of the Column Web Panel, Paper 2A, Proceedings of the International Conference on Joints in Structural Steelwork, Teeside Polytechnic, Middlesbrough, April 1981.

41 Mann A.P. and Morris L.J. Significance of Lack of Fit - Flush Beam - Column Connections, Paper 2B, Proceedings of the International Conference on Joints in Structural Steelwork, Teeside Polytechnic, Middlesbrough, April 1981.

42 Bouwman L.P. The Structural Design of Bolted Connections Dynamically Loaded in Tension, Paper 3, Proceedings of the International Conference on Joints in Structural Steelwork, Teeside Polytechnic, Middlesbrough, April 1981.

43 Tarpy T.S. and Cardinal J.W. Behaviour of Semi-Rigid Beam-to-Column End Plate Connections, Paper 10, Proceedings of the International Conference on Joints in Structural Steelwork, Teeside Polytechnic, Middlesbrough, April 1981.

44 Steel Designer's Manual, CONSTRADO, 4th Edition, Crosby Lockwood and Staples, London 1972.

45 Morris L.J. and Randall A.L. Plastic Design, CONSTRADO, 1975.

46 CHRAC Research Report 3, Structural Stability, Appendix B, Department of the Environment, London, 1975.

47 Cheal B.D. Design Guidance Notes for Friction Grip Bolted Connections, Technical Note 98, CIRIA, May 1980.

48 Plastic Design in Steel - A Guide and Commentary, Manual No. 41, ASCE, New York, NY, 1971.

49 Graham J.D. Sherbourne A.N. and Khabbaz R.N. Welded Interior Beam to Column Connections, AISC, New York, 1959.

50 European Recommendations for Steel Construction, European Convention for Constructional Steelwork, March 1978.

51 Gill P.J. The Specification of Minimum Preloads for Structural Bolts, Report No. 130, GKN Group Research Laboratory, Feb., 1966.

52 British Standard 4395, Specification for High Strength Friction Grip Bolts and Associated Nuts and Washers for Structural Engineering, Part 1, General Grade, 1969.

53 British Standard 4604, Specification for the Use of High Strength Friction Grip Bolts in Structural Steelwork, Part 1, General Grade, 1970.

54 New Civil Engineer, Magazine of the Institution of Civil Engineers, Thomas Telford Ltd., 16 August 1979.

55 Drew F.P. Tightening High Strength Bolts, Proceedings Paper 786, Structural Division, ASCE, Vol. 81, August 1955.

56 Easton F.M. Lewis E.M. and Wright D.T. Some Notes on the Use of High Preload Bolts in the United Kingdom, The Structural Engineer, Vol. 35, London, May 1957.

57 Ball E.F. and Higgins J.J. Installation and Tightening of High Strength Bolts, Transactions, ASCE, Vol. 126, Part 2, 1961.

58 Cullimore M.S.G. Basic Factors in the Behaviour of Friction Grip Bolt Joints, Civil Engineering and Public Works Review, March/April 1963.

59 Rumpf J.L. and Fisher J.W. Calibration of A325 Bolts, Journal of the Structural Division, ASCE, Vol. 89, ST6, Dec., 1963.

60 Prynne P. Fundamentals of the Use of High Tensile Bolts in Structural Connections, Civil Engineering and Public Works Review, March/April 1965.

61 Sterling G.H. Troup E.W.J. Chesson E. and Fisher J.W. Calibration Tests of A490 High Strength Bolts, Journal of the Structural Division, ASCE, Vol. 91, ST5, Oct., 1965.

62 Gill P.J. Load Indicating Bolts, The Consulting Engineer, April/May 1962.

63 Cullimore M.S.G. and Boston R.M. Performance of High Strength Friction Grip Bolts with Countersunk Heads, Civil Engineering and Public Works Review, Oct., 1972.

64 Struik J.H.A. Oyeledun A.O. and Fisher J.W. Bolt Tension Control with a Direct Tension Indicator, Engineering Journal, AISC, Vol. 10, No. 1, 1973.

65 Blagden B.J. Thread Friction Tests, Report No. 748, GKN Group Research Laboratory, Oct., 1964.

66 British Standard 4360, Specification for Weldable Structural Steels, Dec., 1972.

67 Kennedy N.A. Vinnakota S. and Sherbourne A.N. The Split-Tee Analogy in Bolted Splices and Beam-Column Connections, Paper 17, Proceedings of the International Conference on Joints in Structural Steelwork, Teeside Polytechnic, Middlesbrough, April 1981.

68 Douty D.T. Strength Characteristics of High Strength Bolted Connections with Particular Application to the Plastic Design of Structures, PhD Thesis, Cornell University at Ithaca, New York, NY, 1964.

69 Benham P.P. and Warnock F.V. Mechanics of Solids and Structures, Pitman, 1976.

70 Chen W.F. and Newlin D.E. Column Web Strength in Beam to Column Connections, Journal of the Structural Division, ASCE, Vol. 99, ST9, Sept., 1973.

71 Timoshenko S. and Woinowsky-Krieger S. Theory of Plates and Shells, 2nd Edition, McGraw-Hill, 1959.

72 Horne M.R. Plastic Theory of Structures, 2nd Edition, Pergamon Press, 1979.

73. Holmes M. Universal Beams as Runway Beams, Civil Engineering and Public Works Review, May 1964.

74. Bahia C.S. Bolted Joints at the Ultimate Limit State Subject to Torsion and Shear, Ph.D. Thesis, University of Aston in Birmingham, 1980.